

INFORMATION TO USERS

This manuscript has been reproduced from the microfilm master. UMI films the text directly from the original or copy submitted. Thus, some thesis and dissertation copies are in typewriter face, while others may be from any type of computer printer.

The quality of this reproduction is dependent upon the quality of the copy submitted. Broken or indistinct print, colored or poor quality illustrations and photographs, print bleedthrough, substandard margins, and improper alignment can adversely affect reproduction.

In the unlikely event that the author did not send UMI a complete manuscript and there are missing pages, these will be noted. Also, if unauthorized copyright material had to be removed, a note will indicate the deletion.

Oversize materials (e.g., maps, drawings, charts) are reproduced by sectioning the original, beginning at the upper left-hand corner and continuing from left to right in equal sections with small overlaps. Each original is also photographed in one exposure and is included in reduced form at the back of the book.

Photographs included in the original manuscript have been reproduced xerographically in this copy. Higher quality 6" x 9" black and white photographic prints are available for any photographs or illustrations appearing in this copy for an additional charge. Contact UMI directly to order.

UMI

A Bell & Howell Information Company
300 North Zeeb Road, Ann Arbor MI 48106-1346 USA
313/761-4700 800/521-0600

University of Alberta

**PARTIAL FREEZING BY SPRAYING AS A TREATMENT
ALTERNATIVE OF SELECTED INDUSTRIAL WASTES**

by

Wa Gao ©

A thesis submitted to the Faculty of Graduate Studies and Research in partial fulfillment
of the requirements for the degree of Doctor of Philosophy

in

Environmental Engineering

Department of Civil and Environmental Engineering

Edmonton, Alberta

Fall, 1998



National Library
of Canada

Acquisitions and
Bibliographic Services

395 Wellington Street
Ottawa ON K1A 0N4
Canada

Bibliothèque nationale
du Canada

Acquisitions et
services bibliographiques

395, rue Wellington
Ottawa ON K1A 0N4
Canada

Your file Votre référence

Our file Notre référence

The author has granted a non-exclusive licence allowing the National Library of Canada to reproduce, loan, distribute or sell copies of this thesis in microform, paper or electronic formats.

The author retains ownership of the copyright in this thesis. Neither the thesis nor substantial extracts from it may be printed or otherwise reproduced without the author's permission.

L'auteur a accordé une licence non exclusive permettant à la Bibliothèque nationale du Canada de reproduire, prêter, distribuer ou vendre des copies de cette thèse sous la forme de microfiche/film, de reproduction sur papier ou sur format électronique.

L'auteur conserve la propriété du droit d'auteur qui protège cette thèse. Ni la thèse ni des extraits substantiels de celle-ci ne doivent être imprimés ou autrement reproduits sans son autorisation.

0-612-34767-2

University of Alberta

Library Release Form

Name of Author: GAO, WA

Title of Thesis: PARTIAL FREEZING BY SPRAYING AS A TREATMENT
ALTERNATIVE OF SELECTED INDUSTRIAL WASTES

Degree: DOCTOR OF PHILOSOPHY

Year this degree Granted: 1998

Permission is hereby granted to the University of Alberta Library to reproduce single copies of this thesis and to lent or sell such copies for private, scholarly, or scientific research purposes only.

The author reserves all other publication and other rights in association with the copyright in the thesis, and except as hereinbefore provided, neither the thesis nor any substantial portion thereof may be printed or otherwise reproduced in any material form whatever without the author's prior written permission.




226 RH, Michener Park
Edmonton, Alberta
T6H 4M5

Date: July 31, 98

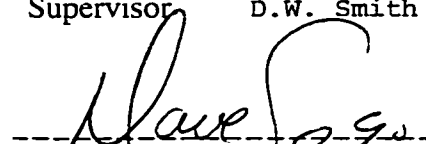
University of Alberta

Faculty of Graduate Studies and Research

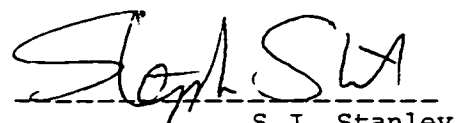
The undersigned certify that they have read, and recommended to the Faculty of Graduate Studies and Research for acceptance, a thesis entitled PARTIAL FREEZING BY SPRAYING AS A TREATMENT ALTERNATIVE OF SELECTED INDUSTRIAL WASTES submitted by WA GAO in partial fulfillment of the requirements for the degree of DOCTOR OF PHILOSOPHY in ENVIRONMENTAL ENGINEERING.



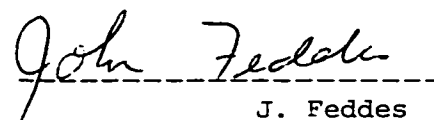
Supervisor D.W. Smith



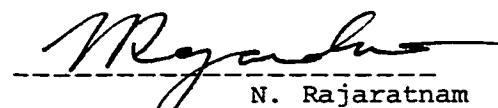
Co-supervisor D.C. Sego




S.J. Stanley



J. Feddes



N. Rajaratnam



External Examiner D.S. Mavinic

Date: 23 July 98

ABSTRACT

The principle objective of this study was to evaluate the spray freezing process as a treatment alternative for industrial wastewater. It included the investigation of the ice nucleation characteristics of pulp mill effluent, piggery wastewater and oil sands tailings pond water droplets, the freezing behavior of freely suspended wastewater droplets and impurity rejection and concentration phenomena occurred in the freezing and melting process.

The laboratory experiments showed that wastewater droplets made from different wastewaters froze at different temperatures when they were tested under the same experimental conditions. When a water drop was freely suspended in the cold air, the freezing started at the bottom of the drop and then spread over the entire surface enveloping the drop in an ice shell. The freezing temperature of a droplet was influenced by the nature of the wastewater, the ambient air temperature, the droplet size, the impurity concentration and the pH of the wastewater.

When wastewater was sprayed into a cold atmosphere, the contaminants in the wastewater were rejected by the growing ice crystals and were concentrated in the liquid phase as part of the sprayed water froze. The unfrozen water generated in the spray freezing process could carry away more than 50% of the impurities in the source water from the ice mound. The spray ice impurity concentration could be predicted by a mathematical model based on the mass balance of the impurity in the continuous spray freezing process.

Impurities remained in the spray ice would redistribute and were concentrated in the early meltwater. Experimental results indicated that the fractionation of impurities from melting ice column was affected by the nature of the wastewater, the impurity concentration in the spray ice, the age of the ice (or storage time), the distribution of the impurities within the ice column and the ice column density. The initial 30% of the meltwater removed between 50% and 80% of the total impurities (indicated by TOC, COD, color, conductivity, Cl^- and SO_4^{2-} concentrations) in the ice columns. The meltwater impurity concentration can be predicted using empirical equations.

Dedication

To: my husband, Muren and my son, Aoqi (Brian)

ACKNOWLEDGMENTS

The author wishes to express sincere gratitude to her supervisors: Dr. D.W Smith and Dr. D.C. Sego, for their guidance, supervision and encouragement throughout this study.

Sincere thanks go to Dr. D. Mavinic, Dr. J. Feddes, Dr. N. Rajaratnam and Dr. S. Stanley for their suggestions in preparing this thesis.

Grateful acknowledgment is given to Dr. T. Forest (Department of Mechanical Engineering) for providing access to laboratory space and equipment and Dr. E.P. Lowzosky (Department of Earth and Atmospheric Science) for supplying literature related to this study.

Special acknowledgment is also extended to Mr. S. Gamble, Mr. G. Cyre, Ms. C. Hereygers (Geotechnical Group, Department of Civil and Environmental Engineering), Mr. R. Gitzel and Mr. D. Lathe (Electronic Shop, Department of Civil and Environmental Engineering), Mr. N. Chernucka, Mr. G. Solonynko, Ms. M. Demeter and Ms. C. Schumacher (Environmental Engineering Group, Department of Civil and Environmental Engineering) and Mr. A. Muir (Mechanical Engineering shop, Department of Mechanical Engineering) for their cooperation and assistance

TABLE OF CONTENTS

CHAPTER 1	INTRODUCTION	1
CHAPTER 2	ICE NUCLEATION IN LIQUID WATER.....	4
2.1	HOMOGENEOUS NUCLEATION	4
2.2	HETEROGENEOUS NUCLEATION	6
2.2.1	Hypothesis of heterogeneous ice nucleation in water droplets	8
2.2.1.1	<i>Stochastic (statistical) model</i>	9
2.2.1.2	<i>Singular hypothesis</i>	10
2.2.1.3	<i>Differential and cumulative nucleus concentrations</i>	12
2.3	LITERATURE REVIEW OF EXPERIMENTAL STUDIES OF HETEROGENEOUS NUCLEATION	16
2.3.1	Ice nucleating materials and their influences	17
2.3.2	Some factors affecting freezing of water drops	21
2.3.2.1	<i>Drop volume</i>	21
2.3.2.2	<i>Cooling rate</i>	22
2.3.2.3	<i>Influence of aqueous solution on freezing temperature</i>	23
2.3.2.4	<i>The effect of pH on the ice nucleation</i>	24
2.3.2.5	<i>Atmospheric gases and freezing of supercooled water drops</i>	24
2.3.2.6	<i>Effect of evaporation on the drop freezing temperature</i>	25
2.4	SUMMARY.....	26
CHAPTER 3	FREEZING CHARACTERISTICS OF WASTEWATER DROPLETS	27
3.1	CHARACTERIZATION OF THE INDUSTRIAL WASTEWATERS.....	28
3.1.1	Characteristics of liquid swine waste.....	28
3.1.2	Contaminants in Kraft pulp mill effluent.....	29

3.1.3 Oil sands tailings pond water (T.P.W.).....	30
3.2 EXPERIMENTAL PROCEDURES AND METHODOLOGY	31
3.2.1 Wastewater Samples and Preparation	31
3.2.2 Experimental Design and Procedures	32
3.3 RESULTS AND DISCUSSION.....	33
3.3.1 Comparison of nucleus concentration.....	33
3.3.2 The effect of pH on the nucleus concentrations.....	39
3.3.3 The influence of impurity concentration on the wastewater freezing temperature	43
3.3.4 The volume effect	47
3. 4 SUMMARY.....	47
 CHAPTER 4 FREEZING BEHAVIOR OF FREELY SUSPENDED WATER	
DROPLETS	51
4.1 DESIGN OF THE VERTICAL WIND TUNNEL.....	53
4.1.1 Velocity profiles of the wind tunnel	57
4.2 EXPERIMENTAL FACILITIES AND SET-UP	60
4.2.1 Experimental facilities	60
4.2.2 Experimental set-up	61
4.3 FREEZING OF FREELY SUSPENDED WASTEWATER DROPS	62
4.3.1 General freezing characteristics of wastewater drops	62
4.3.2 The motion of frozen wastewater drops.....	73
4.3.3 Fragmentation of freezing water drops	75
4.4 THE FREEZING TIME REQUIRED FOR A FREELY SUSPENDED WASTEWATER DROP ..	82
4.5 COOLING AND ICE FRACTION IN A FREELY FALLING WASTEWATER DROP.....	93
4.5.1 The terminal velocity of a freely falling water drop	93
4.5.2 Cooling of a freely suspended wastewater drop.....	94
4.5.3 The heat balance of a freezing drop and ice production	105
4.6 SUMMARY.....	111

CHAPTER 5	WASTEWATER CONTAMINANTS CONCENTRATION AND SEPARATION BY FREEZING PROCESS.....	115
5.1	FUNDAMENTALS OF IMPURITY SEPARATION BY FREEZING	115
5.1.1	Impurity rejection during freezing	115
5.1.2	Freezing potential.....	118
5.1.3	Incorporation of impurities in the ice.....	120
5.2	APPLICATION OF FREEZING TECHNOLOGY IN WATER OR WASTEWATER PURIFICATION.....	124
5.3	IMPURITY SEPARATION IN THE SPRAY FREEZING PROCESS	128
5.4	PREDICTION OF IMPURITY CONCENTRATION IN THE SPRAY ICE	138
CHAPTER 6	SPRAY FREEZING TO TREAT INDUSTRIAL WASTEWATER ..	143
6.1	EXPERIMENTAL MATERIALS AND METHODS	143
6.1.1	Spraying equipment and method.....	143
6.1.2	The melting experiments.....	146
6.1.2.1	<i>Water samples and analysis</i>	147
6.2	RESULTS AND DISCUSSIONS	149
6.2.1	Impurity removal by runoff during the spraying operation.....	149
6.2.2	Impurity concentrations in the spray ice	151
6.2.3	Impurity removal during melting process	155
6.2.3.1	<i>Impurity removal from the spray ice obtained in a - 10 °C ambient air environment</i>	155
6.2.3.2	<i>Impurity removal from the spray ice obtained in a - 24 °C ambient air environment</i>	180
6.2.3.3	<i>Comparison of the impurity removal efficiency for the spray ice obtained under different ambient air temperatures</i>	199
6.2.3.4	<i>Results of Microtox toxicity test</i>	205
6.3	PREDICTION OF MELTWATER IMPURITY CONCENTRATION	209
6.4	APPLICATION OF THE SPRAY FREEZING PROCESS	213

6.5 SUMMARY.....	217
CHAPTER 7 SUMMARIES AND CONCLUSIONS	219
CHAPTER 8 RECOMMENDATIONS FOR FUTURE STUDIES	230
REFERENCES	231
APPENDIX - A CHAMICAL ANALYSIS DATA.....	246
APPENDIX - B FREEZING TIME REQUIRED BY FREELY SUSPENDED WASTEWATER DROPLETS	285
APPENDIX - C PHOTOGRAPHS OF THE EXPERIMENTS	297

LIST OF FIGURES

FIGURE 3-1 COMPARISON OF THE WASTEWATER ICE NUCLEUS CONCENTRATIONS.....	34
FIGURE 3-2 CONCENTRATIONS OF FREEZING NUCLEI IN THE WASTEWATERS WITH 50% OF THE ORIGINAL IMPURITY CONTENT: (A) DIFFERENTIAL NUCLEUS SPECTRA; (B) CUMULATIVE NUCLEUS SPECTRA.	37
FIGURE 3-3 THE INFLUENCE OF pH ON THE NUCLEUS CONCENTRATION OF THE INDIVIDUAL WASTEWATER (THE DROPLETS CONTAIN ORIGINAL WASTEWATER IMPURITY CONTENT).	40
FIGURE 3-4 COMPARISON OF CUMULATIVE NUCLEUS CONCENTRATIONS AT DIFFERENT pH CONDITIONS.	42
FIGURE 3-5 CUMULATIVE NUCLEUS SPECTRA FOR WASTEWATERS WITH DIFFERENT IMPURITY CONTENTS.....	44
FIGURE 3-6 CUMULATIVE ICE NUCLEUS CONCENTRATIONS OF THE WASTEWATERS WITH 2% OF THEIR ORIGINAL IMPURITY CONTENT.....	46
FIGURE 3-7-A DIFFERENTIAL ICE NUCLEUS CONCENTRATIONS FOR DISTILLED WATER AND PULP MILL EFFLUENT DROPS WITH DIFFERENT VOLUMES (4.2 μL AND 33.5 μL).	48
FIGURE 3-7-B DIFFERENTIAL ICE NUCLEUS CONCENTRATIONS FOR PIGGERY WASTEWATER AND OIL SANDS TAILINGS POND WATER DROPS WITH DIFFERENT VOLUMES (4.2 μL AND 33.5 μL).....	49
FIGURE 4-1 THE SCHEMATIC DIAGRAM OF THE VERTICAL WIND TUNNEL.....	54
FIGURE 4-2 THE SMALL SCREEN USED TO GET VELOCITY SAG.....	56
FIGURE 4-3 VELOCITY PROFILES TAKEN ABOVE THE WORKING AREA	58
FIGURE 4-4 THE AVERAGE FREEZING TIME REQUIRED BY THE 4.2 MM DIAMETER WASTEWATER DROPS AS A FUNCTION OF THE AMBIENT AIR TEMPERATURES	90

FIGURE 4-5	THE DROPLET FREEZING TIME AS A FUNCTION OF THE UPDRAFT TEMPERATURE AND THE DROPLET DIAMETER.....	92
FIGURE 4-6-1	COOLING OF FREELY SUSPENDED WASTEWATER DROPS: (A) COOLING FROM + 5 °C TO - 10.3 °C AND (B) COOLING FROM + 5 °C TO - 17.7 °C.....	100
FIGURE 4-6-2	COOLING OF FREELY SUSPENDED WASTEWATER DROPS: (C) COOLING FROM + 5 °C TO - 6.7 °C AND (D) COOLING FROM + 5 °C TO - 7.4 °C.	101
FIGURE 4-7	THE ICE FRACTION IN A SINGLE PULP MILL EFFLUENT DROP VS. THE DROPLET AIR RESIDENCE TIME.....	107
FIGURE 4-8	THE ICE FRACTION IN A SINGLE OIL SANDS TAILINGS POND WATER DROPLET VS. THE DROPLET AIR RESIDENCE TIME.	108
FIGURE 4-9	THE FRACTION OF FROZEN WATER IN A 1 MM AND 3.4 MM DIAMETER PIGGERY WASTEWATER DROP VS. AIR RESIDENCE TIME IN A - 10.3 °C ENVIRONMENT.....	110
FIGURE 4-10	THE ICE FRACTION IN A PULP MILL EFFLUENT DROP AS A FUNCTION OF DROPLET DIAMETER AND DROPLET AIR RESIDENCE TIME IN A - 10.3 °C ENVIRONMENT.....	112
FIGURE 4-11	THE ICE FRACTION IN A OIL SANDS TAILINGS POND WATER DROP AS A FUNCTION OF DROPLET DIAMETER AND DROPLET AIR RESIDENCE TIME IN A - 10.3 °C ENVIRONMENT.....	112
FIGURE 4-12	THE FRACTION OF FROZEN WATER IN DIFFERENT SIZES OF PULP MILL EFFLUENT DROPS AFTER SUSPENDING IN THE AIR FOR 7 SECONDS.	113
FIGURE 4-13	THE FRACTION OF FROZEN WATER IN DIFFERENT SIZES OF OIL SANDS TAILINGS POND WATER DROPS AFTER SUSPENDING IN THE AIR FOR 7 SECONDS.....	113
FIGURE 5-1	SCHEMATIC DIAGRAM OF A SPRAY FREEZING PROCESS	139
FIGURE 6.1	THE EXPERIMENTAL CONFIGURATION FOR THE LABORATORY MELTING TESTS.....	145
FIGURE 6-2	VARIATION OF THE NORMALIZED COD CONCENTRATION IN THE SEQUENTIAL MELTWATER SAMPLES OF THE SPRAY ICE MADE FROM PULP MILL EFFLUENT	156

FIGURE 6-3	VARIATION OF THE NORMALIZED COLOR CONCENTRATION IN THE SEQUENTIAL MELTWATER SAMPLES OF THE SPRAY ICE MADE FROM PULP MILL EFFLUENT.	156
FIGURE 6-4	VARIATION OF THE NORMALIZED TOC CONCENTRATION IN THE SEQUENTIAL MELTWATER SAMPLES OF THE SPRAY ICE MADE FROM PULP MILL EFFLUENT.	157
FIGURE 6-5	VARIATION OF THE NORMALIZED IONIC STRENGTH (CONDUCTIVITY) IN THE SEQUENTIAL MELTWATER SAMPLES OF THE SPRAY ICE MADE FROM PULP MILL EFFLUENT.	157
FIGURE 6-6	VARIATION OF THE NORMALIZED pH VALUE IN THE SEQUENTIAL MELTWATER SAMPLES OF THE SPRAY ICE MADE FROM PULP MILL EFFLUENT.....	159
FIGURE 6-7	VARIATION OF THE CONCENTRATION RATIOS OF THE SELECTED IMPURITIES VERSUS MELTWATER VOLUME FOR THE 20-DAY OLD SPRAY ICE MADE FROM PULP MILL EFFLUENT IN A - 10 °C ENVIRONMENT.....	162
FIGURE 6-8	VARIATION OF THE CONCENTRATION RATIOS OF THE SELECTED IMPURITIES VERSUS MELTWATER VOLUME FOR THE 40-DAY OLD SPRAY ICE MADE FROM PULP MILL EFFLUENT IN A - 10 °C ENVIRONMENT.	163
FIGURE 6-9	VARIATION OF THE NORMALIZED COD CONCENTRATION IN THE SEQUENTIAL MELTWATER SAMPLES OF THE SPRAY ICE MADE FROM OIL SANDS TAILINGS POND WATER (SPRAY ICE WAS OBTAINED IN A - 10 °C AMBIENT AIR TEMPERATURE)	165
FIGURE 6-10	VARIATION OF THE NORMALIZED TOC CONCENTRATION IN THE SEQUENTIAL MELTWATER SAMPLES OF THE SPRAY ICE MADE FROM OIL SANDS TAILINGS POND WATER (SPRAY ICE WAS OBTAINED IN A - 10 °C AMBIENT AIR TEMPERATURE)	165
FIGURE 6-11	VARIATION OF THE NORMALIZED Cl ⁻ CONCENTRATION IN THE SEQUENTIAL MELTWATER SAMPLES OF THE SPRAY ICE MADE FROM OIL SANDS TAILINGS POND WATER (SPRAY ICE WAS OBTAINED IN A - 10 °C AMBIENT AIR TEMPERATURE.....)	166

FIGURE 6-12	VARIATION OF THE NORMALIZED SO_4^{2-} CONCENTRATION IN THE SEQUENTIAL MELTWATER SAMPLES OF THE SPRAY ICE MADE FROM OIL SANDS TAILINGS POND WATER (SPRAY ICE WAS OBTAINED IN A - 10 °C AMBIENT AIR TEMPERATURE	166
FIGURE 6-13	VARIATION OF THE NORMALIZED IONIC STRENGTH (CONDUCTIVITY) IN THE SEQUENTIAL MELTWATER SAMPLES OF THE SPRAY ICE MADE FROM OIL SANDS TAILINGS POND WATER (SPRAY ICE WAS OBTAINED IN A - 10 °C AMBIENT AIR	169
FIGURE 6-14	VARIATION OF THE NORMALIZED pH VALUE IN THE SEQUENTIAL MELTWATER SAMPLES OF THE SPRAY ICE MADE FROM OIL SANDS TAILINGS POND WATER (SPRAY ICE WAS OBTAINED IN A - 10 °C AMBIENT AIR TEMPERATURE	169
FIGURE 6-15	VARIATION OF THE CONCENTRATION RATIOS OF THE SELECTED IMPURITIES VERSUS MELTWATER VOLUME FOR THE 20-DAY OLD SPRAY ICE MADE FROM OIL SANDS TAILINGS POND WATER IN A - 10 °C ENVIRONMENT.	171
FIGURE 6-16	VARIATION OF THE CONCENTRATION RATIOS OF THE SELECTED IMPURITIES VERSUS MELTWATER VOLUME FOR THE 40-DAY OLD SPRAY ICE MADE FROM OIL SANDS TAILINGS POND WATER IN A - 10 °C ENVIRONMENT.	172
FIGURE 6-17	VARIATION OF THE NORMALIZED IONIC STRENGTH (CONDUCTIVITY) IN THE SEQUENTIAL MELTWATER SAMPLES OF THE SPRAY ICE MADE FROM TAP WATER (THE SPRAY ICE WAS OBTAINED IN A - 10 °C ENVIRONMENT)	174
FIGURE 6-18	VARIATION OF THE NORMALIZED SO_4^{2-} CONCENTRATION IN THE SEQUENTIAL MELTWATER SAMPLES OF THE SPRAY ICE MADE FROM TAP WATER (THE SPRAY ICE WAS OBTAINED IN A - 10 °C ENVIRONMENT)	175
FIGURE 6-19	VARIATION OF THE NORMALIZED Cl^- CONCENTRATION IN THE SEQUENTIAL MELTWATER SAMPLES OF THE SPRAY ICE MADE FROM TAP WATER (THE SPRAY ICE WAS OBTAINED IN A - 10 °C ENVIRONMENT)	175
FIGURE 6-20	VARIATION OF THE NORMALIZED pH VALUE IN THE SEQUENTIAL MELTWATER SAMPLES OF THE SPRAY ICE MADE FROM TAP WATER (THE SPRAY ICE WAS OBTAINED IN A - 10 °C ENVIRONMENT)	176

FIGURE 6-21	VARIATION OF THE CONCENTRATION RATIOS OF THE SELECTED IMPURITIES VERSUS MELTWATER VOLUME FOR THE 20-DAY OLD SPRAY ICE MADE FROM TAP WATER IN A - 10 °C ENVIRONMENT.....	178
FIGURE 6-22	VARIATION OF THE CONCENTRATION RATIOS OF THE SELECTED IMPURITIES VERSUS MELTWATER VOLUME FOR THE 40-DAY OLD SPRAY ICE MADE FROM TAP WATER IN A - 10 °C ENVIRONMENT.....	179
FIGURE 6-23	VARIATION OF THE NORMALIZED TOC CONCENTRATION IN THE SEQUENTIAL MELTWATER SAMPLES OF THE SPRAY ICE MADE FROM PULP MILL EFFLUENT (THE SPRAY ICE WAS OBTAINED IN A - 24 °C ENVIRONMENT).	182
FIGURE 6-24	VARIATION OF THE NORMALIZED COD CONCENTRATION IN THE SEQUENTIAL MELTWATER SAMPLES OF THE SPRAY ICE MADE FROM PULP MILL EFFLUENT (THE SPRAY ICE WAS OBTAINED IN A - 24 °C ENVIRONMENT)	182
FIGURE 6-25	VARIATION OF THE NORMALIZED COLOR CONCENTRATION IN THE SEQUENTIAL MELTWATER SAMPLES OF THE SPRAY ICE MADE FROM PULP MILL EFFLUENT (THE SPRAY ICE WAS OBTAINED IN A - 24 °C ENVIRONMENT)	183
FIGURE 6-26	VARIATION OF THE NORMALIZED IONIC STRENGTH (CONDUCTIVITY) IN THE SEQUENTIAL MELTWATER SAMPLES OF THE SPRAY ICE MADE FROM PULP MILL EFFLUENT (THE SPRAY ICE WAS OBTAINED IN A - 24 °C ENVIRONMENT).	183
FIGURE 6-27	VARIATION OF THE NORMALIZED pH IN THE SEQUENTIAL MELTWATER SAMPLES OF THE SPRAY ICE MADE FROM PULP MILL EFFLUENT (THE SPRAY ICE WAS OBTAINED IN A - 24 °C ENVIRONMENT)	184
FIGURE 6-28	VARIATION OF THE CONCENTRATION RATIOS OF THE SELECTED IMPURITIES VERSUS MELTWATER VOLUME FOR THE 20-DAY OLD SPRAY ICE MADE FROM PULP MILL EFFLUENT IN A - 24 °C ENVIRONMENT.....	185

FIGURE 6-29 VARIATION OF THE CONCENTRATION RATIOS OF THE SELECTED IMPURITIES VERSUS MELTWATER VOLUME FOR THE 40-DAY OLD SPRAY ICE MADE FROM PULP MILL EFFLUENT IN A - 24 °C ENVIRONMENT.	186
FIGURE 6-30 VARIATION OF THE NORMALIZED COD CONCENTRATION IN THE SEQUENTIAL MELTWATER SAMPLES OF THE SPRAY ICE MADE FROM OIL SANDS TAILINGS POND WATER (THE SPRAY ICE WAS OBTAINED IN A - 24 °C ENVIRONMENT).	188
FIGURE 6-31 VARIATION OF THE NORMALIZED TOC CONCENTRATION IN THE SEQUENTIAL MELTWATER SAMPLES OF THE SPRAY ICE MADE FROM OIL SANDS TAILINGS POND WATER (THE SPRAY ICE WAS OBTAINED IN A - 24 °C ENVIRONMENT).	188
FIGURE 6-32 VARIATION OF THE NORMALIZED IONIC STRENGTH (CONDUCTIVITY) IN THE SEQUENTIAL MELTWATER SAMPLES OF THE SPRAY ICE MADE FROM OIL SANDS TAILINGS POND WATER (THE SPRAY ICE WAS OBTAINED IN A - 24 °C ENVIRONMENT)	189
FIGURE 6-33 VARIATION OF THE NORMALIZED pH IN THE SEQUENTIAL MELTWATER SAMPLES OF THE SPRAY ICE MADE FROM OIL SANDS TAILINGS POND WATER (THE SPRAY ICE WAS OBTAINED IN A - 24 °C ENVIRONMENT).	189
FIGURE 6-34 VARIATION OF THE NORMALIZED Cl^- CONCENTRATION IN THE SEQUENTIAL MELTWATER SAMPLES OF THE SPRAY ICE MADE FROM OIL SANDS TAILINGS POND WATER (THE SPRAY ICE WAS OBTAINED IN A - 24 °C ENVIRONMENT).	190
FIGURE 6-35 VARIATION OF THE NORMALIZED SO_4^{2-} CONCENTRATION IN THE SEQUENTIAL MELTWATER SAMPLES OF THE SPRAY ICE MADE FROM OIL SANDS TAILINGS POND WATER (THE SPRAY ICE WAS OBTAINED IN A - 24 °C ENVIRONMENT).	190
FIGURE 6-36 VARIATION OF THE CONCENTRATION RATIOS OF THE SELECTED IMPURITIES VERSUS MELTWATER VOLUME FOR THE 20-DAY OLD SPRAY ICE MADE FROM OIL SANDS TAILINGS POND WATER IN A - 24 °C ENVIRONMENT.	191

FIGURE 6-37	VARIATION OF THE CONCENTRATION RATIOS OF THE SELECTED IMPURITIES VERSUS MELTWATER VOLUME FOR THE 40-DAY OLD SPRAY ICE MADE FROM OIL SANDS TAILINGS POND WATER IN A - 24 °C ENVIRONMENT.	192
FIGURE 6-38	VARIATION OF THE NORMALIZED Cl^- CONCENTRATION IN THE SEQUENTIAL MELTWATER SAMPLES OF THE SPRAY ICE MADE FROM TAP WATER (THE SPRAY ICE WAS OBTAINED IN A - 24 °C ENVIRONMENT)	194
FIGURE 6-39	VARIATION OF THE NORMALIZED SO_4^{2-} CONCENTRATION IN THE SEQUENTIAL MELTWATER SAMPLES OF THE SPRAY ICE MADE FROM TAP WATER (THE SPRAY ICE WAS OBTAINED IN A - 24 °C ENVIRONMENT)	194
FIGURE 6-40	VARIATION OF THE NORMALIZED IONIC STRENGTH (CONDUCTIVITY) IN THE SEQUENTIAL MELTWATER SAMPLES OF THE SPRAY ICE MADE FROM TAP WATER (THE SPRAY ICE WAS OBTAINED IN A - 24 °C ENVIRONMENT)	195
FIGURE 6-41	VARIATION OF THE NORMALIZED PH IN THE SEQUENTIAL MELTWATER SAMPLES OF THE SPRAY ICE MADE FROM TAP WATER (THE SPRAY ICE WAS OBTAINED IN A - 24 °C ENVIRONMENT)	195
FIGURE 6-42	VARIATION OF THE CONCENTRATION RATIOS OF THE SELECTED INORGANIC CONTAMINANTS VERSUS MELTWATER VOLUME FOR THE 20-DAY OLD SPRAY ICE MADE FROM TAP WATER IN A - 24 °C ENVIRONMENT.....	196
FIGURE 6-43	VARIATION OF THE CONCENTRATION RATIOS OF THE SELECTED INORGANIC CONTAMINANTS VERSUS MELTWATER VOLUME FOR THE 40-DAY OLD SPRAY ICE MADE FROM TAP WATER IN A - 24 °C ENVIRONMENT.....	196
FIGURE 6-44	EC_{50} VALUES (%) OF THE MELTWATER SAMPLES (PH-ADJUSTED AND FILTERED) VERSUS THE CUMULATIVE MELTWATER VOLUME (%) FOR THE SPRAY ICE OF OIL SANDS TAILINGS POND WATER (SPRAY ICE WAS OBTAINED AT - 24 °C)	207
FIGURE 6-45	PREDICTED AND MEASURED MELTWATER TOC CONCENTRATION RATIO FOR THE SPRAY ICE MADE FROM PULP MILL EFFLUENT (SPRAY ICE WAS OBTAINED AT - 24 °C AND STORED FOR 40 DAYS).	211

FIGURE 6-46	PREDICTED AND MEASURED MELTWATER CONDUCTIVITY RATIO FOR THE SPRAY ICE MADE FROM PULP MILL EFFLUENT (SPRAY ICE WAS OBTAINED AT - 24 °C AND STORED FOR 40 DAYS).	211
FIGURE 6-47	PREDICTED AND MEASURED MELTWATER TOC CONCENTRATION RATIO FOR THE SPRAY ICE MADE FROM OIL SANDS TAILING POND WATER (SPRAY ICE WAS OBTAINED AT - 10 °C AND STORED FOR 20 DAYS).	212
FIGURE 6-48	PREDICTED AND MEASURED MELTWATER CONDUCTIVITY RATIO FOR THE SPRAY ICE MADE FROM OIL SANDS TAILINGS POND WATER (SPRAY ICE WAS OBTAINED AT - 10 °C AND STORED FOR 20 DAYS).	212

LIST OF TABLES

TABLE 3-1 LIST OF T_{90} 'S OF DIFFERENT WATER SAMPLES	36
TABLE 3-2 THE T_{90} 'S OF THE WASTEWATER DROPS WITH DIFFERENT PH.....	41
TABLE 4-1 THE FREEZING TIME REQUIRED FOR PIGGERY WASTEWATER DROPS	85
TABLE 4-2 THE FREEZING TIME REQUIRED FOR PULP MILL EFFLUENT DROPS	86
TABLE 4-3 THE FREEZING TIME REQUIRED FOR OIL SANDS TAILINGS POND WATER DROPS.....	88
TABLE 4-4-A THE ESTIMATED FREEZING TEMPERATURE OF PULP MILL EFFLUENT DROPS ..	102
TABLE 4-4-B THE ESTIMATED FREEZING TEMPERATURE OF OIL SANDS TAILINGS POND WATER DROPS	103
TABLE 4-4-C THE ESTIMATED FREEZING TEMPERATURE OF PIGGERY WASTEWATER DROPS	103
TABLE 6-1 SUMMARY OF SAMPLE ANALYTICAL METHODS	148
TABLE 6-2 COMPARISON OF THE SOURCE WATER AND THE RUNOFF IMPURITY CONCENTRATIONS	150
TABLE 6-3 IMPURITY CONCENTRATIONS OF THE SPRAY ICE CORES OF PULP MILL EFFLUENT.....	152
TABLE 6-4 IMPURITY CONCENTRATIONS OF THE SPRAY ICE CORES OF OIL SANDS TAILINGS POND WATER.....	153
TABLE 6-5 PH VALUES OF VARIOUS PULP MILL EFFLUENT SAMPLES COLLECTED	160
TABLE 6-6 PERCENTAGE OF THE TOTAL AMOUNT OF THE IMPURITY REMOVED FROM THE SPRAY ICE OF PULP MILL EFFLUENT BY THE FIRST 30% OF MELTWATER.....	161

TABLE 6-7	COMPARISON OF pH VALUES OF VARIOUS OIL SANDS TAILINGS POND WATER SAMPLES COLLECTED (AIR TEMPERATURE = - 10 °C WHEN SPRAY FREEZING TESTED WAS CONDUCTED).....	167
TABLE 6-8	PERCENTAGE OF THE TOTAL AMOUNT OF THE IMPURITY REMOVED FROM THE SPRAY ICE OF OIL SANDS TAILINGS POND WATER BY THE FIRST 30% OF MELTWATER	168
TABLE 6-9	THE PERCENTAGE OF THE TOTAL AMOUNT OF INORGANIC COMPONENTS IN THE SPRAY ICE PREPARED FROM TAP WATER RELEASED WITH FIRST 30% OF THE MELTWATER	177
TABLE 6-10	PERCENTAGE OF THE TOTAL AMOUNT OF THE IMPURITY REMOVED FROM THE PULP MILL EFFLUENT SPRAY ICE OBTAINED AT - 24 °C AIR TEMPERATURE BY THE FIRST 30% OF MELTWATER	181
TABLE 6-11	PERCENTAGE OF THE TOTAL AMOUNT OF THE IMPURITY REMOVED FROM THE SPRAY ICE OF OIL SANDS TAILINGS POND WATER BY THE FIRST 30% OF MELTWATER (SPRAY ICE WAS OBTAINED IN A - 24 °C ENVIRONMENT)	193
TABLE 6-12	COMPARISON OF IMPURITY REMOVAL EFFICIENCY BY THE SPRAY FREEZING PROCESS CONDUCTED AT DIFFERENT AMBIENT AIR TEMPERATURES (PULP MILL EFFLUENT, THE SPRAY ICE WAS STORED IN THE COLD ROOMS FOR 20 DAYS).....	200
TABLE 6-13	COMPARISON OF IMPURITY REMOVAL EFFICIENCY BY THE SPRAY FREEZING PROCESS CONDUCTED AT DIFFERENT AMBIENT AIR TEMPERATURES (PULP MILL EFFLUENT, THE SPRAY ICE WAS STORED IN THE COLD ROOMS FOR 40 DAYS)	201
TABLE 6-14	COMPARISON OF IMPURITY REMOVAL EFFICIENCY BY THE SPRAY FREEZING PROCESS ONDUCTED AT DIFFERENT AMBIENT AIR TEMPERATURES (OIL SANDS TAILINGS POND WATER, THE SPRAY ICE WAS STORED IN THE COLD ROOMS FOR 20 DAYS)	202

TABLE 6-15	COMPARISON OF IMPURITY REMOVAL EFFICIENCY BY THE SPRAY FREEZING PROCESS CONDUCTED AT DIFFERENT AMBIENT AIR TEMPERATURES (OIL SANDS TAILINGS POND WATER, THE SPRAY ICE WAS STORED IN THE COLD ROOMS FOR 40 DAYS)	203
TABLE 6-16	COEFFICIENTS OF THE MELTWATER IMPURITY CONCENTRATION PREDICTION MODELS FOR PULP MILL EFFLUENT	213
TABLE 6-17	COEFFICIENTS OF THE MELTWATER IMPURITY CONCENTRATION PREDICTION MODELS FOR OIL SANDS TAILINGS POND WATER	214

CHAPTER 1 INTRODUCTION

For some industries located in cold regions, selection of an effective wastewater treatment method is restricted by technical, economical or both reasons due to the cold climate and the wastewater volume. Government regulations have also forced industries to search for better methods for the processing, discharge or reuse of their wastewater. A technically and economically achievable treatment method which can be easily applied in the cold regions is needed. Natural freezing technology could be the one method that provides a practical treatment alternative for some industrial wastewaters.

The spray freezing process is a modified natural freezing process, which utilizes natural winter conditions to concentrate contaminants and remove them by the unfrozen water during the freezing process, then use warm spring air temperatures to melt the spray ice mound. Impurities in the spray ice mound are concentrated and discharged with first meltwater, leaving a purified ice mound for the later spring melt. Wastewater can be purified by these two stages of impurity removal. The advantages of the spray freezing process over other freezing techniques are its accelerated freezing rate, simple operation and low capital and operating cost. Although some applications were found, no research information was found on using spray freezing technology to treat industrial wastewater.

In the spray freezing process, wastewater is atomized through a nozzle and sprayed into atmosphere. Formation of spray ice is a complicated dynamic and thermodynamic process which involves ice nucleation, heat and mass transfer processes. The meltwater impurity concentration of a ice column is influenced by many factors such

as the distribution of impurities within and on ice crystals and within the ice column. water flow in the column, and melt-freeze cycles which are directly related to the weather conditions.

The objectives of this study were to evaluate the spray freezing process as a treatment alternative for industrial wastewater, to gain qualitative and quantitative understanding of the ice nucleation in wastewater drops, the freezing behavior. the cooling rate and ice formation of a freely suspended wastewater drop as well as impurity rejection and concentration phenomena which occur during freezing and melting processes.

The research discussed in this thesis can be divided into three distinct phases. The initial research phase involved ice nucleation in water drops (Chapter 2 and Chapter 3). The literature review of the ice nucleation theory and experimental studies of heterogeneous nucleation are presented in Chapter 2. A group of experiments were conducted to investigate the freezing characteristics of piggery wastewater, pulp mill effluent and oil sands tailings pond water droplets (Chapter 3). The freezing ability of these three types of industrial wastewaters was determined by quantitative evaluation of the ice nuclei concentrations in the wastewater. The effect of droplet volume, impurity concentration and pH on the droplet freezing temperatures was also determined.

The second phase of the research was to examine freezing behavior of freely suspended wastewater droplets. The behavior of a freely suspended wastewater droplet during freezing was studied in a small vertical wind tunnel. The experimental findings and results obtained from the suspended wastewater droplet tests are given in Chapter 4. The cooling rate, ice nucleation temperature as well as ice production rate of a freely suspended wastewater droplet were also determined based on the heat and mass transfer theory and experimental data under various experimental conditions.

The final phase of the research included theoretical and experimental studies of the impurity separation and concentration during the freezing and melting process (Chapters 5 and 6). The fundamentals of impurity rejection during the freezing process are reviewed in Chapter 5. An impurity removal hypothesis for the spray freezing process was proposed and a mathematical model was developed to predict spray ice impurity concentrations based on the impurity rejection theory. Treatability of pulp mill effluent and oil sands tailings pond water by spray freezing process was evaluated by an experimental study. Fractionation of impurities during the melting of spray ice columns was examined in detail. The impurity removal efficiency was determined for the spray ice formed under different spraying and storage conditions. Chapter 6 presents the experimental results of this test. Two empirical models which could be used to estimate the meltwater impurity concentrations were obtained from the relationship between the cumulative meltwater discharge and the impurity release from the melting ice column.

Chapter 7 summarizes the findings of this research and the final chapter (Chapter 8) gives the recommendations for future research.

CHAPTER 2 ICE NUCLEATION IN LIQUID WATER

All three phases of water are in the stable equilibrium at 0 °C and 101.32 kPa. Ice may form either by deposition from the vapor phase or by the freezing of liquid water. Phase changes are associated with the changes of the internal energy of the substance, i.e. the amount of release or uptake of heat which is called the latent heat of phase changes. When a liquid is supercooled it is energetically favorable for it to change to solid phase (ice).

2.1 Homogeneous Nucleation

A small water droplet can be cooled well below its equilibrium temperature: it does not immediately freeze but remains for some time in a metastable supercooled state although it is impossible to cool large quantities of liquid water such as in a lake or pond far below 0 °C. Initiation of the phase transition from water to ice occurs by the nucleation of a small ice embryo. Homogeneous nucleation of ice occurs in pure liquid water which is deeply supercooled. Extremely pure water can be supercooled to near - 40 °C before homogeneous nucleation appears (Hobbs, 1974). There are always random fluctuations in structure which provoke microscopic variations in such quantities as density, temperature, and pressure in supercooled water (Frenkel, 1946). These fluctuations are caused by the continual formation and disintegration of small embryos of ice – small groups of water molecules becoming locked by change to ice-like configurations within the liquid phase. However, when the embryo is small, it is in an energetically unfavorable state because of its very large surface to volume ratio and the additional energy required with the creation of new interface with the liquid. There is

thus a free energy barrier to be overcome before freezing can commence and this barrier can only be surmounted by a nucleation process which depends upon thermal fluctuations (Fletcher, 1970). The average size of the embryo increases with increased supercooling. When an ice embryo reaches a critical size, the probability of growth equals to the probability of dissipation. Once an ice embryo exceeds the critical size, growth becomes energetically favorable. Addition of further molecules lowers the total free energy of the system and the embryo can grow into a macroscopic ice crystal at very high rate. Therefore, homogeneous nucleation of ice in liquid water is intrinsically probabilistic, with the probability of occurrence depending on the nature of the molecular interactions in the parent phase and in the embryos, and it also depends on external variables such as temperature and sample size (Götz et al., 1991). The free energy of formation of ice embryos can be estimated using a thermodynamic approach that assumes that the ice water interface is a sharp one. If an embryo has a spherical shape, then the critical free energy and critical embryo radius can be calculated by following equation (Fletcher, 1970):

$$\Delta G^* = \frac{16\pi\sigma_{sl}^3}{3(\Delta G_v)^2} \quad \text{and} \quad (2.1)$$

$$r^* = \frac{-2\sigma_{sl}}{\Delta G_v} \quad (2.2)$$

where:

ΔG^* = the critical (or maximum) free energy difference per unit volume between ice and water

ΔG_v = the free energy difference per unit volume between ice and water

σ_{sl} = the solid-liquid interfacial energy

r^* = the critical embryo radius

The rate of homogeneous freezing nucleation J , or the number of critical embryos forming per unit time and per unit volume is expressed as (Götz et al., 1991):

$$J = K \exp \frac{-\Delta G^*}{k_B T} \text{ m}^{-3} \text{ s}^{-1} \quad (2.3)$$

where:

J = the homogeneous freezing nucleation rate, $\text{m}^{-3} \text{s}^{-1}$

ΔG^* = the energy of formation of a critical size embryo, J

T = temperature, K

k_B = Boltzmann's constant = $1.381 \times 10^{-23} \text{ J K}^{-1}$, and

K = the rate of addition of molecules to the (sub-critical size) embryo, $\text{m}^{-3} \text{s}^{-1}$

It was found that the pre-exponential factor K has a numerical value in the range of 10^{32} to 10^{38} depending on the form and numerical inputs to the calculations (Götz et al., 1991).

2.2 Heterogeneous Nucleation

If an ice embryo grows closely upon a foreign particle, the nucleation process is called heterogeneous. In heterogeneous nucleation less supercooling is required for an embryo to reach critical size because of the smaller values of the free energy difference which is associated with the formation of the embryo. The same concepts used in homogeneous nucleation can be applied to heterogeneous nucleation with modifications that account for the influence of the substrate, the foreign particle, on which the embryo

develops. Fletcher (1970) developed the macroscopic theory for the heterogeneous nucleation of ice. Without considering the details of the microscopic mechanisms involved in nucleation, the theory includes these effects in an adjustable macroscopic parameter, m , a contact angle parameter. The shape of an ice embryo growing on a foreign particle of arbitrary size and the shape is defined by the contact angle, the cosine of which is related to the interfacial energies of the three types of contacts (solid/liquid, solid/particle, particle/liquid) between substances:

$$m = \frac{\sigma_{pl} - \sigma_{sp}}{\sigma_{sl}} = \cos \theta \quad (2.4)$$

where σ is the interfacial energy and the subscripts p , s , and l refer to the particle, solid and liquid, respectively. θ is the angle of contact between the ice embryo and the particle. m is in the range of -1 for a surface incompatible with ice to +1 for a surface which 'wet' by ice.

The free energy to grow an ice embryo on the surface of a particle with characteristic dimensions R is:

$$\Delta G_H^* = \Delta G^* f(m, R) \quad (2.5)$$

where ΔG^* is the energy of formation of a critical size embryo in homogeneous nucleation as given by equation (1.3), $f(m, R)$ is the geometrical factor, which is always less than unity. If the nucleation particle is a sphere of radius R and the ice embryo grows on it as a spherical cap, Fletcher (1958) indicated that:

$$f(m, R) = \frac{1}{2} \left\{ 1 + \left[\frac{1 - mx}{h} \right]^3 + x^3 \left[2 - 3 \left(\frac{x - m}{h} \right) + \left(\frac{x - m}{h} \right)^3 \right] + 3mx^2 \left[\frac{x - m}{h} - 1 \right] \right\} \quad (2.6)$$

where: $h = (1 + x^2 - 2mx)^{1/2}$, and $x = R / r^*$ (2.7)

r^* is the critical embryo radius in homogeneous nucleation, given by equation (2.2). For a spherical particle of radius R (m), the nucleation rate per particle is (Fletcher, 1970):

$$J \sim 10^{20} R^2 \exp\left(-\frac{\Delta G_H^*}{k_B T}\right) \text{ s}^{-1} \quad (2.8)$$

The pre-exponential factor is smaller than that in homogeneous nucleation (K in equation 2.3) by a factor of 10^7 . However, the theory has a number of fundamental limitations, as indicated by Fletcher (1970). The most important limitation is that the theory neglects the phenomena on a molecular level and the treatment of m as a simple parameter characterizing all surfaces of the nucleating particle.

2.2.1 Hypothesis of heterogeneous ice nucleation in water droplets

It is known that a collection of macroscopically identical drops of a particular type of water or solution do not freeze at a single temperature but over a range of temperatures. For any phase change caused by a statistical event, there exist a

relationship between the probability of nucleation, the volume of the unstable phase, and the duration and degree of the supercooling. Several hypothesis have been suggested to explain the heterogeneous nucleation of freezing in water droplets.

2.2.1.1 Stochastic (statistical) model

The stochastic theory assumes that if a sample of supercooled drops with the same origin and volume are observed in an experiment, then, at any given instant all the drops have the same probability of freezing if all the drops have the same nucleus content. Similar to homogeneous nucleation, in this case, the nucleation process is controlled by molecular kinetics i.e. the critical ice embryo size is reached by random fluctuations and the nature of the nucleating sites induced by impurities (foreign particles) produces only negligible variations within a given sample. Bigg (1953) explained the phenomena of the volume dependence and the time dependence of freezing temperatures in his experiments by the assumption that the probability of freezing per unit time (P) is proportional to the volume of drops and increases exponentially with decreasing temperature at a steady cooling rate:

$$P = \frac{1}{N} \frac{dN}{dt} = BVe^{\frac{T}{\tau}} \quad (2.9)$$

where B and τ are constants, V is the volume of droplets, T is the temperature (always a negative value), t is time and N is the number of drops that are still unfrozen at temperature T. The stochastic model predicts that at a constant temperature freezing events should occur continually, with higher frequency as the temperature is lowered. If

the cooling rate $\alpha = -dT/dt = \text{constant}$, the probability of freezing per degree decrease in temperature is:

$$P(T) = -\frac{1}{N} \frac{dN}{dT} = \frac{BV}{\alpha} e^{-\frac{T}{\tau}} \quad (2.10)$$

Integration of equation (2.10) with boundary condition $N = N_0$ at $t = 0$, yields

$$\ln\left(-\ln \frac{N}{N_0}\right) = \ln \frac{BV\tau}{\alpha} - \frac{T}{\tau} \quad (2.11)$$

provided $e^{-T/\tau} \gg 1$ ($T < -5^\circ\text{C}$). Therefore, equation (2.10) predicts a linear relationship between $\ln[-\ln(N/N_0)]$ and the temperature T .

2.2.1.2 Singular hypothesis

An alternative model for the heterogeneous nucleation was presented by Levine (1950), and in a different form by Langham and Mason (1958) which is referred to as the Singular model. The basic assumptions of this hypothesis are that every impurity (nucleus) has a characteristic temperature and a drop nucleates at a temperature determined by the most effective ice nucleus it happens to contain. Therefore, according to the singular model, no freezing events would occur at a fixed temperature, since heterogeneous nucleation only happens when the temperature of the droplets is lowered to

the characteristic temperatures of the impurities. The concentration of ice nuclei which become effective between 0 °C and T is given by

$$n(T) = n_o e^{-\frac{T}{\tau}} \quad (2.12)$$

where $n(T)$ is the concentration of ice nuclei that become effective at temperature between 0 °C and T °C , n_o and τ are constants. For a drop of volume V, if it contains a random distribution of ice nuclei, the probability that it will freeze on reaching temperature T is given by Poisson distribution:

$$P(T) = 1 - \frac{N}{N_o} = 1 - e^{-n(T)V} \quad (2.13)$$

so that,
$$N = N_o \exp[-n_o V \exp(-\frac{T}{\tau})] \quad (2.14)$$

or

$$\ln(-\ln \frac{N}{N_o}) = \ln(n_o V) - \frac{T}{\tau} \quad (2.15)$$

Let $B' = n_o / \tau$, then equation (2.15) can be rewritten as

$$\ln(-\ln \frac{N}{N_o}) = \ln(B' \tau V) - \frac{T}{\tau}$$

The difference between equation (2.11) and equation (2.15) is only the form of the constant.

Both the stochastic and singular hypotheses predict that the probability of freezing per degree fall in temperature increases exponentially with decreasing temperature. Stochastic hypothesis assumes that the probability of freezing is dependent on temperature only, while in the singular theory, it is assumed that the number of ice nuclei increases exponentially with decreasing characteristic temperature so it is independent of the cooling rate.

2.2.1.3 Differential and cumulative nucleus concentrations

Vali and Stansbury (1966) investigated the relative importance of kinetic effects and nucleus content on the heterogeneous nucleation of a drop. They found that their experimental results were inconsistent with both stochastic and singular hypotheses and they concluded that probability of freezing a drop depends on the properties of the nucleating site as well as on the random fluctuations. They deduced that the probability of a drop freezing at temperature T and time t can be written as

$$P(T, t) = \int P_1(T, T_c) P_2(T_c, t) dT_c \quad (2.16)$$

where T_c values are the characteristic temperatures of the nuclei. The probability function P_1 defines the chance of nuclei becoming active within a unit time interval at temperatures other than their particular characteristic temperatures. The function P_2 represents the number of nuclei which at time t have not yet become active. Vali (1971) indicated that the singular model is equivalent to replacing $P_1(T, T_c)$ in equation (2.16) by a Dirac δ -function at $T = T_c$. The time-dependence in P_2 can then be omitted so that the probability of freezing, $P(T)$ is determined only by the distribution of characteristic temperatures for the nuclei.

In order to quantitatively evaluate the ice nucleus content of water droplets from a nucleation experiment, Vali (1971) developed a differential and a cumulative nucleus spectrum, the concentration vs. temperature functions. The singular approximation that each particular freezing nucleus becomes active at its characteristic temperature independently of the rate of change of temperature was used in the derivation of the spectra.

Differential nucleus spectra. A function $k(T)$ which describes the concentrations of nuclei active in a unit volume of sample within $\pm 1^\circ\text{C}$ of the temperature T needs to be derived from the droplet freezing temperatures obtained from droplet freezing tests. With the definition of $k(T)$, the average number of nuclei \bar{n} which are active within a unit temperature interval of T in a drop of volume V is then

$$\bar{n}(T) = k(T)V \quad (2.17)$$

The number of nuclei per drop active between T and $(T-dT)$ is equal to

$$\bar{n}(T)dT = k(T)VdT \quad (2.18)$$

If $\bar{n}(T)dT$ is less than 1, equation (2.18) represents the probability that a given drop will contain a nucleus active in the specified temperature interval.

Setting a total of N_0 drops observed in an experiment, then $N(T)$ is the number of drops that are still unfrozen at temperature T . The number of drops frozen at T would be $N_0 - N(T)$. As temperature is decreased to $(T-dT)$, dN more drops may freeze. Then, $dN/N(T)$ is the fraction of unfrozen drops nucleated within this interval and it is the probability of freezing, $P_d(T)$, for one of the unfrozen drops:

$$P_d(T) = \frac{dN}{N(T)} \quad (2.19)$$

The quantities on the right-hand side of above equation can be determined in an experiment.

The chance of finding a nucleus active between T and $(T-dT)$ in any one of the original number (N_0) of drops can also be represented by $P_d(T)$ because the chance allocations of the various nuclei of different activities into the drops are independent of one another. Therefore, the drops that change phase at temperatures above T have the same opportunity to contain nuclei active between T and $(T-dT)$ as the other drops which did not contain nuclei active above T . Hence, although equation (2.19) is derived from observations on the N unfrozen drops, it can be equated to the probability of containing a nucleus in any one of the N_0 drops tested as given by equation (2.18), namely:

$$\frac{dN}{N(T)} = k(T)VdT \quad (2.20)$$

so $k(T)$, the differential nucleus concentration is:

$$k(T) = \frac{1}{VN(T)} \frac{dN}{dT} \quad \text{m}^{-3} \text{ } ^\circ\text{C}^{-1} \quad (2.21)$$

Without some modifications, equation (2.21) can not be used in practice since in an experiment with a finite number of drops, temperature intervals have to be sufficiently large to yield appreciable numbers of freezing events ΔN . After some modifications, Vali (1971) gave the finite-difference form of $k(T)$ as follow:

$$k(T) = -\frac{1}{V\Delta T} \ln\left(1 - \frac{\Delta N}{N(T)}\right) \quad (2.22)$$

and

$$N(T) = N_o - \sum \Delta N \quad (2.23)$$

The differential nucleus concentration, $k(T)$ can be calculated using equation (2.22) from the observed number of frozen drops in each temperature interval.

Cumulative nucleus concentration. The differential nucleus concentration $k(T)$ describes the concentration of nuclei active at a specific temperature. By integrating equation (2.21) from 0 °C to T, the cumulative nucleus concentration, $K(T)$ can be obtained:

$$K(T) = \frac{\ln N_o - \ln(N_o - N)}{V} \text{ m}^{-3} \quad (2.24)$$

Equation (2.24) allows the calculation of the concentration of nuclei active at all temperatures warmer than T. The accuracy of above spectra was examined by Vali (1971) and the differential spectra were found to be reliable to within factors of 2 to 4. The cumulative spectra showed somewhat less scatter.

2.3 Literature Review of Experimental Studies of Heterogeneous Nucleation

Heterogeneous nucleation of ice is a very complex phenomenon. Scientists have studied heterogeneous nucleation for several hundred years to understand the exact nature of heterogeneous nucleation. Numerous experimental investigations have been conducted with different methods and conditions to search for effective ice nucleating materials. In spite of the intensive efforts, heterogeneous ice nucleation is still poorly understood. Observation and theories which were derived mainly from the thermodynamic treatment of homogeneous nucleation have not yet been matched with any generality (Götz et al., 1991). A literature review of some of the experimental studies related to this research is presented below.

2.3.1 Ice nucleating materials and their influences

Current theories of ice nucleation suggest that almost any substance which causes some ordering in liquid water should result in a higher nucleation temperature. Ice nucleating materials range from minerals to alkali halides to metal oxide and a variety of organic compounds. Some bacteria can serve to nucleate ice on their surface, or in them at just a few degrees of supercooling and some organism have special strategies for preventing ice nucleation.

Vonnegut (1947) chose AgI in his experiment as an ice nucleate to be used in weather modification based on the fact that AgI has a hexagonal crystal structure differing from that of ice by only a few percent in the spacing of atoms. The threshold temperature at which a particle of AgI can cause ice to form is -2.6°C (Fukuta, 1958).

Fukuta (1958) measured the ice nucleating ability of a large number of materials dispersed as smokes or powders into a thermostat type cloud chamber. Seventy eight chemicals were found to be effective as ice nuclei at temperatures above -20°C . Fukuta concluded based on his experimental results that water-insoluble substances, materials with the greatest structural similarity to ice and stronger ionic nature are highly effective nuclei.

Mason and Maybank (1958) reported the threshold temperature of twenty-eight minerals; covellite (CuS) with a freezing threshold of -5°C is the most active ice nucleus among the materials tested. Roberts and Hallett (1968) conducted a laboratory study of the ice nucleating properties of some mineral particles. They found that for initial ice nucleation water saturation was necessary, but below a critical temperature a constant ice supersaturation (water subsaturation) was sufficient, i.e. nucleation would occur directly from the vapor phase.

Bryant et al. (1959) conducted a detailed study of 10 inorganic substances and found AgI, PbI₂ and CuS as being the most effective nucleating substances having threshold temperature of -4 °C, -6 °C and -6 °C, respectively.

Phloroglucinol is the first organic ice nucleating material discovered (Bashkirova and Krasikov, 1957). It was found to have a threshold temperature of -8 °C. Phloroglucinol was further tested by Langer et al. (1963). Phloroglucino acted after 10 seconds at -2 °C to give easily noticeable crystals in a deepfreeze chamber. Head (1961) discovered that 7 out of 30 steroid compounds he tested were almost as effective as silver iodide. Komabayasi and Ikebe (1961) studied a number of aromatic compounds including sucrose, naphthalene, pyrogalllic acid, anthraquinone, phthalic acid and terephthalic acid by introducing the finely powdered material into a supercooled cloud, allowing the ice crystals to form and fall into a tray of supercooled sugar solution and measuring the highest temperature at which 1 particle in 10⁴ produced an ice crystal. Apart from the last four compounds, which were active at -16 °C, others did not show significant activity. Power and Power (1962), Barthakur and Maybank (1963), Fukuta and Mason (1963), Evans (1966) and Parungo and Lodge (1967a) all studied the nucleation of freezing and supercooling drops by various amino acids. Power and Power (1962) reported the following amino-acids to be active at temperatures above -10 °C: l-leucine at -4.5 °C, l-tryptophane at -5.5 °C, d-l-aspartic acid at -6 °C and d-l-alanine at -7 °C. Barthakur and Maybank (1963) found that racemic variety of amino acids was less effective than the optically active type. Based on his experimental results, Evans (1966) indicated that d-valine was more active when immersed in supercooled water than in a cloud chamber.

The nucleation of ice on well defined faces of single-crystalline substrates (some organic crystals) under controlled environmental conditions was studied by Fukuta and Mason (1963). The organic substances tested had lattice dimensions quite different from that of ice but ice crystals grew with uniform orientations and the nucleation temperatures were only a few degrees below 0 °C. The researchers suggested that the arrangements of

the hydrogen-bonding groups on the compound surfaces determined the nucleating abilities of these crystals. Ice crystals appeared preferentially at steps and cracks on the surface where OH groups were likely to be exposed. Parungo and Lodge (1965) investigated the ice nucleating ability of a series of substituted phenols and benzoic acids. Reactivity was found to vary with the potential strength of a hydrogen bond between the hydroxyl or carboxyl group and a water molecule, therefore, there may be a free-energy relationship between molecular structure and nucleating power.

Fukuta (1965, 1966) discovered from his experimental study that ice nucleation ability of some organic compounds might be further enhanced by spraying solutions of these materials in suitable organic solvents. The enhancement was caused by the evaporative cooling of the solvent. However, the nucleation ability of organic substances was found to be affected by the method of preparation; particles prepared by condensation were less active and when crystals were freshly ground, the ice nucleation above -5°C was no longer uncommon. Nucleation by contact of some organic particles with supercooled water drops occurred at temperatures 2 to 3°C warmer than those when the same drops were melted and re-frozen with the nuclei already partly immersed (Fukuta, 1975). This was likely due to the movement of the water front along the surface of the nucleus during the contact process. Fletcher (1972) tested over 1000 organic materials in a contact-nucleation experiment at -3°C and only 47 were considered as active. Fletcher pointed out that ice nucleation occurred on the most active site on a substance: less active sites or impurities mainly served to dilute the proportions of active sites. Therefore, "inactive" insoluble impurities only had little effect on the ice nucleation. Since soluble impurities could change the nature of water and thus would affect the ice nucleation process.

Urea has unusual ice nucleation properties. Due to the high endothermic heat of solution and the high solubility of urea, when it dissolves in water this organic causes a local cooling which enables it to become an active ice nucleant even when ambient temperature is as high as $+6^{\circ}\text{C}$ (Knollenberg, 1966, 1969a). Any soluble compound with

an endothermic heat of solution produces a local cooling during dissolution. The amount of cooling produced during the dissolution of a microscopic particle varies with soluble compounds and variations in local cooling will result in corresponding changes in ice nucleation activity. Knollenberg (1969b) developed a local cooling ice nucleation model. The model showed that the amount of local cooling was controlled by the heat and mass transfer processes in the boundary layer immediately adjacent to dissolving ice nucleus: local cooling was a function of the particle dissolution rate which could change markedly with the experimental technique.

Natural ice-forming nuclei in aerosol particles in Colorado and Montana, U.S.A. were found to be mostly clay particles (Rosinski et al., 1976). According to the study, at -12 °C feldspar-like and illite-like particles were predominant in nucleating ice while montmorillonite contributed substantially to the ice-nucleus population between -19 °C and -20 °C. It was also found that a large number of particles which exhibit ice-nucleating properties are the clay particles presumably with nucleating sites containing silver iodide, copper compounds, etc. Ice nucleating ability of rare earth oxides was found to be moderate (Matsubra, 1973).

Ice nucleation rate was determined by freezing droplets of distilled water either unseeded or seeded with aerosol dust (Stoyanova et al. 1994). Water drops were placed on thin polyethylene foil adhering to a thick cooling metal plate. A TV camera was used for the observation of the freezing process of droplets through a heat insulating window. The experimental data indicated that ice nucleation in unseeded distilled water was heterogeneous and was controlled by only one type of active center while in seeded water nucleation was stimulated by three types of active centers introduced by aerosol dust. One of the three activities was close to that of unseeded water. The type of the active center is determined by the effective specific surface energy, activity factor and wetting angle.

Researchers (e.g. Soulage, 1958; Telford, 1960a; Serpolay, 1958, 1959; Mason and Van den Heuvel, 1959 and many others) have confirmed that many metallic oxides such as those of iron, copper, aluminum, manganese, nickel as well as smokes from domestic and most industrial fires are able to act as ice nuclei. The threshold temperature of some of these materials is as high as -6°C .

Some bacteria were found to have the ability to nucleate ice at warm temperature (warmer than -5°C) in natural habitats such as atmosphere, soil, water and decaying vegetable matter (Schnell and Vali, 1976). All identified ice nucleation active (INA) bacteria are known plant epiphytes and potential pathogens such as *Pseudomonas syringae* and *Erwinia herbicola* that cause plant diseases having nothing to do with freezing (Levin and Yankofsky, 1988). The surfaces of frost sensitive plants usually have high concentrations of INA bacteria but the atmosphere is quite low in biogenic nuclei. In order to improve the quality of manufactured snow in ski resorts dead bacterial cells have been used extensively as artificial ice nuclei. It is believed that the ice nuclei of INA bacteria are functionally heterogeneous structures bound to the cells themselves.

2.3.2 Some factors affecting freezing of water drops

The influence of nucleating materials and the influences induced by them, such as substrate surface and surface irregularities on the formation of ice embryos is on the molecular scale, i.e. embryos themselves. According to the macroscopic theory of heterogeneous nucleation, the ice nucleation in a supercooled water drop is also affected by the impurity content of the drop, the volume of the drop, the rate of cooling and some other factors.

2.3.2.1 Drop volume

The results of many experiments on the freezing of water drops indicated that there is a logarithmic relation between the droplet volume and the mean freezing

temperature. Dorsch and Hacker (1950) froze large numbers of drops on metal surfaces. The average freezing temperature for groups of drops showed that there is a linear relationship between the average freezing temperature and the logarithm of the drop diameter. Bigg (1953) confirmed this relationship and found that for drops with diameters greater than about 30 μm , the relationship of drop volume and freezing temperature could be represented by the equation:

$$\ln\left(\frac{1}{V}\right) = aT_s + b \quad (2.25)$$

where: V is the volume of the drop, T_s , the temperature below which 50% of the drops was frozen, a and b are constants for particular sample of water used.

2.3.2.2 *Cooling rate*

Heverly (1949) studied the freezing of water drops and diluted aqueous solutions. The diameters of the drops ranged from 50 μm to 1.1 mm and the cooling rates from 1 to 20 $^{\circ}\text{C}$ per minute. The drops were supported either on the tip of a fine thermocouple or on waxed paper in a cryostat. The freezing temperature appeared to be independent of the cooling rate.

Bigg (1953) observed the freezing to be dependent on the cooling rate. With a cooling rate of 0.05 $^{\circ}\text{C}/\text{min}$, he found that the median freezing point of 164 drops of 1 mm diameter to be - 21.8 $^{\circ}\text{C}$; this is 2 $^{\circ}\text{C}$ higher than the median freezing temperature for a cooling rate of 0.5 $^{\circ}\text{C}/\text{min}$. Gokhale (1965), Vali and Stansbury (1966) all found from their study that deeper supercooling is possible with higher cooling rates. However, Gokhale's results also showed that for cooling rates greater than 5 $^{\circ}\text{C}/\text{min}$ a reverse trend was indicated and the drops freeze at warmer temperatures.

2.3.2.3 Influence of aqueous solution on freezing temperature

The freezing temperature of water is influenced by the presence of salts in solution. Hevely (1949) conducted freezing experiment of droplets with quite dilute soluble salt solution. The differences were inconsequential between the freezing temperatures of the water used as a standard and the salt solution. But when Lafarque (1958) froze droplets of soluble salt solutions, he discovered that the freezing temperature was, in all cases, about 6 °C warmer than that of pure water. Determination of the freezing temperature of large numbers of 1-mm diameter drops of aqueous solutions of NaCl, $(\text{NH}_4)_2\text{SO}_4$, HNO_3 and HI over a wide range of concentrations was carried out by Bigg (1953; see also Mason, 1953,). He found that in freezing sodium chloride solution, the freezing temperature decreased with increasing solution concentration: the maximum change occurred from one-tenth saturation to fully-saturated solution. At moderate concentrations (molar fraction about 10^{-2} or less) NaCl had no significant effect while the other three electrolytes raised the mean freezing temperature. Hoffer (1961) carried out a laboratory investigation of droplet freezing. He used drops containing MgSO_4 with a diameter of 100 μm . Hoffer's experimental results was similar to Bigg's. De Pena et al. (1962) also tested the freezing characteristics of supercooled droplets of electrolytic solutions. Ethyl alcohol was also tested. For some solutions, freezing temperature increased with increasing concentration and some behaved the opposite way. Ethyl alcohol had no effect at any concentration between 10^{-2} and 1 molar. Pruppacher and Neiburger (1963) indicated that the higher freezing temperature of some solutions was caused by the introduction of insoluble foreign particles with the salts. When the solutions were filtered through millipore filters of 0.01 micron pore-size in their test, the freezing temperature of 2-mm diameter drops of all solutions investigated (solutions contain various halides, dextrose, surface active agents), decreased with increasing solution concentration. The freezing characteristics of rain water drops with different solutes was investigated by Murty and Murty (1972) under various temperatures. The experimental results revealed that sulfates present in rain drops accelerated the freezing

process and the effect became stronger with increasing concentration. On the contrary, chlorides, decelerated freezing process under most experimental conditions.

Although experimental studies have demonstrated that dissolved materials affect the freezing points of heterogeneous freezing nucleation, the reasons for this are not well understood (Reischel and Vali, 1974) because the effects were found to be specific to each nucleant tested, and were different from those reported for purified water. Based on their experimental results, Reischel and Vali (1974) concluded that the influence of dissolved salts on heterogeneous ice nucleation was not due to changes in the bulk water structure, but resulted from modifications at the nucleant-embryo interface.

2.3.2.4 The effect of pH on the ice nucleation

The influence of pH on the effectiveness of clay minerals, humic acid and humates, fulvic acid and fulvates, lead iodide and silver iodide as a freezing nucleus in the presence of various additives was carefully examined by Rosinski and Nagamoto (1972) in a laboratory study. The freezing temperature of water drops containing various additives depends on pH while the freezing temperatures of water suspensions of different minerals show little dependence on pH. The effectiveness of AgI as an ice nucleus was only slightly affected by pH, the acidic drops froze at slightly higher temperatures than natural or alkaline drops. However, the nucleating ability of PbI_2 which has a relatively high solubility was strongly affected by pH. The researchers indicated that pH should be considered in nucleation studies.

2.3.2.5 Atmospheric gases and freezing of supercooled water drops

Many gases react with water at low temperature to form hydrates (clathrates). Non-polar gases such as helium, neon, methane, propane etc. were used to test their influence on the freezing of water drops with volume of 0.006, 0.06, 0.1 mL (Parungo and Lodge, 1967a). It was found that the gases tested raised freezing temperature to

various levels and the effect was largest for the largest drop size. The authors considered it was caused mainly by loss of solute to the air in the cooling cup which would be greatest for smaller drops. Kuhns and Mason (1968) also found the dependence of the freezing temperature of small water drops (30 to 40 μm) on the nature of the environmental gas; when compared with air, carbon dioxide depressed the freezing temperature by 0.7 °C while argon raised the temperature by 0.5 °C and the differences could not be explained by experimental error. Interpreting their results, Kuhns and Mason suggested that the warmer temperature for argon might be caused by the formation of an argon clathrate which assisted in the formation of stable clusters in the supercooled water. Pena and De Pena (1970) examined the influence of different gases on the freezing of supercooled droplets. Their results were different from Parungo and Lodge's. Gases with very low solubility in water were found to have no effect or very small effect on the freezing of water droplets. Supercooling was increased when gases with higher solubilities were present, the increase in supercooling was greater when compared with that of dissolved gases. Based on their experimental results, Pena and De Pena concluded that the clathrate structure had an inhibiting effect on the freezing of supercooled water droplets. They thought that direct comparison of their results with Parungo and Lodge's could not be made due to the differences of the two experiments. In a more recent study, experiments were performed to determine the freezing temperatures of water saturated with argon or propane gas with artificial or natural nucleants (Reischel, 1984). He indicated that these clathrate forming gases affected heterogeneous freezing by modifying the nucleant-embryo interface not by changing the bulk water structure.

2.3.2.6 Effect of evaporation on the drop freezing temperature

The increased nucleation ability of supercooled drops under evaporation has been reported by some researchers (Murty and Murty, 1972a, and 1972b). In their work rainwater drops with size about 2 mm were frozen under simultaneous supercooling and evaporation or supercooling only. The fraction of drops frozen at certain time intervals for a given temperature was compared for the two experimental conditions used. It was

found that the supercooled drops, when subjected to evaporation, froze more rapidly than under supercooling alone although there was no noticeable difference in the final drop temperature. They indicated that the evaporation process was always accompanied by the dynamic effect, favoring increases in temperatures of ice nucleation by 4 to 5 °C; evaporation also influenced the time required for freezing of all the drop, especially, at warmer temperatures.

2.4 Summary

Heterogeneous nucleation is the most important process in ice formation in nature. Ice embryos grow on foreign particles in the water in heterogeneous nucleation. The presence of impurity nuclei usually limits the amount of supercooling that can be sustained in a liquid compared to homogeneous nucleation. Freezing is a very structured process highly influenced by chemical and particle variability. Therefore, a given sample has only a statistical probability of freezing at a particular temperature. Freezing is initiated at the nucleation temperature which is a function of the droplet size, the cooling rate and the nature of the ice nucleation materials. The detailed mechanism of heterogeneous nucleation is not well understood. For heterogeneous nucleation, the spread in the observed freezing temperature of water droplets has been shown to arise from the presence of ice nuclei of different activities in the sample. The freezing characteristics and the nucleus content of a liquid can only be determined by freezing experiments.

CHAPTER 3 FREEZING CHARACTERISTICS OF WASTEWATER DROPLETS

Spray freezing is a process which utilizes air temperatures below 0 °C to freeze a portion or all of a liquid solution by atomization of the liquid through a nozzle and spraying it into ambient air. The process involves heat and mass transfer and ice nucleation in response to the cold air. Knowledge of the ice nucleation in the sprayed water droplets is important for the design and the optimization of the spray freezing operation since the freezing characteristics of the sprayed liquid drops affect the operating temperature, the selection of the nozzle size as well as ice production rate. Wastewater which contains numerous soluble and insoluble substances has a different ice nucleation nature than pure water or rain water. Wastewater generated from different industries contain different components, therefore, they may not freeze at the same temperature. No studies have been reported on ice nucleation characteristics of industrial wastewaters.

An experimental study was conducted to determine the freezing ability of three types of industrial wastewaters and to quantitatively evaluate the concentrations of freezing nuclei in the wastewaters as well as the influences of drop volume, impurity concentration and pH on the drop freezing temperatures. The industrial wastewaters chosen for the study were oil sands tailings pond water (T.P.W.), pulp mill effluent and a piggery wastewater.

3.1 Characterization of the Industrial Wastewaters

“ Water pollutant ” is defined as any substance whose character and quantity can alter the natural quality of water so as to impair its usefulness or to render it to offensive to sense of sight, smell or taste. U.S. EPA broadly classified water pollutants into eight types (U.S. EPA, 1982; Springer, 1986): 1) oxygen-demanding substances as biological demand (BOD); 2) disease-causing agents as pathogenic microorganisms; 3) organic compounds as color, various toxicants and industrial chemicals; 4) plant nutrients as nitrogen and phosphorus; 5) inorganic chemicals and mineral substances as pH and heavy metals; 6) sediments as total suspended (TSS); 7) radioactive substances. and 8) thermal discharges. The general information about the major contaminants in the three types of wastewaters used in this study is given in the following section. “Impurity” , a term used in the studies of nucleation of ice includes anything in water that is not a water molecule. therefore, it has a much broader range including both water pollutants and those which are not considered as pollutant but may affect the formation of ice.

3.1.1 Characteristics of liquid swine waste

The characteristics of swine waste change with the physical plant, ration fed, manure management system and animal weight. The liquid pig manure usually contains high solid content, high concentrations of BOD, COD, and nutrients (N and P). The liquid waste also contains potassium, iron, manganese, calcium, sodium, magnesium, and some trace elements such as copper, zinc, arsenic and selenium. The concentrations of the trace elements in the liquid waste are influenced by the amount of these components in the feed (Priem and Maton, 1980). The majority of the total solids in the liquid pig waste is suspended volatile solids. According to Schmid and Lipper (1969), the volatile solids of raw swine waste averaged 80% of the total solids. The suspended solids were 79.5% of the total solids, although these were 84.1% volatile. More than 100 specific volatile compounds have been identified in solid, liquid pig manure, gases emitted from manure, and dust in the swine house. These compounds are end products and

intermediates of various biological reactions. Some researchers (Yasuhara and Fuwa, 1979; Hammond et al., 1974; Miner, 1982; Merkel et al., 1969; and Hartung et al., 1970) have concluded that phenols and carboxylic acids, amines, H₂S and organic sulfur compounds are probably the most noticeable contributors to the odors in swine houses.

3.1.2 Contaminants in Kraft pulp mill effluent

The principal pollutants in kraft pulp mill effluent are suspended solids, oxygen demanding substances, pH, color causing materials and toxic chemicals.

The suspended solids may contain fine bark particles and silt from the wood room, fibers and fiber particles from both the pulp making operations, coating and filling materials etc. Color in the effluent is from natural lignin, which binds the wood fibers together. Lignin and lignin derivatives are solublized and removed from the wood during the pulping process. The dissolved lignin is washed from the pulp. The wash water is highly colored and large amounts of color are ultimately discharged to the receiving water despite some treatment. The principle toxic chemicals of kraft pulping are resin acids (abietic, dehydroabietic, isopimaric, palustric, pimartie, sandaracopimaric, neoabietic) and unsaturated fatty acids (oleic, linoleic, linoenic and palmitoleic) (Spinger, 1986). Except resin acids and fatty acids unbleached pulp mill effluents also contain diterpene alcohols, soaps, sugars, aliphatic and aromatic hydrocarbons (Kringstad and Lindstrom, 1982; Crooks and Sikes, 1991). After bleaching, the effluents contain some chlorinated organic compounds. Organochlorines refer to the chlorine that is attached to a chlorinated organic molecule. The compositions of chlorinated organic compounds in bleached pulp mill effluents vary with raw wood materials used and operating conditions. It has been estimated that only about 10 to 40% of low molecular weight (MW < 1000 g/mol) chlorinated organic compounds in bleached pulp mill effluents have been characterized (Kringstad and Lindstrom, 1984; Leach and Thakore, 1975; McKague, 1988). To completely characterize effluents on the basis of individual substances is not practical, if not possible at this time. For instance, Kringstad and Lindström (1984) and Suntio et al.

(1988) discovered more than 250 chlorinated organic compounds in pulp and paper mill effluents and thousands of chemicals remained unknown regarding their physical-chemical characteristics. Therefore, generic tests such as Absorbable Organic Halogen (AOX) and Total Organic Halogens (TOX) have been used as indices of organochlorine concentrations in pulp and paper mill effluents and receiving waters. Some heavy metals may be present in these effluents although it is unlikely that toxic heavy metals reach critical levels (Springer, 1986). Alberta Environmental Protection has established permissible limits of manganese discharge for one pulp mill because of high concentrations of manganese can create a metal-like taste and laundry staining. Numerous studies have been conducted on the contaminants in pulp mill effluent and the problems associated with them by regulatory authorities and industry over last several decades, therefore, the detailed discussion will not be presented in this study.

3.1.3 Oil sands tailings pond water (T.P.W.)

The extraction of bitumen and its upgrading to produce synthetic crude oil from the oil sands deposits in Alberta requires the use of large volumes of process water. At Syncrude Canada Ltd., yearly extraction and upgrading operations require the use of about $110 \times 10^6 \text{ m}^3$ of water. This water requirement is met by importing about $34 \times 10^6 \text{ m}^3$ of water from the Athabasca River and the recycling and reuse of about $76 \times 10^6 \text{ m}^3$ of clarified water from the Mildred Lake settling basin which stores about $40 \times 10^6 \text{ m}^3$ of water. This requires that the water be recycled from the settling basin for use in the plant about 2 times each year.

According to a study conducted by Dearborn Chemical Company Ltd. (1991), the water in the settling basin (or pond) contains fine tails and other contaminants. The major contaminants are suspended and dissolved solids, oil and grease and COD causing matter. The dissolved solids are mainly inorganic substances such as sodium, chloride and sulfate. The wastewater is relatively soft with high bicarbonate concentration resulting from the caustic extraction process. High concentration of dissolved organic matter

(TDS) is another characteristic of this wastewater. The toxic organic matter present in the wastewater is carboxylic acids, specifically, 2,8-naphthenic acids which are the derivatives of cyclic hydrocarbons and exist naturally in oil sand. The presence of organic toxics in the tailings pond water is considered very likely because of the complex blend of organic materials exposed to the water during hot caustic extraction process. The organic contaminants in the tailings pond water include fish-flesh-tainting agents. The caustic extraction process and the recycling of the tailings pond water results in high concentrations of boron and fluoride. The water also contains certain amount of cyanide, some trace elements and heavy metals. Dearborn Chemical Company Ltd. (1991) indicated that there were no significant levels of priority pollutants (volatile, base-neutrals, acids, resin acids, PCB's, as listed in the MISA Effluent Monitoring Priority Pollutants List, 1987) in the raw tailings pond water. The reuse of the settling pond water results in the gradual increase in the organic and inorganic contaminant concentrations in this water. The gradual build-up of chloride in the recycle water has been identified as a potential problem for the continued future reuse of the water in the extraction process.

3.2 Experimental Procedures and Methodology

3.2.1 Wastewater Samples and Preparation

The piggery wastewater was collected from a pit inside of a barn at the Swine Research Center, University of Alberta, Edmonton, Alberta. Since there were visible suspended materials in the piggery wastewater, the wastewater was filtered through a Whatman No. 1 filter paper. The pH of the piggery wastewater was in the range of 6.9 to 7.2 (average: 7.1) and the electrical conductivity of the wastewater was about 11.1 ms/cm. Pulp mill effluent and oil sands tailings pond water were transported from Weyerhaeuser Canada, Grande Prairie Operation and Syncrude Canada Ltd. mine site, respectively. The pulp mill effluent had a pH of 7.3 to 7.8 (average: 7.6) and conductivity of 1.71 ms/cm. The pH of the oil sands tailings pond water was from 7.8 to 8.3 (average: 8.1) and the conductivity was 2.69 ms/cm. Standard Methods for the Examination of

Water and Wastewater (American Public Health Association et al., 1995) were followed for the determination of pH and conductivity.

HCl and NaOH were used for pH adjustment. High purity water which was produced by a water purifier (Maxima Ultra Pure Water System) was used to dilute wastewater samples. Droplets were produced with an Eppendorf pipettor (model 4710, 10 to 100 μL) and a Nichiryo pipettor (model 5000, 0.5 to 10 μL).

3.2.2 Experimental Design and Procedures

The effect of droplet volume (size), impurity concentration and pH on the freezing temperature of wastewater droplets was examined by conducting a $3 \times 2 \times 2$ factorial experiment. Droplets with two different average volumes, 4.20 μL (the standard deviation of the volume = 0.14) and 33.5 μL (the standard deviation of the volume = 0.26) were tested. The equivalent spherical diameter is 2.0 mm for 4.20 μL drops and 4.0 mm for 33.5 μL drops. Two levels of wastewater impurity concentration (original wastewater concentration and 50% of the original concentration) and three levels of wastewater pH (original liquid pH, pH = 4.0 and 11.0). Thus, there were a total of 12 possible combinations among the three factors and four replicated runs were conducted.

In each trial all three types of wastewater droplets and distilled water (purified by an Option 4 Water Purifier) droplets which served as a reference were placed on the copper surface of a cooling device. The surface of the cooling device was coated with water repellant films using Dow Corning silicone lubricant to separate the droplets from the cooling plate. The silicone lubricant which is often used in droplet ice nucleation tests prevented the deformation of the droplets from sphericity and the presence of any solid material in contact with the droplets that might cause a change in their freezing properties. Nucleation of a water drop from its neighbors was avoided by placing them far apart from each other. The cooling device was connected to a two stage cooling system which provided a constant cooling rate of 0.44 $^{\circ}\text{C}/\text{min}$. The cooling device was

sealed from the top with a glass cover. After each experimental run, the copper surface of the cooling device was cleaned with methanol using soft paper wiper and rinsed with high purity water.

Once cooling started, the number of drops changing phase at successive one-minute time interval was observed until all the drops on the cold surface froze. The instantaneous temperature of the surface of the cooling device was recorded as a function of time by 4 precision thermistors (YSI 44007). A PC with a data logger (Ultra-Logger, model-REV UL-16D) was used to record the temperature throughout the cooling test.

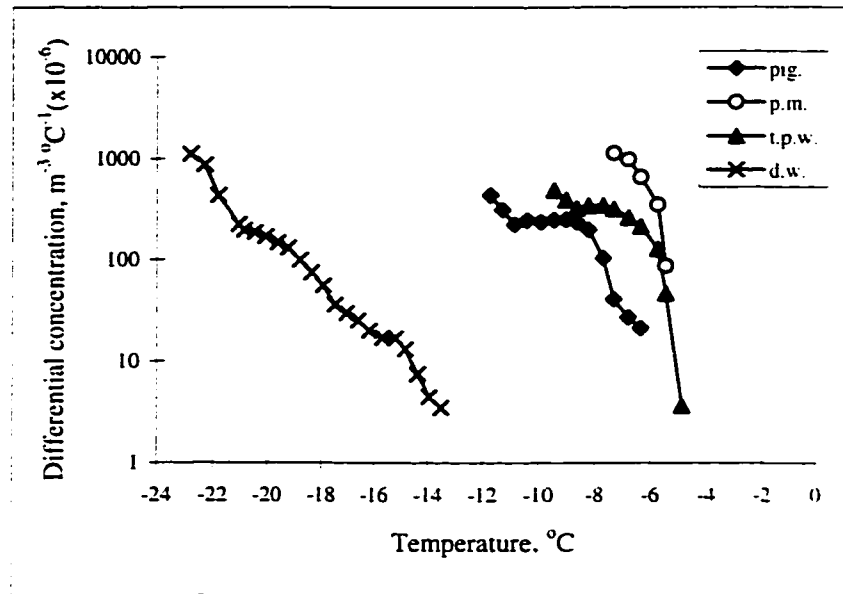
In one series of trials conducted, droplets were produced from wastewater samples diluted to 2% of the original wastewater impurity concentration without any pH adjustment.

3.3 Results and Discussion

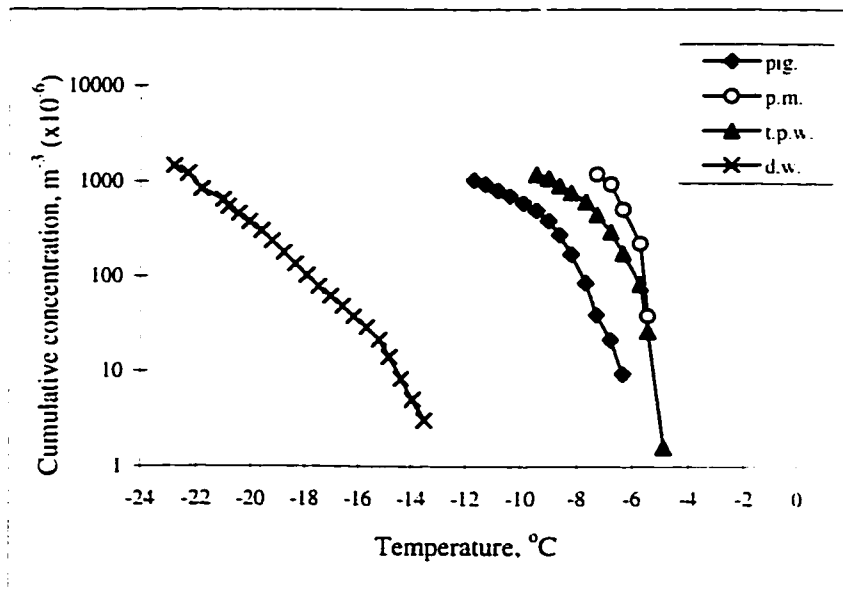
Most of the experimental results of the heterogeneous freezing nucleation of supercooled liquid studies were presented in the form of histograms. Because of the dependence of the results on the drop volume, histograms can only be used for qualitative comparison. In this study the experimental results are evaluated quantitatively using differential nucleus spectra and cumulative nucleus spectra derived by Vali (1971).

3.3.1 Comparison of nucleus concentration

Differential and cumulative nucleus spectra of piggery wastewater (pig.), pulp mill effluent (p.m.), oil sands tailings pond water (t.p.w.) and distilled water (d.w.) samples are shown in Figure 3-1. The results are obtained by averaging the data of the replicated tests. The variation in the median freezing temperature among the replicated runs was within 1 °C. The concentrations are calculated at each 0.44 °C interval and a three-interval weighted smoothing (1/4, 1/2, 1/4) is applied. The differential spectrum is



(a)



(b)

Figure 3-1 Comparison of the wastewater ice nucleus concentrations. 156 drops for each type of wastewater and 432 drops for distilled water. The droplet volume = 4.2 μL . (a) differential nucleus spectra, (b) cumulative nucleus spectra.

obtained from equation (2.22) and the cumulative spectrum is calculated from equation (2.24). Under each experimental condition, 156 drops were made from each type of wastewater and 432 drops for distilled water were tested. The droplet volume is $4.2 \times 10^{-9} \text{ m}^3$ (or $4.2 \text{ }\mu\text{L}$).

As can be postulated from the data presented in Figure 3-1, the wastewaters contain significantly higher concentrations of ice nuclei than the distilled water and all wastewater drops froze before distilled water drops even started to freeze. There seem to be differences in the nucleus content among the wastewaters. Oil sands tailing pond water (T.P.W.) contains active nuclei at temperatures warmer than $-5 \text{ }^{\circ}\text{C}$ while droplets of pulp mill effluent started to freeze with a much higher nucleation particle concentration at a temperature about $0.5 \text{ }^{\circ}\text{C}$ colder than that of T.P.W. The nucleus concentration of pulp mill effluent increases dramatically with the decreasing temperature and the concentration was highest among the wastewaters tested. All pulp mill wastewater drops tested froze at about $-7.3 \text{ }^{\circ}\text{C}$. The initial freezing temperature of piggery wastewater drops was more than $1 \text{ }^{\circ}\text{C}$ colder than that of the oil sands tailing pond water and it was observed repeatedly during the tests. The nucleus concentration of piggery wastewater increased gradually with decreasing temperature and the freezing was complete at $-11.7 \text{ }^{\circ}\text{C}$ which was more than $4 \text{ }^{\circ}\text{C}$ colder than that of pulp mill effluent. The general trend of the curves in Figure 3-1 is toward an exponential increase in nucleation particle concentration with decreasing temperature.

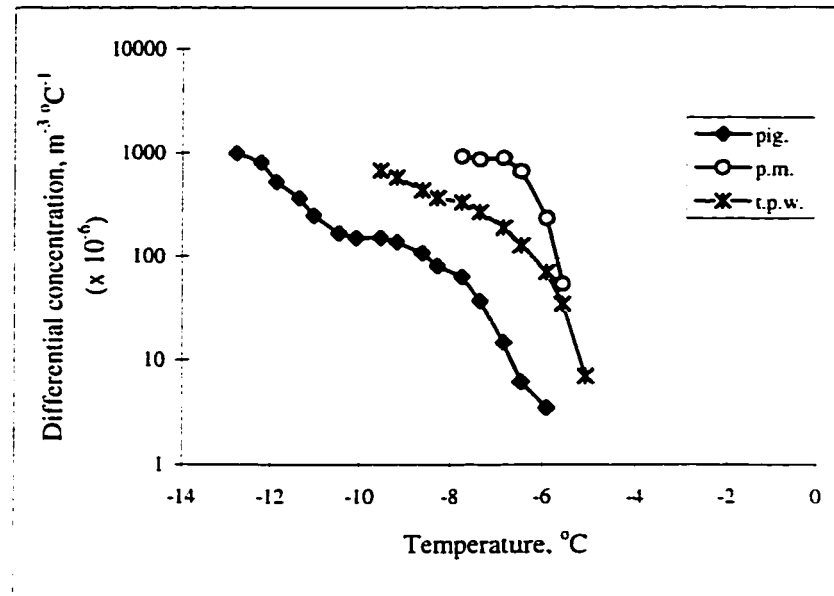
Instead of comparing the entire spectrum, T_{90} , a temperature at which 90% of the sample drops in a given experiment are frozen, was used as a measure of nucleus concentration. T_{90} corresponds to a particular value of cumulative nucleus concentration $K(T)$. If droplet volume $= 4.2 \times 10^{-9} \text{ m}^3$ and since the number of unfrozen drops $N(T) = 0.9N_0$ at T_{90} , then, $KT_{90} = 548 \times 10^6 \text{ nuclei/m}^3$, i.e. there were 548×10^6 active nuclei per m^3 at temperatures warmer than T_{90} . The T_{90} of all the water samples tested are listed in Table 3-1.

As Table 3-1 reveals, the differences in T_{90} among the wastewaters were obvious. Pulp mill effluent had more active nuclei between - 5 °C and - 8 °C and at - 6.4 °C the nucleus concentration had already reached $548 \times 10^6/\text{m}^3$. The increase in nucleus concentration was slower for T.P.W. when temperature was lowered. The T_{90} of T.P.W. was 1.1 °C lower than that of pulp mill effluent while piggery wastewater had lowest nucleus concentration among the three types of wastewaters and its T_{90} was more than three degrees lower than that of pulp mill effluent.

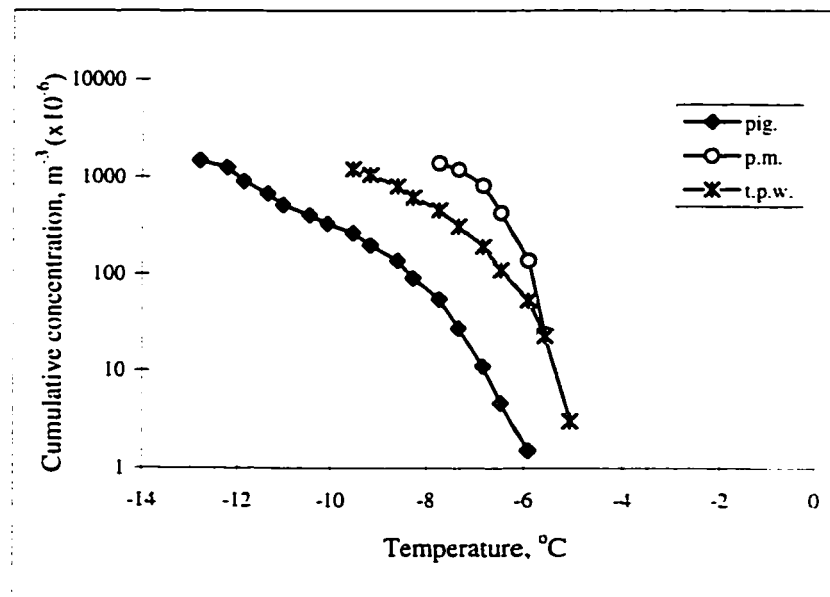
Table 3-1 List of T_{90} 's of different water samples

Water Samples	T_{90} (°C)
Pulp mill effluent	-6.4 ± 0.5
Oil sands tailings pond water	-7.5 ± 0.5
Piggery wastewater	-9.7 ± 0.5
Distilled water	-20.8 ± 0.5

All wastewaters contain numerous particulate and dissolved substances and some of them were even unidentified or with unknown physical-chemical characteristics as mentioned in the wastewater characterization section. It was not possible to determine the effect of the individual component on the freezing temperature of a wastewater drop and to determine exactly what substances which had the highest effective temperature and cause the differences in the freezing temperature among the wastewaters. Only the general influence of the entire complement of impurity components can be detected. The differences in the nucleus concentrations among the wastewaters become more clear when the wastewaters were diluted with high purity water to 50% of their original impurity concentrations as revealed in Figure 3-2. Compare to Figure 3-1, the differential



(a)



(b)

Figure 3-2 Concentrations of freezing nuclei in the wastewaters with 50% of the original impurity content: (a) differential nucleus spectra; (b) cumulative nucleus spectra.

or cumulative nucleus concentration spectra in Figure 3-2 cover a broader temperature range (or increased in the ranges of the spectra). The nucleus spectra in Figure 3-2 had similar patterns as those shown in Figure 3-1. Nucleus concentrations of the wastewaters were reduced by the dilution. The peak which may indicate the presence of specific groups of nuclei in the sample was more pronounced in the differential nucleus spectrum for the piggery wastewater.

Dilution increased the differences in the T_{90} . The T_{90} of the original samples as shown in Table 3-1 was in the range of -6.4°C to -9.7°C and it was broadened to the range of -6.6°C to -11.1°C . The effect of dilution on the T_{90} of individual wastewater varied. It had the most notable effect on the piggery wastewater. T_{90} of the piggery wastewater was lowered from -9.7°C to -11.1°C , a 1.4°C difference while T_{90} of pulp mill effluent was only changed by 0.2°C (from -6.4°C to -6.6°C). The reduction in the nucleus content by dilution for T.P.W. was between the piggery wastewater and the pulp mill effluent. The T_{90} of T.P.W. was decreased from -7.5°C to -8.1°C after dilution. Once again, as indicated in Figure 3-2, pulp mill effluent had the highest concentration of freezing nuclei.

The piggery wastewater had high suspended solid content, while most of these solids did not act as ice nuclei at least not at temperatures warmer than -10°C . On the other hand, pulp mill effluent must contain very effective ice nucleation particles. Substances such as lignins which are not present in piggery wastewater and in T.P.W. are the chemical source of color and chlorinated organics of pulp mill effluent. Lignins are insoluble in water, in most organic solvents, and in strong sulfuric acid. Lignins have a variable elementary compositions and methoxyl content. Lignins react readily with sodium bisulfite or thioglycolic acid to form soluble products. They are unhydrolyzable with acids, readily oxidizes, and are soluble in hot alkali, and readily condenses with alcoholic and phenolic compounds (Freudenberg, 1955). Not all the lignins can be dissolved in the pulping process; some undissolved lignins may reach the final effluent.

Therefore, the undissolved lignins and lignin derivatives in pulp mill effluent might be one origin of the highly active nuclei.

3.3.2 The effect of pH on the nucleus concentrations

The effect of wastewater pH on the droplet freezing temperature was investigated. If the droplet freezing temperature is affected by the pH of the wastewater from which the drops originated, then, in a spray freezing operation the wastewater pH can be adjusted to a value at which the sprayed wastewater will freeze at a warmer temperature to increase ice production rate (or to avoid a pH that causes the sprayed liquid to freeze at a lower temperature). The effect of sample pH on the droplet freezing temperature was examined by comparing the differential nucleus concentration of the individual wastewater with different pH values (Figure 3-3).

As mentioned above, the average sample pH for piggery wastewater, pulp mill effluent and T.P.W. is 7.1, 7.6 and 8.1, respectively. Figure 3-3 reveals that liquid pH influences the droplet freezing temperature but the effect is specific to each wastewater. Compare to the samples with original pH and pH at 11.0, the samples with acidic pH (pH = 4.0) usually have fewer active nuclei, at least over certain temperature range in the entire spectrum. The nucleus concentration was consistently high for the piggery wastewater, when liquid pH was adjusted to 11.0. The active nucleus content of pulp mill effluent decreases apparently at acidic pH while the adjustment of pH to basic value did not change a great deal in nucleus concentration. The pH modification had the least effect on the freezing temperature of T.P.W. drops. The pH change only showed some influences on the nucleus concentration of T.P.W. in the warmer temperature range (-4.7 °C to -6.4 °C) and the effect diminished as temperature decreased.

The effect of changing pH on the nucleus concentrations may be caused by the change in the solubility of the compounds contained in the wastewaters. Solubility of many compounds is markedly influenced by the solution's pH (Barth and Polkowski, 1972; Merkel et al., 1969). The change of solubility of the chemical compounds in the

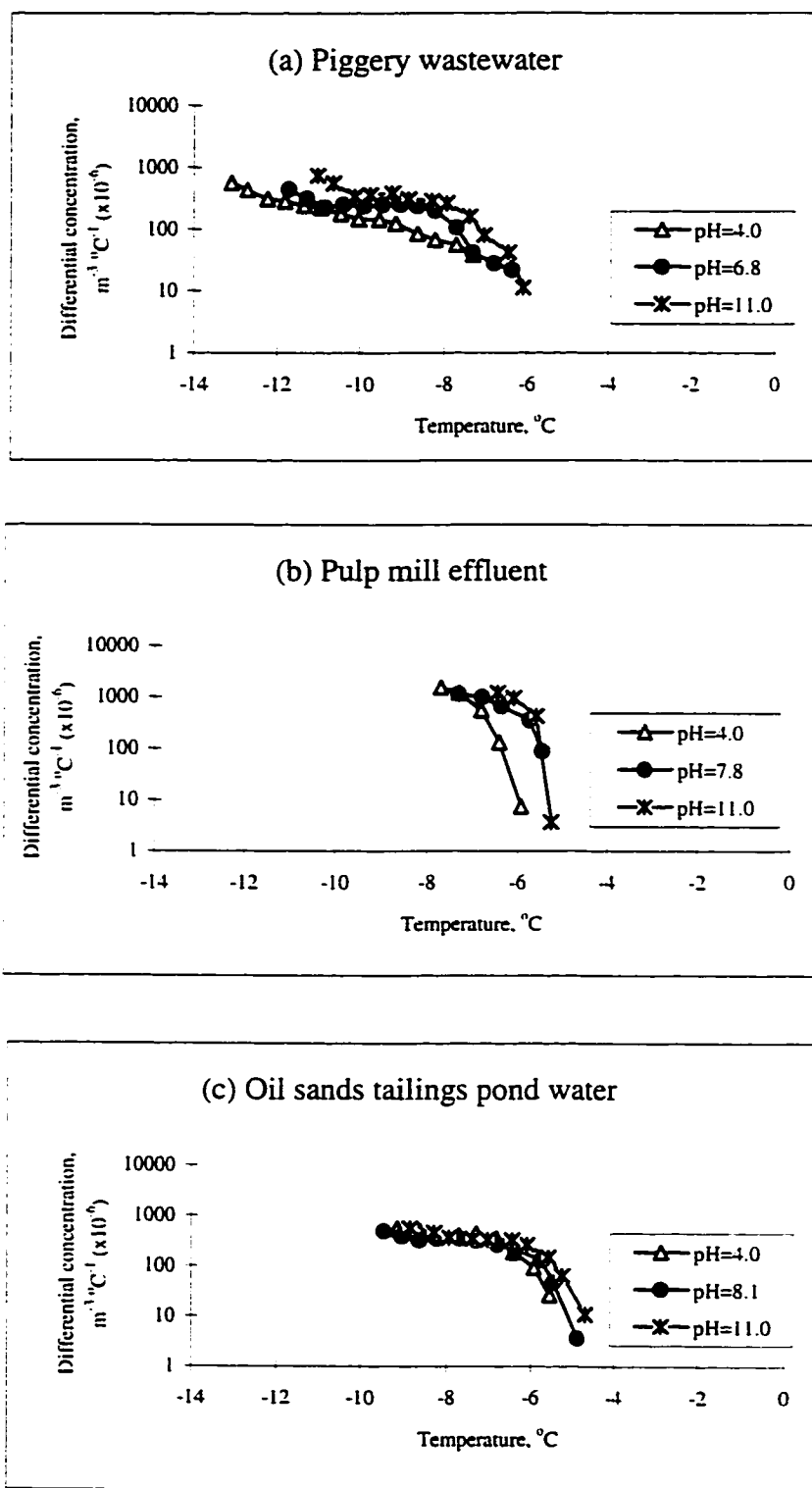


Figure 3-3 The influence of pH on the nucleus concentration of the individual wastewater (The droplets contain original wastewater impurity content).

wastewater by a simple pH adjustment may result in the alteration in the substances available as active nuclei, consequently, the change in the nucleus concentration. Thus, the influence is chemical species (or in general, wastewater) and temperature dependent. In particular, at pH 11.0 all $\text{Ca}(\text{HCO}_3)_2$ in water will change to $\text{CaCO}_3 \downarrow$ (precipitates). The solution pH change also has significant effect on the odor causing materials in swine waste, for instance, at high pH, the emission of volatile acids and H_2S was limited and almost no odor was detected while, under acidic conditions, the H^+ and HS^- ions combines, escapes and produces the typical sulfide odor but the release of NH_3 and amines will diminish (Barth et al., 1982; Merkel et al., 1969). The T_{90} 's of the wastewater drops under different pH are recorded in the Table 3-2.

Table 3-2 The T_{90} 's of the wastewater drops with different pH

Wastewater Sample	Sample pH	T_{90} ($^{\circ}\text{C}$)
Piggery wastewater	4.0	-11.3
	7.1 (original)	-9.7
	11.0	-9.0
Pulp mill effluent	4.0	-7.0
	7.6 (original)	-6.4
	11.0	-6.0
Oil sands tailings pond water	4.0	-7.4
	8.1 (original)	-7.5
	11.0	-7.1

Comparison of the cumulative nucleus concentrations of the three types of wastewaters tested under different pH conditions are displayed in Figure 3-4. Figure 3-4 indicates that when the wastewater pH is adjusted to 4.0, the differences in the T_{90} increases and the differences decreases when pH was 11.0. The comparisons are based on the values obtained when there is no pH adjustment on the wastewaters.

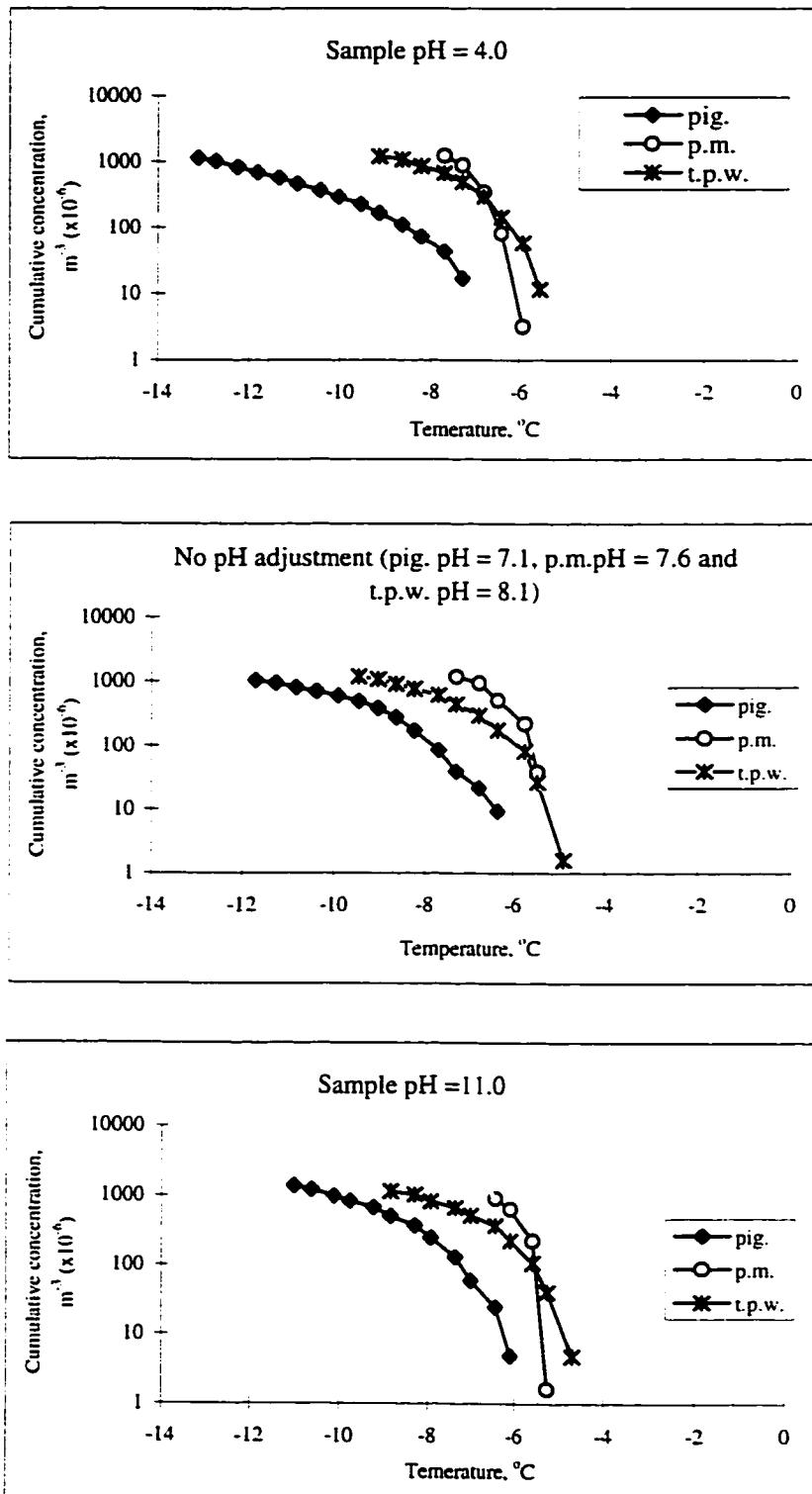


Figure 3-4 Comparison of cumulative nucleus concentrations at different pH conditions.

3.3.3 The influence of impurity concentration on the wastewater freezing temperature

The changes in the freezing temperatures caused by the variation in the amount of impurities in the wastewaters are demonstrated in Figure 3-5. The effect of impurity content on the droplet freezing temperature becomes more intense when the impurity content is reduced to 2% of the original amount by a 1:50 dilution with high purity water. With 2% of the original impurity, the initial freezing of the drops starts at colder temperatures than those drops made from the original wastewater samples.

The initial freezing temperature was 0.7 degree lower for pulp mill effluent and T.P.W. and 1.3 degree lower for piggery wastewater while there were almost no differences in the starting points when the wastewaters were diluted to 50% of their original impurity concentration. Furthermore, the cumulative nucleus spectra cover much broader temperature ranges, especially, for pulp mill effluent. The freezing of the macroscopically identical pulp mill effluent drops spreads over a 13.8 degree temperature range at 2% of the original impurity content; the range was 2.1 degrees at 50% impurity concentration and only 1.8 degrees with original impurity content. There were considerably fewer active ice nuclei available in the wastewaters after the impurity content was reduced by 50 times.

The accuracy of the predicted nucleus concentrations (equation 2.22 and equation 2.24) and the acceptability of the experimental procedures can be checked by using different droplet sizes or samples with various dilutions. Compare with the drops with original impurity content, in the same temperature range the calculated cumulative nucleus concentration decreased an average value of 97.1% for piggery wastewater, 83.1% for pulp mill effluent and 96.2% for T.P.W. at 2% of the original impurity concentration. Ideally, the nucleus concentration should decrease by 98%. The model prediction was quite satisfactory for piggery wastewater and T.P.W. but discrepancy was higher for pulp mill effluent. The difference from the ideal value (98%) is 0.9% for

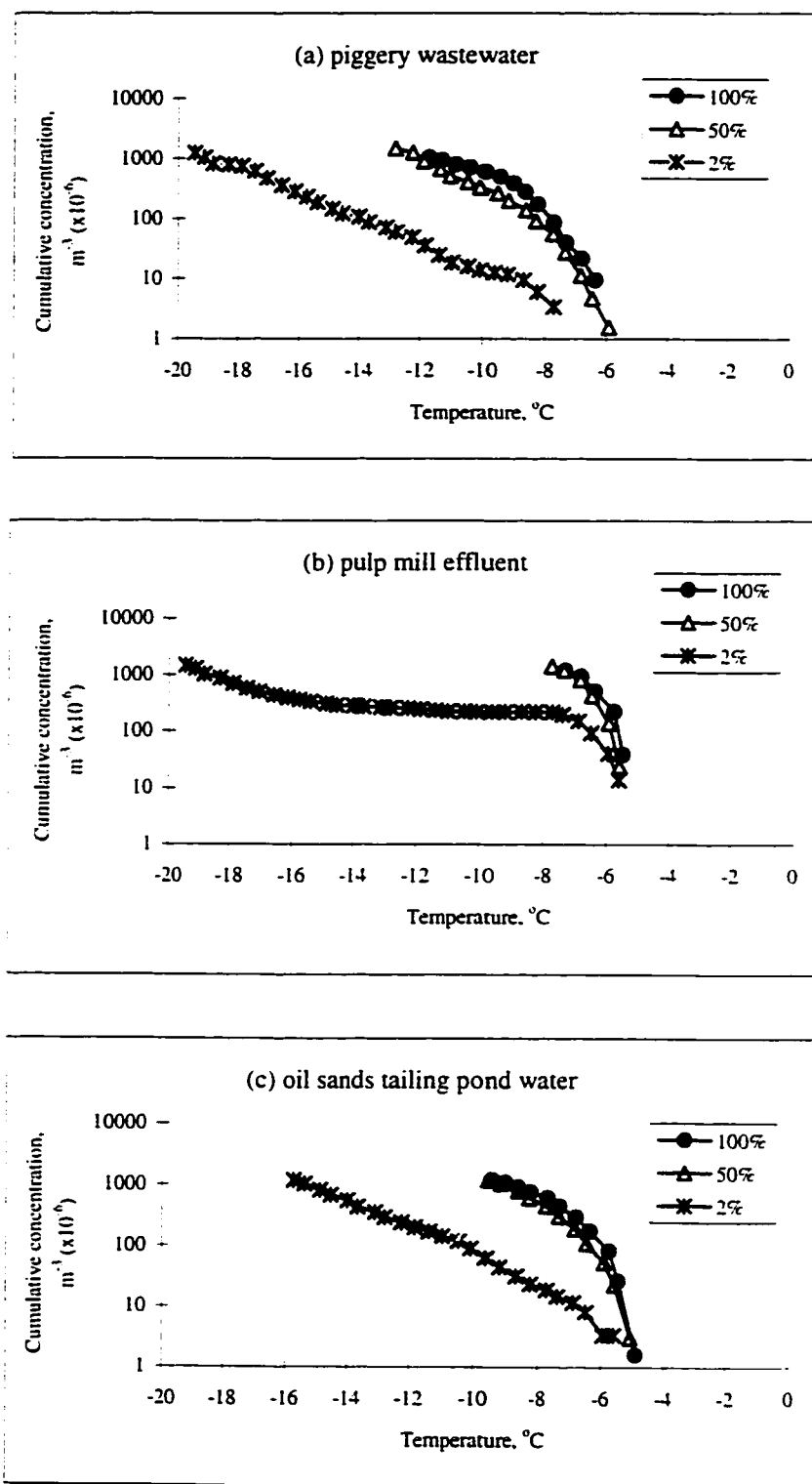


Figure 3-5 Cumulative nucleus spectra for wastewaters with different impurity contents.

piggery wastewater, 1.8% for T.P.W. and 15.2% for pulp mill effluent. The discrepancies between the expected nucleus concentration (or the ideal value) and the calculated concentration based on the results obtained from droplet freezing test increased as dilution ratio decreased. At 50% of the original impurity content, the reduction in the nucleus concentration was up to 50% for piggery wastewater (average: 40%), 38% for T.P.W. and pulp mill effluent (average: 20%). It seems that Vali's model had better prediction when the water samples had relatively lower nucleus content such as piggery wastewater (or diluted T.P.W) and the accuracy of the model decreased if samples contained high ice nuclei such as pulp mill effluent. The accuracy of the model will be checked again later in this section by using different sizes of drops.

As shown in Figure 3-6, with 2% of the original impurity content, the spectrum of the piggery wastewater and T.P.W. is similar to that of distilled water in Figure 3-1. But the spectrum of the pulp mill effluent is different. The amount of active nuclei increased sharply with decreasing temperature in the warm temperature range (-5 °C to -8 °C) then the nucleus concentration stays at that level (i.e. no freezing events happened) until temperature is lowered to about -12 °C. The nucleus content in pulp mill effluent then increased slowly after the temperature is colder than -12 °C. Between -12 °C and -16 °C, T.P.W. actually had higher nucleus concentration than that of pulp mill effluent. There are almost the same amount of ice nuclei in the pulp mill effluent as in the piggery wastewater when temperature is lower than -16 °C although the nucleus concentration in the pulp mill effluent is much higher than that of piggery wastewater at the warm temperature range. The sharp increase in the nucleus content in pulp mill effluent at the warm temperature range indicates that even at 2% of the original impurity there were still some nuclei which are active at the warm temperatures but these nuclei are not uniformly distributed among the drops. About 50% of the droplets tested froze in the warm temperature range (-5 °C to -8 °C). The T_{90} 's of the wastewaters with different impurity concentrations are listed in the Table 3-3.

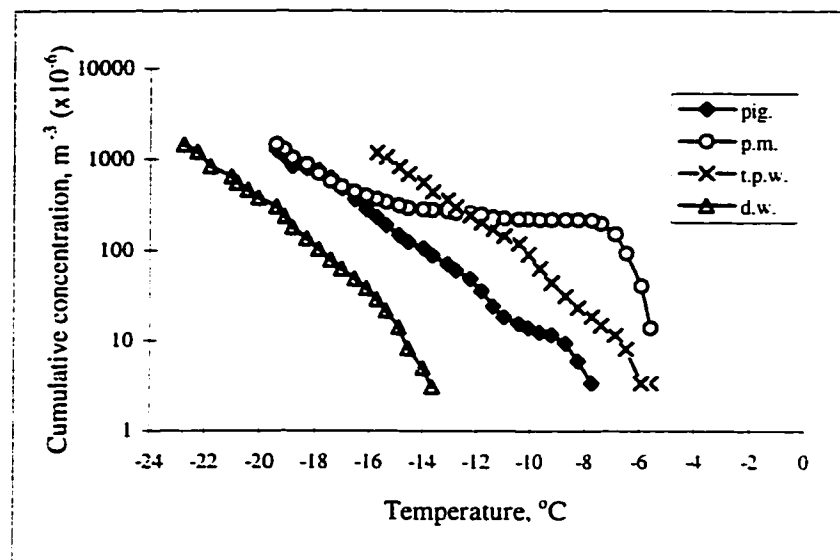


Figure 3-6 Cumulative ice nucleus concentrations of the wastewaters with 2% of their original impurity content.

Table 3-3 List of the T_{90} 's of the wastewaters with different impurity contents

Wastewater Sample	Impurity concentration (%C*)	T_{90} (°C)
Piggery wastewater	100%	-9.7
	50%	-11.1
	2%	-17.3
Pulp mill effluent	100%	-6.4
	50%	-6.6
	2%	-17.3
Oil stands tailings pond water	100%	-7.5
	50%	-8.1
	2%	-14.0
Distilled water		-20.8

*C = original wastewater impurity concentration

3.3.4 The volume effect

The nucleus concentrations of the drops with different volumes were compared. The calculated differential nucleus concentrations obtained from the droplets with different volumes (4.2 μL and 33.5 μL) are shown in Figure 2-7. The calculated concentrations cover different ranges for the two different volumes of the drops but the curves follow the same trend in general. Some overlapping occurs over portions of the spectra. The drops with larger volume have lower nucleus concentration generally, especially for pulp mill effluent. This is because the range of the nucleus spectra is determined by droplet volume V and the total number of the drops tested N_0 (equation 2.22 or equation 2.24). For larger drops, fewer nuclei per cubic meter of water are needed to freeze all the drops in the sample, therefore, relatively low nucleus concentration are obtained from the experiment. The larger drops freeze at warmer temperatures than the small drops because the chance that the droplet contains a high activity nucleus is increased with increasing droplet size. The difference in the calculated concentration increases for the wastewater with higher nucleus concentration such as pulp mill effluent.

3.4 Summary

The wastewater generated from different industries freezes at different temperatures. The 'freezability' of the wastewater can be evaluated by quantitative determination of the ice nucleus concentrations. The pulp mill effluent has highest nucleus concentration or highest 'freezability' among the three types of wastewaters tested, and piggery wastewater had the lowest nucleus concentration. The nucleus concentration of oil sands tailings pond water (T.P.W.) was between the other two.

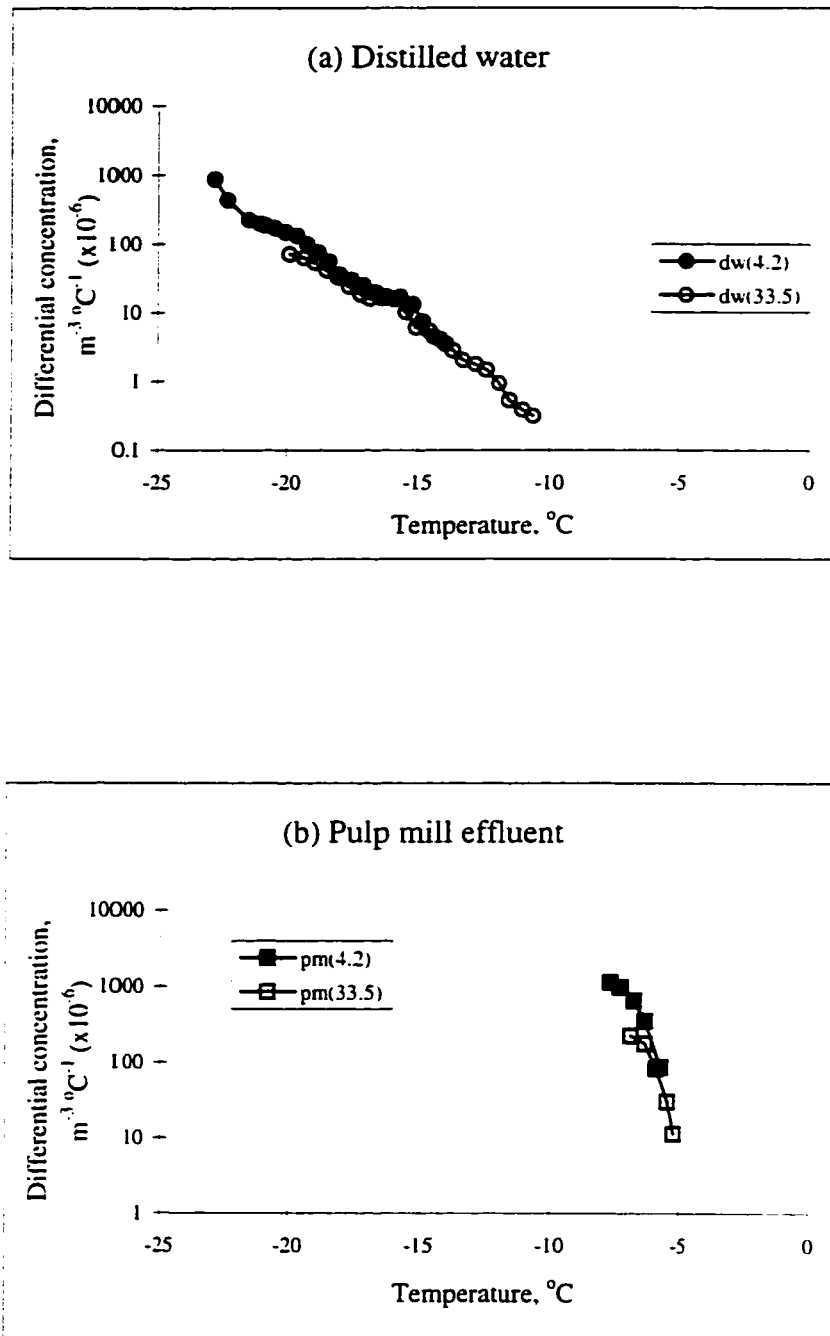


Figure 3-7-a Differential ice nucleus concentrations for distilled water and pulp mill effluent drops with different volumes ($4.2 \mu\text{L}$ and $33.5 \mu\text{L}$). Wastewater samples are not diluted and no pH adjustment on the samples.

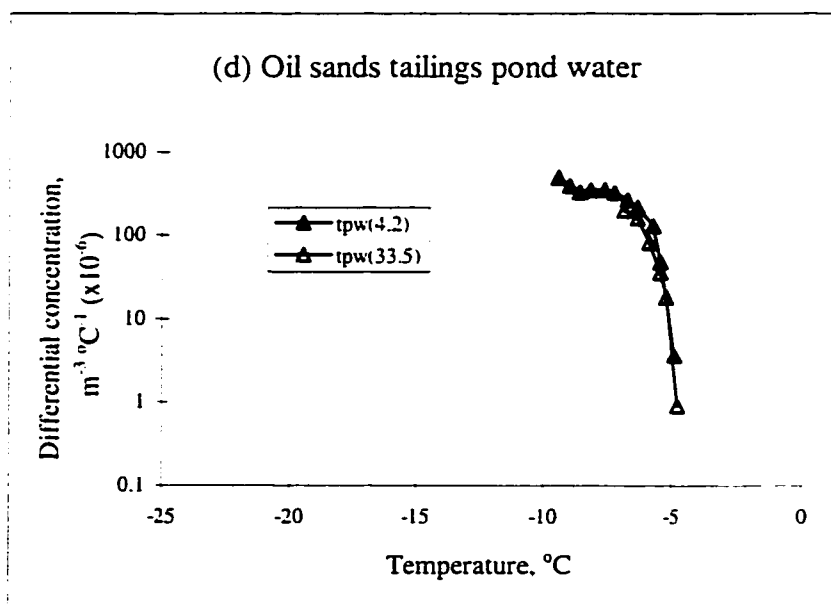
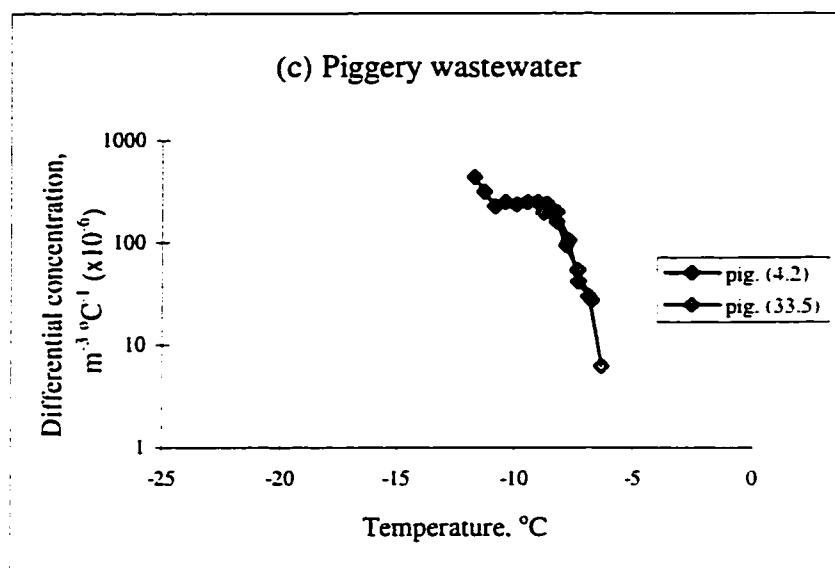


Figure 3-7-b Differential ice nucleus concentrations for piggery wastewater and oil sands tailings pond water drops with different volumes (4.2 μL and 33.5 μL). Wastewater samples are not diluted and no pH adjustment on the samples.

pH of the wastewater affected the freezing temperature of the wastewater droplets. The effect was specific to each wastewater. The wastewater droplet ice nucleation temperature was influenced by the amount of the impurities contained in the wastewater. The wastewater with lower impurity concentration froze at colder temperatures while high impurity concentrations induced freezing to occur at warmer temperatures. The freezing temperature of the wastewater drops were volume dependent. The larger drops froze at warmer temperature than the small ones. Lower freezing nucleus concentration was required for larger drops to freeze.

In summary the pulp mill effluent had the highest freezability; it started freezing at warm temperatures and the droplet freezing temperature of the pulp mill effluent was less affected by the change in pH (when $\text{pH} > 7$), impurity concentration and droplet volume. The droplet freezing temperature of piggery wastewater was about 2 to 3 degree ($^{\circ}\text{C}$) colder than that of T.P.W and pulp mill effluent. The freezing temperature of piggery wastewater was sensitive to the change in the impurity concentration, drop volume and pH.

CHAPTER 4 FREEZING BEHAVIOR OF FREELY SUSPENDED WATER DROPLETS

Spray freezing is a complicated dynamic and thermodynamic process. During spraying a water jet breaks up into small drops, the drops are supercooled and some nucleate into ice as they travel through the air to the ground. Although the droplet air residence time during a spraying operation is short, the large exposed surface area per unit volume of water provided by the sprayed water drops greatly enhances the cooling rate and subsequently increases the ice formation rate and it makes the spray freezing technique different from other freezing methods.

In most experimental studies on the freezing of supercooled water drops reported in literature, drops are either placed on the surface of a hydrophobic solid support or suspended at the interface of two organic, immiscible liquids which are insoluble in water. In this type of experimental study the water drops usually freeze under constant cooling rate. The laboratory study of freezing of wastewater droplets reported in Chapter 2 falls in this category. It is a simple method to obtain information about the nucleus contents of the wastewaters and compare freezing characteristics of the wastewaters investigated. The experimental conditions differ from the conditions under which drops freeze in the atmosphere during a spraying freezing operation. Therefore, more sophisticated experimental methods are required to study water drops under conditions which simulate those in the atmosphere a water is sprayed.

Little engineering design information is available related to the water droplet ice nucleation and growth rates that can be achieved during the spray freezing process. Some research work has been conducted on the heat and mass transfer of a droplet falling in a

gas stream (Ranz and Marshall, 1952; Dickinson and Marshall, 1968; Yao and Schrock, 1976; Chen and Trezek, 1977). Hughes and Gilliland (1952) studied the behavior of drops and sprays from a dynamic perspective. The study involved the gross motion of drops and detailed motion in and around individual drops, the correlation in connection with the effect of acceleration on drag, the equilibrium distortion or oscillation from prolate to oblate spherical shapes, and the internal circulation caused by skin friction. Lane (1951) studied the shattering of the free falling drops due to aerodynamic forces under both transient and steady state conditions. Lane (1951) indicated that for a drop with 4 mm diameter which was the largest drops he tested, the critical velocity for shatter in a steady stream of air was 12.5 m/s. Higher shattering velocity were required for smaller drops, for example, the shattering velocity of a 1 mm diameter drop was 35 m/s. Unfortunately, none of the above mentioned studies involve freezing of the free falling droplets. The freezing characteristics of freely suspended wastewater drops under the influence of steady cold updraft can best be studied in a laboratory with a vertical wind tunnel.

Behavior of free falling water droplets have been studied for a better understanding of the formation of precipitation in the atmosphere. In order to study the behavior of freely falling water drops or the characteristics of the collision or coalescence between water drops and breakup of water drops, drops are usually freely suspended in a vertical wind tunnel. Lenard (1904) built the first vertical wind tunnel and determined that a 5.5 mm diameter drop was the largest drop that will not be broken up by turbulence. Later Blanchard (1950) stabilized 9 mm diameter drops in his wind tunnel. List (1959), Bailey and Macklin (1968) used wind tunnel in their hailstone study. There are some other wind tunnel studies related to behavior of water drops (Komabayasi et al., 1964; Montgomery and Dawson, 1969; Richards and Dawson, 1971). More recently study of the behavior of freely suspended water droplets were conducted by Spengler and Gokhale (1972) and Kamra and Ahire (1985). Spengler and Gokhale (1972) investigated the interactions of freely suspended, supercooled water drops and frozen pellets in a large vertical wind tunnel. The size of drops studied were in the range of 200 μm to 8 mm.

These authors observed the freezing process. Kamra and Ahire (1985) built a small vertical wind tunnel. Up to 5 water drops could be simultaneously suspended in an air stream.

In the study presented in this thesis, a vertical wind tunnel similar to Kamra and Ahire's (1985) was designed to examine the freezing behavior of freely suspended wastewater droplets under different experimental conditions.

4.1 Design of the Vertical Wind Tunnel

Any wind tunnel design is limited by various factors. Perhaps the most important ones are funds and space available. Due to the limited funds and the space available a small wind tunnel similar in many respects to that used by Kamra and Ahire's (1985) was designed. The cold room where the vertical wind tunnel will be located has a floor area of 2 x 3.5 m. The height of the tunnel was also restricted to be less than 2 m (the original height limit was 1.5 m, it was later increased to 1.89 m).

A schematic diagram of the vertical wind tunnel is presented in Figure 4-1. The entire tunnel consists of the following components: a squirrel-cage blower driven by a dc motor with speed controller, a wooden diffuser section, the plenum, the vertical section with air flow straighteners and wire mesh screens, the working section and the back pressure plate.

The stability of a water drop in terms of lifetime in the working area of the tunnel is dependent on the level of turbulence it encounters. Therefore, in order to keep water droplets suspending in the air stream, the most important design factor in the vertical wind tunnel is to obtain a low turbulent airflow. Several steps were taken to reduce turbulence in the air stream within the wind tunnel. The wooden diffuser and plenum were used to smooth out the flow fluctuations produced by the fan. The critical component of the tunnel was the vertical section. The airflow was straightened and most

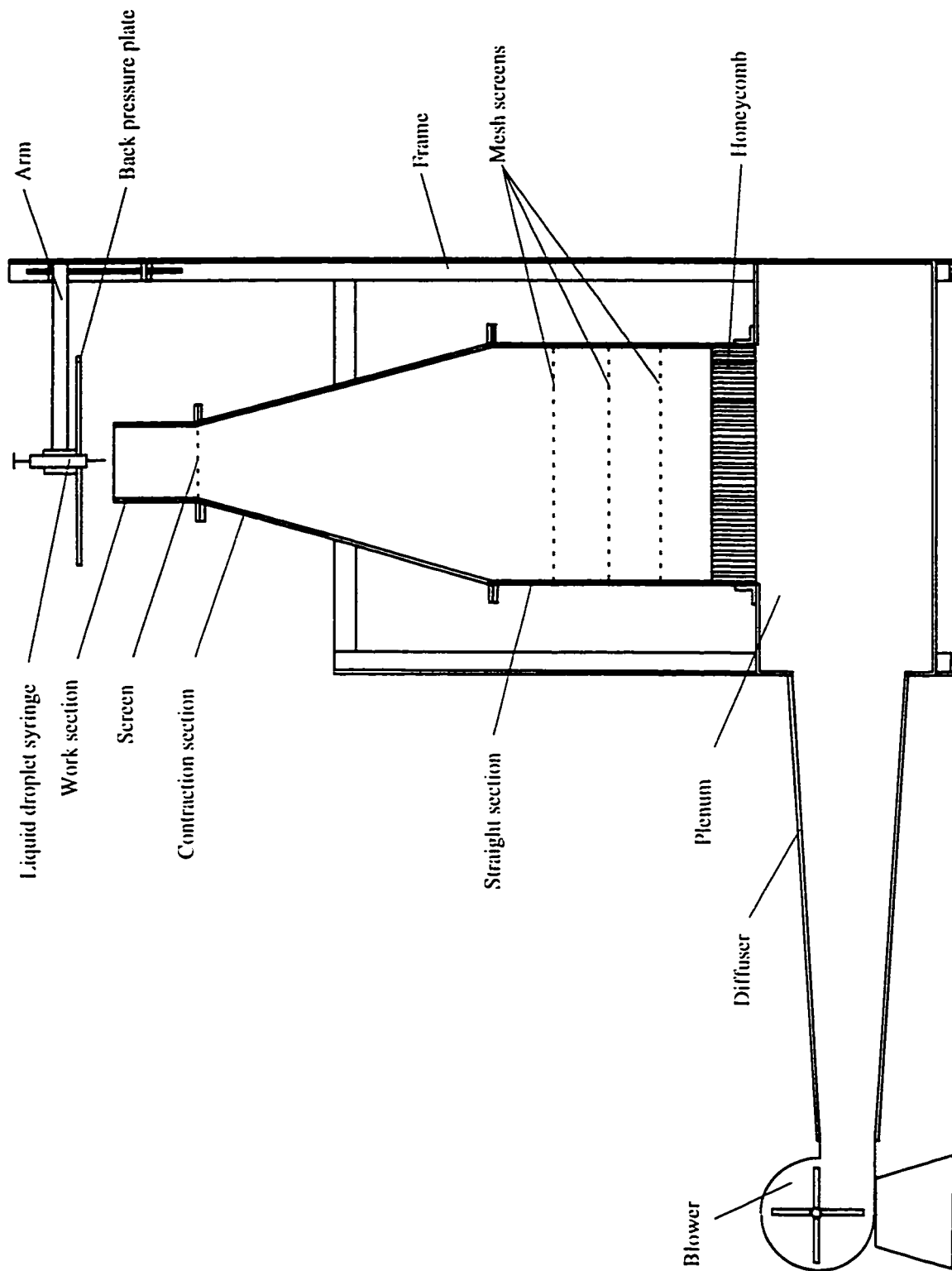


Figure 4-1 The schematic diagram of the vertical wind

of the turbulence was reduced in this section. In order to reduce turbulence in the airflow, a large contraction ratio (14) was used in the vertical section. The principal advantage of using a large contraction ratio was that the ratio of turbulent intensity to the mean air speed decreased through the contraction area as the mean speed increased (Prandtl, 1933; Taylor, 1935). The use of the wire mesh screen (or damping screen) in the vertical section was again to reduce turbulence in the working section. Based on their study, Dryden and Schubauer (1947) indicated that the effect of a damping screen in reducing the turbulence of an air stream depended on the pressure-drop coefficient, k , of the screen. The theoretical reduction of turbulence by one screen was $1/(1+k)^{1/2}$ and by n identical damping screens was approximately $1/(1+k)^{n/2}$. The lower limit of the turbulence level attainable by the use of damping screen was determined by the fineness and the uniformity of the screen used in the wind tunnel. By trying several different mesh size screens, three damping mesh screens were selected, two 24-mesh size (0.19 mm diameter wire) and one 60-mesh size (0.18 mm diameter wire).

The working section was a 120 x 120 mm open ended cross section made of perspex. A drop was suspended in the air stream at its terminal velocity. According to previous studies a “velocity well” or velocity sag, a slightly lower vertical velocity required to stably suspend a water drop at the center of the working section. Usually a specially designed screen was needed to lower the velocity at the center part of the air stream. A screen with same design but made with different material as the one in Kamra and Ahire’s (1985) wind tunnel was used. The screen had a 120 x 120 mm internal cross section and a plastic glass frame. The screen is shown schematically in Figure 4-2. A 22 gauge electrical wire with plastic cover was used to make the screen. The wire passed through the holes drilled in the frame. Air velocity should be lower at those places where wires of the screen cross each other. The screen was placed between the converging section and working section of the tunnel.

A back pressure plate was required to maintain a desired velocity profile in the working area and to prevent the water drops from accelerating upward. The distance

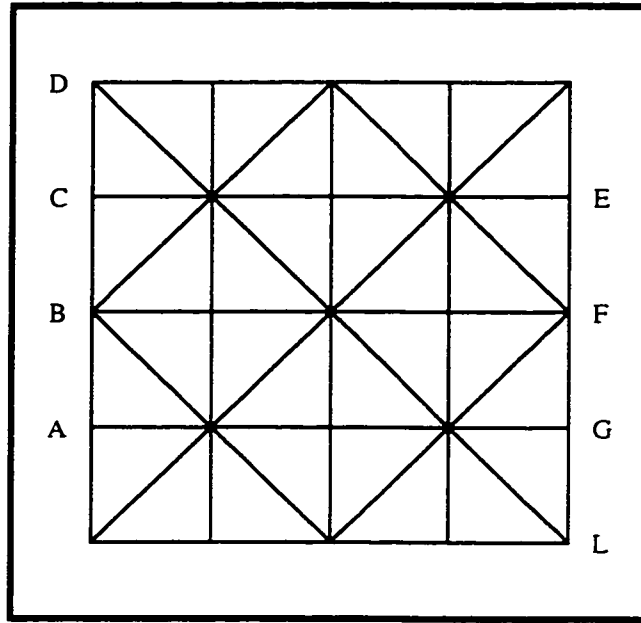


Figure 4-2 The small screen used to get velocity sag

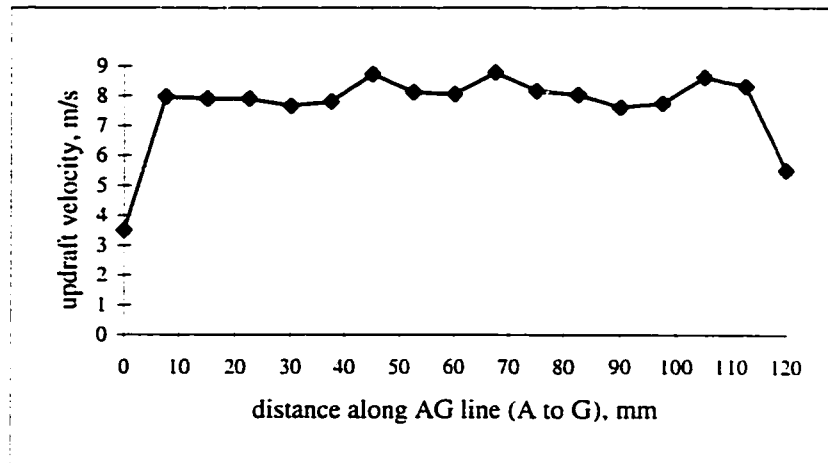
between the back pressure plate and the working area can be adjusted by vertically shifting the position of the back pressure plate.

4.1.1 Velocity profiles of the wind tunnel

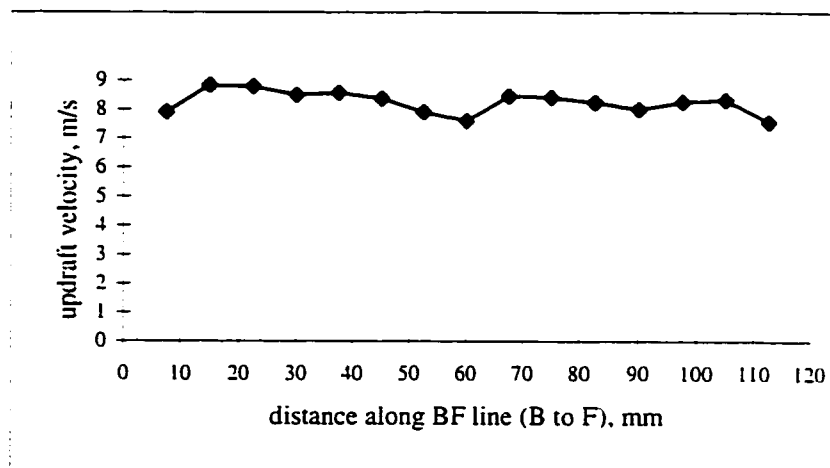
It is important to know the velocity profiles in an investigation using a wind tunnel. A plot of velocity profile above the working area can be used to determine the size of the suspended drops, their location and their stability in the working area. A small pitot tube (PAA-12-KL, United Sensor) was used to obtain the horizontal velocity profiles along different lines of the small screen at the height where droplets were suspended. Velocity profiles are shown in Figure 4-3. The velocity profiles are similar to those obtained by Kamra and Ahire (1985). It is obvious that air velocity declined at the points where wires of the screen (see Figure 4-2) cross each other. Greater reduction in the velocity was obtained at the points where eight wires crossed each other and smaller reduction where four wires crossed.

Numerous trials were made to increase the air residence time of the water drops by preparing the small screen with different types (copper wire and electrical wire) and different thickness of wires, by changing the position of damping screens in the vertical section as well as the position of the back pressure plate.

Preliminary investigation of the stability and the behavior of different sizes (or volumes) of droplets made from pulp mill effluent, oil sands tailings pond water, piggery wastewater and tap water was conducted under room temperature. Droplets with equivalent diameters in the range of 2.7 to 5.0 mm were tested. It was found that pulp mill effluent and piggery wastewater drops were much easier to suspend, i.e. they could be suspended for longer times without breaking. Tap water drops had highest stability among the water drops. It was very difficult to suspend oil sands tailing pond water drops under room temperature, especially, the larger drops. These oil sands tailings pond water drops deform radically from the spherical shape once introduced into the air stream then

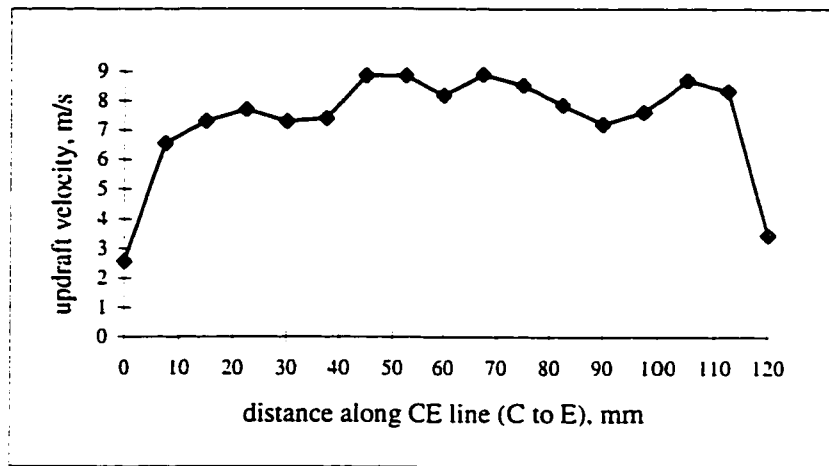


(a) Velocity profile along AG Line

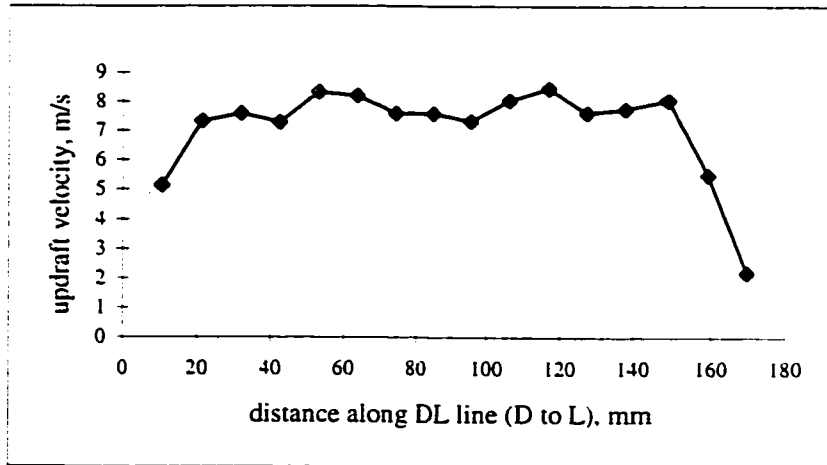


(b) Velocity profile along BF line

Figure 4-3 Velocity profiles taken above the working area (at about the height where a water drop suspends). The distances are measured along the wires of the small screen (Figure 4-2) and start from the edges of the tunnel.



(c) Velocity profile along CE Line



(d) Velocity profile along DL line

Figure 4-3 (continued) Velocity profiles taken above the working area (at about the height where a water drop suspends). The distances are measured along the wires of the small screen (Figure 4-2) and start from the edges of the tunnel.

they break up. The low surface tension of the oil sands tailing pond water drops was probably caused by the surfactants which had been added during the bitumen extraction process.

4.2 Experimental Facilities and Set-up

The objectives of this experiment were to examine the behavior of freely suspended wastewater droplets during the freezing process and determine the time required for freezing under different experimental conditions, then to use these experimental results to estimate the ice nucleation temperature of the suspended wastewater droplets and ice fraction contained within the droplets.

4.2.1 Experimental facilities

The experiment was conducted in a small cold room (CEB 20) located at the basement of Civil and Electrical Engineering Building, University of Alberta. The vertical wind tunnel was housed in the cold room. The cold room temperature could be adjusted from room temperature to - 40 °C. The cold air was circulated by two distribution fans in the cold room.

Three video cameras (JVC Color video camera head, Model No. TK-12800) were used to record the droplet freezing process from different directions. A 75 mm lens (Rainbow G75mm 1:1.8) was installed on each camera. Three JVC video cassette recorders record the entire freezing process on the video tapes for review after the experiment. A timer connected to VCRs shows the time of the experiment (hour, minute, second and the frame numbers). The video cameras had a speed of 30 frames per second. The distance between the cameras and a drop suspending in the air was varied between 1 and 1.5 m.

4.2.2 Experimental set-up

All three wastewaters, piggery wastewater, pulp mill effluent and oil sands tailings pond water, were examined in these experiments. Drops with average volumes of 12.0 (the standard deviation = 0.89) and 37.7 μL (the standard deviation = 2.1) were made from pulp mill effluent and oil sands tailings pond water. The equivalent spherical diameter is 2.8 mm (for 12.0 μL) and 4.2 mm (for 37.7 μL). The droplet volumes selected for piggery wastewater were 21.2 μL (with the standard deviation = 2.9 and the equivalent diameter: 3.4 mm) and 37.7 μL . It was difficult to make smaller droplets at cold temperature as the wastewater viscosity increases, especially. the piggery wastewater.

Droplets were produced using an Eppendorf pipette (model 4710, 10 to 100 μL) and a Nichiryo pipettor (model 5000, 2.0 to 25 μL). The pipettors were calibrated under the working conditions in the cold room.

Droplets were tested under various temperatures: - 17.7, - 10.3, -7.4, -6.7 and -5.5 °C. Five precision thermistors, four of them were attached to the top of the working section of the vertical wind tunnel (YSI 44007), and a humidity sensor (Humitter- 50U, Vaisala) were used to monitor the air temperature and humidity near the suspending droplet. A PC with a data logger (Ultra-Logger, model-REV UL-16D) was used to record the temperature and humidity data during the testing.

One drop was suspended in the air stream each time and the entire freezing process was observed both visually and videographically. Drops with initial temperature of +5 °C were supercooled and froze while suspended in the updraft of the wind tunnel. The time required for a drop to freeze under different experimental conditions could be determined by replaying the video record. The number of frames which were recorded while a drop was suspended in the air stream could be used for calculating the freezing time.

4.3 Freezing of Freely Suspended Wastewater Drops

Videography played an important role in understanding of the freezing process of the freely suspended wastewater drop. Freezing of drops which occurred too rapidly to observe visually was studied with videography. The freezing process could be observed on the video tape due to the sudden increase in the brightness of the image as droplet freezing occurred.

4.3.1 General freezing characteristics of wastewater drops

Numerous wastewater drops were tested in this study. All the video tapes (about 50 tapes from each VCR) were examined carefully after the experiments were carried out. After a wastewater drop was introduced in the updraft, it remained liquid as it was supercooled. The larger water drop suspending in air did not maintain a 'spherical' shape; it exhibited a marked flattening on its lower surface and smoothly rounded curvature on its upper surfaces. The deformation increased as the droplet volume increased. McDonald (1954) conducted a very thorough study of the equilibrium shape of large water drops falling at terminal velocity and found that the shape of large water drops was mainly controlled by surface tension, hydrostatic pressure, external aerodynamic pressure. Water drops bounced up and down in the updraft and did not drift horizontally or rotate before freezing initiated.

The video recording reveals that freezing starts at the bottom edge of a water droplet and then envelopes the whole surface area of the drop progressively at all ambient temperatures used for this study. Then, it freezes inward and the ice shell thickens as phase change continues. The Plates 4.1 to 4.5 illustrate the proceeding of the freezing of various water droplets. Plate 4.1 shows the freezing process of a 2.8 mm diameter pulp mill effluent drop. The ambient air temperature was - 5.5 °C and humidity 80.2%. The droplet was introduced into the updraft of the wind tunnel at 10(hour):53(minute):24(second);05(frame number) (Plate 4.1-a). The droplet suspended

in the updraft in the liquid form until 10:53:52;02 (the rightmost drop in the upper row of Plate 4.1-b), then, 1/30 second later, freezing started at the bottom edge of the droplet (the bright spot in the second drop from the right of the upper row in Plate 4.1-b). the freezing proceeded to the entire surface of the droplet as observed from Plate 4.1-b. starting at the second drop (from right) in the upper row to the leftmost drop in the lower row. the bright spot grew and covered the entire surface of the drop. The droplet surface freezing was completed in 7/30 second. The Plate 4.1-b was obtained by merging 8 frames (frames 10:53:52;02 to 10:53:52;09). The Plate 4.1-c shows the moment before the droplet left the updraft after being suspending in the updraft for 30.4 seconds.

The time required to envelop the entire drop surface area of different drops varied. It depended on the freezing temperature (or cooling rate) and the type of the water. Under the same conditions, tap water or distilled water (with food color) drops. only needed 2/30 to 3/30 second (2 or 3 video frames) to finish the surface freezing but it took more time to envelop the surface of wastewater drops (3 to 4 frames or even longer) although the time required to initiate the freezing by the wastewater drops was much shorter. Plate 4.2 displays the freezing of a 3.4 mm diameter piggery wastewater drop in a - 17.7 °C environment and the pH of the droplet was adjusted to 11.0. It again took 7/30 seconds (from the second drop (from right) of the upper row to the second (right) drop of the bottom row) while it only took 4/30 second for a 4.2 mm tap water droplet to finish the surface freezing (see Plate 4.3, ambient temperature: - 17.7 °C). It was even shorter. 2/30 seconds, for the ice formation on the surface of a 4.2 mm distilled water drop to which red food coloring had been added (Plate 4.4, ambient air temperature: -17.7 °C).

Blanchard (1955) observed freezing of large water drops suspended in a vertical wind tunnel. In his work Blanchard showed that the manner of freezing is a function of drop temperature. Blanchard indicated that -5 °C was the approximate dividing temperature between clear ice which forms at warmer temperature and opaque ice. which forms at colder temperature. Blanchard observed freezing process visually although he

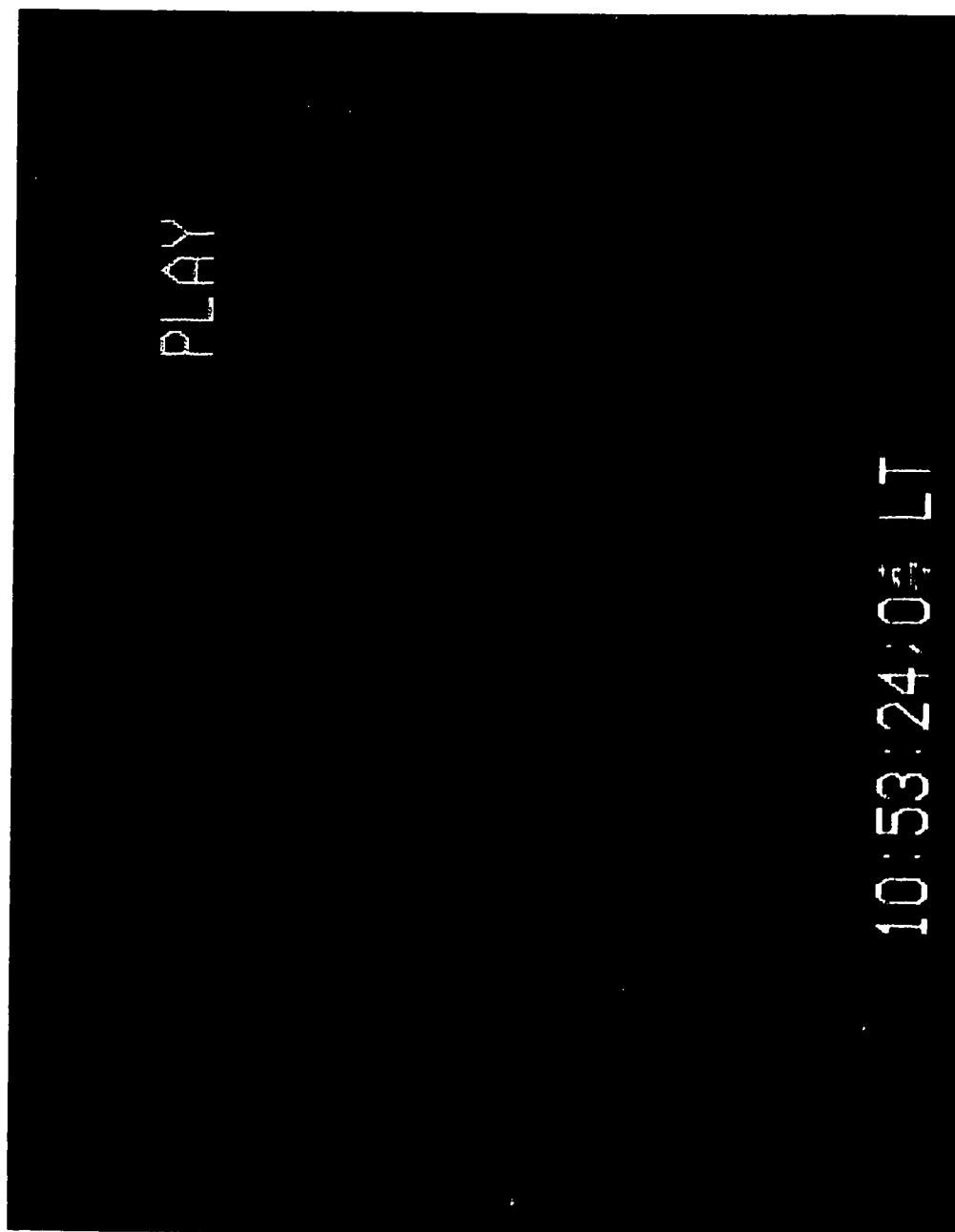


Plate 4.1 The illustration of the process of freezing of a freely suspended pulp mill effluent drop: plate 4.1-a, the moment after the droplet was introduced into the updraft of the wind tunnel; plate 4.1-b, the freezing of the droplet surface; plate 4.1-c, the moment before the droplet left the updraft.

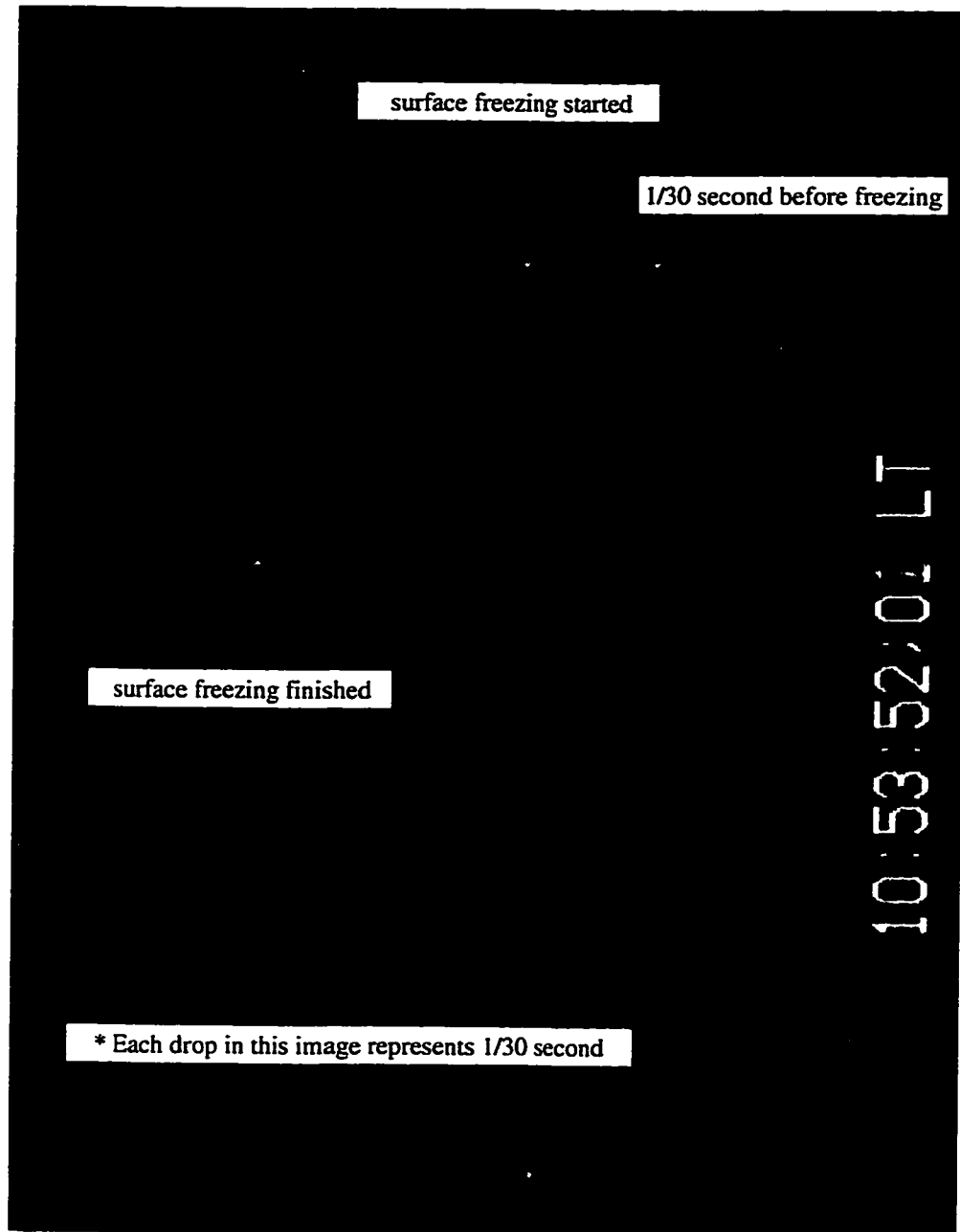


Plate 4.1-b The freezing of the droplet surface.

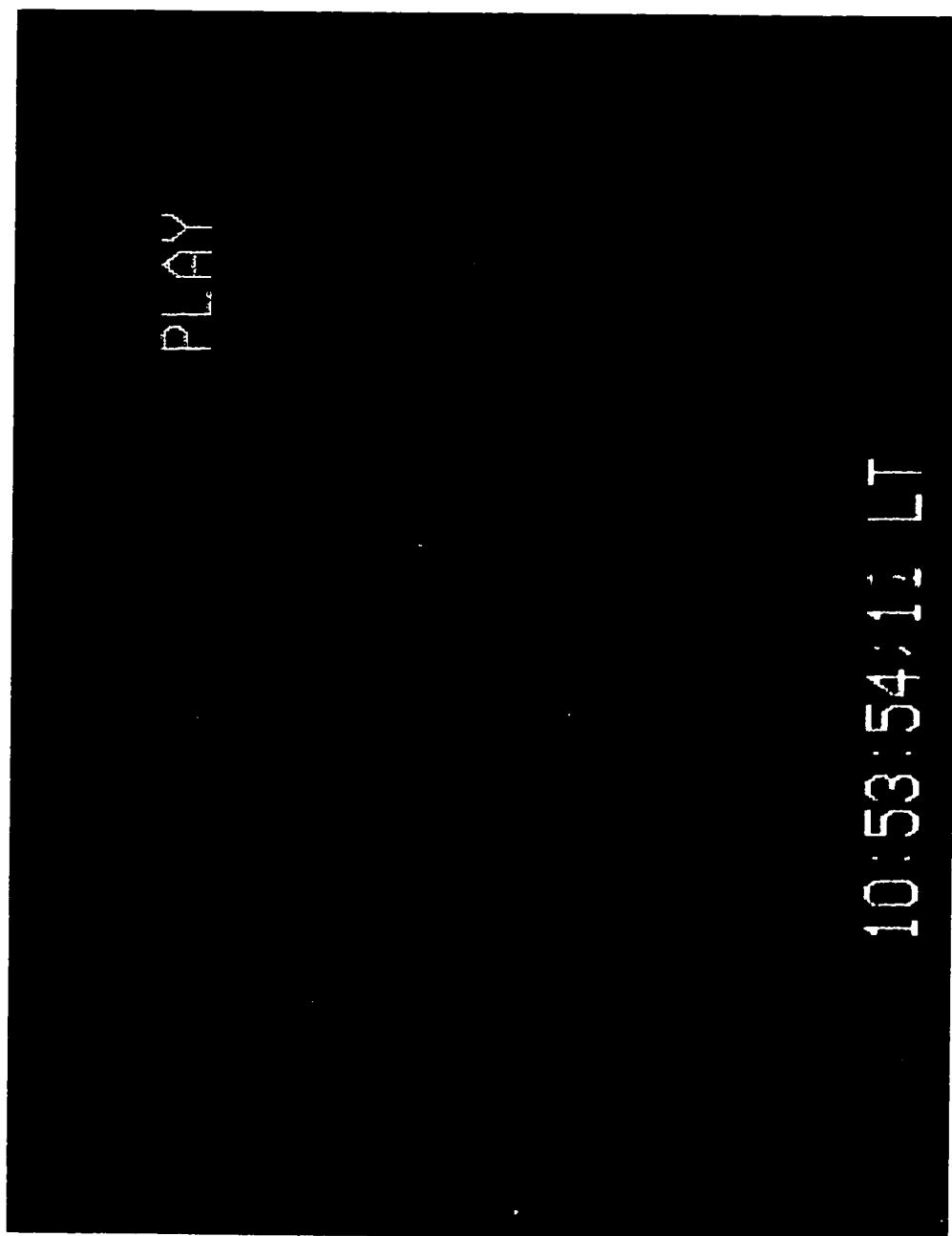


Plate 4.1-c The moment before the droplet left the updraft.



Plate 4.2 The illustration of the ice formation on the surface of a 3.4 mm diameter piggery wastewater drop.

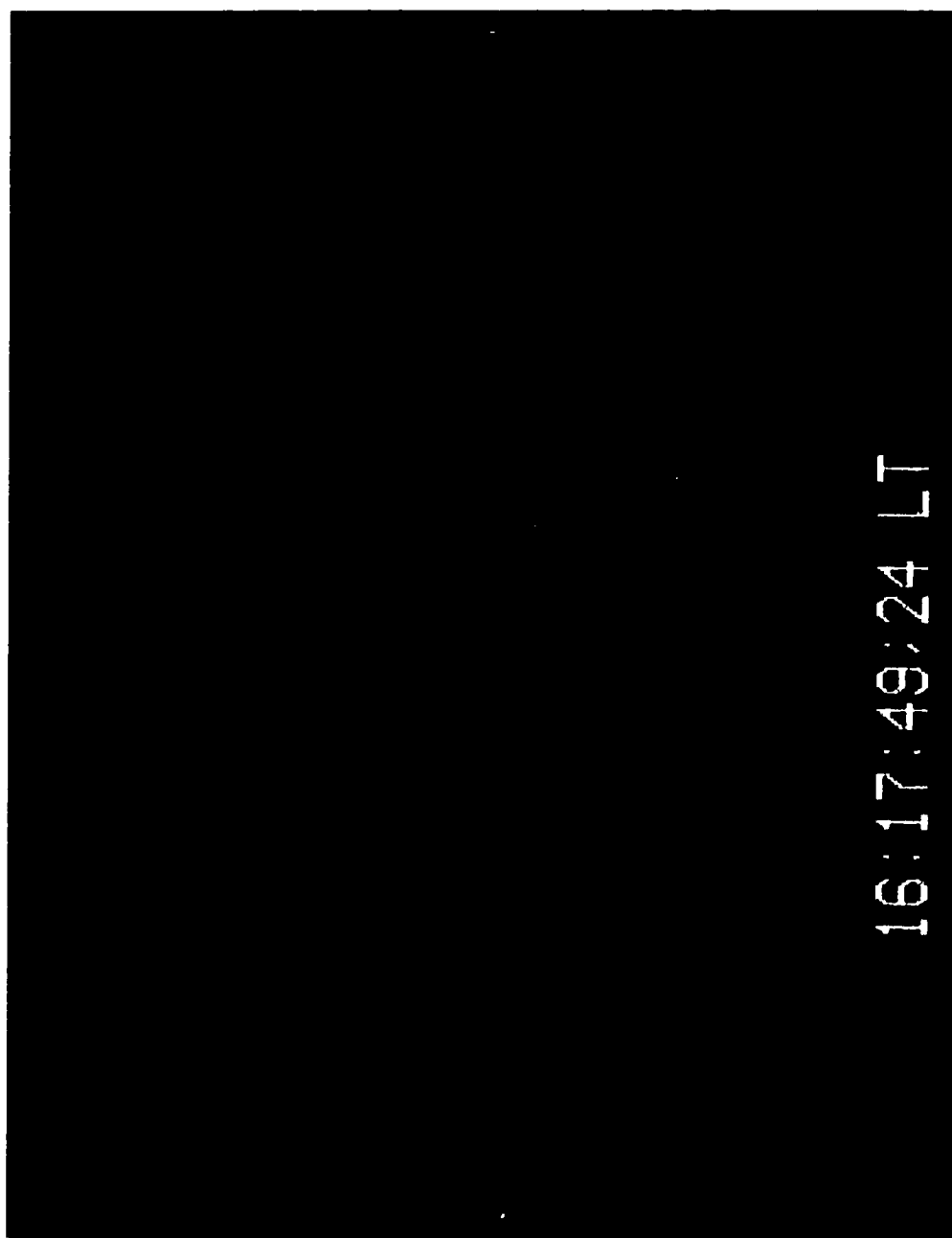


Plate 4.3 The illustration of the ice formation on the surface of a 4.2 mm tap water drop.

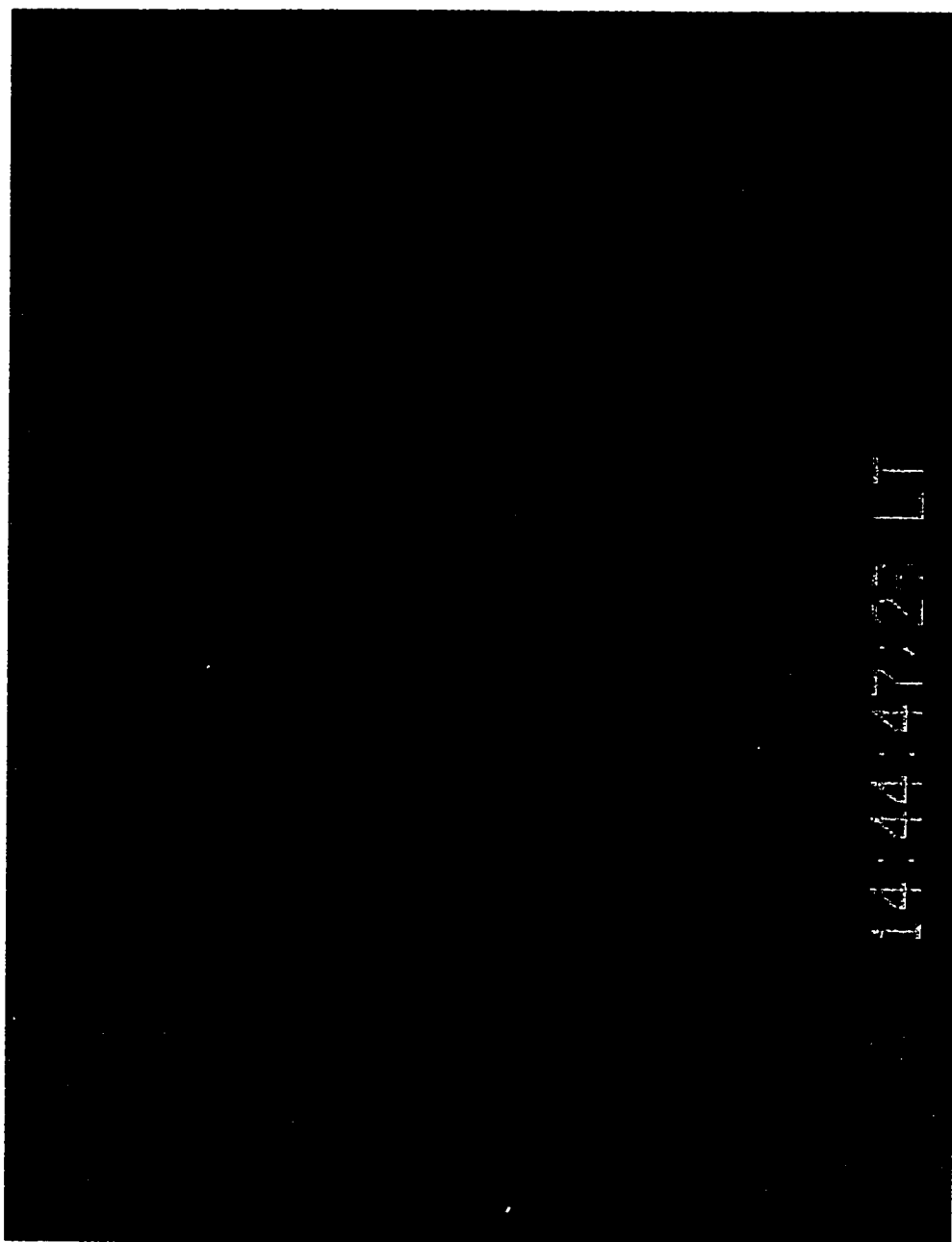


Plate 4.4 The illustration of the ice formation on the surface of a 4.2 mm diameter distilled water drop added with red food color.

could see that ice first forms in one region on the bottom of the drop and then progress slowly around the drop at warm temperature (warmer -4 or -5 °C) but Blanchard had difficulty to determine visually the initial freezing point at colder temperature (temperature colder than -4 or -5 °C). Blanchard said that freezing appears to occur nearly simultaneously over the entire surface of the drop at these colder temperatures. He explained that the clear and opaque freezing is partially caused by the scattering of light by minute air bubbles that form as air comes out of solution as the water freezes.

As was mentioned above there are two distinct stages in the freezing of a supercooled water drop. The water drop was cooled towards updraft temperature when it was introduced in the wind tunnel. The surface temperature of the drop was colder than that of the interior and the drop was not in thermal equilibrium with the environment before ice nucleation begins. When the surface temperature of the drop reached its ice nucleation temperature, freezing began. The first stage of freezing involved the formation of the surface ice shell which contained numerous tiny air bubbles. The total mass of water frozen in this initial stage causes the droplet temperature to rise rapidly to near 0 °C due to the latent heat released as phase change occurs. During the second stage, the liquid interior gradually freezes and the latent heat of fusion must be transferred to the environment. Plate 4.5 illustrated the initial freezing of a 4.2 mm diameter pulp mill effluent drop (Plate 4.5-a) and the thick ice formed during the second stage of the freezing process (Plate 4.5-b). The updraft temperature was -5.5 °C.

T.P.W drops reduced deformation from spherical shape at colder temperatures but the shape change was still significant as compared with pulp mill and piggery wastewater drops. The liquid T.P.W. drop was not very stable while suspended in the updraft, but once freezing started the shape change was confined and the drop became stabilized. It suspended in the air stream for long time after freezing when compared to other wastewater drops. There was no obvious decreased deformation in droplet shape for piggery wastewater and pulp mill effluent drops under subzero temperatures.

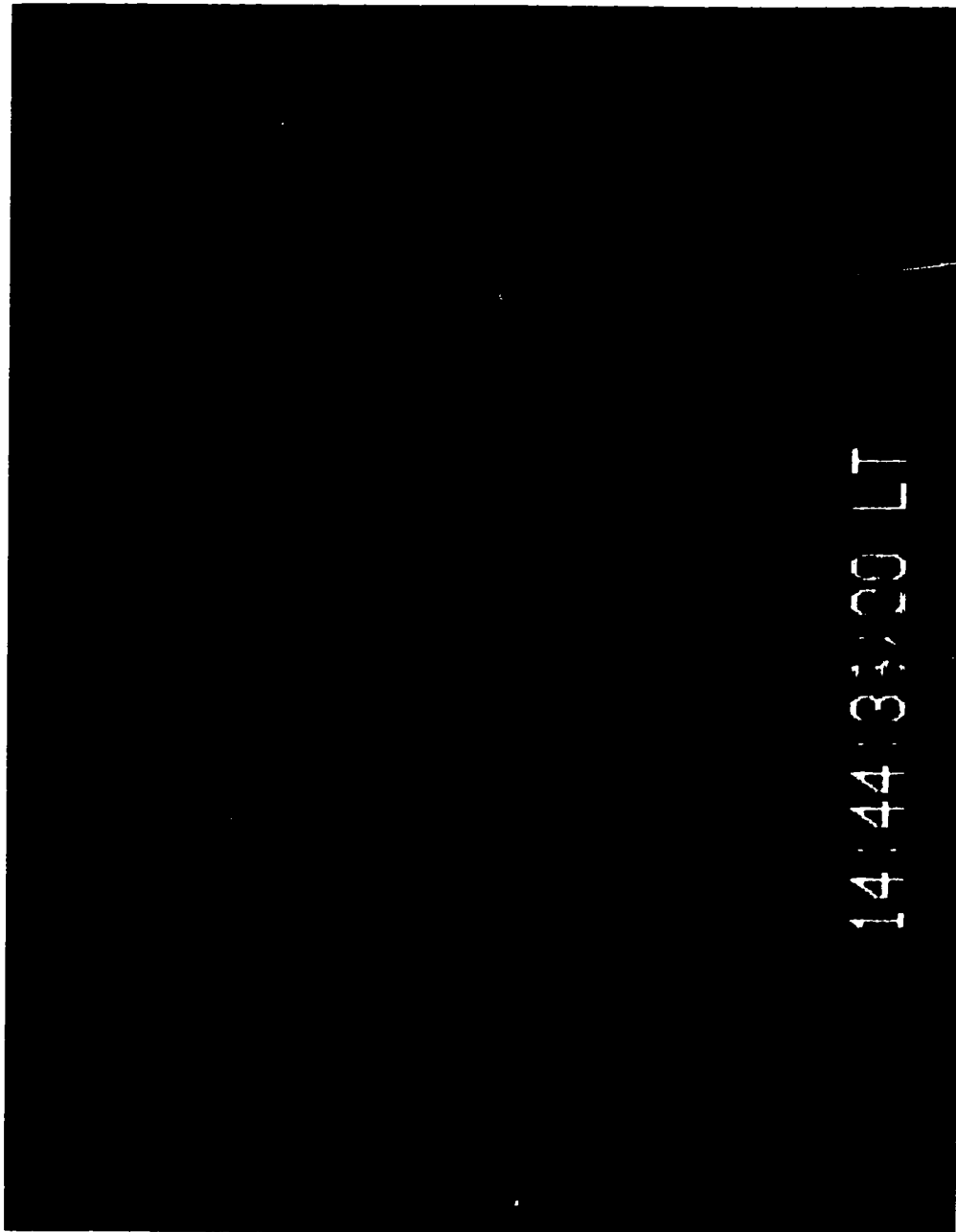


Plate 4.5 The illustration of the freezing process of a 4.2 mm diameter pulp mill effluent drop: plate 4.5-a, the initial freezing and plate 4.5-b, the thickened ice shell after the initial freezing.

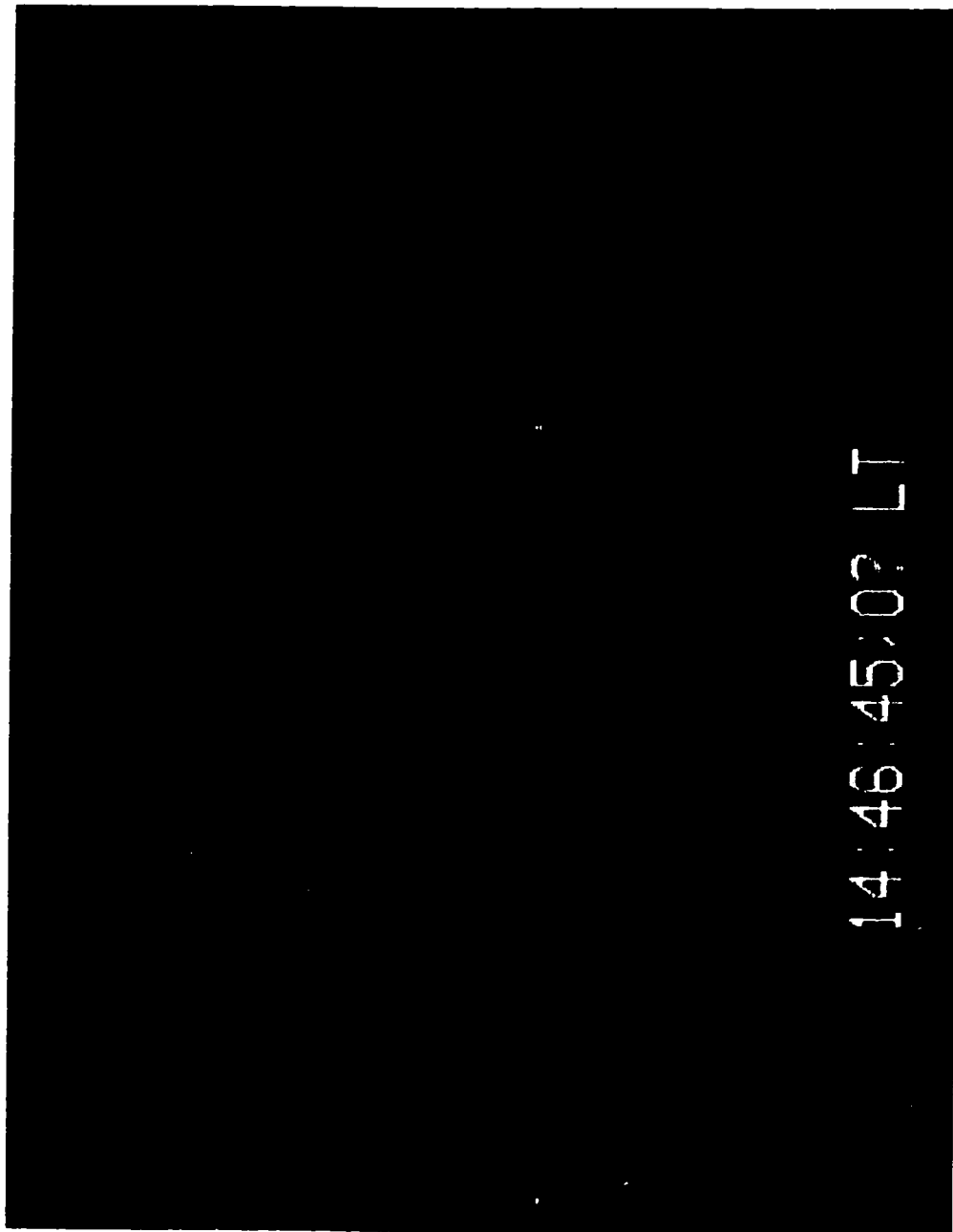


Plate 4.5-b The thickened ice shell after the initial freezing.

4.3.2 The motion of frozen wastewater drops

Some observations on the hydrodynamic behavior of frozen drops were similar to those made by Spengler (1971) and Pitter and Pruppacher (1973). It was apparent that freezing drops displayed interesting and varied patterns of fall:

1. Once freezing starts, a drop will rotate about a vertical axis but no shedding of water was observed.

2. The moment ice nucleation began, some freezing drops would instantly decrease their fall (terminal) velocity and accelerate upwards in the air stream. The decrease in the terminal velocity seems depending on the droplet size and the type of wastewater. The number of freezing drops that exhibited this behavior increased as the droplet size decreased and it happened more frequent with tap water and pulp mill effluent drops than the piggery wastewater and T.P.W. wastewater.

Spengler (1971) observed that the number of the drops showing a decreasing terminal velocity during freezing increased as the temperature of supercooling decreased. He explained that it might be caused by the change in the droplet shape. Liquid drops (especially, the large ones) oscillate about a mean drop shape and the drop terminal velocity is determined by this mean shape. As temperature decreases, the rate of ice crystal growth increases. If these drops oscillating while being suspended at a frequency of 5 to 20 times per second and the surface crystallization propagates rapidly from the point of nucleation, then there is a chance that the drop freezes in some state of oscillation. Ventilation and removal of latent heat from the drop will be increased due to the increased surface area. Therefore, one would expect more oblate than prolate ellipsoids. A drop frozen in an elongated state inevitably would attain a terminal velocity lower than the original unfrozen spherical drop. The decrease of drop terminal velocity during freezing will increase the time needed for a drop to travel from the air to the ground during the spray freezing process, consequently increases ice formation within the drop.

Pitter and Pruppacher (1973) indicated that a drop terminal velocity could be reduced by 6 to 7 percent during the few seconds of freezing. The velocity decrease might be evaluated by using:

$$V_{\infty} = (2gQ(\rho_w - \rho_a) / S\rho C_D)^{1/2} \quad (4.1)$$

where Q and S are the droplet volume and surface area normal to the flow, ρ_w and ρ_a are the densities of the drop and the air, C_D is the drag force coefficient of the drop and g is the acceleration of gravity. ρ_w decreases 8 percent or more while Q/S increases up to 3 percent as the drop undergoes phase change. According to equation (4.1) and the above parameter changes, the drag force coefficient C_D may increase up to 6 percent. i.e. a higher drag force, during the freezing of a drop. The drag force coefficient C_D cannot be computed because it is a derived quantity of the flow field past the drop and depends on the droplet shape and surface roughness.

3. Some drops had the same terminal velocity and shape as the unfrozen drops. It happened mostly in piggery wastewater drops. As mentioned before, liquid piggery wastewater drops were relatively stable in the updraft, after freezing, there was no obvious change in the terminal velocity except for the vertical rotation of the drops.

4. Some drops moved horizontally or in a circle after they froze. While maintaining the basic drop shape (flat on the bottom and round on the top), some drops span and tumbled and followed some mode of a helical trajectory before they moved out of the updraft. However, some drop trajectories became much more regular once they froze, for example, T.P.W. drops. McDonald (1954) indicated that the center of drag forces of a drop is below the center of gravity of the drop. When the drop is liquid it can always adjust its shape to this coupled force. Upon freezing, a shell of ice forms around

the drop, the shape of the drop is fixed and it can no longer adjust its equilibrium shape. It is possible that the coupled force inverts the frozen drop to a more stable and faster fall position. Some frozen drops were observed to remain stable for minutes, especially, the piggery wastewater and T.P.W. drops.

5. Some drops increased in terminal velocity after freezing. Most of them were the larger (37.7 μL) piggery wastewater and T.P.W. drops. These drops suspended in the updraft for a longer time after freezing before they fell slowly on to the top of the small screen located between the working section and the converging section of the tunnel. This phenomenon occurred under all temperatures tested. Spenglar (1971) also observed this phenomenon in his experiment at temperatures $-6\text{ }^{\circ}\text{C}$ and warmer. No explanation can be offered for this slight increase in the droplet falling velocity.

4.3.3 Fragmentation of freezing water drops

The phenomena of fragmentation of freezing water drops was observed by many researchers (e.g. Mason, 1965a; Langham and Mason, 1958; Mason and Maybank, 1960; Dye and Hobbs, 1968; Hallett, 1968 and Hobbs and Alkenzweeny, 1968).

It also was observed in this study that as freezing proceeded the ice shell of some drops fractured and the unfrozen liquid inside of the drop squeezed out on to the ice surface of the drop. The crack usually occurs at the top of the drop. Then a protrusion formed as the drop continued to remain suspended in the updraft. Among the wastewaters tested, formation of protrusion only occurred in pulp mill effluent and T.P.W. and no bulging ever occurred in the piggery wastewater drops. The protrusion grew larger as freezing proceeded. The process of forming a protrusion was recorded on the video tapes. Plate 6 exhibits the process of the stabilizing of a T.P.W. drop after being brought into the updraft of the wind tunnel (Plate 6-a) and the two protrusions formed on the drop after freezing. Plate 7 shows a 4.2 mm diameter pulp mill effluent drop before freezing (Plate 7-a) and formation of a protrusion and a crack during freezing (Plate 7-b). The reason for the interest in this phenomenon is that if it happens to the

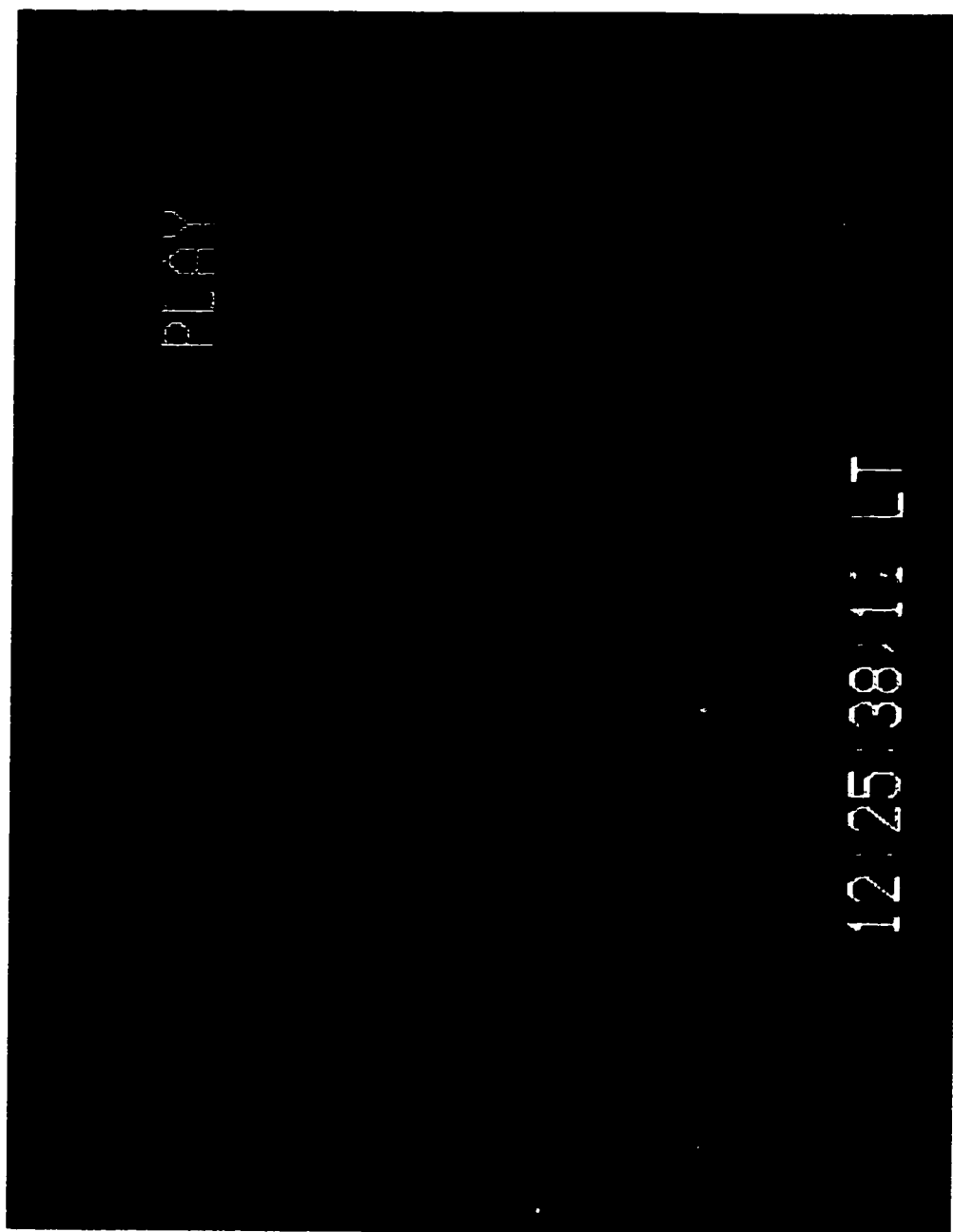


Plate 4.6 The illustration of the stabilizing of a 4.2 mm diameter oil sands tailings pond water drop (a) and (b) the formation of two protrusions on the drop after freezing.

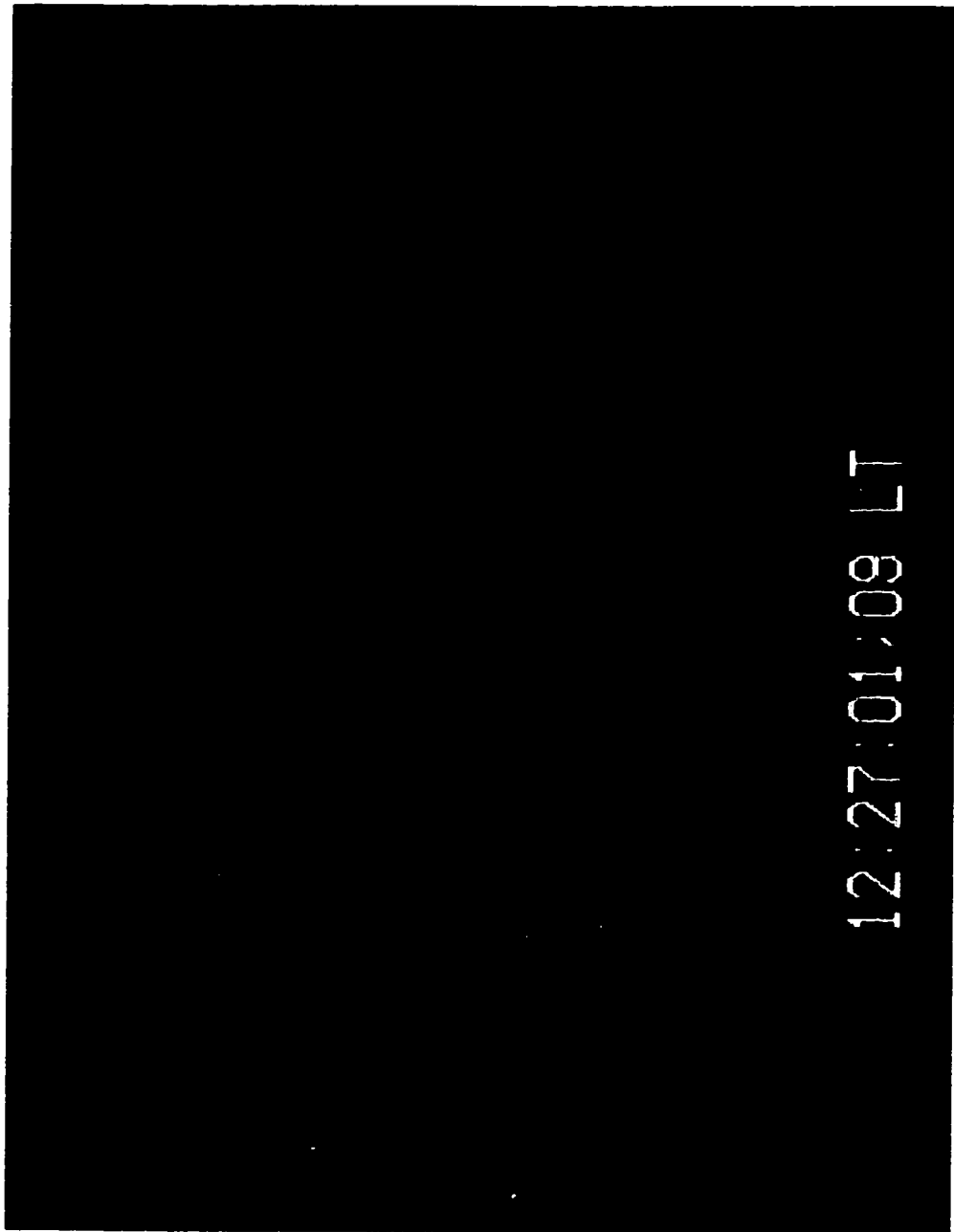


Plate 4.6-b The formation of two protrusions on the drop after freezing.

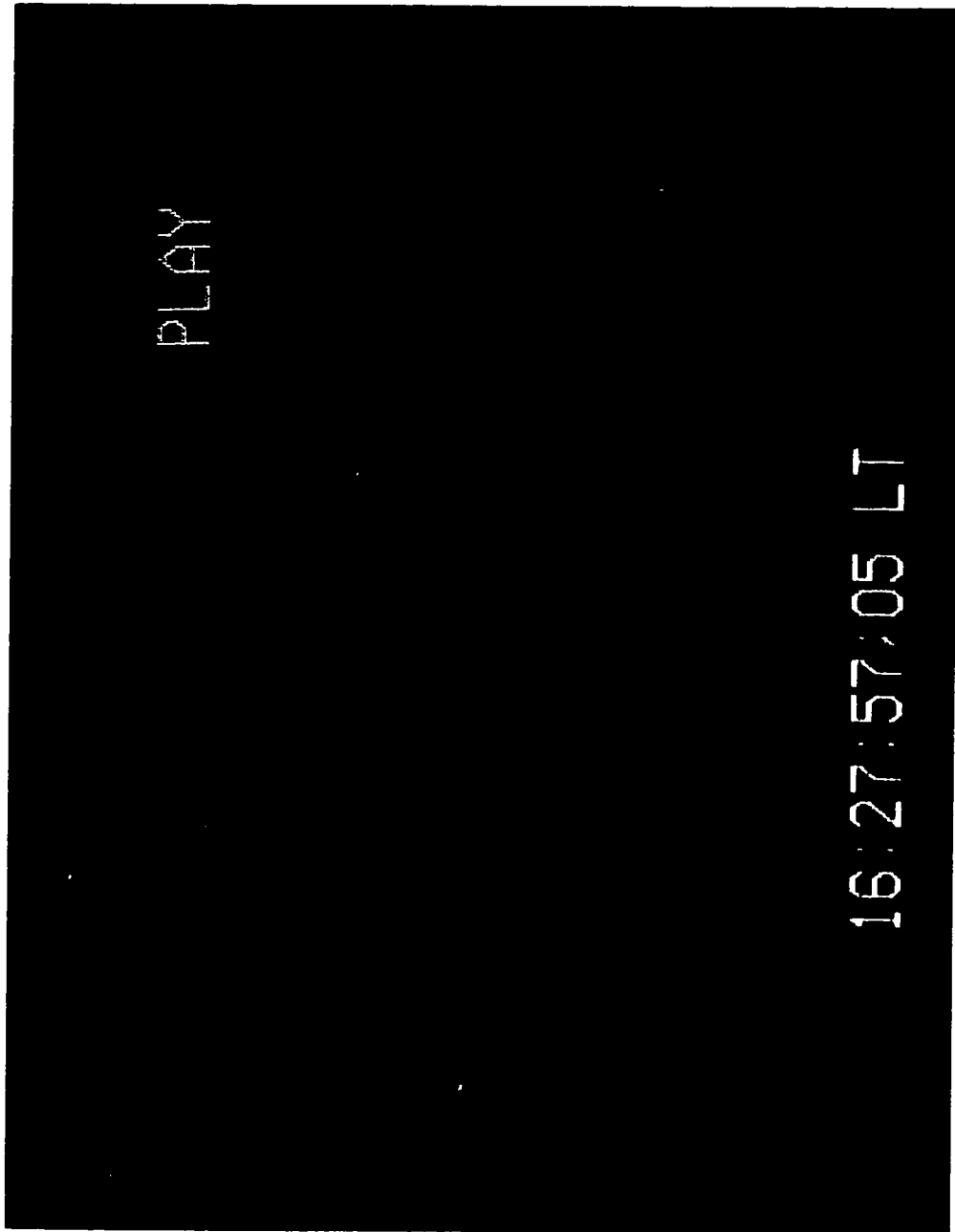


Plate 4.7 The illustration of a 4.2 mm diameter pulp mill effluent drop before freezing (a) and (b) a protrusion and crack formed after freezing.

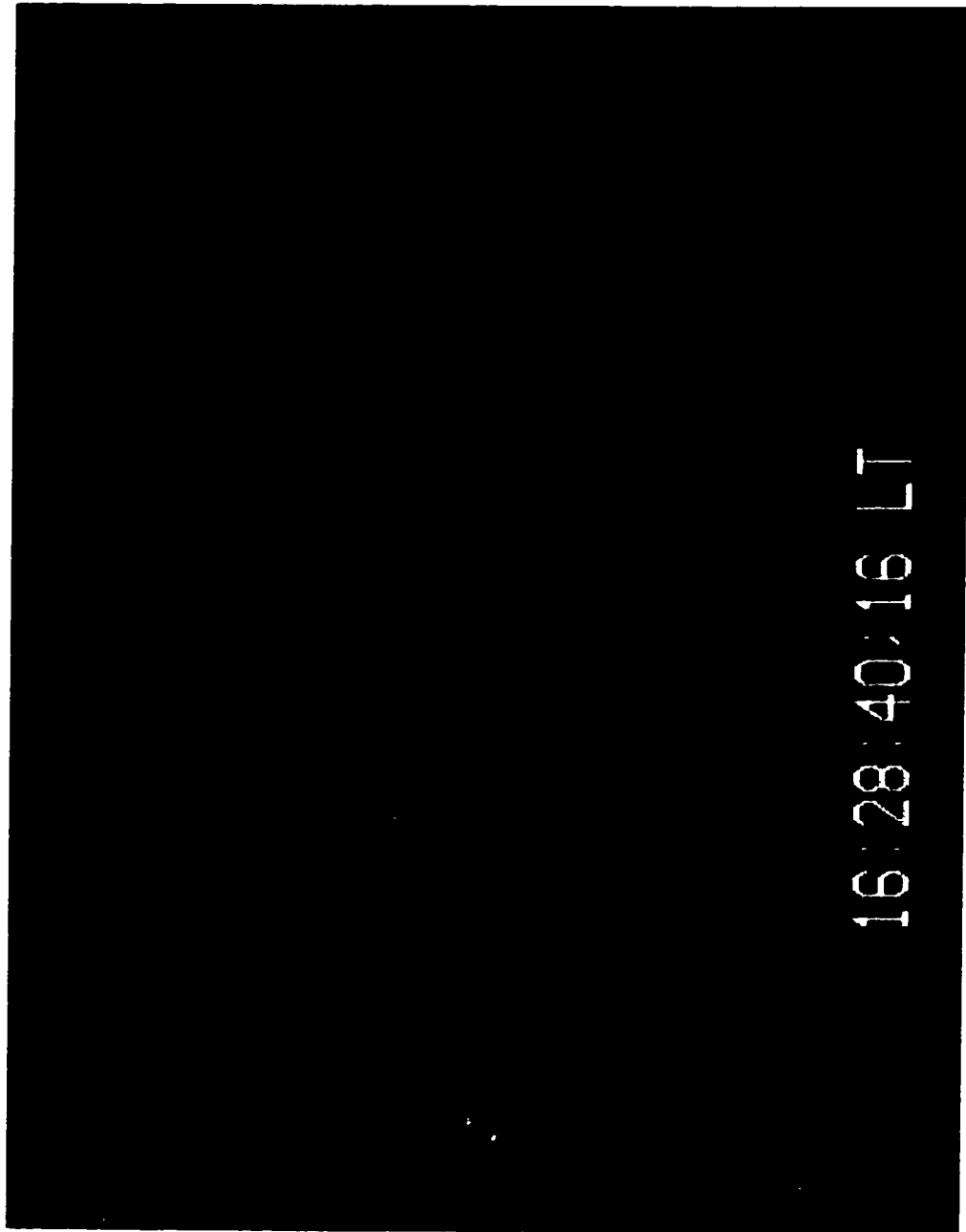


Plate 4.7-b A protrusion and crack formed after freezing.

drops during spray freezing operation, the impurities will be concentrated in the unfrozen liquid and then is squeezed out of the drop. Some impurities may be lost in the air. It is found that the time required to form a protrusion for a drop frozen under -18°C is in the range of 14.7 to 246.5 seconds for T.P.W and 18.0 to 223.8 seconds for pulp mill effluent drops. When a drop frozen under warmer temperature, the time required to crack the drop is increased.

The air residence time of a water during spray freezing operation is determined by many factors such as nozzle pressure, shooting angle, droplet size etc. but it usually takes less than 10 seconds. Therefore, for majority of the sprayed wastewater drops, there is not sufficient time to crack the ice shell while the droplet is travelling through the cold air. Only a portion of the drop froze before it landed on the ground.

Fracture of the ice shell of frozen drops occurs in the second stage of freezing. During this stage of freezing, as mentioned before, ice continues to grow rapidly inwards from the surface of the drop. Expansion caused by phase change of the water inside of the drop during this stage build up pressure in the interior of the drop. Rupture of the shell, occurs at a weak point where a protrusion forms as the liquid from the interior is extruded.

The probability for a drop to fracture or fragment during freezing is affected by many factors. It is known that the nucleation temperature of the drop is one of them. The probability of fragmentation is higher for a drop with higher nucleation temperature since there is a larger amount of water remaining to undergo phase change in the second stage of the freezing. Mason and Maybank (1960) indicated that the air content of the water influence the shattering of freezing water drops. The air content of a drop is controlled by the drop temperature since the solubility of air in water increases rapidly with decreasing temperature. When a drop nucleates at a warmer temperature, a very small amount of air can escape from the surface to the atmosphere and the ice shell formed is mechanically strong. A protrusion may appear at the weak spot and develop into a spike. A drop may

even break into several fragments when the expansion of the interior cannot be held by extrusion through spikes and through the nearly impervious shell. Larger quantities of air would be liberated and trapped in the ice shell and cause a spongy texture in it when a drop freezes under strong supercooling. This yields more readily to the expansion, part of which is taken up by compression of the entrapped air. Numerous cracks and fissures appear in the ice shell through which the liquid is extruded. The occurrence of spikes and violent shattering is rare and fewer ice splinters are produced. The low nucleation temperature of piggery wastewater drops may be one of the reasons that prevent piggery wastewater drops from breaking during freezing. The nucleation temperature of piggery wastewater is several degrees colder than that of pulp mill effluent and oil sands tailing pond water. It also explains why smaller drops are less likely to fragment: drops with smaller diameter have lower nucleation temperature. Only cracking of frozen drops were observed in this study and no shattering of drops occurred.

Dye and Hobbs (1968) pointed out that except for the nucleation temperature of the drop, the nature and concentration of gases dissolved in the drop prior to its nucleation, the condition of the drop with respect to its environment, and the manner in which heat is removed from a drop all affect the freezing behavior of a suspended drop. Dye and Hobbs (1968) found that if drops which are nucleated before coming to thermal equilibrium with the environment, or are nucleated at warmer temperatures and then freeze rapidly at a lower temperature will show more disruptive activity during freezing than do drops frozen at thermal equilibrium. A fast freezing rate and symmetrical heat transfer are likely to favor fragmentation. Since the ice shell has less time to accommodate to the rapidly increasing pressure at fast freezing rate, the chances for a frozen drop to break may increase. If the ice shell freezes asymmetrically, it will not have a uniform strength so the pressure may be relieved at a weak point in the shell by forming a protrusion or a spike without shattering of the drop while the pressure may only be relieved by breaking the drop when an ice shell grow symmetrically with respect to the center of the drop. Theoretically, if the effects of the distribution and growth of gas bubbles on fragmentation are ignored, a drop frozen in air or carbon dioxide at 1 atm

would be less likely to fragment than one frozen in air at 0.1 atm or hydrogen in 1 atm. because heat transfer from the drop is more symmetrical when the ambient air pressure is 0.1 atm or the ambient gas is hydrogen with a pressure of 1 atm. Dye and Hobbs (1968) indicated that all above mentioned parameters interact and make the freezing of a water drop an extremely complex phenomenon; as a result, it is not possible to predict with certainty whether or not a drop will fragment when it is nucleated and frozen under a given set of conditions.

Pruppacher and Schlamp (1975) found that water drops submerged with clay particles and falling at terminal velocity in air within a wind tunnel did not shatter and they produced fewer drops with surface breaks. Mason and Maybank (1960) also noticed that solid impurities contained within the drops had little effect on fragmentation except in so far as they might raise the nucleation temperature of the droplet.

4.4 The Freezing Time Required for A Freely Suspended Wastewater Drop

Following are the experimental results obtained from the freely suspended wastewater drop freezing test. The time required for a freely suspended drop to freeze under various experimental conditions was obtained by examining the video tapes recorded during the experiment. The video tapes with recording time was viewed frame by frame. The time was calculated from the moment of a drop is introduced into the updraft to the moment of freezing of the droplet surface. For most drops the freezing time can be accurate to 1/30 second or 1 video frame. Although the freezing process of water drops was studied using high speed photographic techniques in the past, the videographic technology made it possible not only to inspect the freezing process but also to measure the freezing time accurately in a simple and economical way. The video camera speed selected will be directly related to the time required for viewing the video tapes.

As shown previously, that macroscopically identical drops of any type of water do not freeze at a single temperature but over a range of temperatures. Therefore, it was expected that the time required for freezing of a collection of visibly identical drops would also spread over a certain range. The distribution of the freezing time for each type of freely suspended wastewater drops was presented in the form of histogram for each experimental condition (Appendix B).

The experimental results presented in the Figures AB-1 to AB-11 (Appendix B) revealed that the time required for a wastewater drop to freeze has the following common characteristics:

1. Smaller drops need less time to freeze, which is reasonable since smaller drops have larger surface to volume ratio thus heat and mass transfer rate will be higher as compared to that of larger drops so less time is required for small drops to reach ice nucleation temperature.

2. As expected, droplets freeze faster at colder temperature, this is due to the higher cooling rate. As air temperature decreases, the temperature difference between the drop and the air increases. The heat exchange between the drop and the air is more rapid and this induces a higher rate of cooling in a drop. Under cold air temperature, less supercooling will occur in the drops. The droplet surface is cooled to the nucleation temperature in such a short time that no significant supercooling takes place before freezing begins. While most drops will be supercooled without changing phase when the air temperature is warmer. The driving temperature difference decreases and the heat exchange between the droplet and the air is less, consequently, more time is required to freeze the drop.

3. Droplet freezing time spreads over a wider range as air temperature warms. The probability to find an active ice nucleus declines with increasing air temperature. Some droplets need much longer time than the others to freeze.

4. pH of the wastewater drops affects the time required to freeze. The mean (or the median) freezing time for droplets with basic pH (pH = 11.0) is longer than that of the droplets with original liquid pH except in one case (T.P.W. drops with a 37.7 μ L volume, air temperature is about - 18 °C) in which droplets with basic pH have shorter freezing time. The results are opposite to those obtained from the droplet nucleation test (Chapter 3). In that test droplets froze at slightly warmer temperature when the liquid pH was adjusted to 11.0 (The temperature increase was 0.6, 0.4 and 0.4 for piggery wastewater, pulp mill effluent and T.P.W., respectively). The delay in the freezing time changes with wastewater, droplet size and the air temperature. As in droplet nucleation test, the freezing temperature of T.P.W. is again least sensitive to the pH change but the droplet freezing temperature of piggery wastewater is more easily influenced by the pH modification. The prolongation of the freezing time for piggery wastewater drops including both large and small drops is in the range of 5.9 to 0.6 seconds based on the comparison of the median freezing temperature. The maximum increase in freezing time required was 2.9 (minimum = 1.7) second for pulp mill effluent drops with basic pH and a maximum of 2.5 second (minimum - 1.3 second, i.e. a decrease in freezing time) for T.P.W. The reason why droplets with basic pH needs longer freezing time is not clear but the cooling rate may be the reason (or one of the reasons) that cause the difference in the results obtained from the two experiments. In the droplet nucleation test, a constant cooling rate is used and the cooling rate is much slower while in the freely suspended droplet freezing test droplets are cooled naturally (variable cooling rate) at a faster speed. The effectiveness of the ice nuclei is depressed somehow by the pH adjustment.

The mean and the median freezing times required by wastewater drops under various conditions are summarized in Table 4-1 to Table 4-3.

The average freezing time required by 4.2 mm diameter wastewater drops versus air temperature is displayed in Figure 4-4. There was no pH adjustment on the wastewaters. As displayed in Figure 4-4, under the same conditions piggery wastewater drops take much longer time to freeze. For example, in a -6.7 °C environment, freezing

Table 4-1 The Freezing Time Required for Piggery Wastewater Drops

Air temperature (°C) and Humidity (%)	Droplet volume (μL)	Sample pH	Freezing time required (s)	
			Mean	Median
-6.7, 82	21.2 (equivalent diameter = 3.4 mm)	7.1 (original sample pH)	70.3 max. ¹ = 267.0 min. ² = 13.4 (n ³ = 41)	42.4
	37.7 (equivalent diameter = 3.4 mm)		77.7 max. = 422.4 min. = 22.6 (n = 32)	45.7
-7.4, 84	21.2	7.1	42.0 max. = 104.3 min. = 17.5 (n = 35)	32.1
-10.3, 75	21.2	7.1	16.0 max. = 28.0 min. = 8.3 (n = 70)	15.1
		11.0	23.3 max. = 70.4 min. = 9.2 (n = 65)	20.6
		7.1	19.4 max. = 37.0 min. = 11.0 (n = 90)	18.6
	37.7	7.1	19.4 max. = 37.0 min. = 11.0 (n = 90)	18.6
		11.0	31.4 max. = 221.5 min. = 9.5 (n = 95)	24.5
		7.1	19.4 max. = 37.0 min. = 11.0 (n = 90)	18.6
-17.7, 71	21.2	7.1	7.0 max. = 11.1 min. = 2.6 (n = 48)	6.7
		11.0	7.5 max. = 14.3 min. = 2.8 (n = 56)	7.4

	37.7	7.1	7.4 max. = 12.7 min. = 2.6 (n = 89)	7.4
		11.0	8.4 max. = 19.6 min. = 4.8 (n = 85)	8.0

¹ the maximum freezing time

² the minimum freezing time

³ the number of droplets tested

Table 4-2 The Freezing Time Required for Pulp Mill Effluent Drops

Air temperature (°C) and Humidity (%)	Droplet volume (μL)	Sample pH	Freezing time required (s)	
			Mean	Median
-5.5, 80	12.0 (equivalent diameter = 2.8 mm)	7.6 (original)	43.1 max. ¹ = 271.3 min. ² = 16.0 (n ³ = 32)	27.3
	37.7 (equivalent diameter = 4.2 mm)	7.6	85.4 max. = 329.7 min. = 17.8 (n = 52)	49.5
-6.7, 82	12.0	7.6	21.5 max. = 51.6 min. = 10.9 (n = 60)	18.0
	37.7	7.6	45.5 max. = 274.5 min. = 16.4 (n = 50)	29.9
-7.4, 84	12.0	7.6	15.0 max. = 22.3 min. = 9.7 (n = 42)	14.9
	37.7	7.6	22.4 max. = 30.6	21.2

			min. = 16.7 (n = 31)	
-10.3, 75	12.0	7.6	7.6 max. = 12.8 min. = 3.3 (n = 78)	7.4
		11.0	10.7 max. = 19.6 min. = 5.0 (n = 85)	10.3
		7.6	12.0 max. = 17.5 min. = 8.5 (n = 90)	12.0
		11.0	15.0 max. = 27.0 min. = 6.7 (n = 95)	14.5
-17.7, 71	12.0	7.6	2.5 max. = 4.7 min. = 1.0 (n = 47)	2.3
		11.0	4.2 max. = 7.0 min. = 1.6 (n = 62)	4.0
		7.6	4.3 max. = 7.0 min. = 0.8 (n = 85)	4.3
		11.0	5.8 max. = 8.5 min. = 1.2 (n = 94)	6.0

¹ the maximum freezing time

² the minimum freezing time

³ the number of droplets tested

Table 4-3 The Freezing Time Required for Oil Sands Tailings Pond Water Drops

Air temperature (°C) and Humidity (%)	Droplet volume (μL)	Sample pH	Freezing time required (s)	
			Mean	Median
-5.5, 80	12.0 (equivalent diameter = 2.8 mm)	8.3 (original)	33.1 max. ¹ = 197.4 min. ² = 14.2 (n ³ = 28)	24.6
	37.7 (equivalent diameter = 4.2 mm)	8.3	98.2 max. = 321.8 min. = 24.2 (n = 68)	55.4
-6.7, 82	12.0	8.3	20.1 max. = 77.8 min. = 9.0 (n = 58)	16.7
	37.7	8.3	52.8 max. = 308.0 min. = 17.5 (n = 53)	30.0
-7.4, 84	12.0	8.3	16.9 max. = 30.0 min. = 10.5 (n = 36)	15.8
	37.7	8.3	23.9 max. = 41.1 min. = 10.5 (n = 30)	23.5
-10.3, 75	12.0	8.3	8.4 max. = 12.4 min. = 2.9 (n = 96)	8.3
		11.0	9.5 max. = 15.3 min. = 5.8 (n = 82)	9.3
	37.7	8.3	13.3 max. = 21.7 min. = 6.2	13.2

		11.0	(n = 91) 15.9 max. = 25.6 min. = 6.6 (n = 99)	15.7
-17.7, 71	12.0	8.3	3.1 max. = 4.7 min. = 0.6 (n = 49)	3.0
		11.0	4.1 max. = 7.4 min. = 1.8 (n = 72)	4.0
	37.7	8.3	5.6 max. = 8.8 min. = 1.0 (n = 91)	5.8
		11.0	4.5 max. = 14.4 min. = 1.0 (n = 85)	4.5

¹ the maximum freezing time

² the minimum freezing time

³ the number of droplets tested

was delayed by 31.6 seconds in the piggery wastewater drops as compared to the pulp mill effluent drops or 24.8 seconds when compared to the T.P.W. drops. The difference in the time spent by droplets before freezing suggests that the piggery wastewater drops have the lowest freezing temperature and the pulp mill effluent drops have highest freezing temperature. Several piggery wastewater drops were suspended in the updraft of the wind tunnel at - 5.5 °C during the test. The drops suspended in the air for more than 17 minutes without freezing before they finally floated out of the updraft. According to

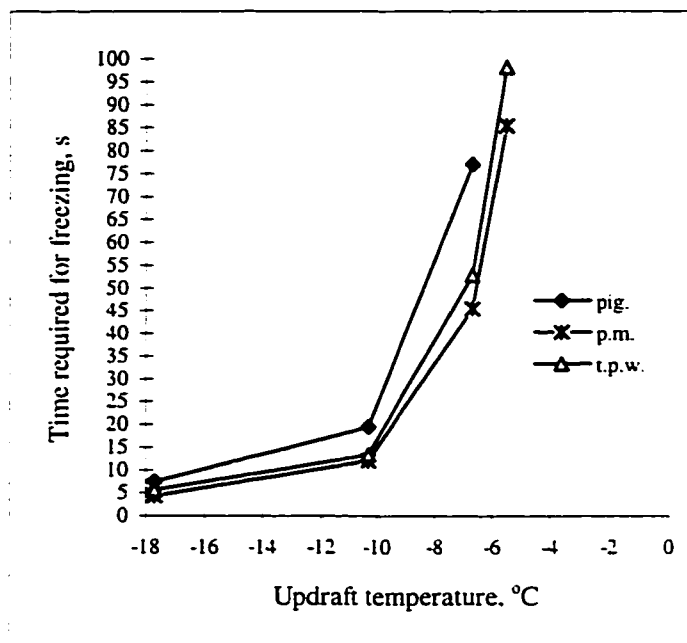
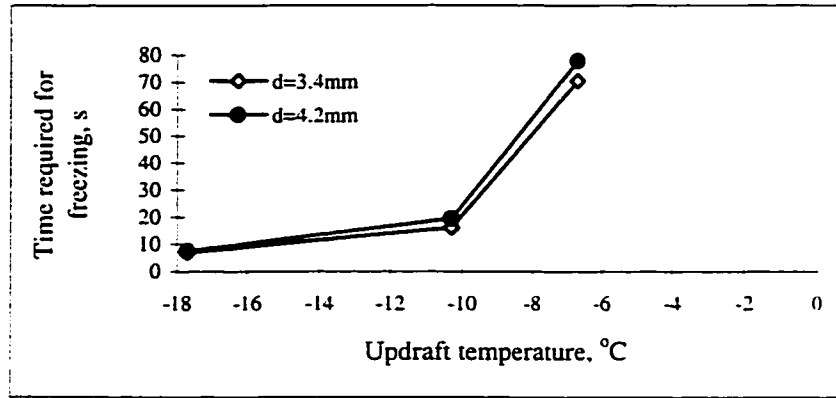


Figure 4-4 The average freezing time required by the 4.2 mm diameter wastewater drops as a function of the ambient air temperatures.

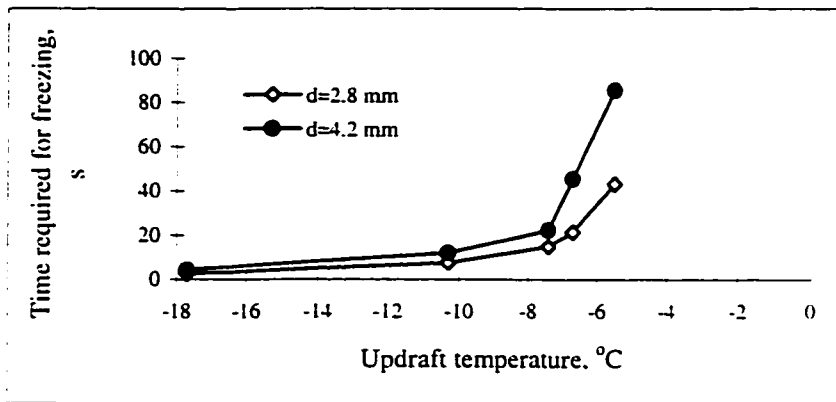
the time required, the freezing temperature of T.P.W. drops was between the other two wastewaters. The discrepancy in the required freezing time decreases with decreasing air temperature. When air temperature falls to about - 18 °C, the difference in the average freezing time between the pulp mill effluent and piggery wastewater was reduced to 3.1 seconds and 1.8 seconds between piggery wastewater and T.P.W. respectively

The average freezing time as a function of the ambient air temperature and droplet size is shown in Figure 4-5. The average time required for freezing dropped dramatically when the ambient temperature fell from -5.5°C to -7.4°C for pulp mill effluent drops and T.P.W. drops, especially, for the large drops. The distinct reduction in the freezing time happened when the air temperature dropped from -6.7°C to about -10°C for piggery wastewater drops. The difference in the freezing time between the 2.8 mm diameter and 4.2 mm diameter drops was enormous in the warm air temperature range (-5.5°C to -6.7°C) for pulp mill effluent and T.P.W. drops. For pulp mill effluent drops with 4.2 mm diameter needed an additional 24 to 42.3 seconds to start the ice nucleation as compared with 2.8 mm diameter drops, while for large T.P.W. drops 32.7 to 65 seconds extra time was necessary for the large drops to freeze in the warm air temperature range. The freezing time difference caused by the droplet size difference lessens as air temperature decreases. At -18°C , it was only 1.8 seconds for pulp mill effluent drops and 2.5 seconds for T.P.W. drops. At warmer air temperature, the cooling of the small drops was faster than the large ones because of the larger exposed surface area per unit volume of water; less time was required for small drops to reach the ice nucleation temperature. As we know from the nucleation test (Chapter 3) that the freezing temperature of the wastewater drops are volume dependent and the larger drops freeze at a warmer temperature than the small ones. The cooling rate increases for both small and large drops as air temperature become colder but freezing occurs at a warmer temperature for the larger drops since fewer ice nuclei (or lower ice nucleus concentration) is required for the ice nucleation and consequently reduces the time difference. The difference in the required freezing time between the large drops and the small drops will keep decreasing with decreasing ambient air temperature. Due to the closeness in the droplet sizes, the difference in the required freezing time for piggery wastewater drops was not apparent, however, the curves follow the same trend as those of the pulp mill effluent and T.P.W. drops.

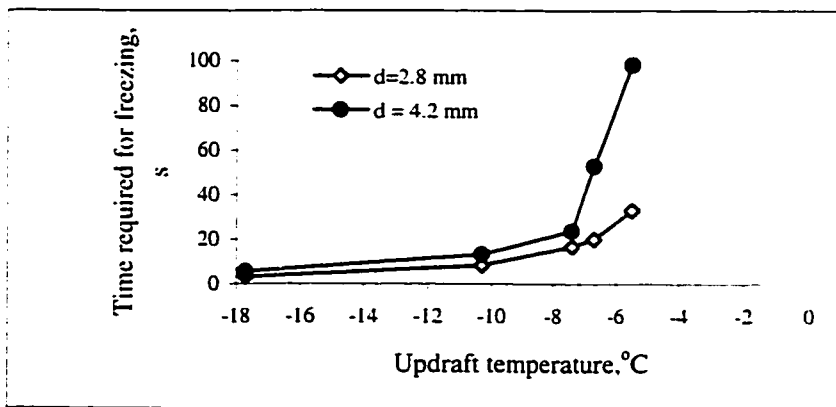
The data for the required freezing time for different volumes (sizes) of drops vs. the air temperature (such as those shown in Figure 4-4 and 4-5) are essential for the



(a)



(b)



(c)

Figure 4-5 The droplet freezing time as a function of the updraft temperature and the droplet diameter. (a) piggery wastewater drops; (b) pulp mill effluent drops and (c) oil sands tailings pond water drops.

optimization of a spray freezing operation. The experimental results obtained from this study indicates that during a spray freezing operation larger size of droplets can be used as ambient air temperature decreases without substantially affecting the ice production rate, it not only increases the volume of the water sprayed but also reduces the energy consumption for producing smaller drops. A lowest operating temperature can also be selected for each type of wastewater if the type of data shown in Figure 4-4 or 4-5 is available. Below this temperature, a spraying operation should be stopped.

4.5 Cooling and Ice Fraction in a Freely Falling Wastewater Drop

4.5.1 The terminal velocity of a freely falling water drop

In order to predict the freezing temperature and the amount of ice formed in a freely suspended or falling water drop, the velocity of the drop and the heat and mass transfer rates from the water drop must be determined first. Combining the information on the droplet freezing time obtained from the experiment and the heat and mass transfer rate under various air temperatures, the droplet nucleation temperature can be predicted.

In a spray freezing operation, the sprayed water jet will break up into individual drops near the apex of its trajectory. The water drops have a zero initial velocity in the vertical direction at the apex of the trajectory where the jet breaks up and the velocity will increase to its terminal velocity as they descend. The terminal velocity for a water drop in the vertical direction is given by Zarling (1980):

$$U = \sqrt{\frac{4dg(\rho_w - \rho_a)}{3\rho_a C_D}} \quad (4.2)$$

Where:

U = velocity, m/s

d = droplet diameter, m

g = gravitational acceleration, m/s²

ρ_w = water drop density, kg/m³

ρ_a = air density, kg/m³

C_D = drag coefficient and it is expressed as a function of Reynolds number. Re , which is the ratio of the inertial to the viscous forces (Chen and Trezek, 1977):

$$C_D = \frac{24}{Re} + \frac{6}{1 + \sqrt{Re}} + 0.27 \quad \text{for } 1 < Re \leq 1000 \quad (4.3)$$

$$C_D = 0.6649 - 0.2717 \times 10^{-3} Re + 1.22 \times 10^{-7} Re^2 - 10.919 \times 10^{-12} Re^3 \quad (4.4)$$

for $1000 \leq Re \leq 3600$.

4.5.2 Cooling of a freely suspended wastewater drop

To predict the droplet freezing temperature, the knowledge of the temperature of a drop versus the length of time in suspension is necessary. If assuming that a drop is completely mixed due to vigorous internal motion and no change in ambient air temperature during the fall, the time rate of change of energy must be equal to the thermal energy transport by convection, evaporation and radiation. The radiation heat can be neglected (Zarling, 1980). Zarling's (1980) differential equation which predicts the droplet temperature change can be simplified as:

$$\rho_w C_p V \frac{dT_w}{dt} = -A[h_c(T_w - T_\infty) + h_D L_{ev} \rho_a (W_s - W_\infty)] \quad (4.4)$$

or

$$\frac{dT_w}{dt} = \frac{-6}{\rho_w C_p d} [h_c(T_w - T_\infty) + h_D L_{ev} \rho_a (W_s - W_\infty)] \quad (4.5)$$

where:

C_p = specific heat of water, kJ/kg °C

V = drop volume, m³

A = surface area of drop, m²

h_c = convective heat transfer coefficient, W/m² °C

h_D = convective mass transfer coefficient, m/s

T_w = water drop temperature, °C

T_∞ = ambient temperature, °C

ρ_a = air density, kg/m³

ρ_w = water density, kg/m³

L_{ev} = latent heat of evaporation, kJ/kg

W_s = saturation humidity ratio

W_∞ = ambient humidity ratio

The heat and mass transfer coefficient, h_c and h_D can be determined using the Nusselt number (Nu), a dimensionless number, which accounts for the enhancement of heat loss by convection and Sherwood number (Sh), which is the analogue of the Nusselt number for mass transfer (Ranz and Marshall, 1952):

$$Nu = \frac{h_c d}{k_a} = 2 + 0.6 \text{Pr}^{1/3} \text{Re}^{1/2} \quad (4.6)$$

$$Sh = \frac{h_D d}{D} = 2 + 0.6 \text{Sc}^{1/3} \text{Re}^{1/2} \quad (4.7)$$

where Pr and Sc are the Prandtl number and Schmidt number, respectively, and D is the diffusivity of vapor in air. The value of h_c and h_D can be calculated using following formulas (Kusuda, 1965; Instanes, 1993):

$$h_c = \frac{k_a}{d} [2.0 + 0.6(\frac{v_a}{\alpha})^{1/3} (\frac{Ud}{v_a})^{1/2}] \quad (4.8)$$

$$h_D = \frac{D}{d} [2.0 + 0.6(\frac{v_a}{D})^{1/3} (\frac{Ud}{v_a})^{1/2}] \quad (4.9)$$

where

$$k_a = (0.0242 + 7.7 \times 10^{-7} T_\infty) \quad (4.10)$$

$$\nu_a = (1.315 \times 10^{-5} + 9.56 \times 10^{-8} T_\infty) \quad (4.11)$$

$$\alpha = (1.855 \times 10^{-5} + 1.32 \times 10^{-7} T_\infty) \quad (4.12)$$

$$D = (2.144 \times 10^{-5} + 1.73 \times 10^{-7} T_\infty) \quad (4.13)$$

where

k_a = thermal conductivity of air; α = thermal diffusivity; ν_a = kinematic viscosity of air, and the others have been defined before. The saturation humidity ratio, W_s , is a polynomial function of temperature. Taking the first three terms of the polynomial function, W_s can be expressed as:

$$W_s = C_1 T_w^2 + C_2 T_w + C_3 \quad (4.14)$$

where C_1 , C_2 , and C_3 are constants, and

$$W_\infty = C_1 T_\infty^2 + C_2 T_\infty + C_3 \quad (4.15)$$

thus the humidity ratio potential is:

$$W_s - W_\infty = C_1 (T_w^2 - T_\infty^2) + C_2 (T_w - T_\infty) \quad (4.16)$$

the values of C_1 , C_2 , and C_3 in the different temperature ranges are (Instanes. 1993):

for $-10\text{ }^{\circ}\text{C} \leq T_w < 0\text{ }^{\circ}\text{C}$

$$C_1 = 8.4709 \times 10^{-6}, \quad C_2 = 3.0125 \times 10^{-4} \quad C_3 = 3.7794 \times 10^{-3}$$

for $-20\text{ }^{\circ}\text{C} \leq T_w < -10\text{ }^{\circ}\text{C}$

$$C_1 = 4.0465 \times 10^{-6}, \quad C_2 = 2.1739 \times 10^{-4} \quad C_3 = 3.3705 \times 10^{-3}$$

for $-30\text{ }^{\circ}\text{C} \leq T_w < -20\text{ }^{\circ}\text{C}$

$$C_1 = 1.8250 \times 10^{-6}, \quad C_2 = 1.3107 \times 10^{-4} \quad C_3 = 2.5265 \times 10^{-3}$$

substituting equation 4.16 into equation 4.5:

$$\frac{dT_w}{dt} = \frac{-6}{\rho_w C_p d} [(h_c + h_D L_{ev} \rho_a B)(T_w - T_{\infty}) + h_D L_{ev} \rho_a A(T_w^2 - T_{\infty}^2)] \quad (4.17)$$

$$\text{let} \quad a = \frac{-6}{\rho_w c_p d} (h_c + h_D L_{ev} \rho_a B) \quad \text{and} \quad b = \frac{-6}{\rho_w c_p d} h_D L_{ev} \rho_a A$$

then equation 4.17 can be simplified as:

$$\frac{dT_w}{dt} = a(T_w - T_{\infty}) + b(T_w^2 - T_{\infty}^2) \quad (4.18)$$

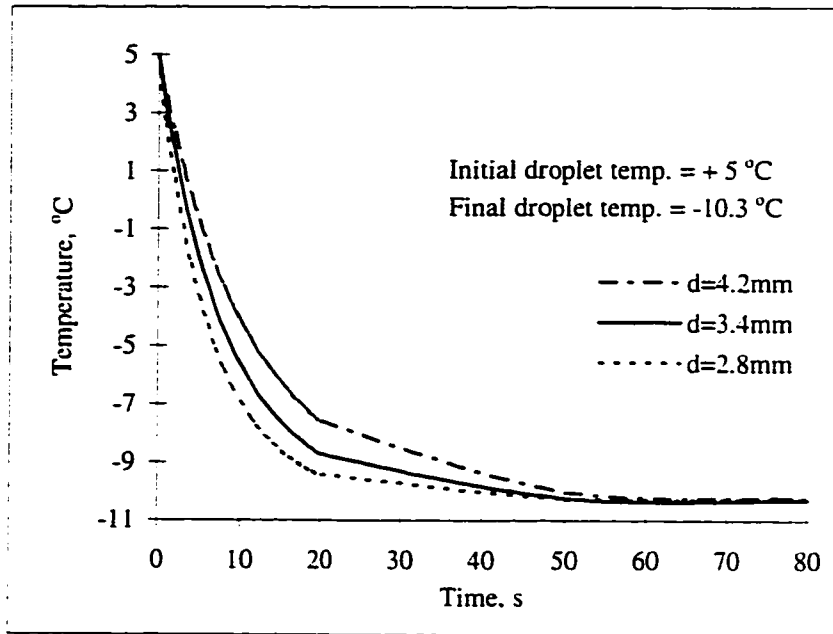
Integrating the above equation, the final equation is in the same form as that given by Instans (1993):

$$T_w = \left\{ -T_\infty \left[1 + \frac{(T_i + T_\infty + \frac{a}{b})e^{-t(2bT_\infty + a)}}{T_i - T_\infty} \right] - \frac{a}{b} \right\} / \left[1 - \frac{(T_i + T_\infty + \frac{a}{b})e^{-t(2bT_\infty + a)}}{T_i - T_\infty} \right] \quad (4.19)$$

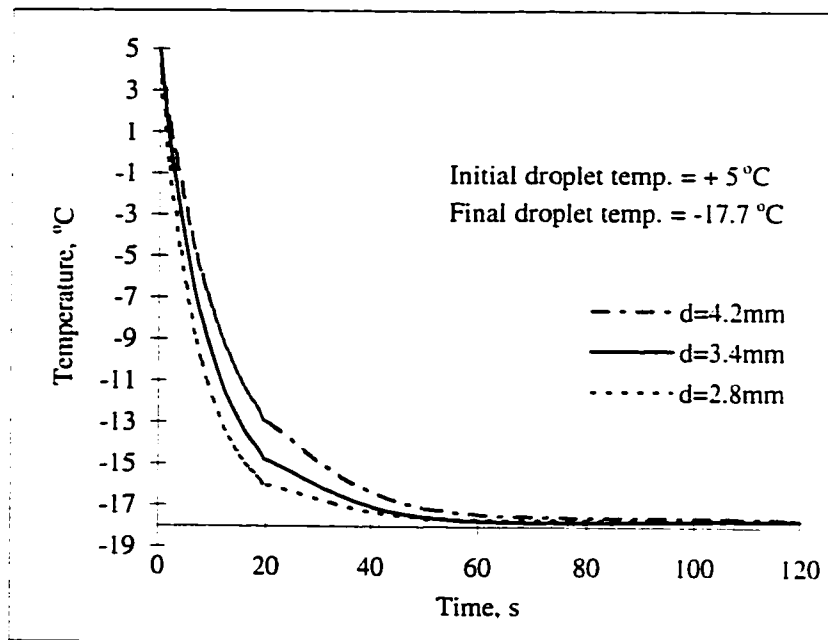
where T_i is the initial temperature of a water drop.

Equation 4.19 can be used to predict the temperature change in a droplet during the time of suspension or falling at its terminal velocity.

The droplet temperature as a function of time in suspension under various updraft air temperatures is presented in Figure 4-6. The cooling rate of the drops is predicted using equation 4.19. The drops entering the updraft of the wind tunnel with an initial temperature of + 5 °C cool to approach the updraft air temperature (wet bulb temperature) with the thermal relaxation time (a time required by a droplet to reach 63% of its equilibrium temperature after it has been transferred to a new environment). As anticipated, the smaller drops reach a lower temperature in a given suspension time (or a given falling distance) as compared to larger drops. Drops with different sizes have the same final temperature, however, the time required to reach the final temperature varies with droplet sizes. It is due to the fact that when the thermal equilibrium condition between the drops and the air is reached, the droplet temperature is the same as the air temperature thus no further cooling takes place. The cooling rate increases with increasing temperature difference between the droplet and the air, for example, the temperature of a 2.8 mm diameter droplet with an initial temperature of + 5 °C falls to

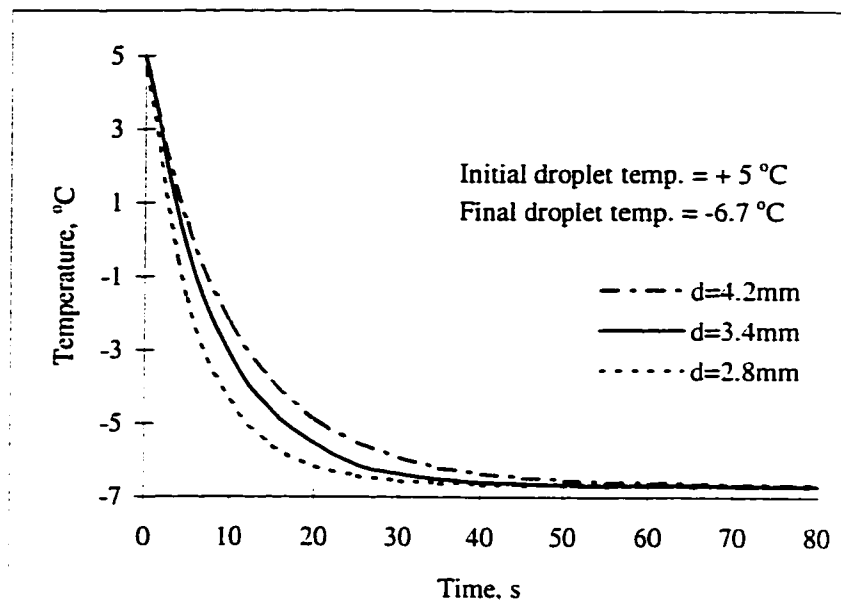


(a)

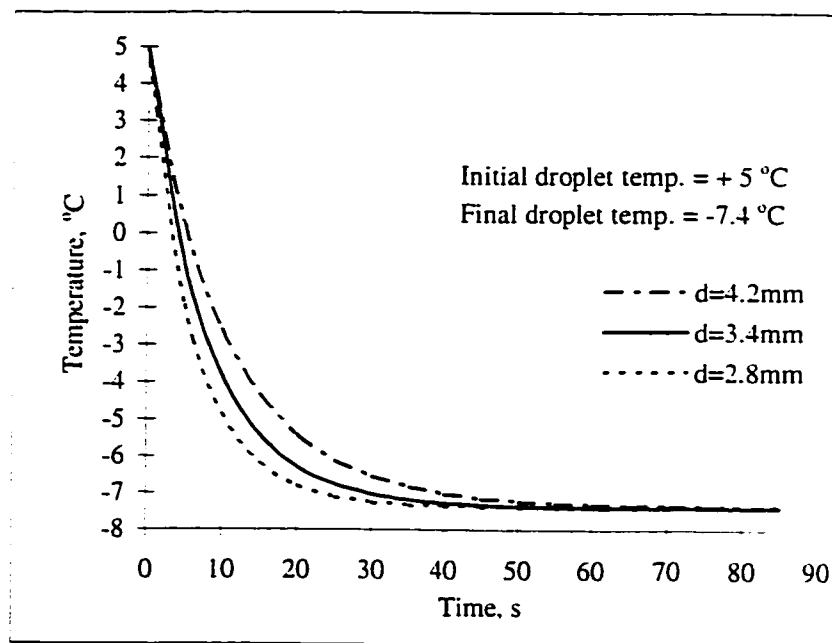


(b)

Figure 4-6-1 Cooling of freely suspended wastewater drops: (a) cooling from + 5 °C to - 10.3 °C and (b) cooling from + 5 °C to - 17.7 °C.



(c)



(d)

Figure 4-6-2 Cooling of freely suspended wastewater drops: (c) cooling from + 5 °C to - 6.7 °C and (d) cooling from + 5 °C to - 7.4 °C.

about - 17 °C after being suspended in the updraft for 20 seconds in a - 17.7 °C updraft temperature. For the same suspension time, the droplet temperature is only about - 6 °C if the air temperature is - 6.7 °C.

The ice nucleation temperatures of various suspended wastewater droplets were determined using equation 4.19. The average required freezing time which was obtained from the suspended droplet tests (Table 4-1 to 4-3) were used to determine the droplet freezing temperature in equation 4.19. The results are tabulated in Table 4-4.

Table 4-4-a The estimated freezing temperature of pulp mill effluent drops

Updraft air temperature (°C)	Estimated droplet ice nucleation temperature (°C)	
	d* = 4.2 mm	d = 2.8 mm
-5.5	- 5.5	- 5.5
- 6.7	- 6.5	- 6.3
-7.4	- 5.8	- 6.2
- 10.3	-5.1	- 5.5
	-6.2 (pH=11.0)	- 7.2 (pH= 11.0)
-17.7	-1.8	- 1.9
	-3.7 (pH=11.0)	- 5.1 (pH= 11.0)

* d = droplet diameter

Table 4-4-b The estimated freezing temperature of oil sands tailings pond water drops

Updraft air temperature (°C)	Estimated droplet ice nucleation temperature (°C)	
	d = 4.2 mm	d = 2.8 mm
- 5.5	- 5.5	- 5.4
- 6.7	- 6.6	- 6.2
-7.4	- 6.0	- 6.5
- 10.3	-5.6	- 6.0
	-6.5 (pH=11.0)	- 6.7 (pH= 11.0)
-17.7	-3.4	- 3.1
	-2.1 (pH=11.0)	- 4.2 (pH= 11.0)

Table 4-4-c The estimated freezing temperature of piggery wastewater drops

Updraft air temperature (°C)	Estimated droplet ice nucleation temperature (°C)	
	d = 4.2 mm	d = 3.4 mm
- 6.7	- 6.7	- 6.7
- 10.3	-7.5	- 7.9
	-9.2 (pH=11.0)	- 9.2 (pH= 11.0)
-17.7	-5.3	- 7.1
	-6.3 (pH=11.0)	- 7.6 (pH= 11.0)

According to the calculated results listed in the Table 4-4, droplet freezing occurs at a warmer temperature when the ambient air temperature is colder and the period of supercooling is only a small part of the entire heat loss process. As shown in Table 4-4-a, both 4.2 mm diameter and 2.8 mm diameter pulp mill effluent drops freeze at a temperature above $-2\text{ }^{\circ}\text{C}$ in a $-17.7\text{ }^{\circ}\text{C}$ environment. Contrarily, drops are deeply supercooled without change of phase when the ambient air temperature is warmer. For instance, in a $-6.7\text{ }^{\circ}\text{C}$ environment, all three types of wastewater drops are supercooled to $-6\text{ }^{\circ}\text{C}$ or below without undergoing phase change. The freezing of the droplets, as shown in Table 4-4, happens at a temperature very close to the ambient air temperature. Table 4-4 also indicates that under the same air temperature larger drops generally freeze at a slightly warmer temperature than those small ones. It is due to the fact that the probability for a droplet to contain a warmer temperature nucleus increases with increasing droplet volume (or diameter) and additionally large drops need fewer ice nuclei to initiate freezing. The calculated results also confirm that pulp mill effluent has the warmest ice nucleation temperature among the wastewaters tested and piggery wastewater drops have the coldest freezing temperature. The freezing temperature of oil sands tailings pond water drops is between the pulp mill effluent and the piggery wastewater drops. Piggery wastewater drops usually freeze at a temperature about 2 to 3 $^{\circ}\text{C}$ colder than the pulp mill effluent and oil sands tailings pond water.

The experimental results of the suspended wastewater droplet test once again demonstrate that the wastewater generated from different industries have distinct characteristics during freezing. The differences in the droplet freezing temperature among the wastewaters in the suspended droplet test are very similar to those results obtained from the droplet ice nucleation test in Chapter 3. As mentioned at the beginning of this Chapter, the ice nucleation test is a simple method to get information on the ice nucleus contents of the wastewaters, the influence of factors such as droplet volume and impurity concentration on the droplet freezing temperature or to compare the freezing characteristics of different water samples. However, the ice nucleation temperature of drops under constant cooling rate is very different from that of freely suspended or falling

drops because the experimental conditions differ from the conditions under which drops freeze in atmosphere during a full scale spraying operation. The ice nucleation temperature of a suspended water droplet varies with the ambient temperature. The results obtained from the freely suspended droplet freezing study can be applied directly to the design and optimization of a spray freezing process because of the similarity in the conditions of a freely suspended drop to a freely falling drop in the cold winter air.

4.5.3 The heat balance of a freezing drop and ice production

When droplet temperature reaches the nucleation temperature, the freezing process begins as the drop suspends or falls at its terminal velocity through cold air. The total amount of heat exchange with the environment determines the rate of freezing of a drop. Based on the assumptions made in section 4.5.2 and neglecting the heat released due to the cooling of the ice shell (the heat is insignificant compared to the latent heat released at the ice-water interface (Hobbs, 1972)), the total amount of the latent heat released at the freezing interface must equal to the heat loss at the surface of the drop by conduction, convection and evaporation:

$$L_f \frac{dm_i}{dt} = q_c + q_e \quad (4.20)$$

where L_f is the latent heat of fusion, m_i is the mass of ice in the droplet, q_c is the heat loss by thermal process (conduction plus convection), and q_e is the heat loss by evaporation process:

$$q_c = h_c A (T_w - T_\infty) \quad (4.21)$$

and

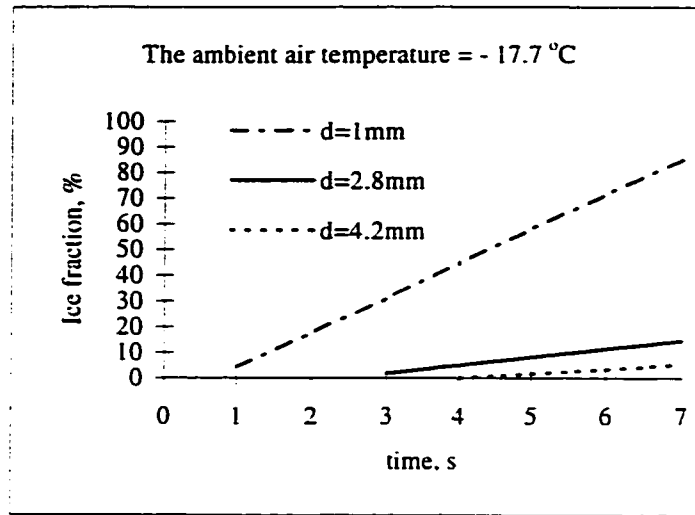
$$q_e = h_D A L_{ev} \rho_a (W_s - W_\infty) \quad (4.22)$$

the items on the right hand side of equation 4.21 and 4.22 have been defined in section 4.5.2. Substitute equation 4.21 and equation 4.22 into equation 4.20, we have

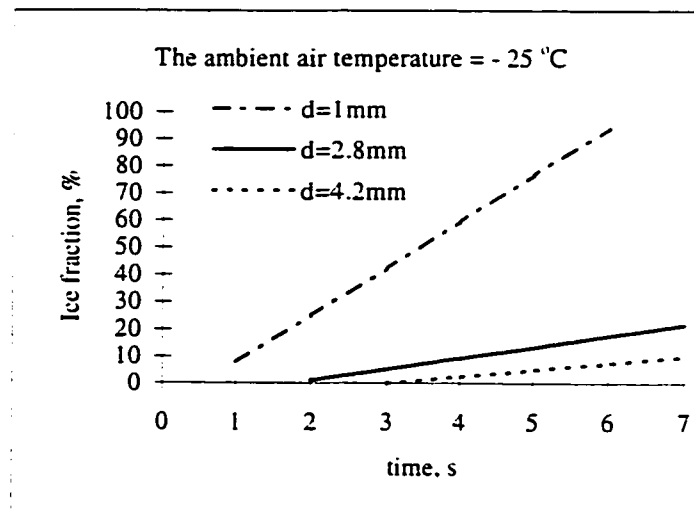
$$L_f \frac{dm_i}{dt} = h_c A (T_w - T_\infty) + h_D A L_{ev} \rho_a (W_s - W_\infty) \quad (4.23)$$

Solving equation 4.23 gives the fraction of ice formed as a function of time. Providing that the heat loss is constant, the ice fraction (m_i/m_w , m_w = mass of a droplet) in a single droplet is calculated against the droplet air residence time. The results are presented in Figure 4-7 and Figure 4-8. Ice formation begins after the droplet nucleation temperature is reached, therefore, the time required for each type of wastewater droplet to reach its nucleation temperature under different air temperature should be included in the air residence time. It is obvious that under a given droplet air residence time, the longer the time for a droplet to reach its nucleation temperature, the less that is available for ice production. Ice fraction in a 1 mm diameter drop is calculated under different conditions. Assumptions are made on the droplet freezing temperatures for those not tested in this study.

A droplet air residence time of 7 seconds is used in the calculation of the ice

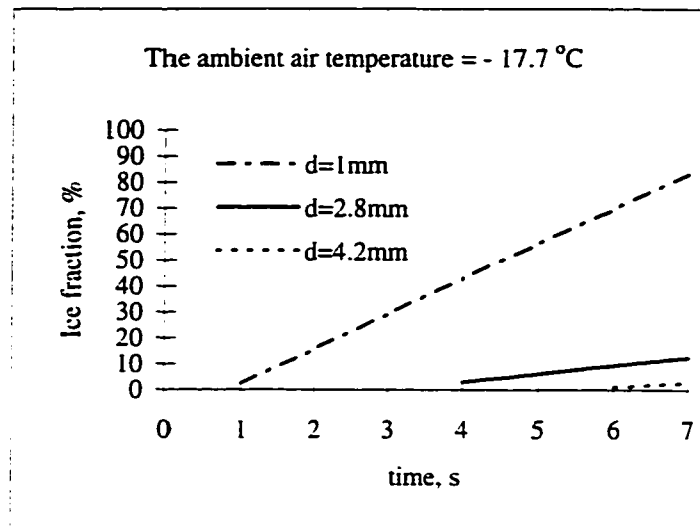


(a)

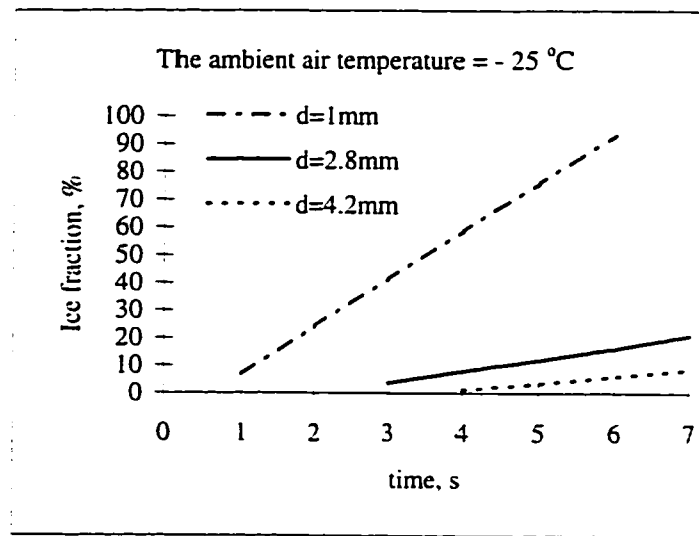


(b)

Figure 4-7 The ice fraction in a single pulp mill effluent drop vs. the droplet residence time in air. The initial droplet temperature = + 5 °C. (a) the ice nucleation temperature (T_n) of 1 mm diameter droplet is assumed as - 2 °C. (b) the assumed T_n : for d = 1 mm, T_n = - 1.85 °C; for d = 2.8 mm and d = 4.2 mm. T_n = -1.0 °C.



(a)



(b)

Figure 4-8 The ice fraction in a single oil sands tailings pond water droplet vs. the droplet residence time in air. The initial droplet temperature = + 5 °C. (a) the ice nucleation temperature (T_n) of 1 mm diameter droplet is assumed as - 3.6 °C. (b) the assume nucleation temperature: for $d = 1$ mm, $T_n = - 3.0$ °C; for $d = 2.8$ mm and $d = 4.2$ mm, $T_n = -2.0$ °C.

fraction shown in Figure 4-7 and 4-8. In a spray freezing operation, the residence time of a droplet in the air is determined by the vertical height of the water jet. Therefore, calculation of ice formation for longer droplet residence time in air is unnecessary for the spray freezing operation. But for the purpose of comparison, the ice fraction is calculated for droplet air residence time of 30 seconds when air temperature is -10.3°C . The results are shown in Figure 4-9 to Figure 4-11.

At -17.7°C , 3.4 mm or 4.2 mm diameter piggery wastewater drops do not freeze within 7 seconds due to its lower nucleation temperature. As shown in Figure 4-7 and Figure 4-8, with an initial temperature of $+5^{\circ}\text{C}$, about 85% of a 1 mm diameter drop will turn into ice in less than 7 seconds under a -17.7°C condition. The assumed ice nucleation temperature for 1 mm diameter pulp mill effluent drop is -2.5°C and -3.6°C for T.P.W. while the estimated freezing temperature is -1.8°C and -1.9°C for 4.2 mm and 2.8 mm diameter pulp mill effluent drops, respectively (Table 4-4-a). Under the same condition, the ice nucleation temperature is -3.4°C (4.2 mm diameter drop) and -3.1°C (2.8 mm diameter drop) for T.P.W. The portion of frozen water in T.P.W. drops is slightly lower than that of pulp mill effluent drops because of the lower ice nucleation temperature of the T.P.W. For a given droplet diameter, the fraction of ice increases as the ice nucleation temperature increases. This effect is mainly due to the fact that less time is required for the freezing event to happen in a droplet having a warmer ice nucleation temperature and once freezing begins the droplet temperature rises up to 0°C and thus increases the driving force for heat transfer. As air temperature decreases to -25°C , the 1 mm diameter drops will freeze completely during the suspension in the air in less than 7 seconds. The ice fraction increases as droplet size decreases. The smaller surface to volume ratio and the higher terminal velocity of large drops are the cause of low ice fraction. When ambient temperature is -10.3°C , the ice fraction in a 1 mm diameter pulp mill effluent and T.P.W. can still reach about 60% after residing in the air for about 10 seconds. Figure 4-9 indicates that approximately 50% of water in a piggery wastewater drop 1 mm in diameter will freeze in 10 seconds if the drop has a nucleation temperature of -9°C . Almost no freezing occurs in the drops with a diameter of 2.8 or

larger within 10 seconds under -10.3°C environment. Figures 4-9 to 4-11 also suggests that for the wastewaters with warmer ice nucleation temperatures such as pulp mill effluent and T.P.W. by changing to smaller sizes of drops it is still possible to freeze most of the water in a spray freezing process when air temperature is around -10°C .

The fraction of frozen water in a single pulp mill effluent or oil sands tailings pond water drop as a function of droplet diameter and ambient air temperature is plotted in Figure 4-12 and Figure 4-13 for a droplet air residence time of 7 seconds.

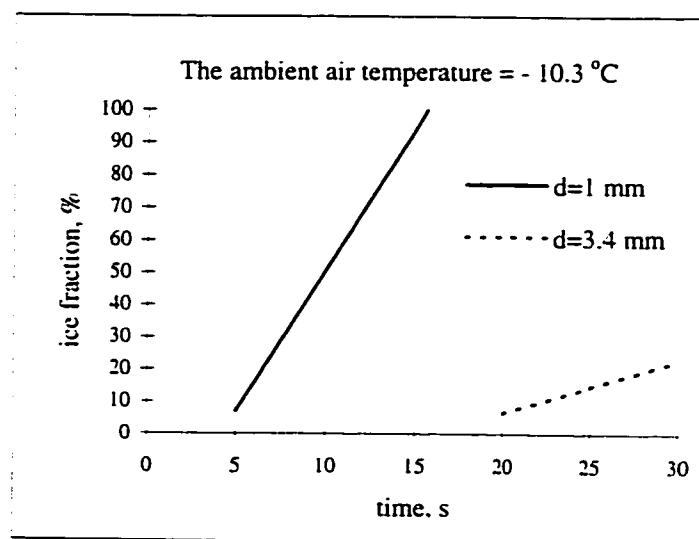


Figure 4-9 The fraction of frozen water in a 1 mm and 3.4 mm diameter piggery wastewater drop vs. air residence time in a -10.3°C environment. The freezing temperature of 1 mm diameter drop is assumed to be -9°C .

In a spray freezing operation, the total amount of ice produced is the sum of the ice formed before droplets landing on the ground and the ice formed on the ground. Some of the unfrozen droplets will freeze after impacting the ground surface because the droplet has been supercooled during its time in the air. Spray freezing is an effective way for ice formation since the droplets have much larger exposed surface area than does ponded water, which accelerates the cooling of the sprayed water. Zarling (1980) compared the exposed surface area of sprayed water droplets with ponded water. for example, a 50 mm layer of ponded water would contain the equivalent of approximately 1.5 million 4 mm diameter drops per square meter of surface area and this yields a drop surface area to water surface area ratio of 75 to 1. The total ice formation in the spray freezing process for the purpose of wastewater treatment can be estimated by measuring the runoff generation rate and it will be discussed in the next chapter. The ice formation rate in the spray freezing process for the construction of ice structures in arctic region was presented by other researchers (e.g. Allyn and Masterson, 1989, Szilder et al., 1991); the discussion of this topic is beyond the scope of this thesis.

4.6 Summary

Freezing of a freely suspended water drop starts at the bottom and propagates over the surface to enclose the drop in an ice shell. The speed of the droplet surface freezing is a function of the ambient air temperature and the nature of the water sample. Most droplets decrease in terminal velocity after freezing. Fracture of ice shell is unlikely to occur to the droplets in a spray freezing operation due to the short air residence time of the sprayed water drops.

The time required for freezing a freely suspended wastewater drop was dependent on the chemical properties of the contaminants in the wastewater, the volume (size) of the drop, the ambient air temperature, and pH of the wastewater. The time required for freezing of a collection of visibly identical drops spreads over a certain range. Under the

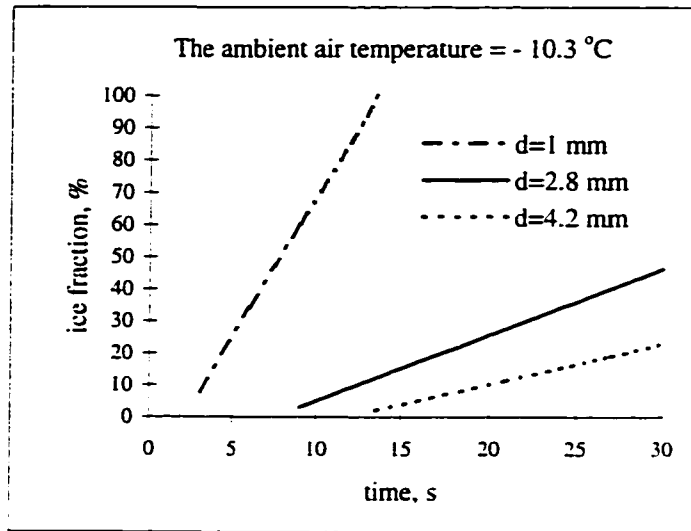


Figure 4-10 The ice fraction in a pulp mill effluent drop as a function of droplet diameter and droplet air residence time in a - 10.3 °C environment. The freezing temperature of 1 mm diameter drop is assumed to be - 6 °C.

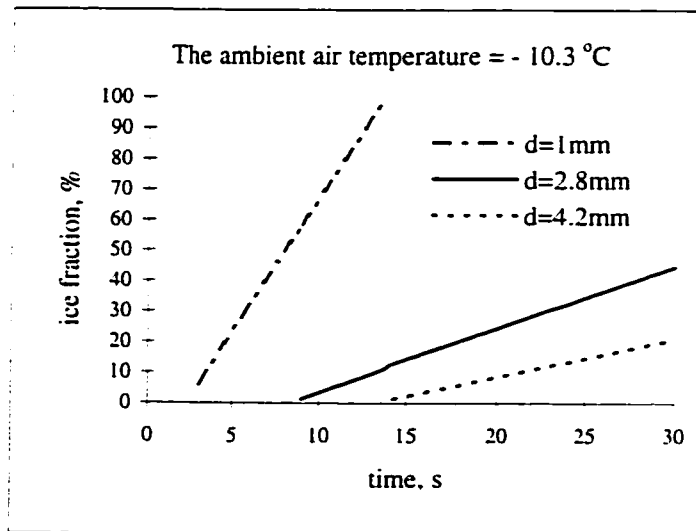


Figure 4-11 The ice fraction in a oil sands tailings pond water drop as a function of droplet diameter and droplet air residence time in a - 10.3 °C environment. The freezing temperature of 1 mm diameter drop is assumed to be - 6.5 °C.

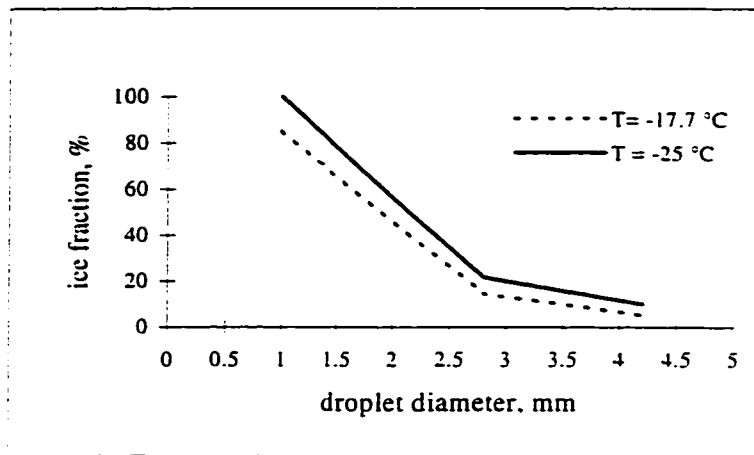


Figure 4-12 The fraction of frozen water in different sizes of pulp mill effluent drops after suspending in the air for 7 seconds. The ambient air temperature of $-17.7\text{ }^{\circ}\text{C}$ and $-25\text{ }^{\circ}\text{C}$ is used for comparison.

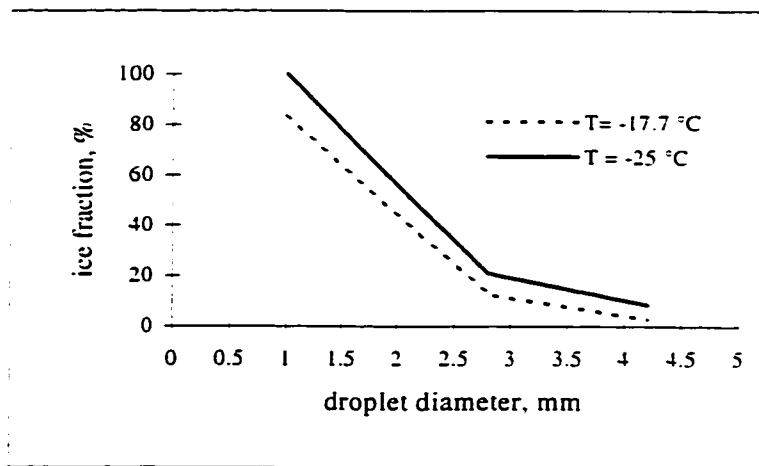


Figure 4-13 The fraction of frozen water in different sizes of oil sands tailings pond water drops after suspending in the air for 7 seconds. The ambient air temperature of $-17.7\text{ }^{\circ}\text{C}$ and $-25\text{ }^{\circ}\text{C}$ is used for comparison.

same conditions, smaller drops needed less time to freeze. Generally, the ice nucleation in the larger droplets occurs at a slightly warmer temperature when compared to smaller drops. The droplet size effect reduced as ambient air temperature decreased. Slightly longer freezing time was needed when droplet pH was adjusted to 11. The difference in the cooling rate experienced by the droplets during the ice nucleation tests and the freely suspended droplet tests might be the reason that caused the variation of the pH effect.

Experimental results and calculated droplet cooling rate indicated that water droplets are less supercooled when ambient air temperature was low while freezing does not occur until droplet temperature approaches the ambient air temperature when the air temperature is close to the wastewater warmest ice nucleation temperature. More ice will be formed for the wastewater droplets that freeze at warmer temperatures.

Under the same experimental conditions, a freely suspended pulp mill effluent droplet has the warmest ice nucleation temperature among the wastewaters tested and piggery wastewater drops have the lowest freezing temperature. The freezing temperature of oil sands tailings pond water drops is between the pulp mill effluent and the piggery wastewater drops. Piggery wastewater drops usually freeze at a temperature about 2 to 3 °C lower than the pulp mill effluent and oil sands tailings pond water.

CHAPTER 5 WASTEWATER CONTAMINANTS

CONCENTRATION AND SEPARATION BY FREEZING PROCESS

Using freezing technology to treat water or wastewater is based on the principle that when water freezes, ice crystals grow of pure water and impurities contained in water being treated are rejected from the ice structure and concentrated in the liquid phase. Through the freezing process contaminants in large volumes of diluted wastewater can be concentrated. The volume separation makes subsequent treatment or disposal of the concentrated smaller volume easier.

5.1 Fundamentals of Impurity Separation by Freezing

5.1.1 Impurity rejection during freezing

Ice is a solid that consists of a crystallographic arrangement of water molecules (Glen, 1974). The structure of the crystals of ice is determined by the interaction forces between its molecules and these forces, which in turn, are determined by the electronic structure of those molecules (Fletcher, 1970). Water molecules are bonded together by the positive charge concentrations of one molecule in contact with the negatively charged concentration of another. The electrostatic attraction between charge concentrations is very strong and is the main factor in determining the mechanical strength of ice (Glen, 1974). Chalmers (1959) indicated that the molecules of water in the crystal structure of ice assume positions farther apart from one another than they do in the liquid state. therefore, ice has a lower density than water.

When an ice embryo reaches a critical size and the freezing process has become dominant, the ice crystal will continue to grow by adding water molecules to its crystal structure, as bricks are added to build a wall. Chalmers (1959) indicated that the structure of an ice crystal has great regularity and symmetry. Because of this highly organized structure, ice can not accommodate other atoms or molecules without severe internal strain. Other solutes (or impurities) in the water are thus rejected by the advancing surface of the growing ice crystal. Impurities concentrated just ahead of the advancing crystal surface and the impurity rejection continues until it limits the availability of water molecules to add to the ice crystal.

It has long been known that salt water can be purified by freezing. The early study of desalination of sea water by freezing actually dated back to 1786 (Nebbia and Menozzi, 1968). Since then numerous studies have been carried out to understand the mechanism of impurity rejection during ice crystal formation, however, it is a complex process which has not been completely understood (Kuo and Wilcox, 1973; Drost-Hansen, 1967). There are many factors that affect the movement of impurities from a moving ice-water interface. Uhlmann et al. (1964) investigated the interaction between particles and the ice-water interface. They found that there was a "critical velocity" for each particular particle below which the particle is trapped in the ice. The critical velocity was a function of particle composition as well as particle size. But for particles smaller than 15 μm (diameter), the critical velocity was observed to be independent of the particle size. If particle radius R_0 was greater than 100 μm , the critical velocity $v_c \propto 1/(R_0)^2$. Therefore, for large particles, the critical velocity decreases as particle size increases. The critical velocity were also found to depend on the shape of the particles. For the same size of particles, irregular particles are expected to have higher critical velocities than smooth ones.

Continuous rejection of a particle demands both a force preventing incorporation of the particle into the ice and a steady feeding of water to the region of the interface

immediately between the particle and the ice. Gilpin (1979, 1980) conducted a theoretical study of particle engulfment and developed a mathematical model to predict the effects of particle radius, temperature gradient and force applied to the particle on the engulfment velocity. Gilpin believed that the presence of a particle in the ice-water interface alters the chemical potential of the water near the particle surface and this altered chemical potential has two consequences of interest to the particle rejection phenomenon: first, a film of unfrozen water will exist next to the particle surface for temperatures below the bulk fusion temperature and the second consequence is that a spreading pressure, exist which tends to maintain the film at a uniform thickness around the particle, i.e. when a fusion front encroaches on the liquid film a pressure gradient develops in the film to drive flow along the particle surface into the region separating the ice and the particle. The particle is pushed ahead of the fusion front. Gilpin predicted that for particles which are engulfed at velocities greater than about 2 $\mu\text{m}/\text{sec}$ the engulfment velocity depends mainly on particle radius and is relatively insensitive to the force (specific gravity) acting on the particle and to the temperature gradient in the ice. For particles engulfed at velocities less than about 0.5 $\mu\text{m}/\text{sec}$ the particle radius is less important but the particle specific gravity and to some extent the temperature gradient in the ice are important. The theory agreed with experimental measurements.

Corte (1962) investigated the vertical migration of particles in front of a moving freezing plane and discovered that particle migration is affected by particle shape or the contact area with the interface, particle size and freezing rate. Increasing the contact area of the particle while the size was constant caused the migration to increase. The fine particles migrated under a wide range of freezing rates while coarser ones only migrated at slower and narrower ranges of rates of freezing.

But Halde's (1980) findings were opposite to Corte's (1962). Halde (1979) found from the sewage sludge freeze concentration study that raw primary sludge containing a larger fraction of coarse particles was much easier to concentrate than a digested sludge containing small particles.

Cissé and Bolling (1971) studied the interaction between inert particles and freezing water. Gravity and viscous drag could be the forces which bring the interface and the particle in contact. Rough particles which have more contact points with the ice-water interface were better rejected since the share of the force developed at each point of a rough particle will be less than the total force required if there is only one point of contact. However, the rate of movement of mineral particles was found not to be systematically related to particle size or temperature gradient (Römkens and Miller, 1973). The migration of mineral particles in ice subjected to a temperature gradient was attributed to osmotic phenomena in an unfrozen liquid film surrounding these particles.

Waller (1966) and Terwilliger and Dizio (1970) studied the effect of rate of freezing on the exclusion of sodium chloride by ice. They discovered that the rejection of the salt was affected by the thickness of the NaCl boundary at the ice-water interface. The boundary thickness varied inversely with freezing rate. High freezing rates caused thin crystals with brine inclusions in the ice aggregation. When the NaCl concentration was increased, the ice content of NaCl increased as well. At a critical concentration range brine entrapment suddenly increased and crystal size changed. Waller (1966) concluded that there was a maximum concentration in the boundary layer that could be tolerated before detrimental effects occurred.

5.1.2 Freezing potential

Workman and Reynolds (1950) noticed that an electrical potential was generated during the freezing of dilute aqueous solutions. The freezing potential (it was named as the Workman and Reynolds effect) occurs when trace amount of inorganic and some organic salts are present in a freezing solution. The charge separation that takes place during freezing at the ice-water interface were primarily attributed to the preferential incorporation into the ice lattice of certain impurity ions compared to others.

Loeb (1958), Drost-Hansen (1967), Gross (1967, 1968) and Cobb and Gross (1969) reviewed early studies on the freezing potential. The direction and magnitude of the freezing potentials depend on the nature and concentration of the ionic impurities. Cobb and Gross (1969) found from their experiment that ammonium salts charged the ice positively, produced high potential and only had a weak dependence on concentration. Lead acetate also gave the ice a positive charge while fluorides charged the ice negatively. No ion separation took place in HF, HCl and H₂SO₄ solutions. Gross (1971) studied the freezing potential in H₂O-NH₃-CO₂ system and found that when the concentration of CO₂ equaled or exceeded that of NH₃ the freezing potential was highest. Atmospheric carbon dioxide interferes with the charge separation process. It will lower the pH and therefore the freezing potential in solutions of salts which charge ice negatively while in basic solutions CO₂ increases the freezing potential (Hobbs, 1974). The hydrogen and hydroxide ions affect freezing potentials since they provide the neutralization current at the interface, their availability determining the interface resistance. Based on charge transfer characteristics during freezing, Gross (1968) distinguished three groups of inorganic solutes: Group I, includes alkali halides and ammonium fluoride. In these solutions the anions are preferentially incorporated into the ice. Freezing potentials are strongly dependent on concentration and freezing rate. Shunting the ice-water interface by a resistor intensifies the freezing current. Group II solutes are the ammonium salts (except NH₄F), sulfates, nitrates, oxalates and acetates of various metals. Positive ions are preferentially incorporated into the ice. Ion incorporation and charge transfer into ice is small. Unlike in Group I, the freezing potential is high and less depends on the solute concentration. Group III includes halogen acids, alkali hydroxides and ammonium hydroxide, no charge separation occurs when these acids and bases are present in a freezing solution.

The differential ion transfer process discussed in this section can be changed by using a shunt resistance, by changing pH of the solution or by varying the freezing rate. Gross (1968) indicated that differential ion transfer is a second order phenomenon

superimposed on the rejection of the major portion of all the impurities. anions and cations alike, from the ice.

5.1.3 Incorporation of impurities in the ice

Impurities are rejected and concentrated in the liquid phase ahead of the phase boundary as soon as freezing starts. The impurities become distributed unequally between the ice and the liquid during freezing. A coefficient k which is a measure of the distribution of a solute between phases can be defined as:

$$k = \frac{C_s(i)}{C_l(i)} \quad (5.1)$$

where C_s is the solute concentration directly adjacent to the interface in the ice and C_l is the concentration directly adjacent to the interface in the liquid. The k value indicates the distortion the solute imposes on the molecular arrangement in the solid. The distortion is zero when k equals to one. Gross (1968) indicated that k is always very much smaller than one for ionic solutes in water. It means that the solute weakens the binding between molecules, increases the intermolecular distances and lowers the melting point. Generally, if ice is grown from a solution free of convection, the value of k is between k_o , the thermodynamic equilibrium coefficient and k_{eff} , the effective distribution coefficient:

$$k_o < k < k_{eff}.$$

The thermodynamic equilibrium coefficient, k_o is obtainable only when the freezing rate is zero, or the liquid is stirred intensively so there is no concentration gradient in the liquid. The concentration of impurities in the liquid phase ahead of the advancing interface will increase as the freezing process progresses. If the advancing ice rejects a solute too rapid for the solute diffusional process, a concentration gradient is built up ahead of the interface. Then, the amount of solute incorporated into the solid phase can

no longer be described by k_o . Under this condition, the relation between concentration in the ice and that in the main body of the liquid can be described by the effective distribution coefficient k_{eff} :

$$k_{eff} = \frac{C_s}{C_o} \quad (5.2)$$

where C_o is the concentration of the liquid at a distance far away from the interface. C_s equals to the concentration of the liquid before freezing starts if a liquid column has infinite length. The effective distribution coefficient is estimated from experimental data. For a long liquid column, the concentration of solute in the ice increases until steady state is reached. Under steady state conditions, the solute diffuses away from the interface as fast as it is rejected by the ice. As a result, the shape and the width of the boundary layer where the concentration of solute is enhanced is a function of freezing rate, distribution coefficient and the diffusion coefficient of the solute. In the steady state and in the absence of convection, $k_{eff} = 1$, the concentration in the ice is the same as that in the original solution before freezing starts. If the temperature at the phase boundary of a highly concentrated freezing solution is below the solidification temperature, constitutional supercooling occurs. The solidification temperature increases sharply from the interface to the bulk solution as a result of the steep concentration gradient (Terwillinger and Dizio, 1970). A consequence of this condition is the formation of cells, spikes and finally dendrites. The highly concentrated solution that develops between these accelerated growth zones may become trapped in the ice (Gross, 1968). The measured distribution coefficient for such a system will be too high. The distribution coefficient does not apply to these bulk entrapment conditions.

To determine the distribution coefficient theoretically, many assumptions have to be made to simplify a real system. Assumptions such as the transport of the rejected solute occurs by diffusion only (no convection), distribution coefficient and diffusion coefficient are constant at certain freezing rate, or uniform freezing rate are usually made.

For example, if the impurity distribution is governed by convection and the freezing rate is uniform, Burton et al. (1953) indicated that a steady state will be reached when:

$$k = \frac{k_o}{k_o + (1 - k_o) \exp(-\frac{Rd}{D})} \quad (5.3)$$

where d = thickness of the diffusion layer, R = the rate of advance of the interface and D = diffusion coefficient. If equilibrium distribution coefficient k_o is known, then from k , and a knowledge of the growth conditions, k can be estimated from equation 5.3. or using the empirical method given by Pfann (1966) equation 5.3 can also be used to determine k_o . Much experimental and theoretical work has been done on distribution coefficients of metals and semiconductors. Little information is available on distribution coefficients in the ice-water system (Gross, 1968). Baker (1967a) pointed out that mechanical transport forces are augmented by electro-, chemical forces which determine the degree to which the ice-water structure is modified, and therefore, the probability of solute inclusion. Thus, the theoretical treatment of the solute movement process inadequately describes the actual case and too little is known about the individual and combined parametric effects in a real system. The following is a review of some experimental work on distribution coefficients in ice conducted by different researchers.

Jaccard and Levi (1961) studied distribution of NH_3 , HF and NH_4F at high concentrations during the freezing process. During the experiment, uniform freezing rates were used and most of the solutions were stirred. The distribution coefficient was found to be strongly depend on the solution concentration. For HF and NH_3 , a minimum distribution coefficient was obtained when concentration of an original solution was above 10^{-1} M while the coefficient increased with concentration for NH_4F . Gross (1967) conducted a similar test as that of Jacard and Levi but at a much lower temperature and convection was minimized. HF was found to have a very low distribution coefficient although it is supposed to enter ice substitutionally with a minimum of distortion of the ice lattice. On the other hand, NH_4F which may also be incorporated into the ice had

highest distribution coefficient. Gross (1967) also found that the distribution coefficients of KF and CsF increased with concentration and for HF k decreased with increasing concentration. For HCl, the coefficient remained approximately constant. In another study, Gross et al. (1975) investigated concentration dependent solute redistribution at the ice-water phase boundary. The distribution curves of HCl, HF, NH_4OH and NH_4F were obtained under different conditions. Gross and his colleagues suggested that the characteristics of solute distribution curves in ice were determined by five processes: convection, a concentration dependent distribution coefficient, solute saturation of the ice solid solution, a eutectic point, and interface breakdown. Specific differences between solutes were observed and measured. The experimental results revealed that the distribution coefficient of NH_4F was about two orders of magnitude greater than others. The coefficient of HCl and NH_4F were independent of concentration. HCl showed a solubility limit around the eutectic point. For HF, the coefficient was strongly depending on the concentration and NH_4F had a very sharp solubility limit that controlled the redistribution of this solute.

De Micheli and Iribarnes (1960) examined distribution coefficient of various salts, acids and bases. The experimental results showed that the salts had higher distribution coefficient than the acids and bases and the coefficients were more dependent on the mother solution concentration for acids and bases than their salts.

Baker (1969, 1970) and Molo and Baker (1968) indicated that in a complex system containing both organic and inorganic solutes, the effective distribution coefficient was not constant but varied with fraction of the solution frozen. Nonionized solutes were rejected more efficiently from the ice than ions.

Terwilliher and Dizio (1970) proposed a theory which was contrary to the theory mentioned above that solute rejection during freezing is controlled by a distribution coefficient which is solely a function of the freezing rate. Based on the results obtained from their investigation, Terwilliher and Dizio (1970) indicated that a distribution

coefficient is only an indirect function of the freezing rate and bulk concentration. Therefore, the distribution coefficient is a passive parameter which describes but does not control the rejection of a solute during freezing. Terwilliher and Dizio (1970) concluded that the liquid phase interface concentration and the thermal driving force were the two main factors controlling NaCl rejection in their experiment.

In summary, the process of incorporation of impurities in ice is very complicated. It is influenced by many factors. Incorporation of solute in ice may be affected by freezing rate, nature and concentration of a solute, the other species present in solution and their concentrations and other factors such as convection, saturation of the ice solid solution, etc. Therefore, the interpretation of solute distribution in ice is difficult (Gross, 1969).

5.2 Application of Freezing Technology in Water or Wastewater Purification

A familiar example of application of freeze process is desalination. Tremendous work has been carried out to study sea water desalination by the freezing process. Despite persistent design problem during the past 30 years, the method is still regarded as an appealing way of purifying sea water. In recent years, new applications of freezing technologies have been created to separate substances in crystalline form at substantial savings in cost and energy. Some pilot-scale work has been conducted to treat industrial wastewater by using the similar equipment and technology utilized in sea water desalination (Douglas, 1989). Test applications included remediation of hazardous waste lagoons, concentration of deep mine reject water, material recovery from ammunition plant wastes, and by-product recovery from organic chemical and pharmaceutical waste streams.

Baker (1967a and b, 1969, 1970) conducted a systematic laboratory study of freeze separation of trace organic materials in aqueous solutions. The effect of mixing rate, concentration of inorganic salts on the separation efficiency of organic materials was

examined. Increasing ionized solute concentration reduced the separation efficiency of organic solutes. Baker indicated that increased salt concentration altered ice morphology by promoting dendritic growth and incorporation of solute-rich liquid in forming the ice phase. Increasing mixing rates improved separation of organic solutes from the liquid. Separation of trace organic solutes from aqueous solution by freezing does not change the chemical composition and so the volatile or reactive compounds are not destroyed. This technique was used to increase the sensitivity of analytical technique (Baker, 1967a).

Bardulin et al. (1963) investigated the feasibility of using the freezing and gas hydrate process to purify municipal wastewater. The process essentially involved partial freezing and draining followed by washing and melting the ice crystals. In a pilot-scale study, 90% impurity removal was achieved. Washing the organics from the ice crystals was found to be difficult and the process had a high cost.

Researchers at the Applied Science Laboratories, Inc. (1971) purified acid mine water by the freezing process. By partial freezing, about 50% conversion to ice, the amount of metals and acid components was reduced by 85 to 90% in the melt water.

More than 90% removal of nickel, cadmium, chromium, zinc and sodium chloride from plating rinsewater was obtained by freezing process in a pilot plant study (Campbell and Emmeman, 1972). The capacity and operating costs were considered to be primarily a function of total flow, and to a limited extent, the initial waste concentration in the feed stream.

Freeze concentration of spent sulfite liquor, a paper mill waste was investigated by Grulich (1969). The percentage of total solids trapped in the ice was higher than that of BOD₅. Grulich indicated that low molecular weight sugars which cause high BOD₅ were transported away from the ice-water interface more readily than high molecular weight, low BOD₅ causing lignosulfonates. A freeze crystallization pilot plant was operated to treat BCTMP pulp mill effluent (Kenny et. al., 1991). The whole pilot plant

consisted of two skids. One truck mounted, and the other truck transportable. The truck transportable skid contained a vertical heat exchanger for producing an ice crystal slurry and vertical ice separation column. The refrigeration system, tankage, pumps, and other auxiliary equipment were mounted on the truck mounted skid. The effluent BOD₅ was in the range of 1300 to 3400 mg/L, COD around 4000 to 8500 mg/L and color concentration was about 280 mg/L. After the freezing process, BOD₅ in the melt water was reduced to between 80 to 280 mg/L while COD and color concentrations were reduced to between 200 to 900 mg/L and 30 to 50 mg/L, respectively.

Müller and Sekoulov (1992) evaluated the potential of freeze concentration to reuse municipal wastewater. A falling film reactor, a cooled double walled vessel, was used in the study. The wastewater was recycled in the falling film reactor while ice films were frozen on the cooled inner walls. The ice was collected from the walls and then melted. Various parameters such as conductivity, TOC, COD, NH₄-N of the melted ice and wastewater concentrate were measured. Up to 99% impurity removal was observed.

Not many references can be found in the literature pertaining to impurity removal by the spray freezing process under natural conditions although the technology has been used in the construction of ice structures in the Arctic and the snow making process for years.

An experimental study of desalination of saline water by spray freezing process was carried out by Elmore (1968). During the winter of 1967-1968, 7192 m³ (1.9 million gallon) of saline water was sprayed on an one-acre site at the University of Wyoming Agricultural Experimental Farm, Laramie, Wyoming, US. The total dissolved solid (TDS) concentration of the source water was in the range of 1736 mg/L to 2297 mg/L. The increase in the source water TDS was caused by recycling of the drainwater (runoff) from the ice mound during the spraying. A total of 4640 m³ (1.226 million gallon) of purified water were produced. The average TDS concentration of the product water was 500 mg/L or less. The highest salt reduction was 97.7%. The feed water with high

concentrations of magnesium carbonate, calcium carbonate, calcium bicarbonate or magnesium bicarbonate was found difficult to purify while high impurity removal was obtained for the feed water with high sodium chloride, potassium chloride or calcium chloride concentrations. Elmore conducted economic evaluation of the spray freezing process and concluded that spray freezing process (under natural conditions) produced water cheaper than any other existing desalination process, even on a small scale.

Krepchin (1985) reported that sea water was desalinated by spray freezing process in the winter of 1984 - 1985 at a Long Island pilot desalination plant (New York). The salt concentration in the water was reduced from 30,000 mg/L to 10 mg/L.

Spyker (1985) studied desalination of brackish water by spray freezing and indicated that a site for spray freezing must be chosen carefully for field study since cumulative effects might be produced by brine seepage into the foundation of the spraying areas. The salts which seep into the underlying soil of the spraying areas were being redissolved in subsequent years as additional spray freezing cycles were completed. The purification efficiency was reduced by the redissolved salts. The purification efficiency was higher for lined area than that of unlined ones.

In order to evaluate the potential use of spray freezing process to remove contaminants from recycled oil sands tailings pond water, a field study was carried out at the Syncrude Canada Ltd. Mine site in February 1994 (Gao et al., 1996). The recycled oil sands tailings pond water was sprayed into a plastic lined containment area. An ice pile measuring 5 m in height and 18 by 12 m in plan was produced over a 15 hour spraying operation. Reduction in the Cl^- concentration was in the range of 90.8 to 98.7% for the ice core samples and the melt water samples collected. The total organic carbon (TOC) removal reached 89.3 to 98.9% while the electrical conductivity was reduced by 91.5 to 99.1%. Removal of Na^+ in the ice core and melt water samples was similar to that of Cl^- .

Several studies in treatment and disposal of sewage effluent through snowmaking have been reported. Some of the experimental results are listed here. 91% BOD₅ and 85% TDS removal from snowpack made from sewage effluent was reported by Wright (1976) in an early study. Secondary sewage effluent was converted to snow with snowmaking equipment (Zapf-Gilje, 1985). The first 20% of the melt water removed, on the average, 65% of the phosphorus, 86% of the nitrogen from the snow made from sewage effluent; and 92% of the potassium chloride from snow made from a potassium chloride solution. The author concluded that snowmaking could provide tertiary treatment and a disposal alternative for disinfected secondary effluent for communities faced with effluent disposal restrictions in the winter. Later, a pilot-scale research program on using snowmaking to treat and dispose wastewater was carried out at the City of Kamloops effluent spray irrigation site at Cinnamon Ridge, British Columbia (Rabinowitz, et. al., 1988). Effluent from the City of Kamloops aerated lagoon system was made into snow. About 90% of the nitrogen and 70% of the phosphorus was removed from the snowpack in the first 30% of the meltwater. The percent reduction in the concentrations of magnesium, sodium, potassium and boron in the initial melt water were similar to that of the nitrogen while metal concentrations were lower. The impurity removal efficiency was increased with decreasing snow density and increasing snow height.

5.3 Impurity Separation in the Spray Freezing Process

Using the spray freezing process to purify water or wastewater, impurity removal is achieved in one or two stages depending on if runoff is generated during the spraying operation.

The first stage of the impurity removal is achieved because runoff is generated during spraying. Rejection of impurities starts as soon as freezing begins. During the spraying operation, there are two main phases of ice formation. In the first phase, ice

starts to grow on the surface of the supercooled droplets when their surface temperature falls below the nucleation temperature as they travel through air to the ground. The stages of supercooling and the amount of ice formed in this stage depends on the atmospheric and spraying conditions such as droplet size, air residence time. As ice forms on the surface of a droplet, impurities are rejected and concentrated in the liquid phase inside of the droplet. Second phase of ice formation commences after the droplets land on the ground (or a previously deposited ice surface). The supercooled droplets freeze upon contact with the cold ground surface or the ice surface. Due to the impact, fracture of the ice shell of the frozen drops may occur, and the water released from the cores contacts the colder outer surfaces of the ice shells and freezes. A layer of ice-water mixture forms. Additional freezing occurs in the ice-water mixture when the layer is exposed to the atmosphere as the nozzle sweeps back and forth during spraying. When the spray ice grows under wet condition, there is a thin liquid layer on the ice surface because not all of the water can freeze before new droplets arrive. The excess water that cannot be held within the ice mound flows away from the surface or flows downward and runoff occurs from the spray ice mound.

Impurities redistribute in the ice phase and the liquid phase as the freezing process occurs by the mechanism described in the previous sections. Impurities rejected by the growing ice are concentrated in the liquid phase and carried away from the ice mound as runoff. The amount of the impurities removed by the runoff is a function of the source water impurity concentration and the freezing rate. The amount of runoff generated during spraying is governed by the freezing rate. Obviously, the efficiency of the impurity removal from the spray ice is determined by the flowrate and the impurity concentration of the runoff. There are two extreme conditions: 1) all the wastewater sprayed turns into runoff, i.e. no ice is formed, therefore, no impurity separation. The concentration of the impurities in the runoff is the same as the source water; 2) no runoff is generated during spraying. In this case, the freezing rate is too high, all the water sprayed turns into ice. All impurities are entrapped into the ice structure, impurity concentration of the ice equals to the source water concentration, again, no impurity

separation occurs. Thus, for the purpose of water or wastewater purification, a certain amount of runoff generation during the spray freezing process is desirable. The optimum condition for maximum amount of impurity removal during spraying would be the one that the runoff generated has highest impurity concentration and lowest flowrate. For a given air temperature, this optimum condition may be achieved by adjusting the spray flow rate, droplet size, droplet air residence time during a spraying operation.

Second stage of impurity removal of the sprayed water or wastewater begins as spray ice mound melts. The mechanisms by which impurities in the ice become concentrated during the melting process is still poorly understood. This is especially true for spray freezing of wastewater. There is very limited literature on laboratory work on the release of ions from thawing ice compared to ion incorporation into crystal lattice (Davise et al., 1986). The limited knowledge of the impurity incorporation in the ice will definitely give rise to the incomplete understanding of the mechanism in impurity release from melting ice.

Elution of impurities from melting snowpack or glacier ice has been studied by researchers for many years. It has been recognized that when an ice mound or snowpack melts, the concentration of solutes (impurities) in the melt water changes with time and the first fraction of melting snowpack or ice mound has a much higher concentration of impurities than that of the bulk snow or ice. The initial 20 to 30% of meltwater from a solute rich snowpack could remove 50 to 80% of the total solutes in the snowpack (Johannessen et al, 1975; Hohannessen and Henrisksen, 1977; Johannes et al., 1981). This phenomenon, now is technically referred to as "fractionation". More detailed studies found that some ions were removed sooner than others from the highly fractionated initial snowpack meltwater, i.e. the degree of partition between the meltwater and ice is not identical for all ions. Davies et al. (1982) first reported this "preferential ion elution" process.

Some field and laboratory studies have been conducted to investigate impurity removal from a snowpack or ice core to get a better understanding of the “fractionation” and the “preferential elution” processes. Most studies were related to snow melting. However, the mechanisms by which impurities in snowpack or ice mound become concentrated during the melting process and the exact cause of preferential elution are still poorly understood. Steinemann (1958) indicated that recrystallization occurred in glacier ice during its deformation. This deformation provided an opportunity for the impurities to reach the grain boundary. The impurities reached the boundary whether by solid-state diffusion from the grain or because the boundary itself was migrating relative to the grain (Glen et al., 1977). Glen et al. (1977) suggested that pressure induced thermal gradient resulted in release of impurities at point of melt, and subsequent freeze concentration of impurities in the cold zones. Therefore, the purification of individual ice grain is a result of grain boundary migration caused by either curvature or pressure. Continuous recrystallization thus brought the impurities out of the ice structure to the surface of individual grains, where they were available for transport by surface water. Römken and Miller (1973) proposed that temperature gradient driven migration of mineral particles in ice could be explained by osmotic transport of water in the film surrounding the particles. The particles might be enclosed by brine pockets and move towards the warmer temperature region, this brought about melt in the warm end and following freezing at the cold end.

Johannessen and Henriksen (1978) studied impurity concentration changes in the snow meltwater. Field lysimeter observations showed that the first 10% melt fraction contained more than 6 times the snowpack impurity concentrations. The concentrations of all components were 3 to 5 times higher in the initial meltwater than in the bulk snow in the laboratory tests. In the laboratory tests roughly homogenized snow samples were used. Johannessen and Henriksen (1978) suggested that the high impurity concentration in the initial meltwater might be caused by a freeze-concentration process during snow recrystallization and melting in which contaminants accumulate preferentially at the surfaces of ice particles.

The high concentrations of contaminants released in the first phase of the snowmelt in spring gives rise to rapid changes in the chemical composition of streams and lakes. These changes have severe ecological effects on the lakes and streams (Hagen and Langeland, 1973; Leivestad and Muniz, 1976; National Research Council of Canada, 1981).

Seip et al. (1980) investigated the fractionation and runoff of the most important ions found in natural acid snow meltwater. The early melt fractions contained significantly higher impurity contents. The initial 30% melt fraction carried about 80% of the sulfate and nitrate and 60% of sodium and chloride.

Clear fractionation was observed in the meltwater of snow made from secondary sewage effluent in Zapf-Gilje's study (1985). As mentioned in section 4.2, the first 20% fraction of the melt removed 65% phosphorus and 86% of nitrogen from effluent snow while 92% potassium chloride removal was reached in the snow made from potassium chloride solutions. Results obtained from melting test of snow made from potassium chloride solution indicated that the degree of impurity concentration was independent of the melting mode (continuous melting or melt-freeze cycles), snow depth, snow temperature and initial solution concentration. Impurity migration in the snowpack was clearly shown by snow samples taken at different depths. Zapf-Gilje (1985) indicated that the maximum degree of concentration of the impurity front could reach 15 to 40 times the bulk snow concentration. The impurity removal efficiency was influenced by the snowpack density and height (Rabinowitz et al., 1988).

Studies by Davies et al. (1982), Brimblecombe et al. (1985) and Tsiouris et al. (1985) revealed that solutes in snowpacks or ice caps were not removed with the same efficiency, hence the proportional ionic composition of snow or ice changed during melting. They discovered that sulfate and nitrate were removed in preference to chloride and the cations in the order potassium > calcium > magnesium > sodium. Field data

implied that H^+ ion was quite closely associated with NO_3^- and SO_4^{2-} ions and was eluted with these ions as a strong acid peak appearing relatively early in the melt season. In contrast to the field data, H^+ was found as a slowly eluted ion in laboratory experiments (Tsiouris et al. 1985). Laboratory tests were carried out Marsh and Webb (1979) using crushed ice made from frozen dilute sulfuric acid. They found that the maximum meltwater impurity concentration occurred in the initial 5 to 10% runoff. The concentration increased with decreasing melting rate and increasing ice column depth. The fractionation was found to be independent of the mean ice column concentration.

Colbeck (1981) mentioned that at lower melt flow rates molecule diffusion was important as diffusion might effectively redistribute the solute front, resulting in a high impurity concentration with small meltwater quantity. High melt rates produce less concentrated early meltwater fractionation. Diurnal melt-freeze cycles, i.e. a favorable sequence of weather event, would also enhance impurity concentration in a natural snowpack (Colbeck and Anderson, 1982).

Brimblecombe et al. (1987) observed fractionation and preferential loss of ions from melting snow and laboratory ice. In order to get homogeneous ice, the laboratory ice was prepared by rapidly freezing dilute salt solutions as thin layers onto the base of a stainless steel beaker containing liquid nitrogen. It was expected that this laboratory ice would show little fractionation because of the homogeneous distribution of solutes in the ice structure. The ice was packed into a precooled perspex column and melting took place by allowing the column to reach room temperature or by using a small heater above the ice column. The melt water was collected from the bottom of the column throughout thawing. Some ice samples were melted immediately after freezing and others were stored 3 to 7 days before melting to check the changes in the ice. Fractionation of ions into the meltwater was clearly seen in the experiments in spite of the expected homogeneity of the ice prepared by rapid freezing. The solute concentrations in the initial melt water was increased by 3 to 4 times over that in the bulk ice. Most of the solute left in the earliest part of thawing. Preferential elution of one ion with respect to another was

also observed in melting of the laboratory ice. Efficiently removed ions showed high initial concentrations in the melt water. Sulfate and nitrate were preferentially eluted with respect to chloride, and magnesium or potassium was preferentially eluted over sodium. The preferential elution was more pronounced in the aged ices (3 or 7 days old) than in fresh ice. The preferential loss of certain ions became noticeable only at the end of the melting. The fractionation observed in the meltwater of the laboratory ice implied that the brine probably had access to the melting surface along fractures or cracks in the ice. i.e. the laboratory ice was heterogeneous at small scales. Brimblecombe et al. (1987) suggested that the composition changes in ice and meltwater throughout the melting process could be explained by the mixing of two different solutions: an intergranular surficial brine with high solute concentration occupies the ice grain boundaries and a more dilute solution derived from ice grain interiors. However, the hypothesis could not explain the melting of aged laboratory ice and it did not give any description on the physical or chemical mechanisms that produced such a liquid/ice system.

Hewitt et al. (1989) proposed another mechanism to explain the preferential ion elution. They presumed that preferential chemical elution in meltwater is a result of preferential ion exclusion from snow grains during snow metamorphosis. Snow crystals undergo continuous metamorphism upon deposition. Larger ice crystals grow at the expense of smaller ones during metamorphosis (Colbeck, 1987). Chemical components (contaminants) will be incorporated into and excluded from the ice crystals with different efficiencies during the growth of the snow grains. Thus, snow grains mature with a non-homogeneous ion distribution. When snow containing these mature grains melts, ions are released or eluted sequentially with time, and the ion concentration in the meltwater is directly related to the rejection efficiency of different ions imposed by the recrystallization process.

Cragin et al. (1993) investigated the snowpack chemical fractionation and preferential ion elution under laboratory conditions. Natural and laboratory-aged snow grains and frozen water droplets were filled in the 18 mm diameter x 300 mm long glass

columns. The columns were washed with deionized water and with synthetic precipitation solutions to simulate flow of meltwater or rainfall through snow. The meltwater was collected from the bottom of the columns in sequential fractions. Ion concentrations of hydrogen, sodium, potassium, calcium, chloride, nitrate and sulfate in the meltwater were determined. The ionic concentrations in the initial fractions of meltwater from natural snow were two to five times higher than that of the bulk snow from which they originated. Although the initial fraction of meltwater from frozen solution droplets also contained higher concentrations than the bulk solution from which they were prepared, concentrations were two to three times lower than comparable fractions from natural snowmelt. Ice grains did not display any chromatographic sorption of chloride, nitrate or sulfate, indicating that the preferential chemical elution observed in snowpack meltwater was not due to an ion chromatographic process proposed by Tranter et al. (1986) as a possible mechanism for preferential elution.

Cragin et al. (1993) also evaluated the importance of metamorphic process upon snowpack elution chemistry. Fresh snow collected was aged under an imposed temperature gradient for various lengths of time (1, 2, 4, and 8 weeks) and then elution experiments were conducted to determine the influence of grain growth on the degree of fractionation and preferential elution. After one week of aging with an imposed 36 °C/m temperature gradient, crystals had grown from 0.1 to 0.3 mm to 0.2 to 0.4 mm. After eight weeks, Crystal size increased up to 3 mm. The crystal habit changed from slightly rounded apexes at the beginning of the aging test to sintered, highly faceted; many of the crystals were hexagonal and cup-shaped, similar to depth-hoar. Experimental results obtained from elution tests indicated that both fractionation and preferential elution were strongly influenced by ion exclusion during the snow crystal growth. Cragin et al. (1993) concluded that preferential chemical exclusion during snow crystal growth strongly affects preferential ion elution. Sulfates, a less soluble chemical impurity were rejected more efficiently from ice lattice and therefore released in high concentrations in the meltwater prior to the more soluble impurities, such as chloride. Fractionation and preferential elution processes are also affected by snow crystal habit directly through

different chemical release rates from crystals with different geometries and surface area volume ratios and indirectly by affecting meltwater flow rate downwards through the snow.

Through the above extensive literature review, we can hypothesize that the impurities incorporated into a spray ice mound will be removed during melting by the following mechanisms: After the spraying operation is finished, cooling of the entire mass of ice takes place. There is always some water entrapped in the spray ice matrix since spray ice is permeable and porous although the excess amount of water has already been discharged as runoff. The water entrapped in the ice matrix will percolate down the ice mound and some of it subsequently freezes due to the further cooling of the ice mound. The impurities rejected by the growing ice crystals are concentrated in the unfrozen water and carried to the lower level of the ice mound. At the same time, recrystallization takes place continuously once ice crystals are formed. Some individual ice crystals grow larger at the expense of the others. As ice crystals undergo metamorphic physical changes, impurity rejection occurs concurrently. Impurities are concentrated at the surface of the ice grains while the grain boundary moves. The rejection is energetically favorable because less strain is produced when impurities are located on the ice grain surface or at disordered grain boundaries than they are located within the ice lattice (Cragin et al., 1993).

Impurities may also be concentrated on the grain surface by the vaporization in the ice mound. Vapor transfers from warmer ice crystals to the colder ice crystals as snowpack gets older (Colbeck, 1987). As warmer crystals shrink due to the vaporization their impurity concentration increase. They will finally vanish as the ice mound matures, leaving their impurities on the surfaces of the mature gains (Cragin et al., 1993). As recrystallization continues individual ice grains are purified and impurities are concentrated on the surface of ice grains, where they are readily available for transport by meltwater when spring thaw starts. The chemical properties of the individual contaminants will influence the efficiency of rejection from the ice grains. The selective

impurity rejection, of course, will result in preferential elution. Impurity exclusion during the recrystallization will be more complicated for wastewaters because of the numerous types of contaminants contained, especially, the organic contaminants. As known, the rejection efficiency of organic substances is different from inorganics and no studies have ever been conducted on the organic contaminants removal from melting ice. In spring, the surface of the ice mound begins to melt due to the warm air and solar radiation. The surface meltwater percolates down through the ice mound. As ice crystals are washed, the impurities concentrated at the surface of the ice grains are carried away by the meltwater as it flows downward. The impurities will be further concentrated as the water refreezes. The first meltwater discharged from ice mound contains high concentrations of impurities (fractionation). As melting proceeds the meltwater become purer and purer.

The magnitude of the impurities removed in the initial meltwater can be affected by vertical variability in solute distribution, ice mound (snowpack) depth, the meltwater flowrate (Davies et al., 1986; Bales et al., 1989; Blaes, 1991), diurnal melting and refreezing, rainfall and the thermal regime during melting (Colbeck, 1981; Tranter et al., 1992; Suzuki, 1991, Cragin et al., 1993), biological activity (Jones and Deblois, 1987, Jones, 1991). The impurity removal efficiency during ice mound (snowpack) melting will also be influenced by the preferential impurity exclusion during the ice crystal growth, ice crystal habit (Cragin et al., 1993) and the nature of the contaminants contained in a wastewater. It is obvious that the nature of impurity migration through spray ice mound is complex, a general quantitative description based on a process-oriented relationship is unlikely to be made, as yet. Therefore, one has to rely on the empirical representation based on the observed results obtained under different conditions. Zapf-Gilje (1985) found from his experimental study that the impurity removal from the melting snow could be described by a simple exponential decay process. The impurity removal efficiency under different spray freezing conditions will be further discussed in chapter 6.

5.4 Prediction of Impurity Concentration in the Spray Ice

In this section a mathematical model is developed based on the principle of mass balance to estimate impurity concentration in the spray ice. In order to calculate the icing rate of saline sea spray on marine structure, Makkonen (1986) developed a mathematical model to predict the initial salt entrapment in ice grown by sea spray. In Makkonen's model the salinity of ice, S_i , could be calculated by the salinity of sea spray, S_w , and the freezing fraction n from the equation $S_i = 0.26S_w/(1-0.74n)$. For water or wastewater purification by spray freezing process, wastewater is continuously sprayed until the desired volumes of wastewater is sprayed. Determination of the freezing fraction of the sprayed water is complicated and unnecessary because in the spray freezing process the flowrate of the runoff generated during spraying can be easily measured. Since the amount of runoff generated is directly related to the ice formation rate, the incorporation of impurity in the spray ice will be a function of runoff flowrate. A schematic diagram of spray freezing process is shown in Figure 5-1. A mass balance of the impurity in the continuous spray freezing process can be written as

$$C_o Q_o = C_i f + C_r Q_r \quad (5.4)$$

where:

Q_o = flowrate of the source sprayed (influent), m^3/s

Q_r = flowrate of the runoff, m^3/s

f = ice formation rate, m^3/s

C_o = impurity concentration in the source water, g/m^3

C_i = impurity concentration in ice, g/m^3

C_r = impurity concentration in runoff, g/m^3

If the amount of water entrapped in the ice mound is small, the ice formation rate (f) can be estimated roughly as the difference of the influent (source water) flowrate (Q_o) and the

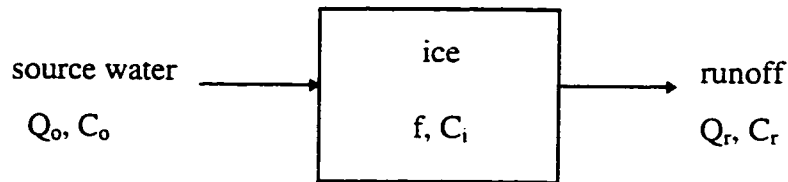


Figure 5-1 Schematic diagram of a spray freezing process

runoff flowrate (Q_r), i.e. $f = Q_o - Q_r$. If one assumes the liquid phase is completely mixed, then, the impurity concentration in the runoff is the same as the concentration in the liquid film on the ice surface. Due to wind drag and impinging droplets, the impurity concentration and the temperature of the liquid layer on the ice surface is usually uniform when spray ice grows in wet condition. Substitute $f = Q_o - Q_r$ in and divide equation 5.4 by Q_o and C_i yields:

$$\frac{C_o}{C_i} = \frac{(Q_o - Q_r)}{Q_o} + \frac{Q_r}{Q_o k^*}$$

where $k^* = C_i/C_r$ is the interfacial distribution coefficient. Since the effective distribution coefficient $k = C_i/C_o$ equation 5.4 can be simplified as:

$$k = \frac{Q_o k^*}{(Q_o - Q_r)k^* + Q_r} \quad (5.5)$$

or

$$k = \frac{C_i}{C_o} = \frac{k^*}{k^* - \frac{Q_r}{Q_o} (k^* - 1)} \quad (5.6)$$

If the value of interfacial coefficient k^* of a solute (impurity) in the sprayed water or wastewater is known, then equation 5.6 can be used to estimate the impurity concentration in the spray ice. It is obvious that the interfacial distribution coefficient k^* is determined by the nature of individual impurities in a water or wastewater. What makes it more complicated is that even for a given solute (impurity) k^* may change with freezing conditions. Makkonen (1986) assumed k^* was a constant in salt entrapment in ice grown by sea spray regardless of growth condition and used $k^* = 0.26$ as first approximation in his work. Makkonen's assumption was based on the hypothesis that salt rejection in the sea spray ice is similar to the salt rejection in dendritic growth of sea ice at low growth rates. Several studies on salt entrapment in growing sea ice (Weeks and Lofgren, 1967; Cox and Weeks, 1975; Weeks and Ackley, 1982) indicated that interfacial

distribution coefficient is a constant when ice growth rate is sufficiently high and the solid/liquid interface has a dendritic substructure, and the value of k^* is about 0.26. Makkonen emphasized that there was a possible connection between salt entrapment in spray ice and the growth of spongy ice by accretion of fresh water droplets. He indicated that the interfacial coefficient k^* may be a function of the liquid fraction λ of the ice deposit. While Baker (1969, 1970) found from his experimental studies of the freezing of complex aqueous solution containing both organic and inorganic solutes that the distribution coefficients of organic solutes were not constant but varied with fraction frozen. In order to determine k^* , the factors that control k^* have to be studied first and then establish clear relationship between k^* and other parameters.

The impurity concentration in the runoff can be calculated from:

$$\frac{C_r}{C_o} = \frac{k}{k^*} \quad (5.7)$$

The concentrations of the source water (C_o) and runoff (C_r) can be easily measured in a spray freezing process. If the concentration ratio of the runoff and source water is known for a given water or wastewater, for instance, if $C_r/C_o = k/k^* = \text{constant}$, then the value of k^* can be determined from equation 5.7, providing that k is known. Any knowledge about interfacial distribution coefficient will certainly help the understanding of impurity incorporation in ice structure so improve the prediction of impurity distribution in a spray ice. For wastewater treatment using the spray freezing process, it is impractical to determine k^* and k value for every contaminant in the wastewater. Therefore, an indicator parameter which is a good measure of the freezing process should be selected and the interfacial distribution coefficient of this indicator can be directly used to estimate the impurity incorporation in the ice. It will be shown in next chapter that electrical conductivity may be used for such purposes.

Equation 5.6 suggested that the impurity concentration in the spray ice is determined by the interfacial distribution coefficient (or the impurity concentration in the runoff) and the runoff flowrate for a given spray condition of a wastewater. It can be easily found out from Equation 5.6 that when $Q_r = Q_o$, $k = k^*$, $C_r = C_o$; i.e. no ice is formed, hence no impurity separation occurs; when $Q_r = 0$, $k = 1$ and $C_i = C_o$. in this case no runoff is generated and the impurity concentration in ice is the same as that of the source water. These are the two extreme spraying conditions mentioned earlier. To produce spray ice under wet growth condition, the runoff flowrate Q_r should be within the range of $0 < Q_r < Q_o$. The impurities contained in the wastewater may affect ice growth rate. Tammann and Büchner (1935), Lindenmeyer (1959) and Prupacher (1967a,b) all found that the dendritic growth rate of the ice at a given supercooling increased with increasing solute concentration until a critical solute concentration was reached then the growth rate decreased with increasing solute concentration and finally became significantly less than that in pure water. The critical concentration of solute necessary to give the maximum dendritic growth rate depend on the nature of the solute and on the supercooling (Hobbs, 1974). A solute may affect the growth of ice in a supercooled aqueous solution by following mechanism: changing the value of the thermal diffusivity of the solution; lowering the equilibrium liquid temperature when the rejected solute build up at the ice-water interface; being absorbed onto the surface of the growing crystal and changing the mobility of the water molecules and therefore the rate at which they can be built into the ice lattice (Hobb, 1974). In equation 5.6, the factors that may influence the ice formation rate is lumped into a single parameter, the runoff flowrate Q_r . Detailed experimental studies should be conducted to verify equation 5.6.

In next chapter the treatability of oil sands tailings pond water and pulp mill effluent by spray freezing process will be evaluated. The amount of impurities removed in the runoff and the early melt water is determined.

CHAPTER 6 SPRAY FREEZING TO TREAT INDUSTRIAL WASTEWATER

The objective of this experiment was to study the treatability of pulp mill effluent and oil sands tailings pond water by spray freezing process. The effects of ambient temperature, the ice age (storage time) on impurity removal were investigated. The fractionation of various impurities including organic impurities into the meltwater were also closely examined.

6.1 Experimental Materials and Methods

6.1.1 Spraying equipment and method

The spraying equipment consisted of a spray gun with a 3.17 mm diameter circular nozzle and a pump operated at 600 to 650 kPa. The wastewaters were contained in 200 L barrels and a submersible pump was used to pump out water from the barrels.

The droplet size distribution from the nozzle was investigated under the working condition. The flour method (Laws and Parson, 1943) was adopted to measure droplet size distribution. The droplet size samples were taken about 4 m from the sprayer. It was found that approximately 56% of the droplets had a diameter less than 1.6 mm (among them 40% with a diameter in the range of 1 to 1.6 mm and 16% with a diameter < 1 mm), and 44% of the droplets had a diameter between 1.7 to 2.8 mm (34%: droplet diameter in the range of 1.7 to 2.3 mm and 10% droplet diameter was between 2.4 to 2.8 mm).

The spraying operation was carried out in the field of the Ellerslie Research Station, University of Alberta, Edmonton, Alberta. The wastewater was pumped out of the barrels and sprayed onto a tarp. The tarp hung between two poles. After the sprayed

water droplets landed on the tarp a mixture of ice and water formed. The ice-water mixture was collected from the lower end of the tarp into Plexiglas columns. The columns were designed for the experiment. The columns had a inside diameter of 240 mm and a height of 300 mm (Figure 6.1). The vertical height of the sprayed water jet was between 10 to 15 m. The spraying method was chosen because all runoff generated during the spraying could be collected in order to prevent any possible pollution of the surrounding areas by the wastewaters and a limited amount of the wastewaters was available. The pulp mill effluent and oil sands tailings pond water were transported from Weyerhaeuser Canada, Grande Prairie Operation and Syncrude Canada Ltd. mine site, respectively. The wastewaters were mixed in the barrel before spraying. City of Edmonton tap water was also sprayed under the same field conditions to serve as "blank".

The spraying operation was carried out on December 17, 1996 and January 23, 1997. The ambient air temperature was about -10 °C (relative humidity: 60 to 75%) on December 17, 1996 and - 24 °C (relative humidity: 50 to 56%) on January 23, 1997. The water sprayed at -10 °C had higher water content in the ice-water mixture which was produced. Most of the droplets froze after they landed on the tarp. After the ice slurry was placed into the Plexiglas columns, drainwater (runoff) was collected from the bottom of the columns. Approximately 30% of the sprayed water was collected as drainwater. No drainwater was generated during the spraying operation with the ambient air temperature around - 24 °C. At - 24 °C, the sprayed water droplets frozen immediately after impinging on the tarp and turned into "wet" snow. Compare to the ice produced under - 10 °C, the ice ("wet" snow) formed under - 24 °C was loose, less cohesive and had numerous airpockets in the ice pack.

The spraying operation had to be stopped from time to time to clean the pump inlet filter. The filter was taken off and soaked in the gasoline to remove the materials which clogged the filter.

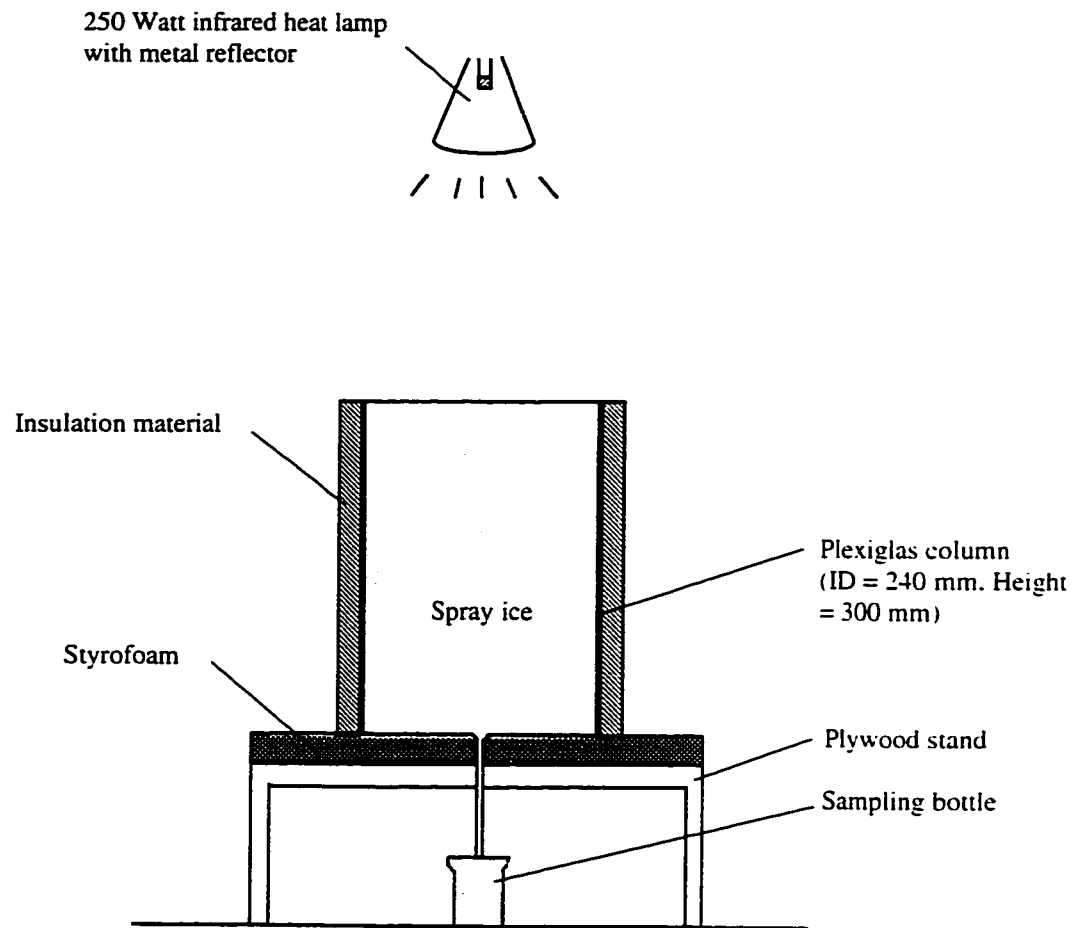


Figure 6-1 Experimental configuration for the laboratory melting tests.

Immediately after finishing the spraying operation, the columns were covered with plastic bags and stored in cold rooms. The cold room temperatures were kept the same as the air temperatures when the wastewaters were sprayed. Half of the columns were stored in the cold room for 20 days and the other half for 40 days to examine the effect of holding period on the impurity removal during the subsequent melt process.

6.1.2 The melting experiments

Before the ice columns were melted, the columns were moved into a cold room with a temperature at -2°C for 24 hours to simulate the gradual warming up of a ice mound during spring. The melting experiments were carried out under room temperature. The columns were wrapped with insulation to reduce edge melting effects. The melting was promoted using a 250 W infrared lamp suspended between 250 to 300 mm above the ice surface (photo, Appendix C). Styrofoam on the base was used to reduce the heating of the column during the melting test. The meltwater from the column was collected at the base of the column at random time intervals. Four melting experiments were conducted, one for each experimental condition:

1. spraying condition: ambient air temperature -10°C , storage time: 20 days;
2. spraying condition: ambient air temperature -10°C , storage time: 40 days;
3. spraying condition: ambient air temperature -24°C , storage time: 20 days. and
4. spraying condition: ambient air temperature -24°C , storage time: 40 days.

The melting tests were completed in a single sequence and they lasted for 14 to 16 hours. The initial meltwater came out after the ice columns were heated for 2 to 4 hours. The spray ice produced at colder temperature (-24°C), needed less time to melt. The rate of meltwater collection was not constant because the percolation of the meltwater through the icepack is a non-uniform process, the water moved along preferred channels or ducts rather than through the full cross-section of the snow as a water front (Colbeck, 1972; Foster, 1978; Hibberd, 1984). Blocking of the drainage hole of the column by ice

also occurred during the melting test. When this occurred, meltwater accumulated in the column and until the drainage hole was unblocked. It happened more frequently during melting of the ice formed at - 10 °C because of the solid ice which had formed at the bottom of the column. It consequently caused fluctuation in the meltwater impurity concentration with time as will be outlined.

6.1.2.1 Water samples and analysis

Source water, runoff (if any) samples were collected during the test. Ice core samples were obtained from one of the replicated columns for each experimental condition (photo, Appendix C). Meltwater samples were collected throughout the thawing process. Standard Methods for the Examination of Water and Wastewater (American Public Health Association et al., 1995) were applied for all sample analysis. The methods used were summarized in Table 6-1.

Sample pH and conductivity were determined using an ACCUMET-25 pH/conductivity meter after the samples were collected. Color of the pulp mill effluent and tap water samples were determined within 48 hours using a ULTROSPEC-3000 spectrometer. The total organic carbon (TOC) content was analyzed with a Dcat-Dohrmann Carbon Analyzer. Cl^- and SO_4^{2-} concentration were also measured for the oil sands tailings pond water and tap water samples. Cl^- concentration was determined using a METTLER-DL-53 Ultratitrator (probe: DM141). A Dionex model ion chromatography, equipped with an IONPAC-AC10 separator column was employed for the determination of SO_4^{2-} . Filtration was performed on the oil sands tailings pond water and tap water samples before SO_4^{2-} determination to removal particles and organic substances. Filter papers with 0.2 μm pore size and Bakerbond cartridge (cap reversed phase C-18) were used for the filtration. The Dichromate Reflux method was used for COD determination.

Microtox toxicity test was used to evaluate toxicity reduction in the meltwater. In this test Microtox results were reported as EC_{50} (15, 15) values (the median effective

Table 6-1 Summary of sample analytical methods

Test	Method
Chemical oxygen demand (COD)	standard method* - 5220 (B)
Cl ⁻	standard method - 4500-Cl ⁻ (D)
Color	standard method - 2120 (C)
Conductivity	standard method - 2510
pH	standard method - 4500-H ⁺
Total organic carbon (TOC)	standard method -5310 (B)
SO ₄ ²⁻	standard method -4500-SO ₄ ²⁻ (B)

*Standard Methods for the Examination of Water and Wastewater (American Public Health Association, 1995)

sample concentration causing a 50% reduction in light output by the test bacteria in 15 minutes as a test temperature of 15 °C). A Microtox toxicity analyzer (Model 500) was used for the test. During the Microtox toxicity test the standard procedure for Microtox analysis issued by WCMUC (Western Canada Microtox Users Committee, 1991) was followed. The Microtox test was performed on the source water and some meltwater samples. For oil sands tailings pond water samples, duplicate Microtox assays of both pH-adjusted and filtered (0.7 µm fiber glass filter paper) and non-adjusted samples (original samples) were conducted to correct/overcome pH and turbidity interferences. For pulp mill effluent samples, pH adjustment and color correction were performed and for the tap water (blank) samples only pH adjustment was made. Original samples (non-adjusted) were also tested for pulp mill effluent and tap water.

6.2 Results and Discussions

6.2.1 Impurity removal by runoff during the spraying operation

The results of the chemical analysis of runoff (drainwater) and source water samples collected during the spraying operation conducted on December 17, 1996 are listed in Table 6-1. The ambient air temperature was about - 10 °C during the spraying. The values listed in Table 6-2 were the average of 3 to 4 samples obtained during the test.

As shown in Table 6-2, the runoff generated during spraying had higher impurity concentrations compared with the source water. The concentration ratio (ratio of the runoff impurity concentration to the source water impurity concentration) indicated that the impurity concentrations in the runoff were about 1.1 to 4.9 times higher than those of the source water for tap water. Apparently higher concentration ratios of organic contaminants in the tap water (COD, 2.5 and color, 4.9) indicated the higher rate of the separation (or removal) of organic contaminants during spray freezing. The concentration ratios for pulp mill effluent were in the range of 1.4 to 1.5. The

Table 6-2 Comparison of the source water and the runoff impurity concentrations

Samples	pH	Conductivity ($\mu\text{S}/\text{cm}$)	TOC (mg/L)	COD (mg/L)	Color (TCU)	Cl^- (mg/L)	SO_4^{2-} (mg/L)
Blank (tap water)							
source (C_o)	7.24	237	2	6	0.7	3	54
runoff (C_r)	7.34	262	3	15	3.4	5	72
Concentration ratio (C_r/C_o)	1.0	1.1	1.5	2.5	4.9	1.6	1.3
Pulp mill effluent							
source (C_o)	7.23	2777	258	546	1314	N/A ¹	N/A
runoff (C_r)	7.74	3955	396	796	1946		
Concentration ratio (C_r/C_o)	1.1	1.4	1.5	1.5	1.5		
Oil sands tailing pond water							
source (C_o)	8.22	3335	148	409	N/A	473	141
runoff (C_r)	8.32	4835	230	662		742	228
Concentration ratio (C_r/C_o)	1.0	1.5	1.6	1.6		1.6	1.6

¹ the wastewater was not analyzed for this parameter

impurity concentrations in the runoff were about 50% higher than those in the source pulp mill effluent. Concentration and separation of organic contaminants by freezing were again more efficient than the inorganics for pulp mill effluent indicated by the slightly higher concentration ratios of the organic parameters measured. For oil sand tailings pond water, the concentration ratios were in the range of 1.5 to 1.6. The increase of the organic and inorganic contaminant contents in the runoff by freeze concentration was at

comparable levels. Most of the concentration ratios of tap water were higher than those of the pulp mill effluent and oil sands tailing pond water except for conductivity and sulfate. The lower concentration ratios (which indicated lower impurity rejection efficiency) obtained from the wastewaters, especially, for the organics, could be caused by higher impurity contents contained in the pulp mill effluent and oil sands tailings pond water. In the freezing process, the impurity rejection efficiency decreases with increasing impurity concentration in the source water since the chances to trap an impurity particle into the ice structure increases. Higher concentrations of inorganic impurities in the wastewaters could result in the lower rejection rate of the organic contaminants. Rejection of organic contaminants by growing ice crystals are affected by the increase in the inorganic contents in a complex solution containing both organics and inorganics. There were slight increases in the pH value for the runoff samples, about 0.1 unit for tap water and oil sands tailing pond water and 0.5 unit for pulp mill effluent. All runoff samples had higher pH values, although the magnitude of increase varied from sample to sample. The runoff carried away the concentrated impurities from the spray ice during the spraying and leave a relatively purer ice, so a certain amount of treatment was achieved during the spraying operation due to the runoff carrying away the impurities.

6.2.2 Impurity concentrations in the spray ice

Ice core samples were obtained from the Plexiglas columns containing the spray ice of the wastewaters using a 100 mm diameter CRREL core barrel. The ice core samples were collected after 20 or 40 day storage (the same day when the ice columns were melted). Each ice core was cut into three pieces (top, middle, and bottom) to check the impurity distribution within the ice column. The results of the chemical analysis were listed in the Tables 6-3 and 6-4. The impurity concentration ratios of the spray ice to source water were also included in the tables.

Table 6-3 Impurity concentrations of the spray ice cores of pulp mill effluent

Sample	ambient air temperature ^a (°C)	storage period, (day)	Impurity Concentrations				
			pH	color (TCN)	TOC (mg/L)	COD (mg/L)	conductivity (µm/cm)
core I: top	- 10	20	9.46 (1.3) ^b	271 (0.2)	74 (0.3)	184 (0.3)	571 (0.2)
middle			9.71 (1.3)	429 (0.3)	94 (0.4)	294 (0.5)	616 (0.2)
bottom			9.37 (1.3)	1033 (0.8)	228 (0.9)	510 (0.9)	2265 (0.8)
Cavg. ^c			(1.3)	(0.4)	(0.5)	(0.6)	(0.5)
core II top	- 10	40	9.90 (1.4)	345 (0.3)	28 (0.1)	235 (0.4)	639 (0.2)
middle			9.87 (1.4)	338 (0.3)	79 (0.3)	212 (0.4)	611 (0.2)
bottom			9.45 (1.3)	494 (0.4)	185 (0.7)	483 (0.9)	1675 (0.6)
Cavg.			(1.4)	(0.3)	(0.4)	(0.6)	(0.4)
core III top	-24	20	10.00 (1.3)	1355 (1.0)	292 (1.2)	686 (1.0)	2073 (0.8)
middle			10.04 (1.3)	1361 (1.0)	268 (1.1)	682 (1.0)	2063 (0.8)
bottom			10.03 (1.3)	1375 (1.0)	257 (1.1)	685 (1.0)	2090 (0.8)
Cavg.			(1.3)	(1.0)	(1.1)	(1.0)	(0.8)
core IV top	- 24	40	10.09 (1.3)	1298 (0.9)	253 (1.0)	633 (1.0)	2153 (0.9)
middle			10.15 (1.3)	1195 (0.9)	227 (1.0)	584 (0.9)	2005 (0.8)
bottom			10.17 (1.3)	1517 (1.1)	268 (1.1)	740 (1.1)	2425 (1.0)
Cavg.			(1.3)	(1.0)	(1.0)	(1.0)	(0.9)

^a ambient air temperature at which the wastewater was sprayed and the spray ice was stored

^b the ratio of the ice (melted) impurity concentration to that of the source water

^c the average concentration ratio of the entire ice core.

Table 6-4 Impurity concentrations of the spray ice cores of oil sands tailings pond water

Sample	air temp. ^a (°C)	storage period, (day)	Impurity Concentrations					
			pH	TOC (mg/L)	COD (mg/L)	conductivity (µs/cm)	SO ₄ ²⁻ (mg/L)	Cl ⁻ (mg/L)
core I: top	- 10	20	9.86	50	196	1085	52	154.0
			(1.2) ^b	(0.3)	(0.5)	(0.3)	(0.4)	(0.3)
middle			9.65	47	99.0	489	21	66.3
			(1.2)	(0.3)	(0.2)	(0.2)	(0.2)	(0.1)
bottom			9.35	130	332	2335	139	414.4
			(1.1)	(0.9)	(0.8)	(0.7)	(1.0)	(0.9)
Cavg. ^c			(1.2)	(0.5)	(0.5)	(0.4)	(0.5)	(0.5)
core II top	- 10	40	10.16	46	146	806	38	117.7
			(1.2)	(0.3)	(0.4)	(0.2)	(0.3)	(0.3)
middle			10.17	38	124	576	26	84.5
			(1.2)	(0.3)	(0.3)	(0.2)	(0.2)	(0.2)
bottom			9.49	115	328	2025	117	370.3
			(1.2)	(0.8)	(0.8)	(0.6)	(0.8)	(0.8)
Cavg.			(1.2)	(0.5)	(0.5)	(0.3)	(0.4)	(0.4)
core III top	-24	20	9.87	98	445	1918	109	358.2
			(1.2)	(0.7)	(1.1)	(0.6)	(0.8)	(0.8)
middle			10.03	95	432	2010	108	371.9
			(1.2)	(0.7)	(1.0)	(0.6)	(0.8)	(0.8)
bottom			9.68	228	449	4930	250	801.8
			(1.1)	(1.7)	(1.1)	(1.5)	(1.8)	(1.7)
Cavg.			(1.2)	(1.0)	(1.1)	(0.9)	(1.1)	(1.1)
core IV top	- 24	40	9.87	143	471	3788	141	484.0
			(1.2)	(1.0)	(1.1)	(1.1)	(1.0)	(1.0)
middle			10.04	146	473	3735	143	486.7
			(1.2)	(1.1)	(1.1)	(1.1)	(1.1)	(1.0)
bottom			9.88	143	455	3788	139	486.1
			(1.2)	(1.1)	(1.1)	(1.1)	(1.0)	(1.0)
Cavg.			(1.2)	(1.1)	(1.1)	(1.1)	(1.0)	(1.0)

^a ambient air temperature at which the wastewater was sprayed and the spray ice was stored

^b the ratio of the ice (melted) impurity concentration to that of the source water

^c the average concentration ratio of the entire ice core.

As expected, the impurity contents in the ice cores obtained in a - 10 °C ambient air environment were significantly less than those in the ice cores obtained at a colder temperature as illustrated in Tables 6-3 and 6-4. The impurities were removed by the runoff generated during the spraying. It demonstrated that substantial amount of impurities could be removed when sprayed wastewater partially froze during the spraying operation. The spray ice was much purer than the source water without further treatment as shown in Tables 6-3 and 6-4. The bottom of the ice cores obtained under warmer temperature conditions (- 10 °C) had relatively higher impurity concentrations induced by the downward flow of the unfrozen water which froze afterwards. Tables 6-3 and 6-4 indicated that the ice cores stored for the longer period (40 days, - 10 °C) had relatively lower impurity concentrations. The ice cores contained about 30% to 57% of the source water impurity concentrations for the pulp mill effluent and 34% to 49% of the source water impurity concentrations for the oil sands tailings pond water (not including pH). The most probable reason for the lower impurity contents in these ice columns was the better discharging of the runoff after the ice slurry was placed in the columns (sometimes the drainage hole was partially blocked by ice and caused less runoff), which happened coincidentally in these columns. The inaccuracy in the measurement might be another reason but loss of impurity during the storage was unlikely as all columns were covered with plastic bags during the entire storage time.

The spray ice cores obtained at colder air temperature (- 24 °C) had nearly the same amount of impurity contents as the source water except conductivity which was lower in most of the ice cores obtained under this air temperature condition. The small difference in the impurity concentrations between the source water and ice cores could be caused by measurement errors. The distribution of the impurities was much more uniform along the length of the ice cores. The pH of the spray ice cores were about 1.1 to 1.4 times higher than that of the source waters. H^+ ions were obviously incorporated into other materials during spraying. The slightly lower ionic strength (conductivity) in the ice cores also suggested the loss of ionic species by spraying.

6.2.3 Impurity removal during melting process

The experimental results of the melting tests were presented in the following sections. The impurity concentrations of the meltwater were expressed as a function of the percentage of the meltwater volume. The meltwater impurity concentrations were normalized to that of the source water concentration (C/C_0). This gives a graph that is similar to those traditionally drawn in this subject (e.g. Johannessen and Henriksen, 1977; Brimblecombe et al., 1987).

6.2.3.1 Impurity removal from the spray ice obtained in a - 10 °C ambient air environment

Samples of spray ice obtained when the air temperature was about - 10 °C was melted after 20 and 40 days storage in a cold room. The impurity concentrations of the meltwater was plotted as a function of meltwater volume and ice age (storage time). The variations of COD, color, TOC concentrations, conductivity and pH of the meltwater during the melting process of the pulp mill effluent spray ice were shown in Figures 6-2 to 6-6.

Figures 6-2 to 6-5 indicated clearly that initial meltwater contained high impurity concentrations i.e. chemical fractionation occurred during the melting process. The concentrations of COD (Figure 6-2), color (Figure 6-3) and total organic carbon (Figure 6-4) in the initial meltwater of the spray ice that had been on storage for 20 days were as much as 3.5 to 5 times as high in the source pulp mill effluent. The ionic impurities (conductivity) in the wastewater were also concentrated by more than 3.5 times in the initial meltwater (Figure 6-5). The horizontal broken line indicates a concentration of the source water. The first portion of the meltwater from the ice stored in the cold room for 40 days was less concentrated; the impurity concentration in the initial meltwater was about 2.5 to 4 times of those in the source water. The meltwater impurity concentrations decreased dramatically in the subsequent portions of the meltwater. The

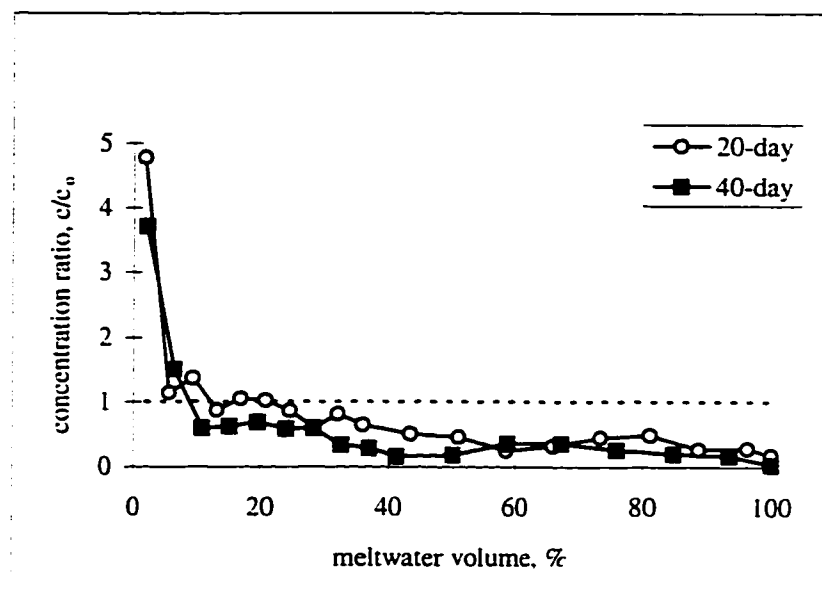


Figure 6-2 Variation of the normalized COD concentration in the sequential meltwater samples of the spray ice made from pulp mill effluent (The spray ice was obtained in a - 10 °C ambient air temperature environment). Source water COD concentration, $c_0 = 546$ mg/L.

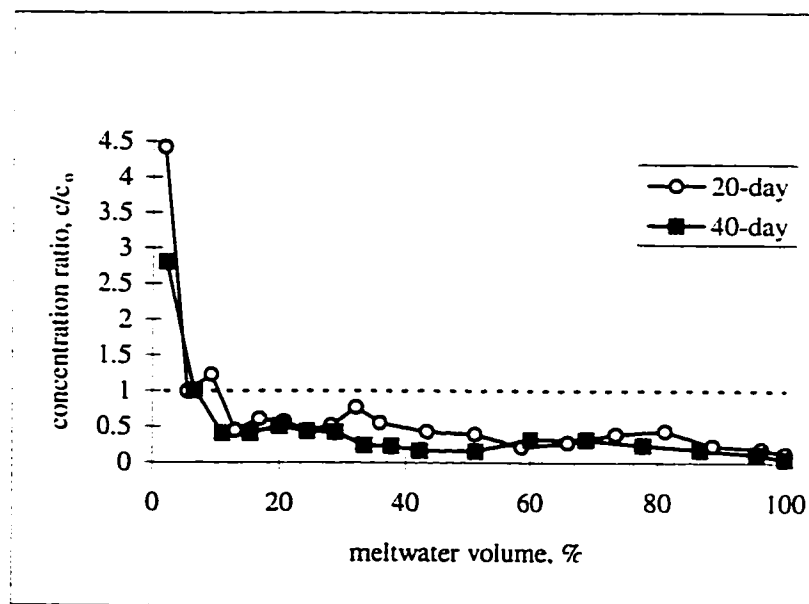


Figure 6-3 Variation of the normalized color concentration in the sequential meltwater samples of the spray ice made from pulp mill effluent (The spray ice was obtained in a - 10 °C ambient air temperature environment). Source water color concentration, $c_0 = 1314$ (TCU).

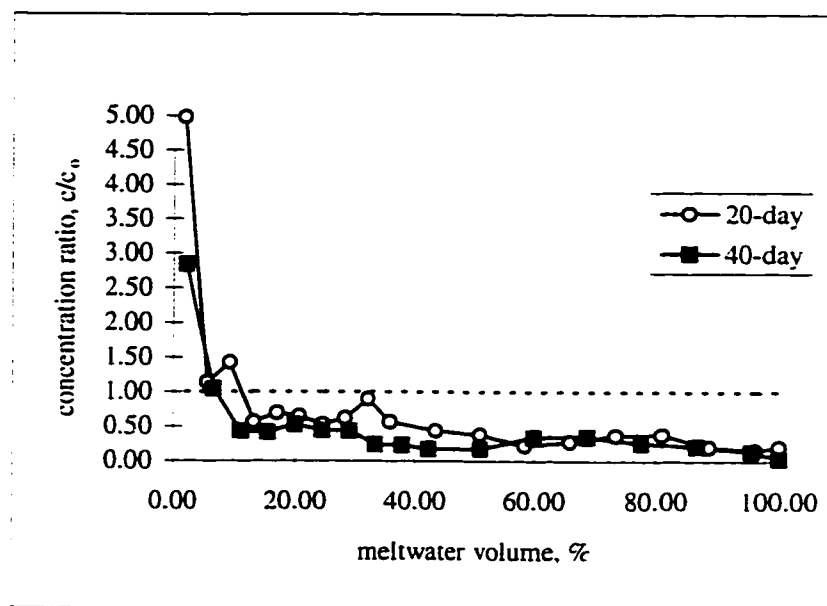


Figure 6-4 Variation of the normalized TOC concentration in the sequential meltwater samples of the spray ice made from pulp mill effluent (The spray ice was obtained in a - 10 °C ambient air temperature environment). Source water TOC concentration, $c_0 = 258$ mg/L.

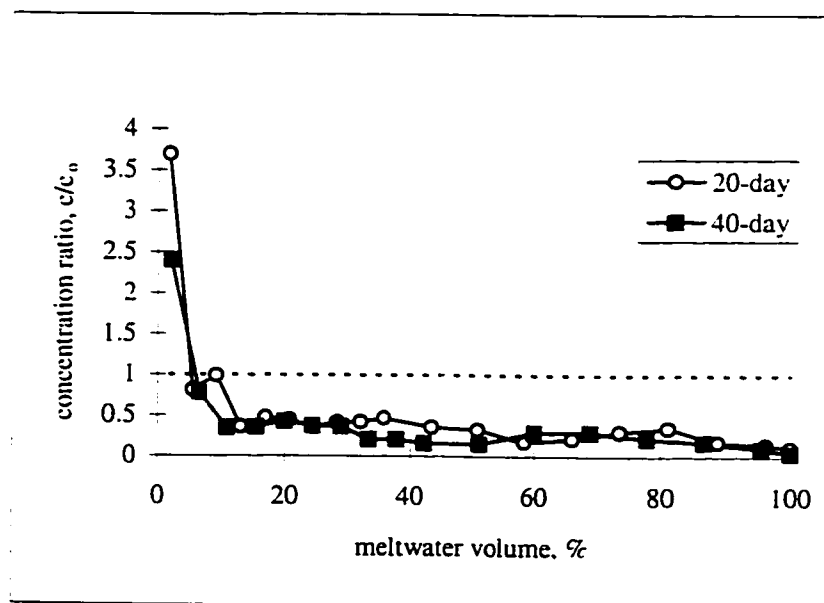
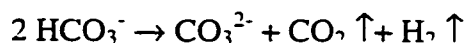


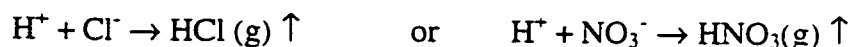
Figure 6-5 Variation of the normalized ionic strength (conductivity) in the sequential meltwater samples of the spray ice made from pulp mill effluent (The spray ice was obtained in a - 10 °C ambient air temperature environment). Source water conductivity, $c_0 = 2777$ μ S/cm.

meltwater became purer and purer as melting continued. Elution of organic and inorganic contaminants during the melting followed the same patterns.

Figure 6-6 indicated that the meltwater pH was consistently higher than that of the source water throughout the melting process. The hydrogen ion concentration (pH) showed little change during the entire melting process. As noticed previously, both runoff and ice core samples had higher pH values than that of the source water. The elevated pH in the runoff, ice core, and meltwater samples implied that some H^+ ions were lost during the spraying operation. Spraying of the wastewater into atmosphere will increase oxygen concentration in the water, just like the aeration process, it causes stripping of the gases such as NH_3 , CO_2 , H_2S and oxidation of volatile organic compounds and some metals. However, stripping of NH_3 during freezing does not increase the sample pH (because $HO^- + NH_4^+ \rightarrow NH_4OH \rightarrow H_2O + NH_3(g) \uparrow$). Sample pH might be increased by losing bicarbonate, HCO_3^- , according to the reaction:



Spyker (1982) noticed the loss of bicarbonate during his spray freezing tests. Acidity of the sprayed wastewater samples might also be lost by the following two reactions during freezing:



But Iribarne and Pyshnov (1990) did not find elution of HCl or HNO_3 during freezing in their study. Release of H_2S gas during spraying will also lose H^+ ions ($2H^+ + S^{2-} \rightarrow H_2S(g) \uparrow$). Based on the fact that pH of the meltwater samples of the spray ice made from tap water which had much lower organic or metal contents was also higher than that of the source water, losing of the bicarbonate during spray freezing was the most possible reason for the increase of pH in the ice core and meltwater samples. The pH of various samples are listed in Table 6-5.

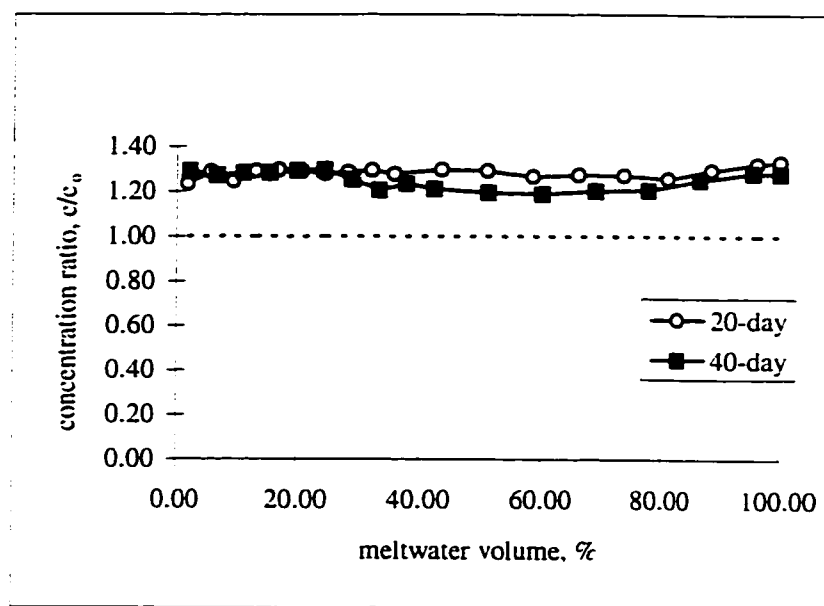


Figure 6-6 Variation of the normalized pH value (hydrogen ion concentration) in the sequential meltwater samples of the spray ice made from pulp mill effluent (the spray ice was obtained in a $-10\text{ }^{\circ}\text{C}$ environment). The source water pH, $c_0 = 7.23$.

Table 6-5 pH values of various pulp mill effluent samples collected

Sample	pH
source water	7.23
runoff	7.74
ice core (20 day storage)	9.51
ice core (40 day storage)	9.74
meltwater (20 day ice, average value of meltwater samples)	9.28
meltwater (40 day ice, average value of meltwater samples)	9.03

As shown in Table 6-5, the pH values of the ice cores and meltwater samples were much higher than that of the source water (about 1.8 to 2.5 units higher). The pH values of the meltwater samples were slightly lower than those of the ice core samples. The small acid pH shift during the melting process was induced by atmospheric CO₂ solution.

Concentration ratios of all impurities analyzed were plotted on one graph against the cumulative volume of the meltwater collected for the spray ice with different storage terms (Figure 6-7 and 6-8). Figure 6-7 and 6-8 revealed that organic contaminants had higher concentration ratios than the ionic species (conductivity) at the beginning of the melting process. The difference of the concentration ratios between the organic contaminants and conductivity decreased afterwards. The difference in the concentration ratio suggested that not all impurities were enriched to the same extent, some impurities were enriched more than others. Higher TOC, COD and color concentration ratios indicated that organic contaminants were removed more efficiently by the early meltwater. The TOC concentration ratio was highest for the 20-day old ice. While for

the 40-day old ice, the COD causing materials were enriched most in the first portion of the meltwater. TOC and color concentrations were about equal but lower than the COD. The conductivity (or ionic strength) ratio was lower than that of the organic contaminants for both 20-day and 40-day old ice. Of the five contaminants studied for pulp mill effluent, hydrogen ion showed the least relative enrichment.

The percentage of impurities removed in the first 30% of the meltwater from the spray ice stored for 20 days and 40 days was calculated and tabulated in Table 6-6.

Table 6-6 Percentage of the total amount of the impurity removed from the spray ice of pulp mill effluent by the first 30% of meltwater

	% of the total amount of impurities within the ice columns removed			
	COD	TOC	color	conductivity
Meltwater from 20-day old ice	55	57	53	54
Meltwater from 40-day old ice	62	57	58	55

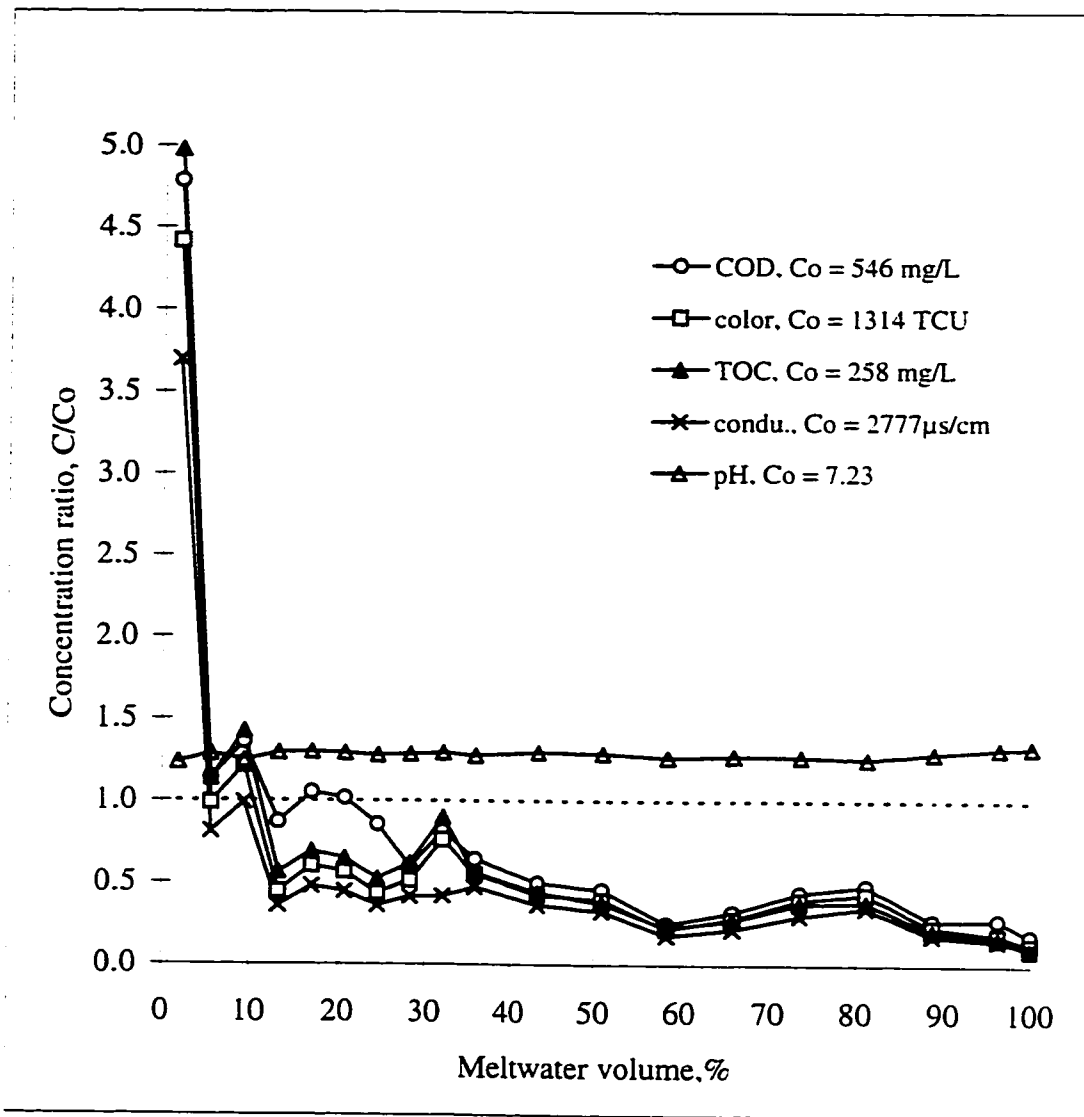


Figure 6-7 Variation of the concentration ratios of the selected impurities versus meltwater volume for the 20-day old spray ice made from pulp mill effluent in a -10°C environment.

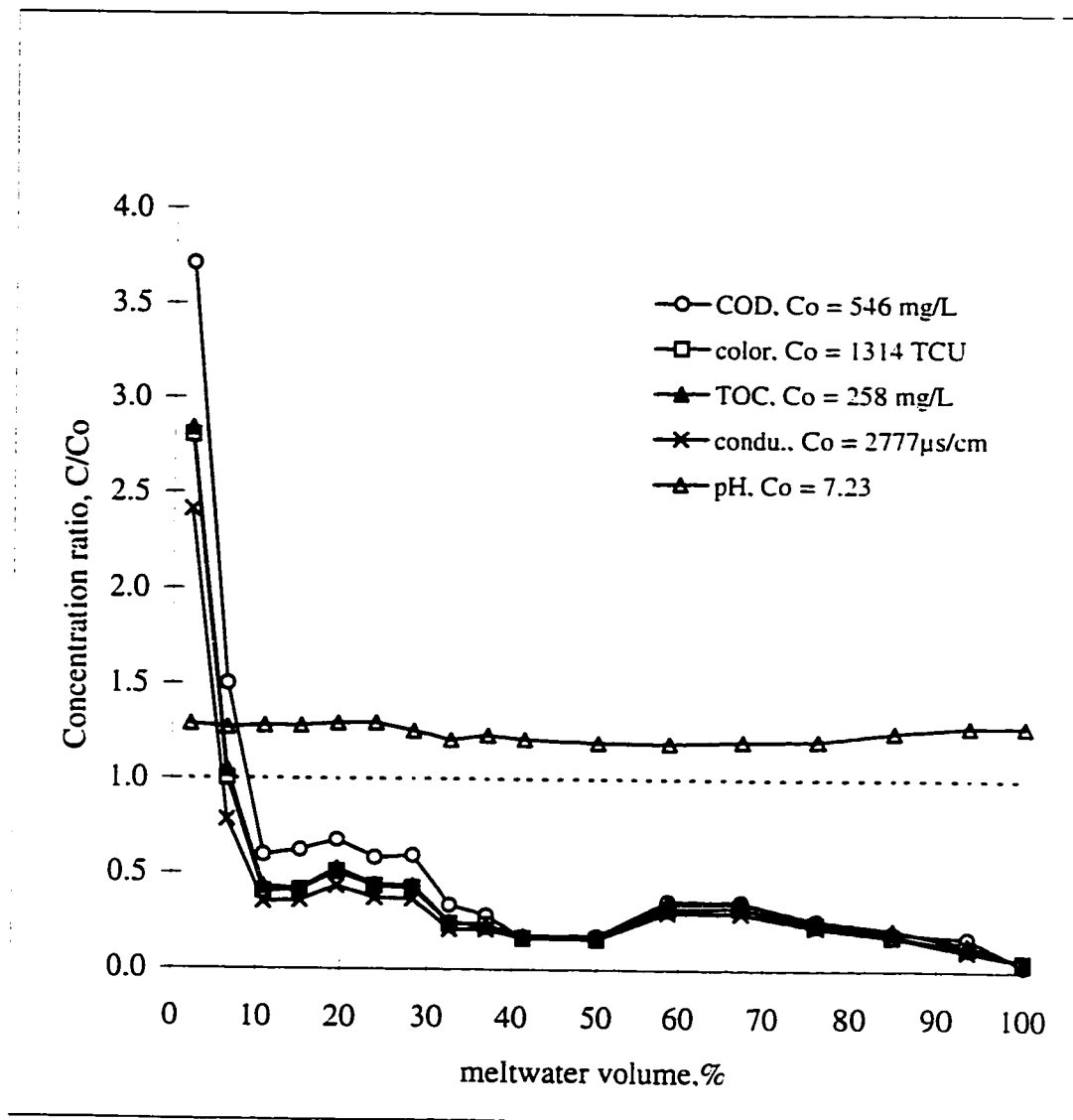


Figure 6-8 Variation of the concentration ratios of the selected impurities versus meltwater volume for the 40-day old spray ice made from pulp mill effluent in a -10°C environment.

As listed in Table 6-6, for the 20-day old spray ice, 57% of the organic carbon content (TOC) was removed with the initial 30% of the meltwater. The amount of TOC removed was slightly higher than COD, conductivity and color. The reduction of the conductivity in the ice was 1% higher than that of the color for the ice stored for 20 days. For the 40-day old ice, the percentage of the total amount of COD causing components in the ice released with the early meltwater was highest. High concentrations of COD or TOC in the initial meltwater suggested that more organic contaminants were removed. The percentage of the impurity removed in the initial meltwater from the older ice increased by 7% for COD, 5% for color and 1% for conductivity, respectively. There was no difference in the TOC removal between the 20-day ice and the 40-day ice. The heterogeneous distribution of impurities within the ice columns and the differential segregation of ionic and nonionized solutes during freezing might result in the larger amount of organic contaminants removal with the early meltwater.

Figures 6-9 to 6-16 present the results obtained from the melting test of the spray ice of oil sands tailing pond water. Fractionation of the chemicals also occurred during the melting of the spray ice of oil sands tailings pond water. The concentrations of all components analyzed were several times higher than those of the source water in the first portion of the meltwater then the impurity concentrations decreased rapidly. The concentrations of the impurities were much lower in the later fractions of the meltwater as compared to those of the source water. Melting of all ice columns followed this typical pattern.

For 20-day old spray ice of oil sands tailings pond water, the concentration ratio, c/c_o , in the first portion of meltwater was about 3 for TOC and 2.5 for COD (Figure 6-9 and 6-10), which were relatively low as compared with pulp mill effluent (TOC and COD

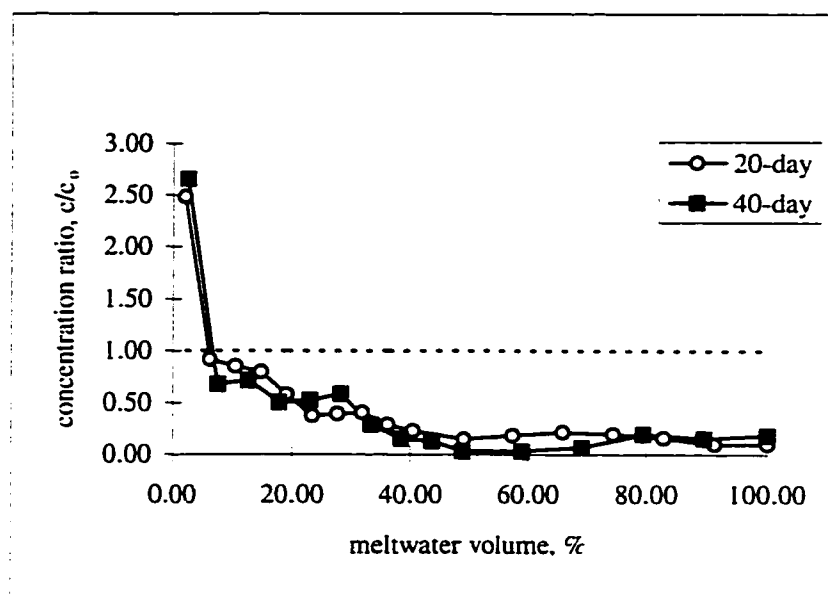


Figure 6-9 Variation of the normalized COD concentration in the sequential meltwater samples of the spray ice made from oil sands tailings pond water (spray ice was obtained in a - 10 °C ambient air temperature environment). Source water COD concentration $c_0 = 409$ mg/L.

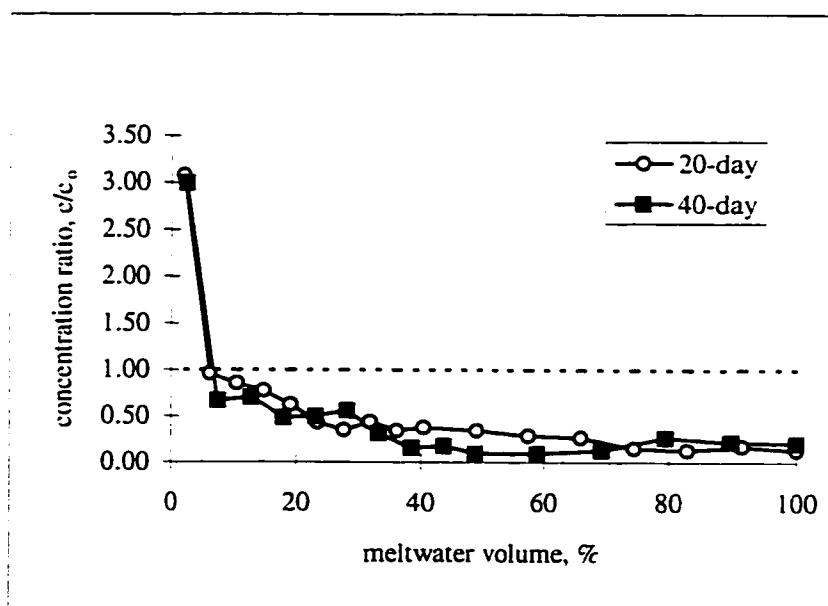


Figure 6-10 Variation of the normalized TOC concentration in the sequential meltwater samples of the spray ice made from oil sands tailings pond water (spray ice was obtained in a - 10 °C ambient air temperature environment). Source water TOC concentration $c_0 = 148$ mg/L.

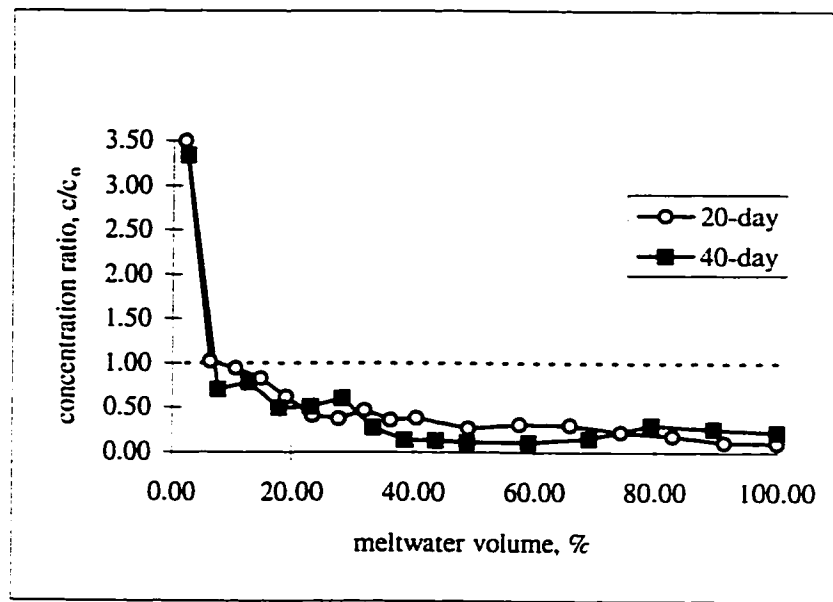


Figure 6-11 Variation of the normalized Cl^- concentration in the sequential meltwater samples of the spray ice made from oil sands tailings pond water (spray ice was obtained in a -10°C ambient air temperature environment). Source water Cl^- concentration $c_0 = 473 \text{ mg/L}$.

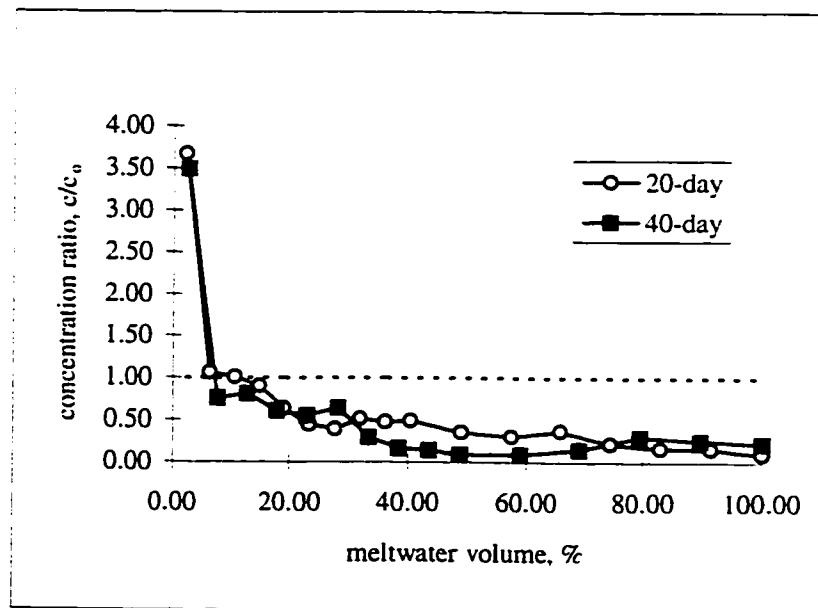


Figure 6-12 Variation of the normalized SO_4^{2-} concentration in the sequential meltwater samples of the spray ice made from oil sands tailings pond water (spray ice was obtained in a -10°C ambient air temperature environment). Source water SO_4^{2-} concentration $c_0 = 141 \text{ mg/L}$.

concentration ratios were about 5). But the meltwater impurity concentrations fluctuated less for the oil sands tailings pond water. The amount of impurities removed with the first 30% meltwater would be close to that from pulp mill effluent. The concentration of sulfate ions and chloride ions in the early meltwater was clearly seen in this experiment. As shown in Figures 6-11 and 6-12, the Cl^- and SO_4^{2-} ions were concentrated by about 3.5 times in the early meltwater. The change of hydrogen ion concentration (pH) versus meltwater volume was demonstrated in Figure 6-13. The pH of the meltwater was low at first then increased slightly and remained almost constant throughout the entire melting process. The difference in the pH value between the first meltwater sample and the second meltwater sample was 0.75 for 20-day ice and 0.68 for 40-day ice. The difference in the pH values means that higher concentration of H^+ ions was released at the beginning of the melting process. The pH value of meltwater samples and ice core samples was steadily higher than that of the source water implying loss of acidity during the spraying. The pH values of the original oil sands tailings pond water (source water), runoff, ice core samples and meltwater samples were listed in the following table for comparison.

Table 6-7 Comparison of pH values of various oil sands tailings pond water samples collected (air temperature = - 10 °C when spray freezing tested was conducted)

Sample	pH
source water	8.22
runoff	8.32
ice core (20 day storage)	9.62
ice core (40 day storage)	9.94
meltwater (20 day ice, average value of meltwater samples)	9.68
meltwater (40 day ice, average value of meltwater samples)	9.62

The pH values of source water and ice core samples shown in Table 6-6 and Table 6-7 suggested that pH values of spray ice core samples were always higher than those of the source waters. Loss of acidity seems typical of the spray freezing. The extent of losing acidity depended on the nature of the liquid sprayed. The pulp mill effluent has a lower buffering capacity as compared with oil sands tailings pond water so it is more sensitive to the bicarbonate lost during the spray freezing process. As a result, the change of pH in the runoff, ice core and meltwater samples was more apparent. The difference in the pH values of ice core samples and source water samples was in the range of 1.8 to 2.3 for pulp mill effluent and it was between 1.40 and 1.72 for oil sands tailings pond water.

The percentage of total amount of impurities in the spray ice released with the first 30% of meltwater was shown in the Table 6-8.

Table 6-8 Percentage of the total amount of the impurity removed from the spray ice of oil sands tailings pond water by the first 30% of meltwater

	% of the total amount of impurities within the ice columns removed				
	COD	TOC	Cl ⁻	SO ₄ ²⁻	conductivity
Meltwater from 20-day old ice	60	56	57	54	54
Meltwater from 40-day old ice	72	65	65	67	64

Table 6-8 shows more clearly that the age of the ice (storage time) affected the fractionation process. The amount of the impurities removed with the first 30% of the meltwater increased by more than 10% for the ice stored for a longer term. The longer

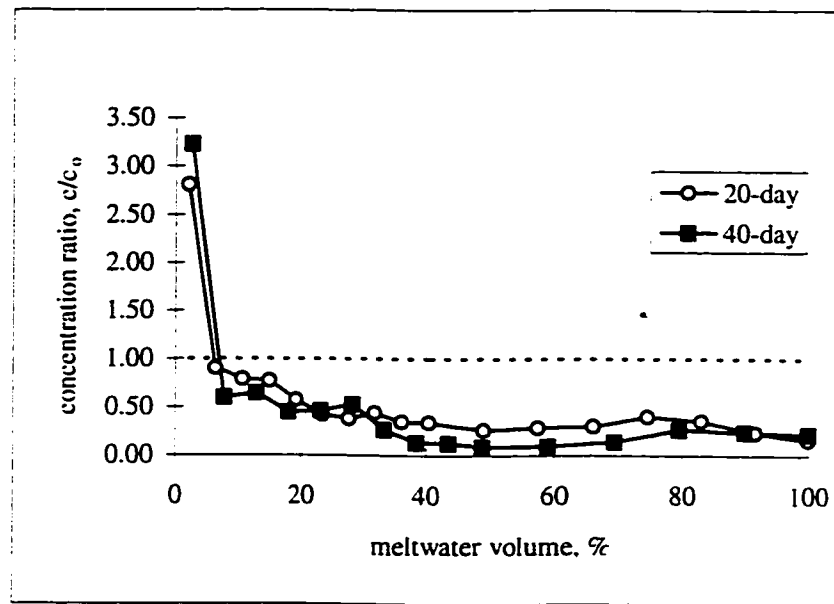


Figure 6-13 Variation of the normalized ionic strength (conductivity) in the sequential meltwater samples of the spray ice made from oil sands tailings pond water (spray ice was obtained in a $-10\text{ }^{\circ}\text{C}$ ambient air temperature environment). The source water conductivity, $c_0 = 3335\text{ }\mu\text{s/cm}$.

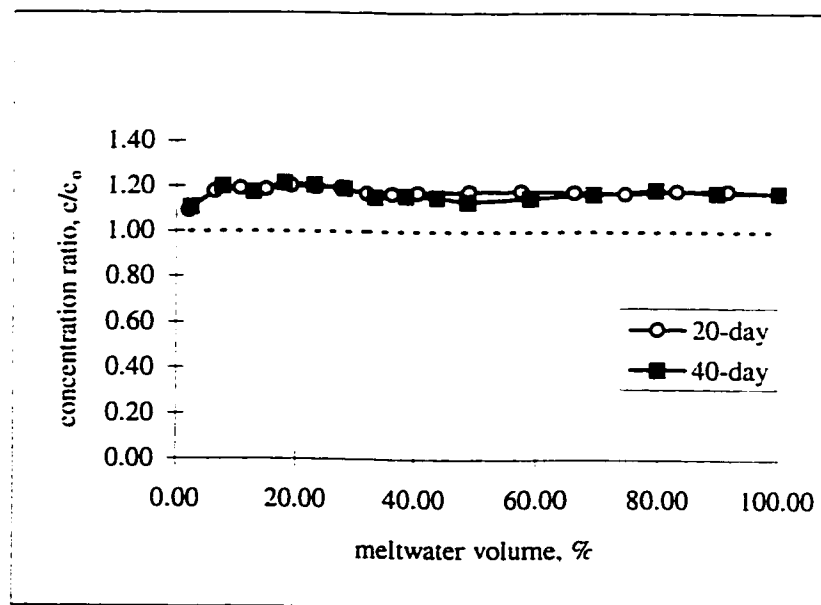


Figure 6-14 Variation of the normalized pH value (hydrogen ion concentration) in the sequential meltwater samples of the spray ice made from oil sands tailings pond water (spray ice was obtained in a $-10\text{ }^{\circ}\text{C}$ ambient air temperature environment). The source water pH, $c_0 = 8.22$.

storage time gave more chances for the ice grains to grow and the recrystallization of the ice crystals under the experimental conditions to improve the rejection of impurities from the ice structure. More impurities might migrate to the surface of the ice crystals so they were readily picked up by the early meltwater percolating down from the top of the column. The effect of the ice age on the fractionation process was more profound for the spray ice of oil sands tailings pond water than for spray ice made from pulp mill effluent. Before doing a more rigorous study, we can only speculate that it was caused by the difference in the nature of the wastewaters. The metamorphic physical changes during the growth of the ice crystals might have induced more efficient rejection of the contaminants in the oil sands tailings pond water. The melting conditions which reduced the fluctuation of the meltwater impurity concentrations for the spray ice of oil sands tailings pond water could also be responsible for the increased amount of impurity removal.

Table 6-8 indicated that early meltwater contained more COD causing substances. COD causing substances were excluded more efficiently from ice grains and therefore appeared sooner and in higher concentrations in the meltwater. The amount of inorganic solutes (SO_4^{2-} and Cl^-) released with the first 30% of the meltwater was slightly less than that of the COD causing matters but comparable with amount of TOC removed. The higher inorganic contents in the oil sands tailings pond water might hinder the release of the organic contaminants. It has been known that the removal efficiency of organic substances would be reduced by the increase of the inorganic contents in an aqueous solution during freezing (Baker, 1970).

Tap water from the City of Edmonton supplies was used as blank in the spray freezing experiment. Similar analysis were conducted on various tap water samples collected and the results were displayed in the Figures AA-1 to AA-3 (Appendix A) and Figures 6-17 to 6-22.

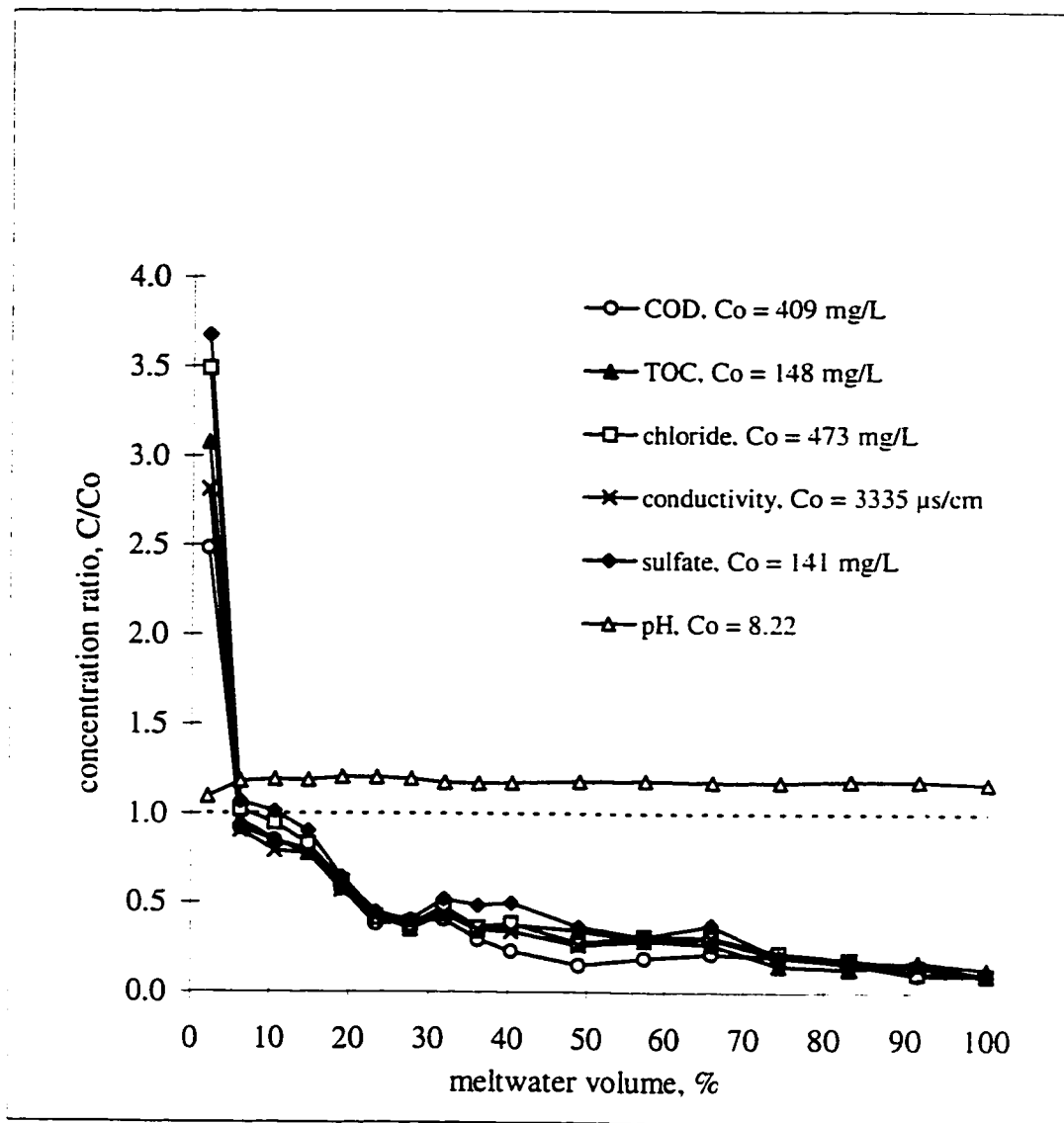


Figure 6-15 Variation of the concentration ratios of the selected impurities versus meltwater volume for the 20-day old spray ice made from oil sands tailings pond water in a $-10\text{ }^{\circ}\text{C}$ environment.

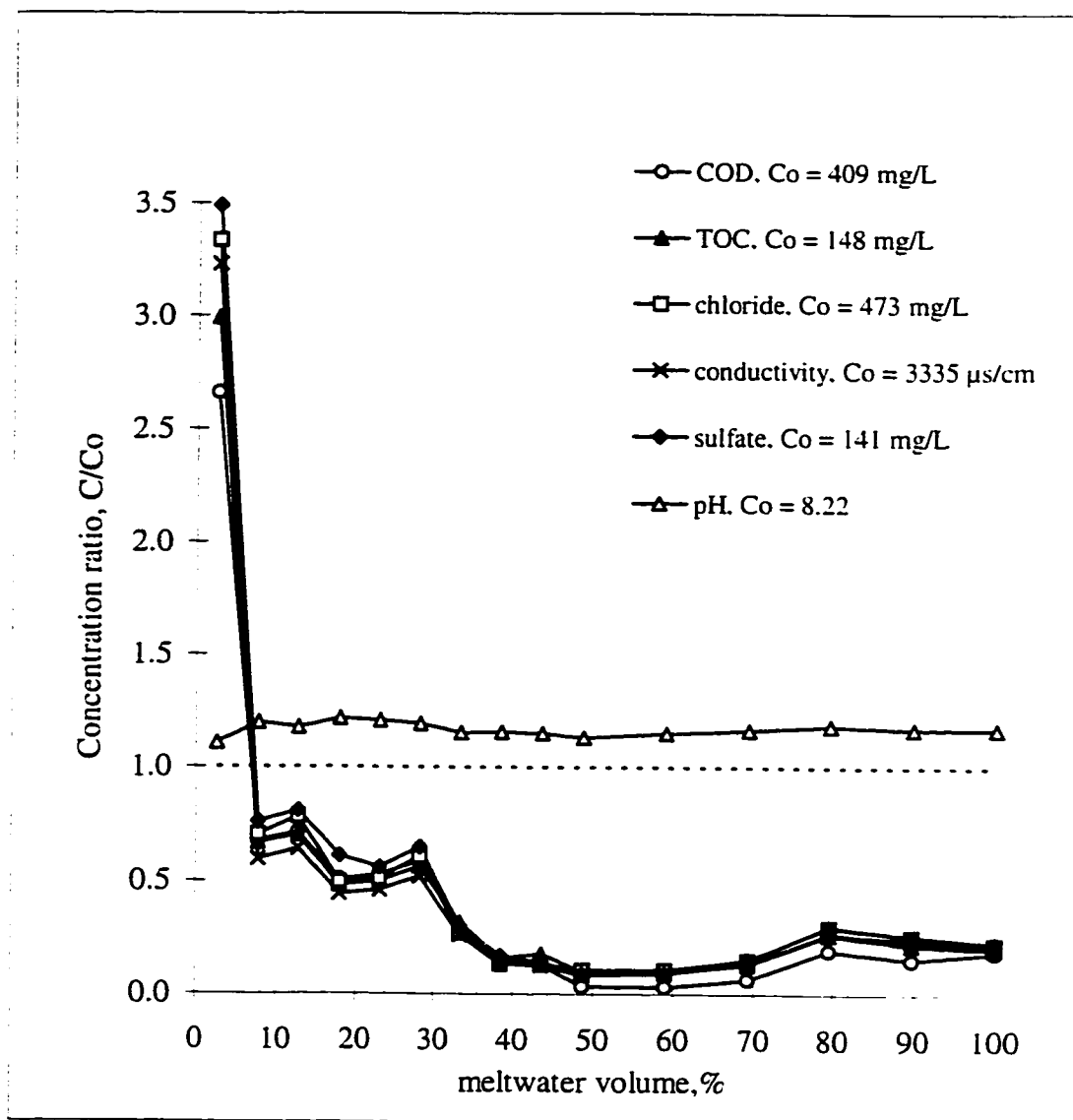


Figure 6-16 Variation of the concentration ratios of the selected impurities versus meltwater volume for the 40-day old spray ice made from oil sands tailings pond water in a $-10\text{ }^{\circ}\text{C}$ environment.

The effects of chemical fractionation were clearly shown in these figures. The enrichment of organic contaminants in the first portion of the meltwater was enormous. the concentration ratios of COD, TOC and color were in the range of 9 to 18 (Figures AA-1 to AA-3). The inorganic contaminants (Cl^- , SO_4^{2-} , or conductivity) were concentrated to a relatively lower degree, about 3.5 to 10 times of the concentrations of the source water. The significant effects of chemical fractionation during melting of ice made from tap water suggested that the concentration factors (ratios) of the first melt fraction were independent of the concentrations in the ice columns. Impurity contents in tap water was much less than those in the wastewaters, but fractionation of chemicals occurred at the same or even higher degree during the melting of the spray ice formed from tap water. Johannessen and Henrisken (1978) and Marsh and Webb (1979) also found from their study that the first meltwater impurity concentrations were several times higher than the bulk concentration in spite of more than a tenfold differences in the concentrations in the bulk snow or ice samples. Absence of any relationship between mean concentration of the ice column (or snowpack) and the early meltwater concentration factor (ratio) indicated it was the accessibility of the solution pockets to the drainage channels which determined meltwater solute concentration (Davies et al. 1986).

As shown in Figures AA-1 to AA-3 (Appendix A), organic contaminant concentrations of the meltwater was higher than that of the source water throughout the melting for some spray ice. This indicated that contamination of the tap water happened during or after the spraying operation. The most likely source of organic contamination was the spraying system (pumps and pipes) although the system was flushed with tap water prior to spraying. The inlet filter of the pump, as mentioned earlier, was cleaned with gasoline during the spraying, it would certainly raise organic contaminant concentration in the tap water. The organic contamination of the sprayed tap water could also occur during the collection of the ice slurry from the surface of the tarp. Analytical inaccuracy or contamination of individual sampling bottles with organic matters might be another source of the error.

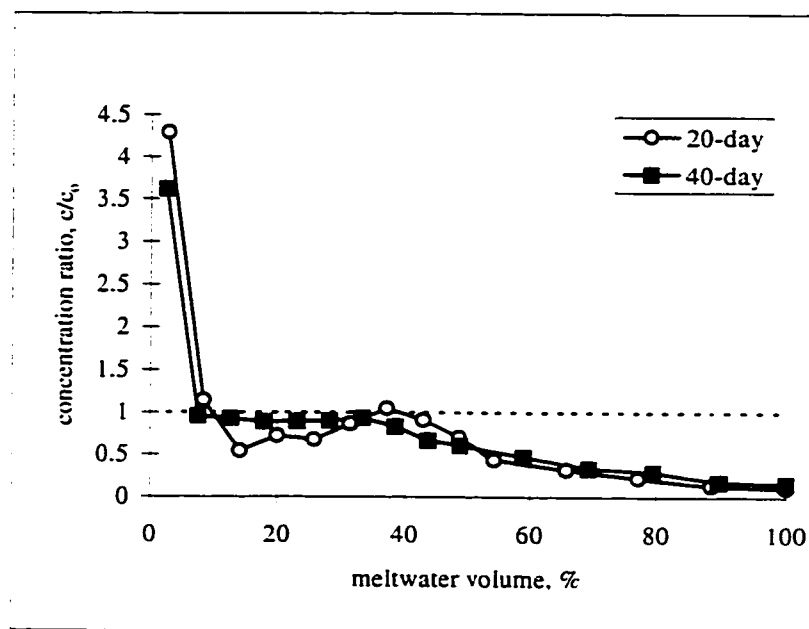


Figure 6-17 Variation of the normalized ionic strength (conductivity) in the sequential meltwater samples of the spray ice made from tap water (the spray ice was obtained in a - 10 °C environment). The source water conductivity, $c_0 = 237 \mu\text{s/cm}$.

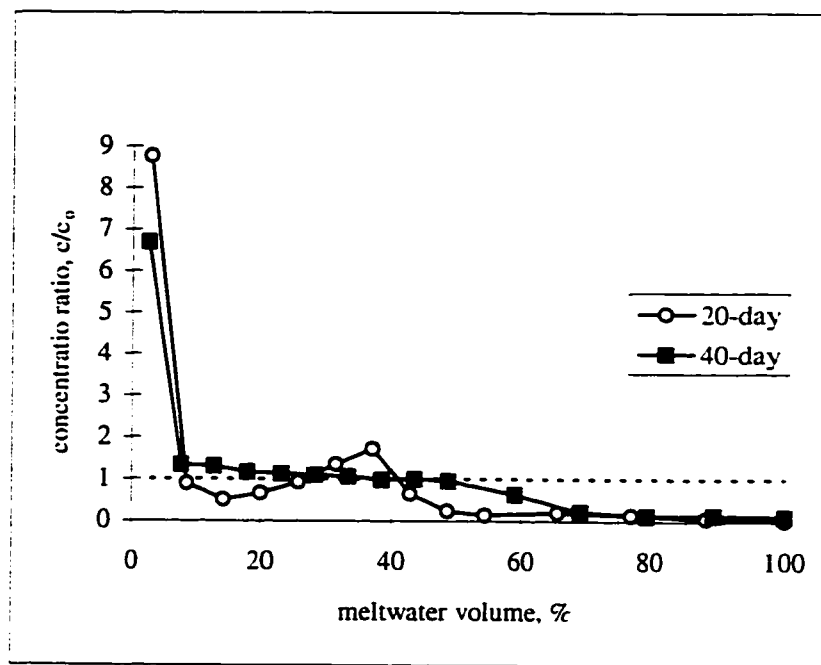


Figure 6-18 Variation of the normalized SO_4^{2-} concentration in the sequential meltwater samples of the spray ice made from tap water (the spray ice was obtained in a -10°C environment). The source water SO_4^{2-} concentration, $c_0 = 54$ mg/L.

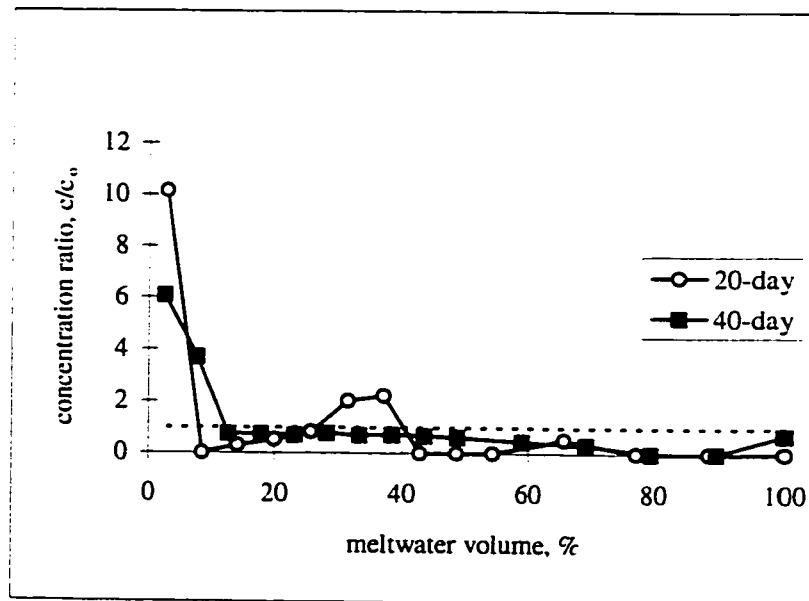


Figure 6-19 Variation of the normalized Cl^- concentration in the sequential meltwater samples of the spray ice made from tap water (the spray ice was obtained in a -10°C environment). The source water Cl^- concentration, $c_0 = 3$ mg/L.

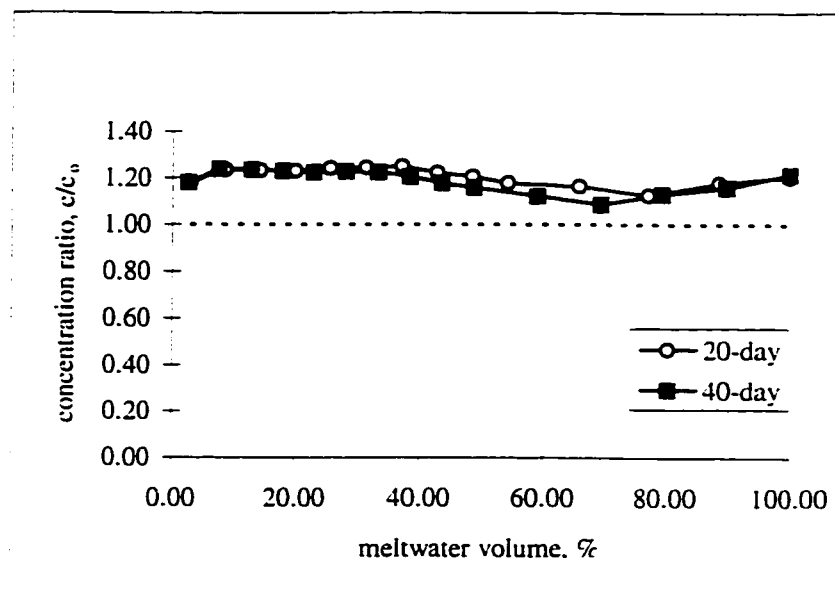


Figure 6-20 Variation of the normalized pH value (hydrogen ion concentration) in the sequential meltwater samples of the spray ice made from tap water (the spray ice was obtained in a $-10\text{ }^{\circ}\text{C}$ environment). The source water pH, $c_0 = 7.24$.

The concentrations of inorganic components (Cl^- , SO_4^{2-} , or conductivity) were much lower in the later fractions of the meltwater as compared to those of the source water (Figure 6-17 to 6-19). Figure 6-20 illustrated the pH value variation of the meltwater. The change of the meltwater pH in Figure 6-20 had the similar pattern as those of the wastewaters. The difference between meltwater pH and the source water pH was smaller as compared with the wastewaters. The less amount of impurities contained in the tap water might explain the relatively lower raise in the meltwater pH.

Comparison of the concentration ratios of inorganic components analyzed in sequential meltwater was illustrated in Figure 6-21 and 6-22. The percentage of total amount of Cl^- and SO_4^{2-} ions as well as conductivity removed with the first 30% of the meltwater was shown in Table 6-9. The organic components were not listed because the exact pollution source could not be determined.

Table 6-9 The percentage of the total amount of inorganic components in the spray ice prepared from tap water released with first 30% of the meltwater

Samples	% of the total amount impurities within the ice columns removed		
	Cl^-	SO_4^{2-}	conductivity
Meltwater of the ice aged for 20 days	69	68	55
Meltwater of the ice aged for 40 days	67	62	55

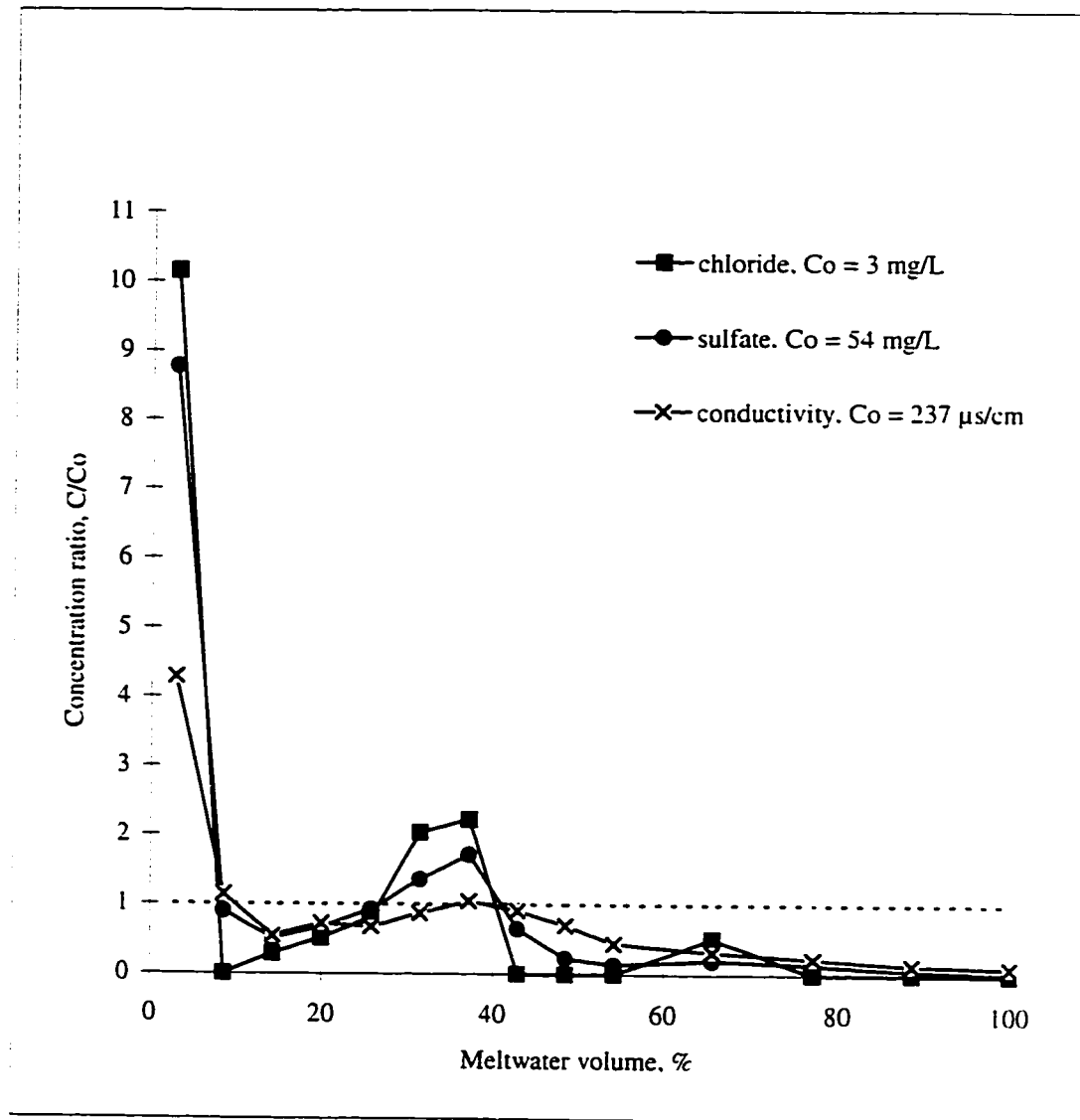


Figure 6-21 Variation of the concentration ratios of the selected impurities versus meltwater volume for the 20-day old spray ice made from tap water in a - 10 °C environment.

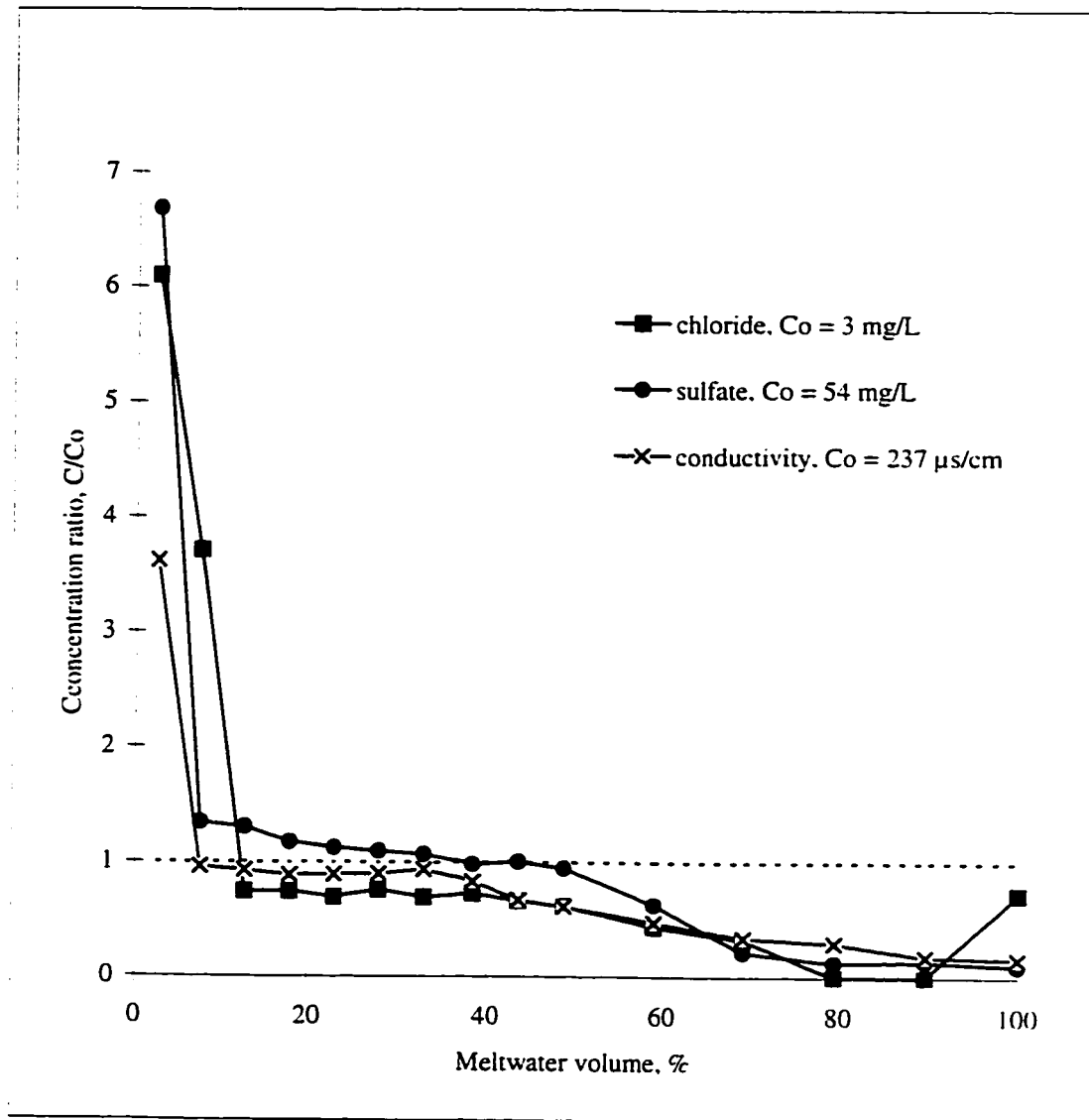


Figure 6-22 Variation of the concentration ratios of the selected impurities versus meltwater volume for the 40-day old spray ice made from tap water in a -10°C environment.

6.2.3.2 Impurity removal from the spray ice obtained in a - 24 °C ambient air environment

Impurity concentrations (normalized) in meltwater released from spray ice made from pulp mill effluent in a - 24 °C environment versus percentage of the cumulative meltwater volume were shown in Figures 6-23 to 6-27. Any water not frozen in the air froze after landing on the tarp and runoff (drainwater) was not generated during the spray freezing operation. The concentrations of all components in the first fraction of the meltwater were 2.5 to 4 times higher than in the source water (or in the ice columns). The chemical fractionation during the melting of the spray ice obtained at colder air temperature (- 24 °C) was different in the following ways from that in the melting of ice obtained under warmer temperature (- 10 °C):

- 1) The meltwater impurity concentration decayed at a much slower rate as compared with the melting of the spray ice obtained at - 10 °C and the meltwater impurity concentration was constantly higher than that of the source water until about 40% of the total meltwater (volume) was discharged. The impurity concentrations were much lower in the last fraction of the meltwater than in the source water but more meltwater was needed to carry away the larger amount of the impurities entrapped in the ice when no impurity removal occurred during the spraying.
- 2) Melting curves were much smoother, the fluctuation in the meltwater solute concentration was reduced greatly. This is due to the relatively lower ice density when the sprayed wastewater completely froze during the spraying operation. The loose ice caused much less clogging of the drainage hole of the columns during the melting.
- 3) At the beginning of the melting process, the meltwater from the 20-day old ice had higher impurity concentration, i.e. more impurities were removed with the meltwater. Consequently, the impurities in the ice depleted faster than those

in the older ice (40-day). Calculation of the amount of the impurities released from the spray ice with first 30% of the meltwater confirmed that the percentage of the total amount of the impurities released from the 20-day ice was about 4% to 7% more than that of the 40-day ice (see Table 6-10). While for the pulp mill effluent spray ice obtained at - 10 °C, the ice with longer storage period (40 days) had higher percentage of impurity removal (up to 7%). These results suggested that chemical fractionation as well as "elution sequences" are not general, but depend on the conditions of the ice columns during melting.

Table 6-10 Percentage of the total amount of the impurity removed from the pulp mill effluent spray ice obtained at - 24 °C air temperature by the first 30% of meltwater

	% of the total amount of impurities within the ice columns removed			
	COD	TOC	color	conductivity
Meltwater from 20-day old ice	72	72	73	73
Meltwater from 40-day old ice	67	66	67	69

The amount of impurities removed with the initial 30% of the meltwater from the ice obtained under colder ambient air temperature (Table 6-10) was more than 10% higher as compared with that shown in the Table 6-6. The lower density and the higher impurity concentrations in the ice were the possible reasons for the higher percentage of impurity removal listed in Table 6-10. Less compacted ice columns might provide higher accessibility to the impurities to the drainage channels within the ice columns during melting so more impurities were discharged with the early meltwater.

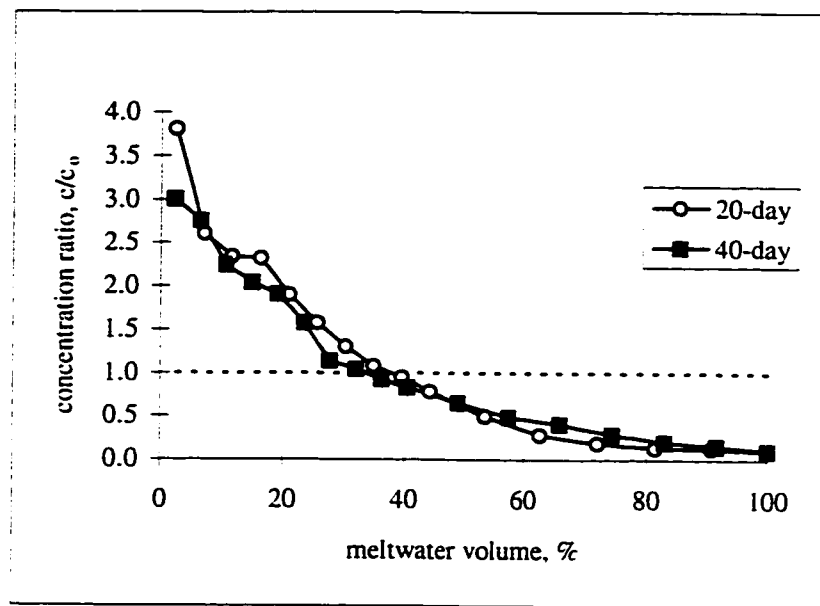


Figure 6-23 Variation of the normalized TOC concentration in the sequential meltwater samples of the spray ice made from pulp mill effluent (The spray ice was obtained in a -24°C environment). The source water TOC concentration, $c_0 = 243 \text{ mg/L}$.

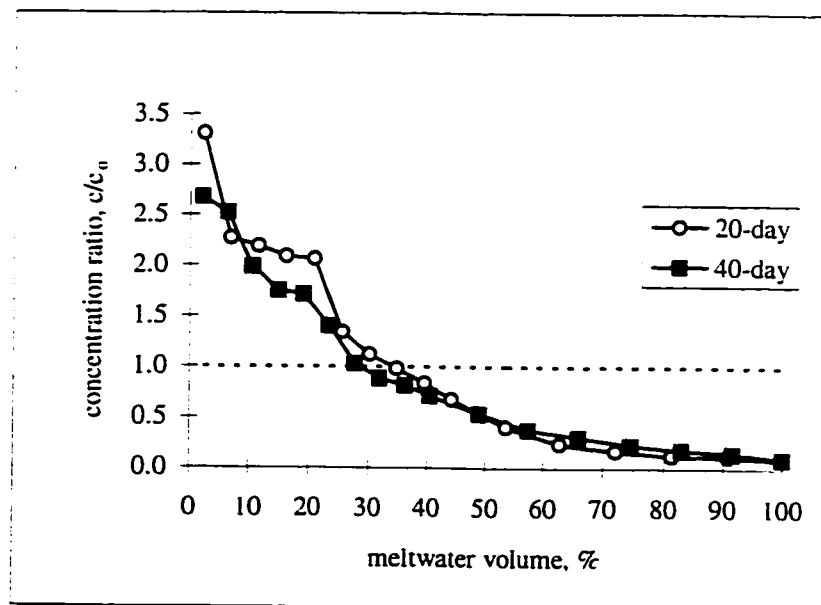


Figure 6-24 Variation of the normalized COD concentration in the sequential meltwater samples of the spray ice made from pulp mill effluent (The spray ice was obtained in a -24°C environment). The source water COD concentration, $c_0 = 667 \text{ mg/L}$.

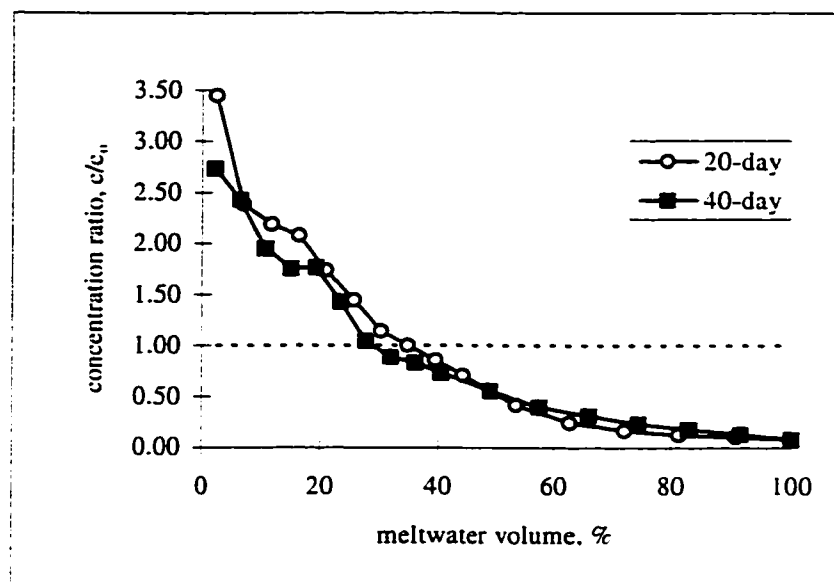


Figure 6-25 Variation of the normalized color concentration in the sequential meltwater samples of the spray ice made from pulp mill effluent (The spray ice was obtained in a -24°C environment). The source water color concentration, $c_0 = 1383$ TCU.

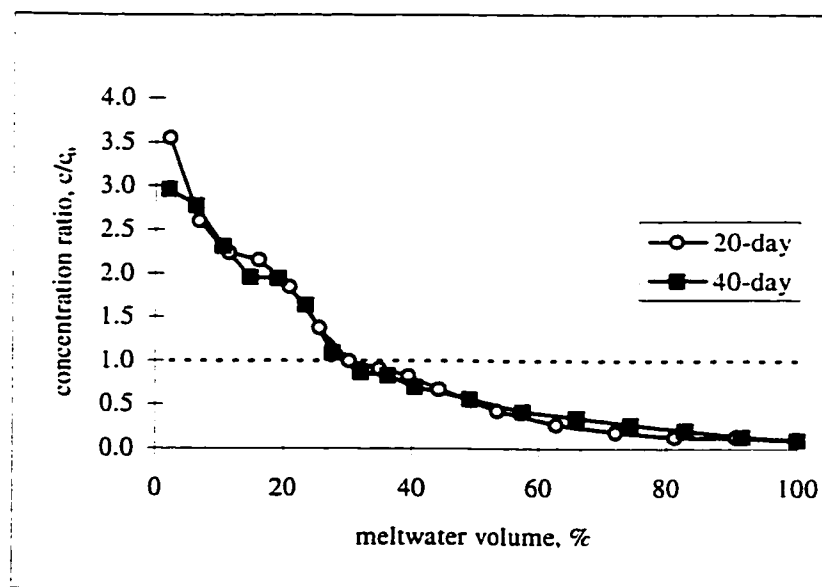


Figure 6-26 Variation of the normalized ionic strength (conductivity) in the sequential meltwater samples of the spray ice made from pulp mill effluent (The spray ice was obtained in a -24°C environment). The source water conductivity, $c_0 = 2503$ $\mu\text{S}/\text{cm}$.

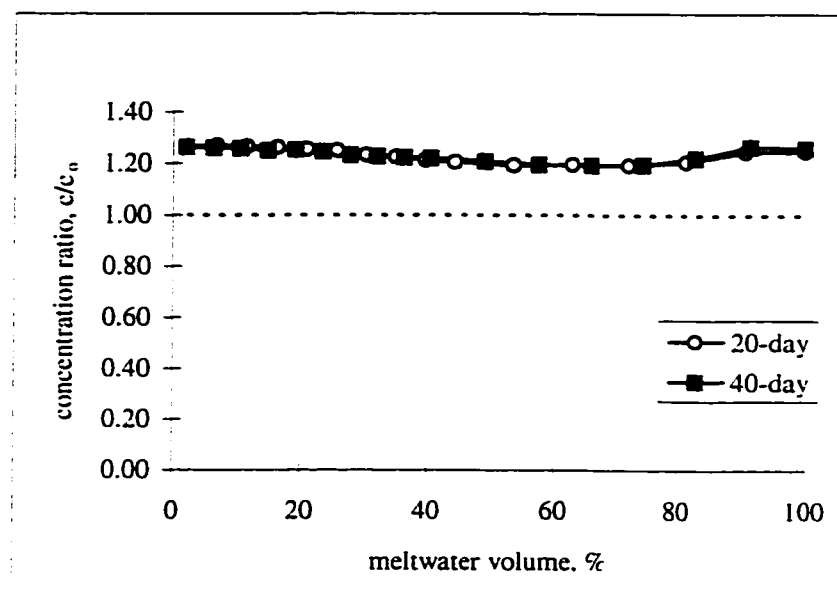


Figure 6-27 Variation of the normalized pH (H^+ concentration) in the sequential meltwater samples of the spray ice made from pulp mill effluent (The spray ice was obtained in a $-24\text{ }^{\circ}\text{C}$ environment). The source water pH, $c_0 = 7.58$.

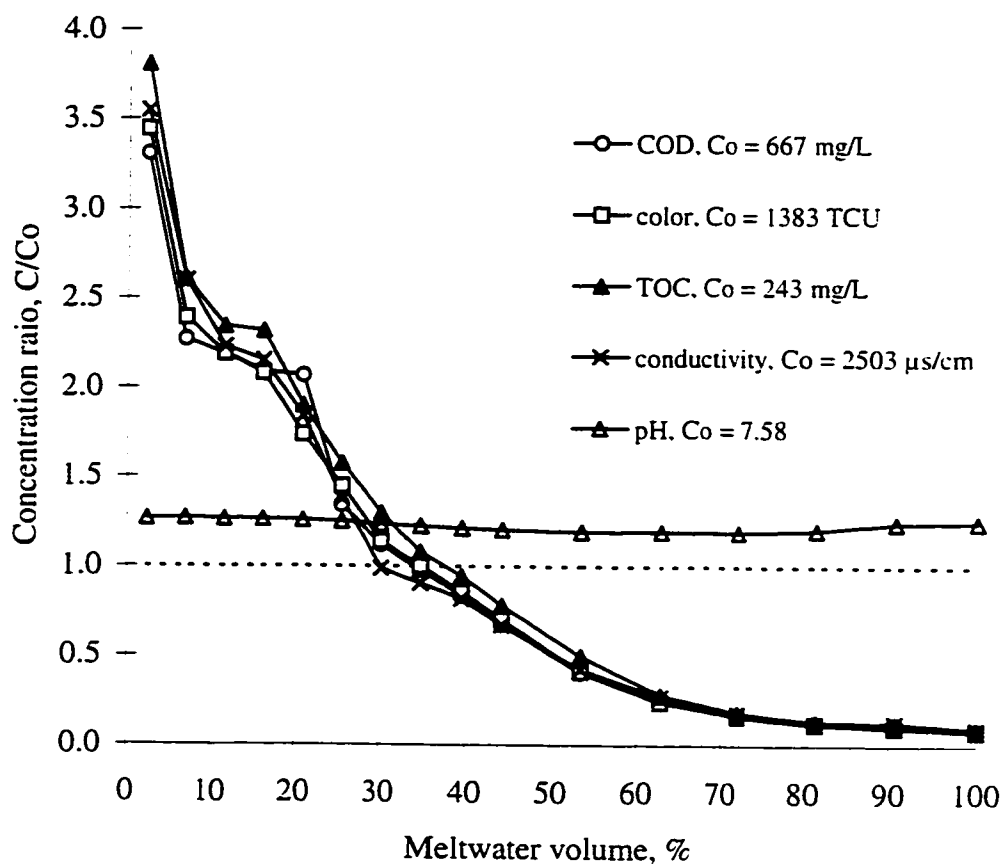


Figure 6-28 Variation of the concentration ratios of the selected impurities versus meltwater volume for the 20-day old spray ice made from pulp mill effluent in a -24°C environment.

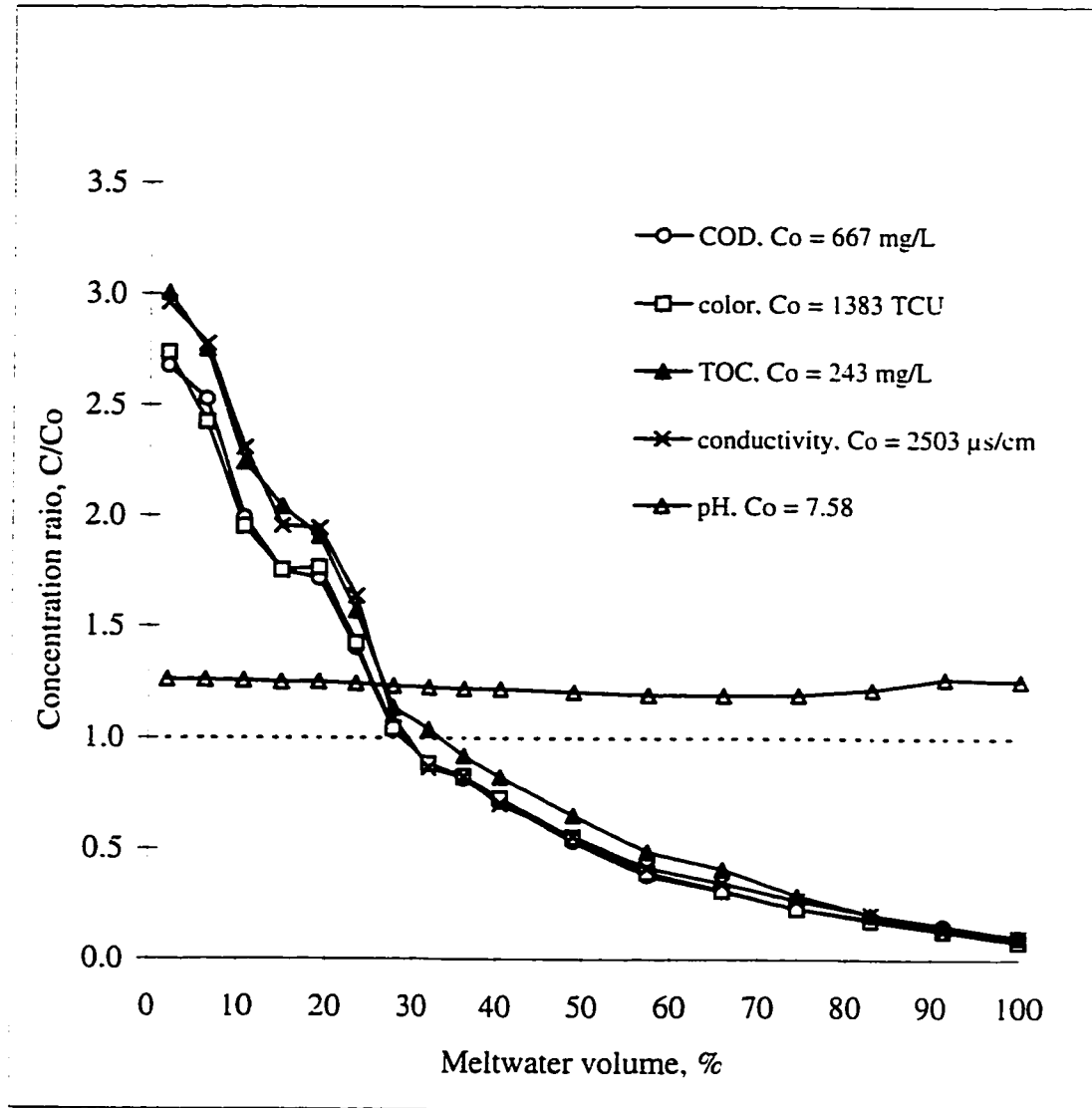


Figure 6-29 Variation of the concentration ratios of the selected impurities versus meltwater volume for the 40-day old spray ice made from pulp mill effluent in a -24°C environment.

Figures 6-28 and 6-29 show the concentration ratios of the impurities in the sequential meltwater. There was no clear indication of preferential elution of a certain type of contaminant over others.

The composition of meltwater of the spray ice made from oil sands tailings pond water was presented in Figures 6-30 to 6-35. The melting pattern was similar to that of the pulp mill effluent shown in Figures 6-23 to 6-27. The initial fraction of the meltwater contained about 3.5 to 6.5 times of the amount of impurities in the source oil sands tailings pond water. The enrichment in the early meltwater from the spray ice of oil sands tailings pond water was at a higher degree than that in pulp mill effluent (the initial concentration ratio was in the range of 2.5 to 4). The concentration ratios of organic contaminants (TOC and COD) were slightly higher for the ice aged for 40 days (see Figures 6-30 and 6-31) in the early meltwater while the concentration ratios of the inorganic components (Cl^- , SO_4^{2-} , pH and conductivity) were very close throughout the melting process as shown in Figures 6-32 to 6-35. Figures 6-36 and 6-37 revealed that Cl^- and SO_4^{2-} ions were released preferentially over organic contaminants. The high concentrations of inorganics in the oil sands tailings pond water might prevent the exclusion of organic contaminants from the ice structure, which resulted in the relatively lower concentrations of organic matters in the early meltwater.

The percentage of the total amount of impurity removed from the ice with first 30% of the meltwater was tabulated in the Table 6-11. Table 6-11 indicated that the amount of the organic matter removal with the first 30% of the meltwater was about 3 to 10% lower than that of the inorganics. The ice storage duration had little influence on the amount of impurity removed by the initial meltwater for the oil sands tailings pond water. The ambient air temperature affects ice crystal growth rate. Ice crystals grow less at colder air temperature. This would reduce the difference in the amount of impurity removed for the ice with different storage time.

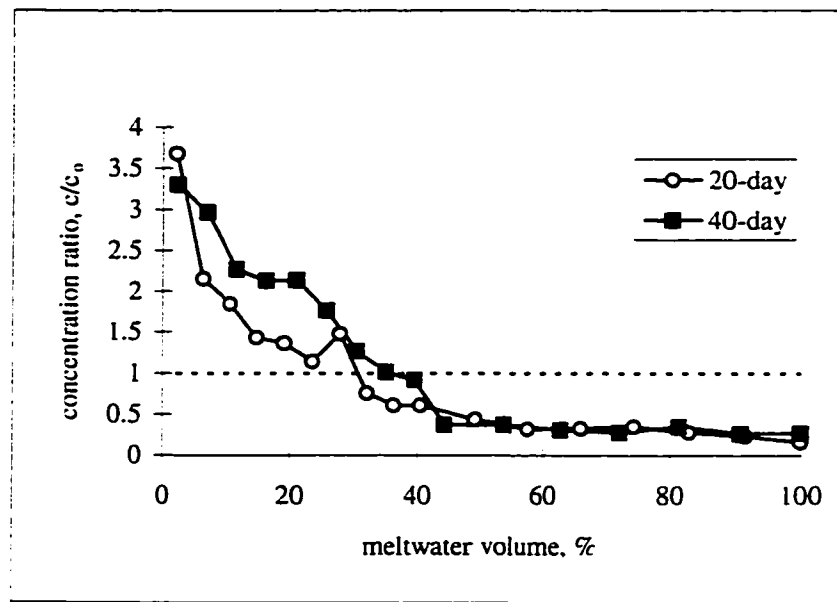


Figure 6-30 Variation of the normalized COD concentration in the sequential meltwater samples of the spray ice made from oil sands tailings pond water (The spray ice was obtained in a - 24 °C environment). The source water COD concentration, $c_0 = 418$ mg/L.

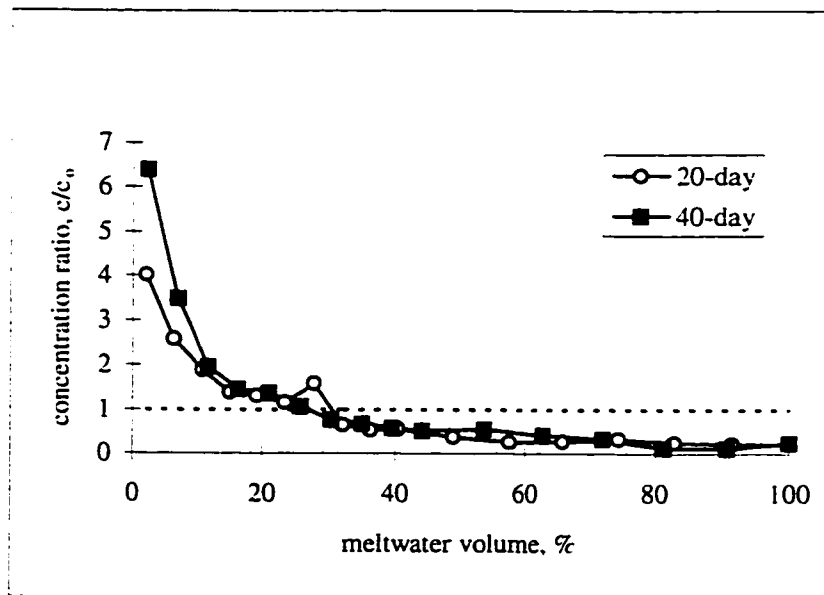


Figure 6-31 Variation of the normalized TOC concentration in the sequential meltwater samples of the spray ice made from oil sands tailings pond water (The spray ice was obtained in a - 24 °C environment). The source water TOC concentration, $c_0 = 136$ mg/L.

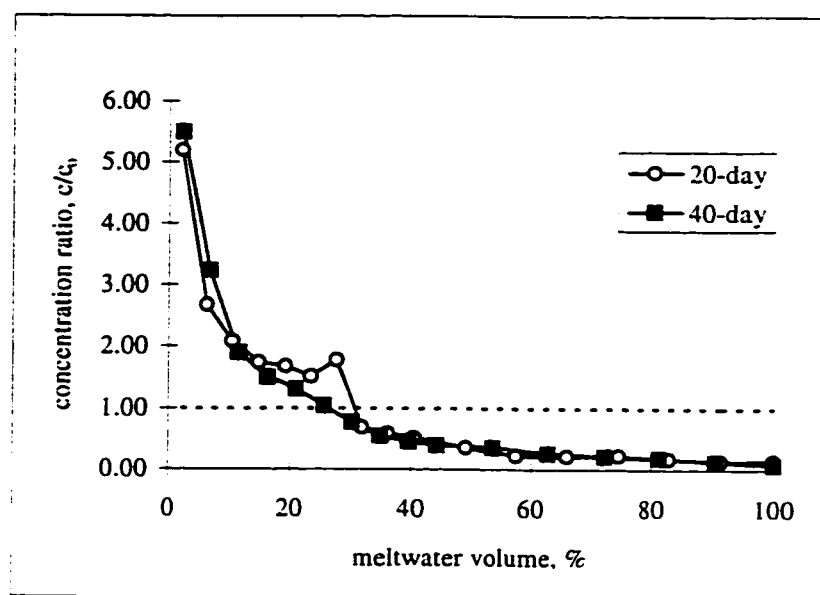


Figure 6-32 Variation of the normalized ionic strength (conductivity) in the sequential meltwater samples of the spray ice made from oil sands tailings pond water (The spray ice was obtained in a - 24 °C environment). The source water conductivity, $c_0 = 3353 \mu\text{s}/\text{cm}$.

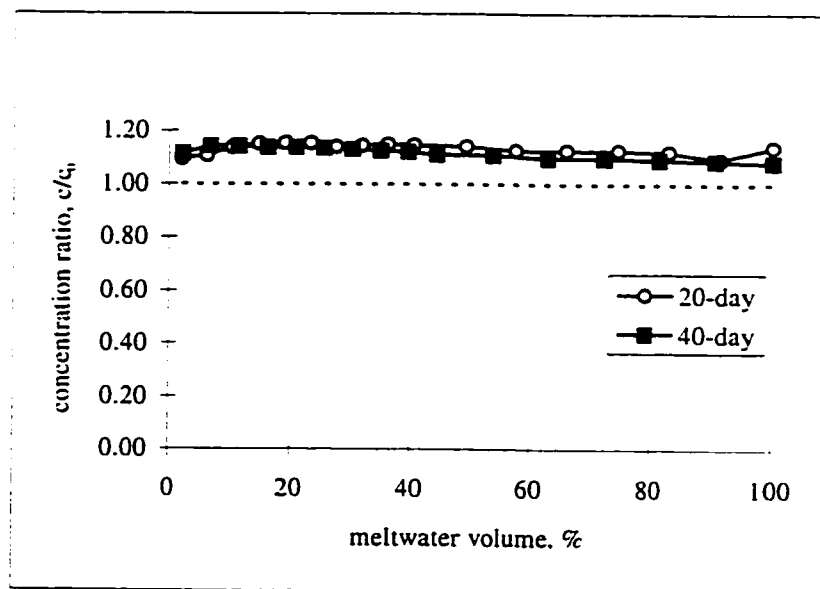


Figure 6-33 Variation of the normalized pH (H^+ concentration) in the sequential meltwater samples of the spray ice made from oil sands tailings pond water (The spray ice was obtained in a - 24 °C environment). The source water pH, $c_0 = 8.60$.

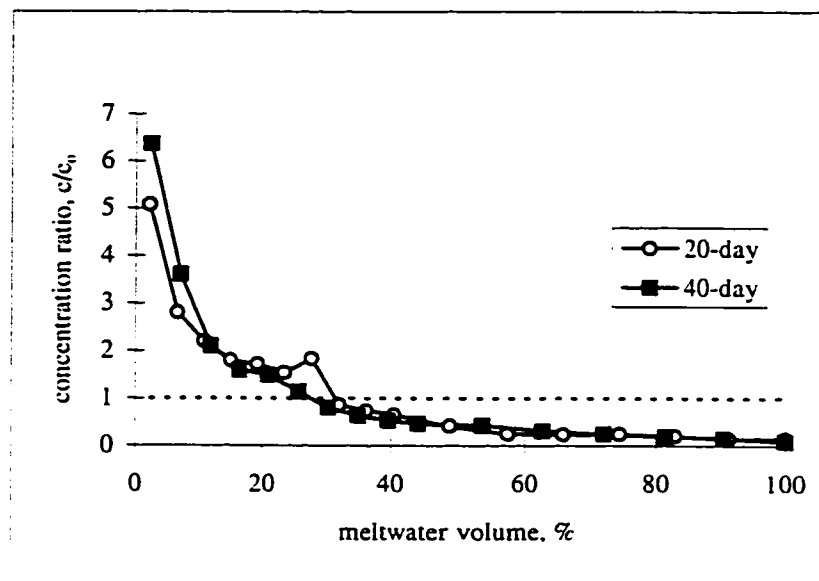


Figure 6-34 Variation of the normalized Cl^- concentration in the sequential meltwater samples of the spray ice made from oil sands tailings pond water (The spray ice was obtained in a -24°C environment). The source water Cl^- concentration, $c_0 = 476 \text{ mg/L}$.

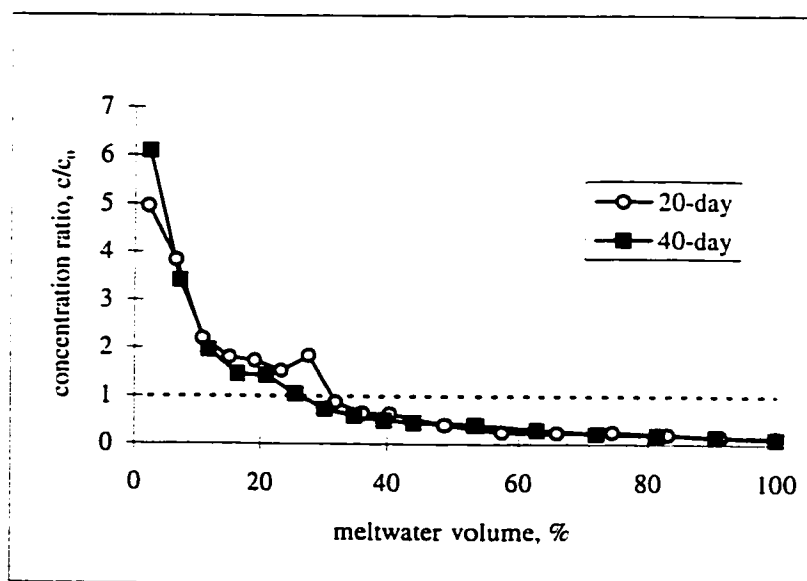


Figure 6-35 Variation of the normalized SO_4^{2-} concentration in the sequential meltwater samples of the spray ice made from oil sands tailings pond water (The spray ice was obtained in a -24°C environment). The source water SO_4^{2-} concentration, $c_0 = 137 \text{ mg/L}$.

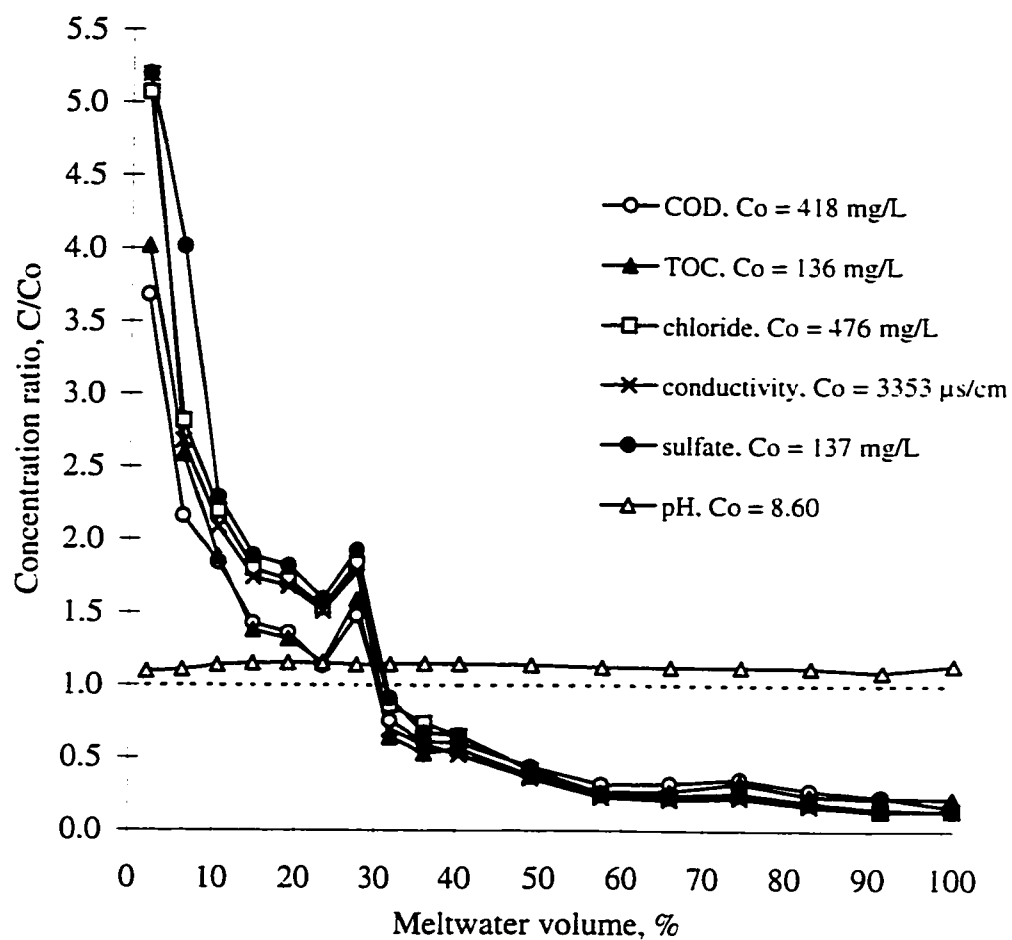


Figure 6-36 Variation of the concentration ratios of the selected impurities versus meltwater volume for the 20-day old spray ice made from oil sands tailings pond water in a - 24 °C environment.

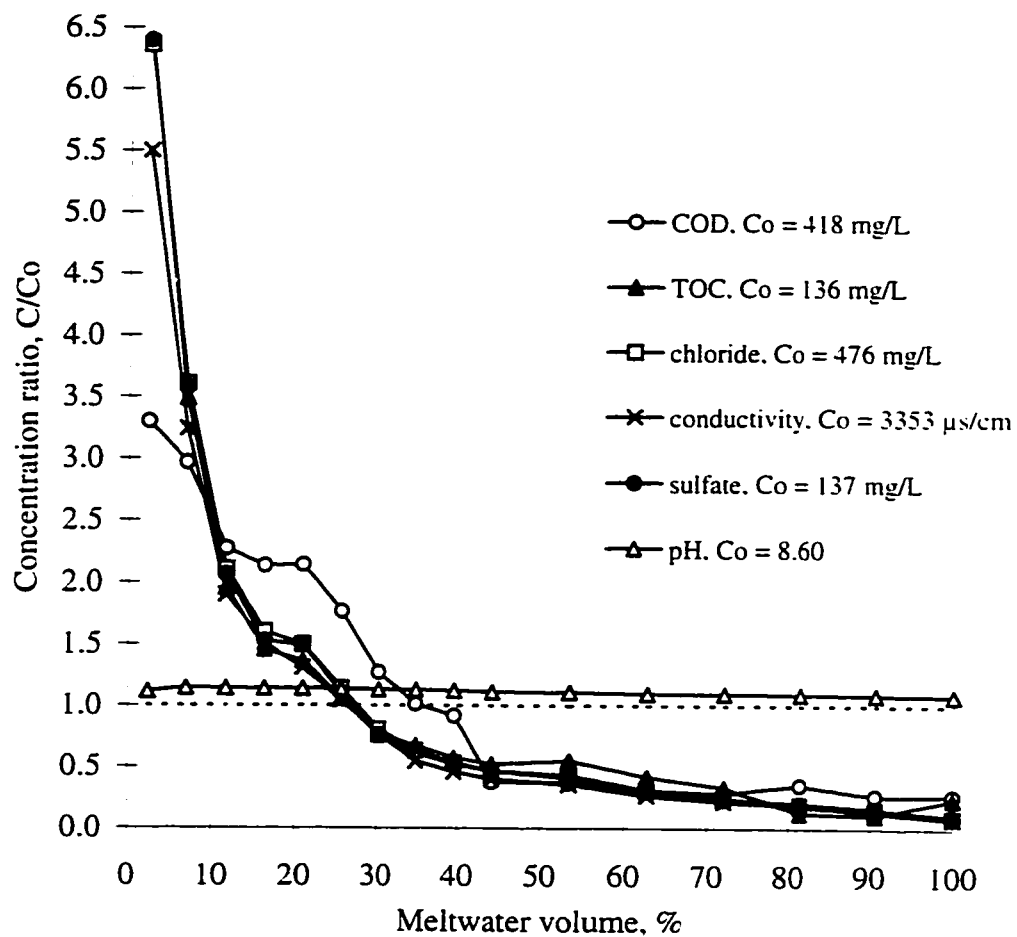


Figure 6-37 Variation of the concentration ratios of the selected impurities versus meltwater volume for the 40-day old spray ice made from oil sands tailings pond water in a - 24 °C environment.

Table 6-11 Percentage of the total amount of the impurity removed from the spray ice of oil sands tailings pond water by the first 30% of meltwater (spray ice was obtained in a - 24 °C environment)

	% of the total amount of impurities within the ice columns removed				
	COD	TOC	Cl ⁻	SO ₄ ²⁻	conductivity
Meltwater from 20-day old ice	66	69	74	75	76
Meltwater from 40-day old ice	68	71	74	74	75

The results of the melting test of the spray ice made from tap water under colder ambient air temperature were displayed in the Figures AA-4 to AA-8 (Appendix A) and Figures 6-38 to 6-43. The concentrations of COD and TOC in the first portion of meltwater was about 2.5 to 5 times higher than in the source water (Figures AA-4 and AA-5). The concentration ratios of TOC and COD in the very first fraction of the meltwater were much lower than those shown in the Figures AA-2 and AA-3 for the spray ice obtained at - 10 °C. No (or much less) organic contamination occurred in the 20-day old spray ice obtained at - 24 °C. TOC concentration in the meltwater of 40-day old ice was higher or equal to that in the source water throughout the melting process indicating possible organic contamination of the samples (see Figure AA-5). COD concentration of these samples seems normal, i.e. lower COD concentration in the late meltwater. So the high TOC concentration in the meltwater of the 40-day old ice might be induced by the measurement error. The color concentration of the meltwater was much lower than that of the source water and most meltwater samples of the ice aged for 40-days by storage had no color (see Figure AA-6). The inorganic components (SO₄²⁻,

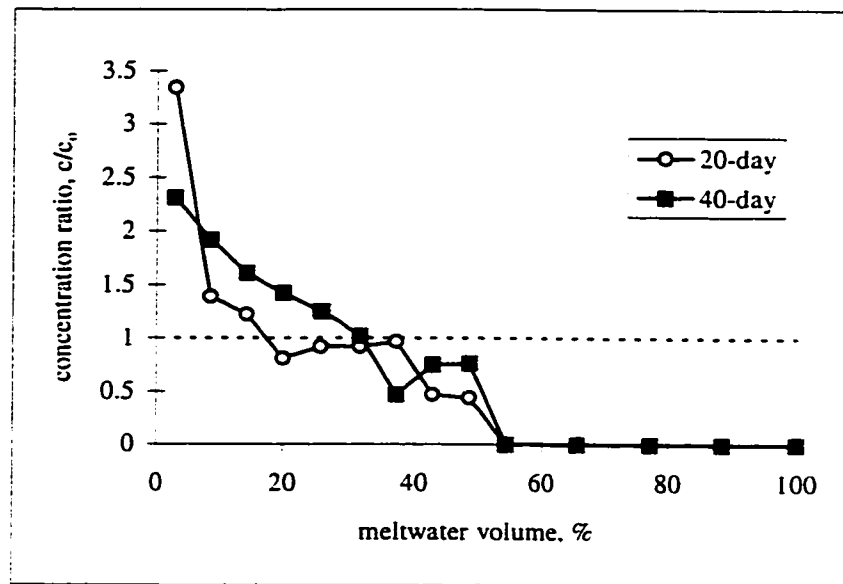


Figure 6-38 Variation of the normalized Cl^- concentration in the sequential meltwater samples of the spray ice made from tap water (The spray ice was obtained in a -24°C environment). The source water Cl^- concentration, $c_0 = 3 \text{ mg/L}$.

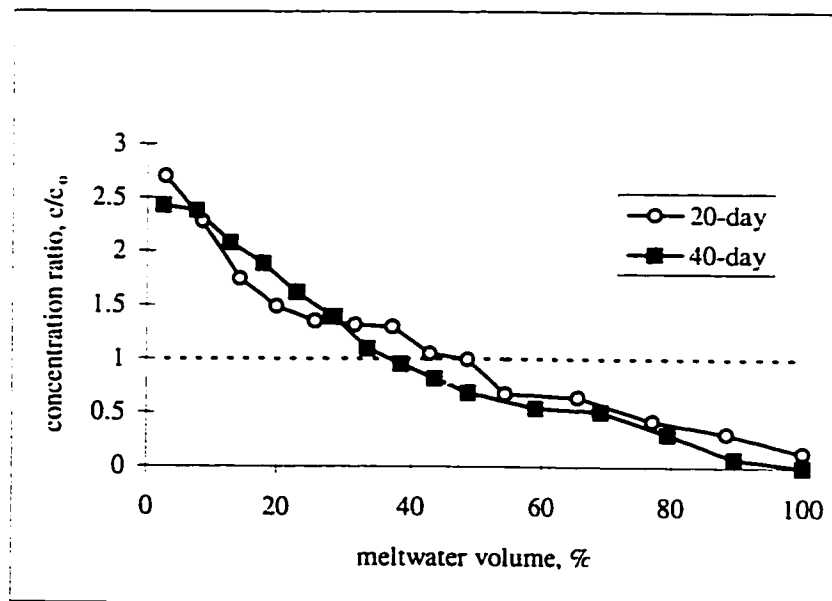


Figure 6-39 Variation of the normalized SO_4^{2-} concentration in the sequential meltwater samples of the spray ice made from tap water (The spray ice was obtained in a -24°C environment). The source water SO_4^{2-} concentration, $c_0 = 60 \text{ mg/L}$.

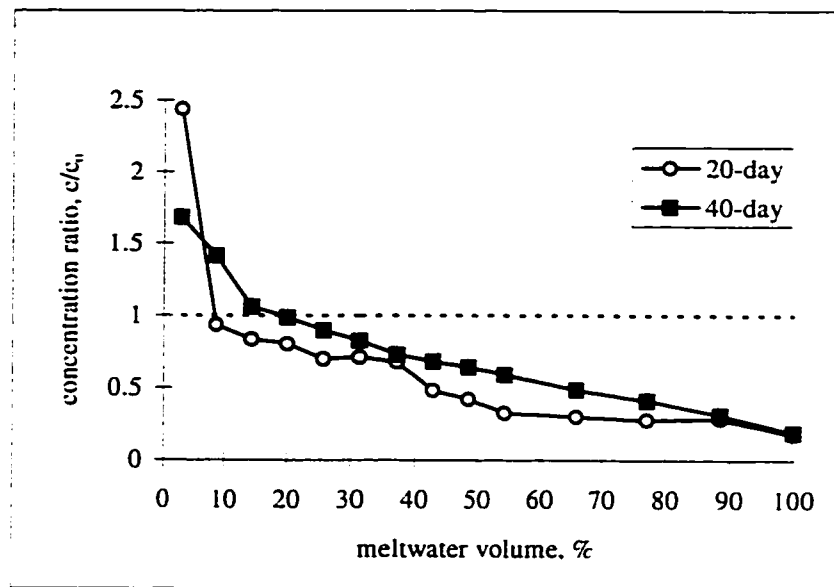


Figure 6-40 Variation of the normalized ionic strength (conductivity) in the sequential meltwater samples of the spray ice made from tap water (The spray ice was obtained in a $-24\text{ }^{\circ}\text{C}$ environment). The source water conductivity, $c_0 = 297\text{ }\mu\text{S/cm}$.

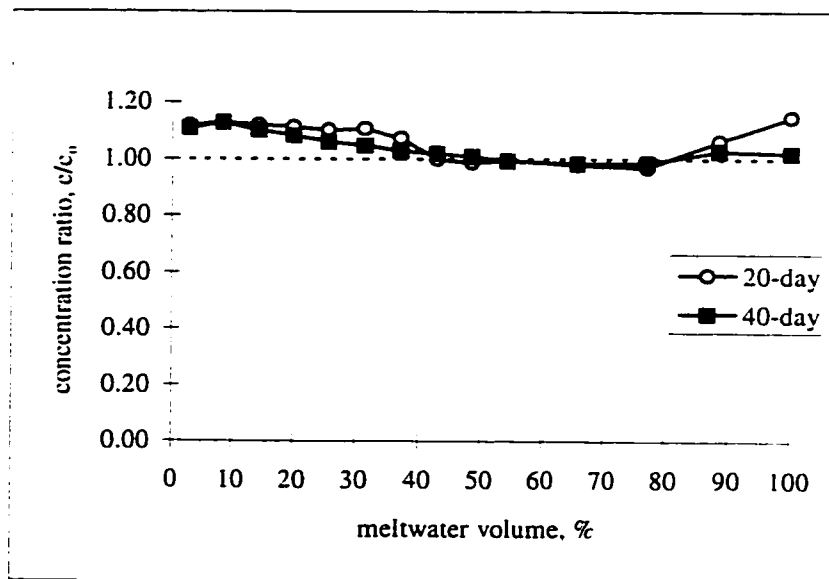


Figure 6-41 Variation of the normalized pH (H^+ concentration) in the sequential meltwater samples of the spray ice made from tap water (The spray ice was obtained in a $-24\text{ }^{\circ}\text{C}$ environment). The source water pH, $c_0 = 7.93$.

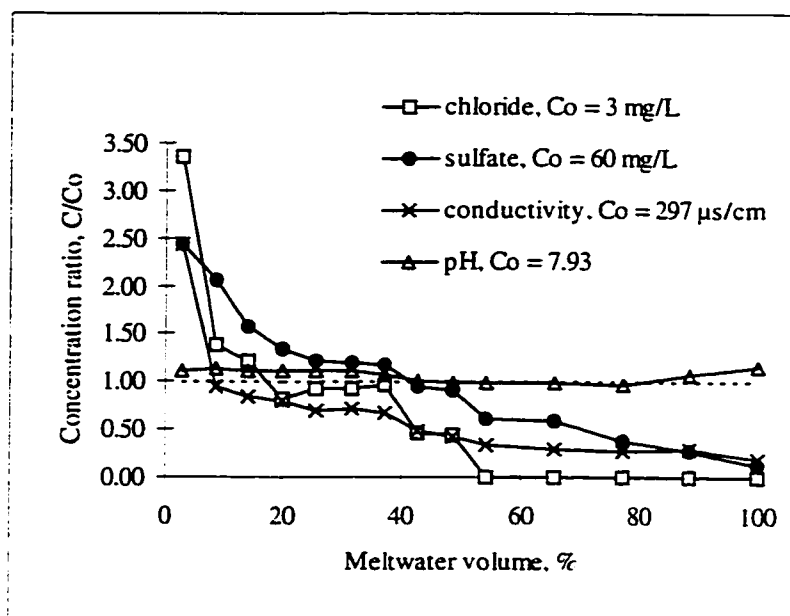


Figure 6-42 Variation of the concentration ratios of the selected inorganic contaminants versus meltwater volume for the 20-day old spray ice made from tap water in a - 24 °C environment.

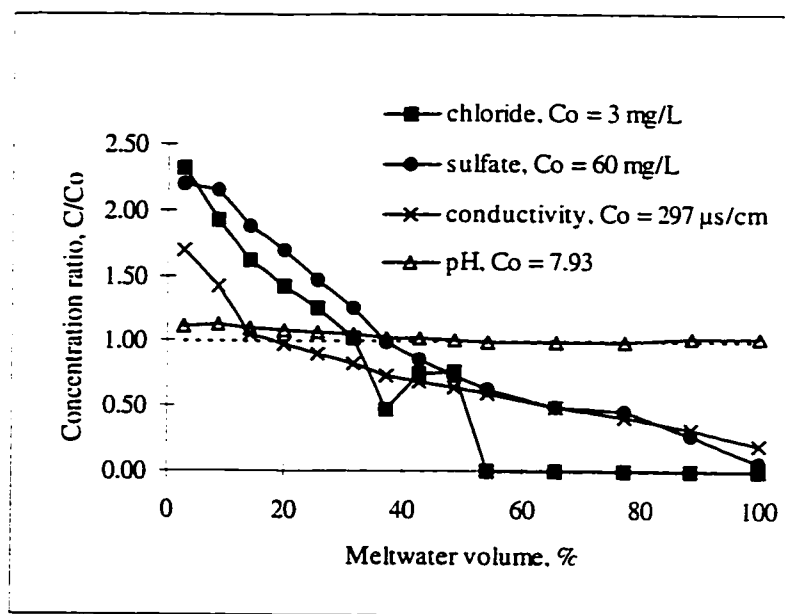


Figure 6-43 Variation of the concentration ratios of the selected inorganic contaminants versus meltwater volume for the 40-day old spray ice made from tap water in a - 24 °C environment.

Cl⁻ and conductivity) in the first fraction of the meltwater were 1.5 to 3.5 times more concentrated than the source water. Cl⁻ ions were removed very effectively and Cl⁻ concentration reduced to lower than the detectable level in late meltwater while SO₄²⁻ ions were released at a relatively slower rate (Figures 6-42 and 6-43). Analytical inaccuracy was possibly higher for the tap water samples because its much lower impurity concentrations as compared with the wastewaters tested.

The results obtained from the melting tests indicated that fractionation of impurities from melting ice columns is a complex process and is affected by physical and chemical properties of ice columns. Concentration factors (ratios) spanning a considerable range were found in the literature. The results of the melting test presented in above sections showed that the ice columns obtained under the same experimental conditions could have different concentration ratios. The efficiency of impurity removal by meltwater seems to be determined by the nature of the wastewater and the melting conditions of individual ice column. Impurities in the ice columns might be redistributed by metamorphism, sublimation and freeze/thaw cycling. This micro-scale distribution of impurities within and on ice crystals is of fundamental importance to meltwater composition because it contributes to the ease of impurity scavenging by meltwater. Unfortunately, very little is known about the distribution of impurities within or on the ice crystals.

Foster (1978) indicated that heterogeneous percolation of the meltwater was the most important factor in controlling the magnitude of the concentration ratio. Drainage might occur through preferred channels, rather than uniformly through the whole matrix (Tranter, 1990). Therefore, the accessibility of the impurities to the drainage channels would limit the impurity content of the meltwater. Ice columns with lower density like the spray ice obtained in the - 24 °C environment might have more drainage channels so that impurities had more opportunities for leaching at the beginning of the melting as compared with the spray ice obtained at warmer air temperature conditions. In addition

the high impurity content in the spray ice formed at the colder temperature increased the probability for the impurities to be discharged from the spray ice with the early meltwater.

Ambient air temperature and the age of the ice columns possibly affected the recrystallization process of the ice crystals. Meltwater of the ice columns stored in a warmer environment (-10 °C) and longer period (40 days) contained higher initial impurity content. Slightly larger amount of organic contaminants were removed with initial meltwater when ice columns were stored in a warmer air temperature (- 10 °C).

Heterogeneous distribution of impurities within ice columns will also affect the meltwater impurity concentration. The ice columns obtained at - 10 °C had higher impurity concentrations at the bottom of the ice cores. More impurities should be discharged with early meltwater but blocking of the drainage holes during the melting probably reduced the observation of this effect. Impurity removal efficiency will increase as ice column depth increases, since the meltwater will have greater opportunity for solute scavenging (Tranter, 1990). If the spray freezing process is conducted under field conditions, higher impurity removal efficiency should be achieved by increasing the depth of the spray ice mound and improved melting conditions (no blocking of drainage channels happens).

Tranter (1990) indicated that meltwater composition of the natural snowpacks were influenced by snowpack hydrology, the micro and meso-scale distribution of solute within the snow column, the occurrence of melt-freeze cycles, the influence of rain-on snow, the occurrence of dissolution reactions and the possibility of biological activity. Currently, the understanding of these controlling factors is largely qualitative. The meltwater quality of the spray ice made from wastewaters will certainly be affected by all or some of the these factors. More study should be conducted at larger scale to get better understanding of these controlling factors.

6.2.3.3 Comparison of the impurity removal efficiency for the spray ice obtained under different ambient air temperatures

The meltwater (product water) quality of the spray ice of the wastewaters was compared based on the meltwater volume obtained (expressed as percentage of the total volume of the sprayed wastewater) in which greater than 50% and 80% impurity removal was achieved (see Tables 6-12 to 6-15). Runoff was generated during the spraying operation carried out at - 10 °C ambient air temperature environment. The volume of the runoff generated was about 30% of the total volume of the wastewaters sprayed. The 30% runoff was included in the calculation of the impurity removal efficiency for the spray ice obtained at - 10 °C. The percentage of the total meltwater volume that reached greater than 50 and 80% impurity removal was also calculated (the bracketed numbers in Tables 6-12 to 6-15). No runoff was generated for the spray ice obtained at - 24 °C so the meltwater volume was the total volume of the sprayed wastewater.

Table 6-12 indicated that the percentage of meltwater which reached above 50% and above 80% impurity removal was higher for the spray ice obtained at - 24 °C for most of the parameters determined than that of the spray ice obtained at - 10 °C based on the total sprayed water volume. The relatively lower impurity removal for the 20-day old spray ice of pulp mill effluent probably caused by the fluctuation of the meltwater impurity concentration during melting due to the blocking of the drainage holes of the columns. The percentage of reduction was the same for all components analyzed for the meltwater of the spray ice obtained at - 24 °C. While Table 6-13 showed that the meltwater of the spray ice obtained under a warmer air temperature condition (40-day old), 51% to 66% (72% to 94% of the total meltwater volume) of the total volume of pulp mill effluent sprayed had above 50% impurity removal and 27% to 39% (38% to 55% of the total meltwater volume) of the total sprayed water volume reached greater than 80% impurity reduction. More meltwater attained higher degree of impurity removal when runoff was generated during the spray freezing process.

Table 6-12 Comparison of impurity removal efficiency by the spray freezing process conducted at different ambient air temperatures (pulp mill effluent, the spray ice was stored in the cold rooms for 20 days)

Parameters	% of impurity removal	% of the total sprayed wastewater volume that reached the level of impurity removal	
		- 10 °C ^a	-24 °C
COD	> 50%	46 (69) ^b	56 (56)
	> 80%	15 (23)	37 (37)
Color	> 50%	53 (76)	56 (56)
	> 80%	20 (29)	37 (37)
TOC	> 50%	48 (69)	56 (56)
	> 80%	20 (29)	37 (37)
Conductivity	> 50%	64 (91)	56 (56)
	> 80%	26 (36)	37 (37)

^a the ambient air temperature at which the spraying operation was conducted

^b the percentage of the total meltwater volume that reached the level of the impurity removal

Table 6-13 Comparison of impurity removal efficiency by the spray freezing process conducted at different ambient air temperatures (pulp mill effluent. the spray ice was stored in the cold rooms for 40 days)

Parameters	% of impurity removal	% of the total sprayed wastewater volume that reached the level of impurity removal	
		- 10 °C ^a	-24 °C
COD	> 50%	51 (72) ^b	51 (51)
	> 80%	27 (38)	26 (26)
Color	> 50%	66 (94)	51 (51)
	> 80%	36 (51)	26 (26)
TOC	> 50%	66 (94)	51 (51)
	> 80%	33 (47)	26 (26)
Conductivity	> 50%	66 (94)	51 (51)
	> 80%	39 (55)	26 (26)

^a the ambient air temperature at which the spraying operation was conducted

^b the percentage of the total meltwater volume that reached the level of the impurity removal

Table 6-14 Comparison of impurity removal efficiency by the spray freezing process conducted at different ambient air temperatures (oil sands tailings pond water, the spray ice was stored in the cold rooms for 20 days)

Parameters	% of impurity removal	% of the total sprayed wastewater volume that reached the level of impurity removal	
		- 10 °C ^a	-24 °C
COD	> 50%	57 (81) ^b	60 (60)
	> 80%	48 (68)	17 (17)
TOC	> 50%	57 (81)	60 (60)
	> 80%	24 (34)	17 (17)
Cl ⁻	> 50%	57 (81)	60 (60)
	> 80%	24 (34)	26 (26)
SO ₄ ²⁻	> 50%	57 (81)	60 (60)
	> 80%	24 (34)	26 (26)
Conductivity	> 50%	57 (81)	60 (60)
	> 80%	24 (34)	26 (26)

^a the ambient air temperature at which the spraying operation was conducted

^b the percentage of the total meltwater volume that reached the level of the impurity removal

Table 6-15 Comparison of impurity removal efficiency by the spray freezing process conducted at different ambient air temperatures (oil sands tailings pond water, the spray ice was stored in the cold rooms for 40 days)

Parameters	% of impurity removal	% of the total sprayed wastewater volume that reached the level of impurity removal	
		- 10 °C ^a	-24 °C
COD	> 50%	54 (82) ^b	60 (60)
	> 80%	46 (67)	0 (0)
TOC	> 50%	58 (82)	47 (47)
	> 80%	39 (56)	19 (19)
Cl ⁻	> 50%	58 (82)	60 (60)
	> 80%	32 (46)	28 (28)
SO ₄ ²⁻	> 50%	51 (72)	65 (65)
	> 80%	32 (46)	28 (28)
Conductivity	> 50%	61 (87)	65 (65)
	> 80%	39 (56)	28 (28)

^a the ambient air temperature at which the spraying operation was conducted

^b the percentage of the total meltwater volume that reached the level of the impurity removal

The percentages of the total sprayed water volume that reached greater than 50% and 80% of impurity reduction were listed in the Tables 6-14 and 6-15 for oil sands tailings pond water. As indicated in the Tables 6-14 and 6-15, slightly higher percentage of the meltwater of the spray ice obtained at - 24 °C attained above 50% impurity reduction as compared with that of the spray ice obtained at - 10 °C when the runoff volume was also considered. But higher degree of impurity removal was achieved in the product water (meltwater) when the sprayed water only partially froze. Only 17% to 28% of the meltwater (volume) of the spray ice obtained at - 24 °C (including both 20-day and 40-day old ice) reach above 80% impurity reduction while 24% to 48% of the meltwater (based on total volume of the sprayed water) reached the same degree of impurity removal when runoff was generated (the percentage of the total meltwater volume that reached above 80% impurity reduction was 34% to 67%).

It is obvious that the product water (meltwater) acquires higher quality when the wastewater only partially freezes during the spraying operation since considerable amount of impurities has been carried away from the spray ice mound by runoff. Therefore, as mentioned early, for the purpose of water or wastewater purification by spray freezing process, certain amount of runoff generation is desirable. But the volume of runoff generated should be kept low, probably less than 30% of the total sprayed water volume, according to the experimental results obtained from this study. Too much runoff will increase energy consumption per unit volume of product water. Under a given air temperature, the volume of runoff can be controlled by adjusting the flowrate, nozzle size or pump pressure. Although above 50% and less than 80% impurity removal can be achieved in most of the product water (meltwater), the amount of meltwater with higher degree (> 80%) of impurity removal is smaller when sprayed wastewater completely freeze (no runoff generation during the spraying operation). Furthermore, under a given ambient air temperature, in order to achieve complete freezing of the sprayed water (such as the artificial snow making process), higher nozzle pressure has to be used to produce smaller water droplets or increase droplet air residence time, which will result in higher energy consumption.

6.2.3.4 Results of Microtox toxicity test

The results of the Microtox test for the oil sands tailings pond water indicated that source water had a $EC_{50}(15,15)$ value, given in percent of the original sample concentration, around 22% in the non-adjusted sample and 28% in the adjusted sample ($EC_{50}(15,15) > 100\%$ indicates no response or inverse response to the sample tested). The removal of toxic substances by the meltwater of the spray ice was indicated by the progressive increase in the EC_{50} values as melting continues. Figure 6-44 illustrated the change of EC_{50} value with percentage of meltwater volume for one group of meltwater samples of the spray ice obtained at - 24 °C. The EC_{50} was obtained on the adjusted samples (pH adjustment and filtration). As shown in Figure 6-44, the EC_{50} value of the first fraction of the meltwater was very low (lower than that of the source water) designating that the initial meltwater contained high concentration of toxic materials. The EC_{50} values of the meltwater then gradually increased to about 100% or greater than 100%.

After analyzing the Microtox test results and the results obtained from chemical analysis, it was found that meltwater samples that had EC_{50} value greater than 100% ($EC_{50} > 100\%$) were the ones that obtained above 80% impurity reduction. About 50% of the total meltwater volume for the spray ice obtained at - 10 °C and with 40-day storage had EC_{50} value greater than 100%. Less than 20% of the meltwater volume for the spray ice obtained at the colder temperature (no runoff) obtained $EC_{50} > 100\%$. This implied that greater than 80% impurity removal is necessary to reduce toxicity from oil sands tailings pond water to the level that the wastewater only causes less than 50% mortality to the test bacteria population ($EC_{50} > 100\%$.) Therefore, for the purpose of water or wastewater purification, spray freezing operation should always be controlled to generate certain amount of runoff.

The pH-adjusted and filtered oil sands tailings pond water samples had higher EC_{50} (15,15) values than those original (non-adjusted) samples. The discrepancy in the EC_{50} (15,15) values between the adjusted samples and non-adjusted samples decreased or vanished when sample EC_{50} (15,15) values were close to 100%. Sometimes the adjusted samples had lower EC_{50} values than the non-adjusted ones when meltwater had higher percentage of impurity reduction. This indicated that high pH might not contribute substantially to the toxicity while the turbidity probably interfered with the Microtox test. When samples EC_{50} (15,15) was very close to 100%, the reproducibility of the test results was lower.

EC_{50} (15,15) of the source pulp mill effluent is greater than 100% for both adjusted and non-adjusted samples. Reduction of lower concentration toxicity (EC_{20}) was found in the meltwater of the pulp mill effluent spray ice. The source pulp mill effluent samples had a EC_{20} value around 77%. The EC_{20} values of the meltwater samples with above 80% impurity reduction were increased to > 100%.

The tap water samples (source water and meltwater) were found not toxic.

The results of the Microtox toxicity test indicated that spray freezing of wastewater is also an effective and simple way to remove toxic substances contained in the industrial wastewater.

6.3 Prediction of Meltwater Impurity Concentration

The impurity release from melting ice columns is a function of the cumulative meltwater discharge. This impurity removal function can be modeled by simple curve fitting. It was found very useful when such models were included into a larger watershed model to predict meltwater flowrate and impurity concentration of the seasonal snowpacks. Many experimental study results have shown that impurity concentration decayed exponentially with the cumulative meltwater discharge. A single-term or two-

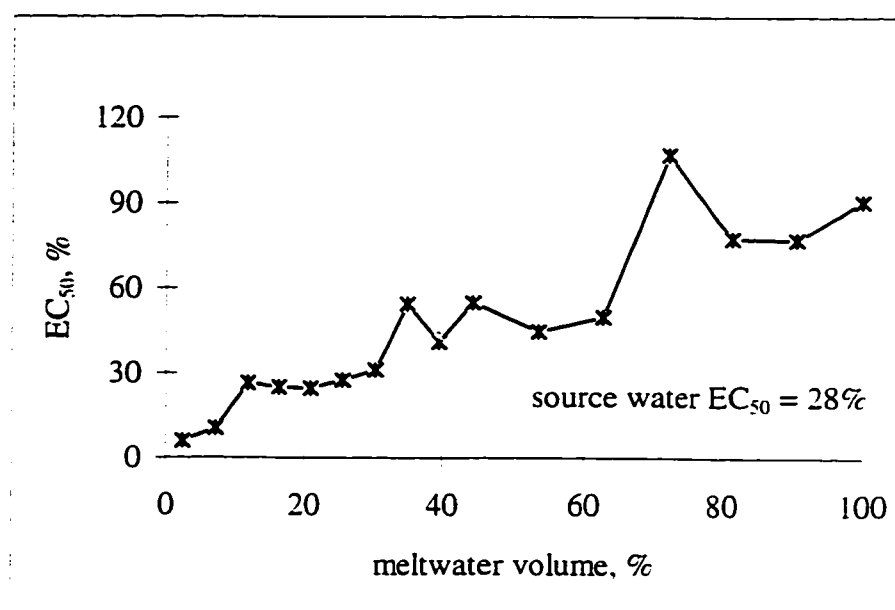


Figure 6-44 EC₅₀ values (%) of the meltwater samples (pH-adjusted and filtered) versus the cumulative meltwater volume (%) for the spray ice of oil sands tailings pond water (spray ice was obtained at - 24 °C). The source water EC₅₀ = 28% (pH-adjusted and filtered).

term exponential function was usually chosen and proven to be very versatile (e.g. Bales. 1991; Zapf-Gilie, 1985).

The shape of the impurity removal (concentration ratio versus cumulative meltwater volume) plots shown in the section 6.2.3.2 indicated that the impurity concentration also decreased exponentially with cumulative meltwater volume for the spray ice made from pulp mill effluent and oil sands tailings pond water in a - 24 °C environment in this study. Based on the figures presented in section 6.2.3.2, a first order exponential wash-out function can be written to approximate the wash-out of the impurity content in the meltwater:

$$y = L_o e^{-k_m x} \quad (6.1)$$

where:

y = meltwater impurity concentration ratio, c/c_o (where c_o is the source water impurity concentration)

L_o = the initial impurity concentration ratio

k_m = wash-out coefficient

x = cumulative meltwater fraction (%)

The wash-out coefficient k_m can be determined by transfer equation (6.1) into logarithmic form:

$$\ln(y) = \ln(L_o) - k_m x \quad (6.2)$$

which is a straight line equation. Coefficients L_o and k_m are obtained by linear regression. L_o , which is the y value when $x = 0$ (i.e. no melting) is approximately equal to the initial

concentration ratio for a melting process. Therefore, the concentration ratio of the first fraction of the meltwater approaches L_o when smaller initial meltwater volume is collected.

L_o and k_m values as well as the correlation coefficient R^2 obtained from linear regression for the spray ice obtained at - 24 °C were given in Tables 6-16 and 6-17. The data obtained from the melting test fit the exponential wash-out model very well for pulp mill effluent. The high R^2 values obtained for the pulp mill effluent (Table 6-16) also indicated the goodness of fit the exponential function (although R^2 is in logarithmic units). Whereas the excellence of fit for oil sands tailings pond water was slightly lower. Figures 6-45 and 6-46 displayed the predicted and measured meltwater conductivity and TOC concentration ratios for the pulp mill effluent tested.

The wash-out of the impurity content with the cumulative meltwater volume did not follow the exponential equation for the spray ice obtained at a warmer air temperature (- 10 °C). Curve fitting for the data obtained from melting of the spray ice obtained at - 10 °C was unsatisfactory when the exponential equation was used. The decay pattern of the meltwater impurity concentration was better described by a power equation due to the dramatic decrease of the impurity concentration after discharging the first portion of the meltwater and the lower amount of impurities contained in the ice column (considerable amount of impurities were removed by runoff generated during spraying operation). The power equation is of the form:

$$y = L_o x^{-k_m} \quad (6.3)$$

The coefficients L_o and k_m and R^2 values for the spray ice obtained at - 10 °C were also listed in Tables 6-16 and 6-17. Again, the data fit the power decay model fairly well for some conditions while was not very satisfactory for others. The model predicted conductivity and TOC concentration ratios as well as measured values were shown in

Figures 6-47 and 6-48 for the meltwater of the spray ice made from oil sands tailings pond water.

The wash-out rate of the meltwater impurity concentration (k_m) is influenced by many factors such as the chemical species, the ambient air temperature at which the spray freezing operation is conducted, the spray ice storage time, the amount of impurities within the spray ice mound, etc. The water flow through the melting ice column will also affect the wash-out rate. If mathematical models which predict water flow through ice columns are available together with the models obtained by curve fitting for impurity concentration decay, the meltwater flux and impurity concentration from spray ice mound may be estimated. Studies on ice mound hydrology and mathematical modeling of water flow through ice mound should be conducted in future. The accuracy of the wash-out coefficient, k_m , might be improved by non-linear regression.

As mentioned in Chapter 5 that determining the impurity distribution coefficient for each contaminant in the wastewater for the spray freezing process is impractical. Thus, a parameter which is a good measure of the freezing process should be selected. Figures in sections 6.2.3.1 and 6.2.3.2 clearly showed that meltwater conductivity always followed other organic and inorganic parameters very closely. The approximation of the conductivity decay coefficient with others listed in Tables 6-15 and 6-16 also indicated that electrical conductivity might be used as an indicating parameter. Meanwhile, measurement of this parameter is easy and can be carried out under field conditions.

6.4 Application of the Spray Freezing Process

One of the advantages of the spray freezing process is the simplicity of the operation. The skill required for the operator personnel is relatively low. The spraying operation can be fully automated, therefore, the operation can be run for 24 hours a day during the winter season.

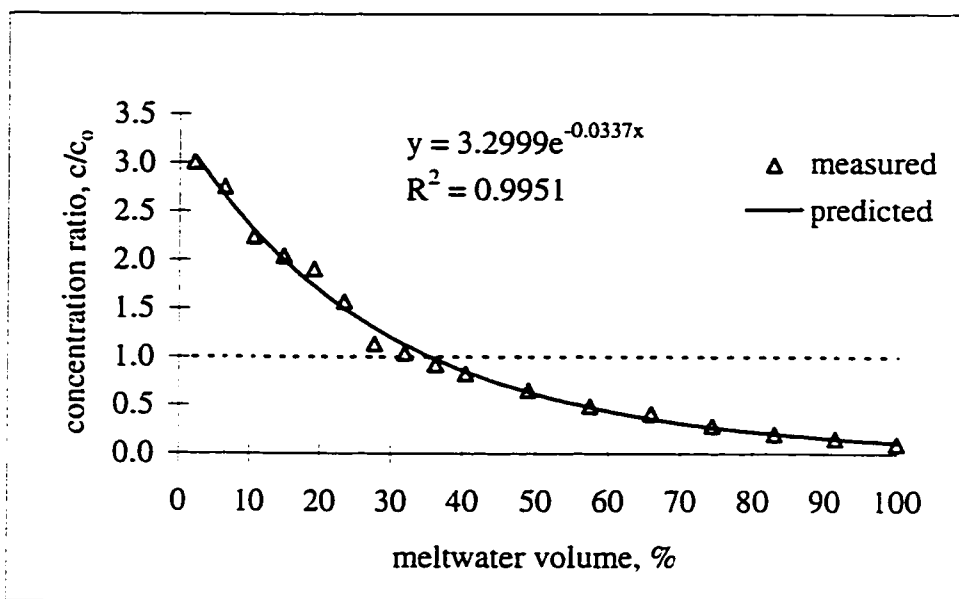


Figure 6-45 Predicted and measured meltwater TOC concentration ratio for the spray ice made from pulp mill effluent (spray ice was obtained at - 24 °C and stored for 40 days).

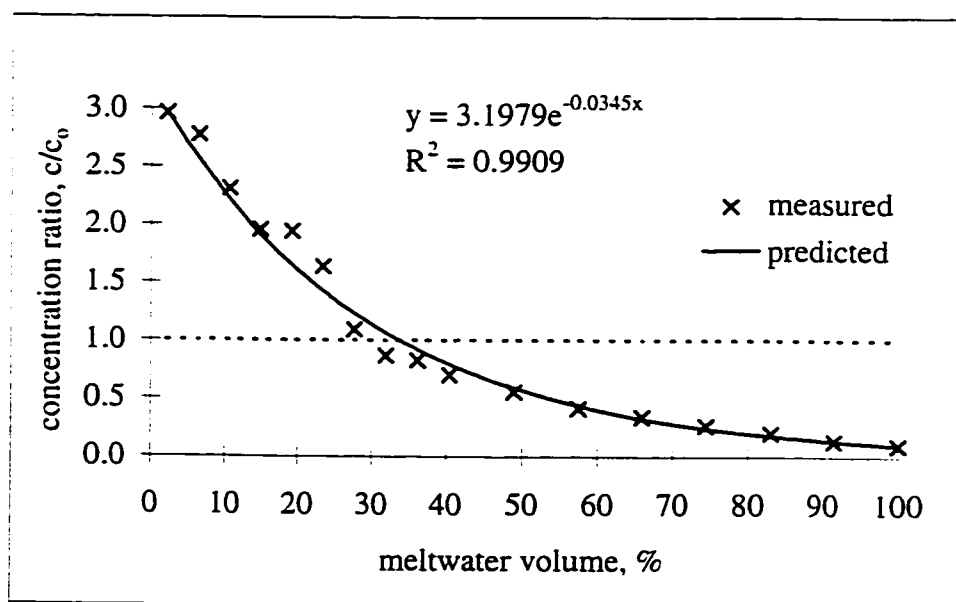


Figure 6-46 Predicted and measured meltwater conductivity ratio for the spray ice made from pulp mill effluent (spray ice was obtained at - 24 °C and stored for 40 days).

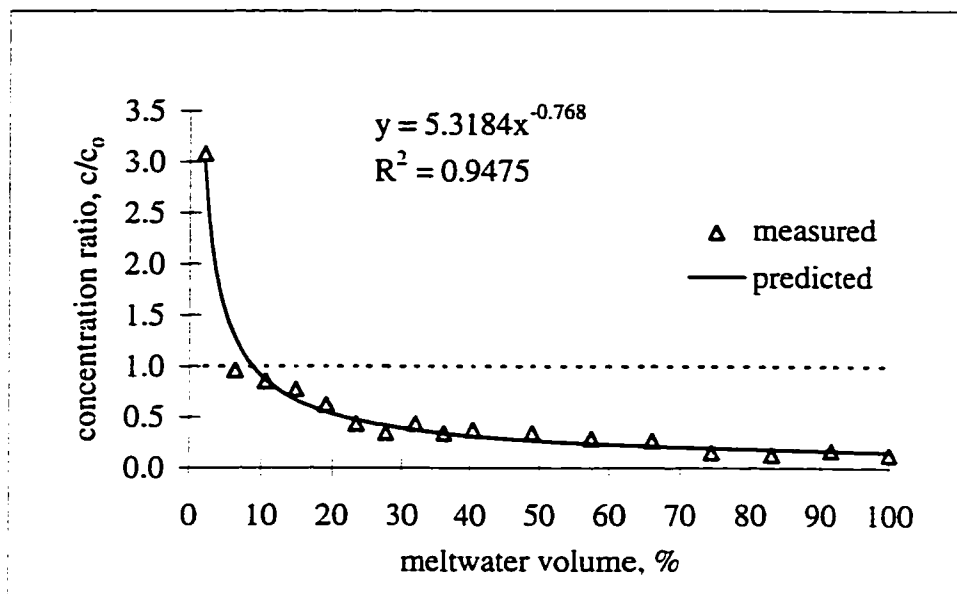


Figure 6-47 Predicted and measured meltwater TOC concentration ratio for the spray ice made from oil sands tailing pond water (spray ice was obtained at $-10\text{ }^{\circ}\text{C}$ and stored for 20 days).

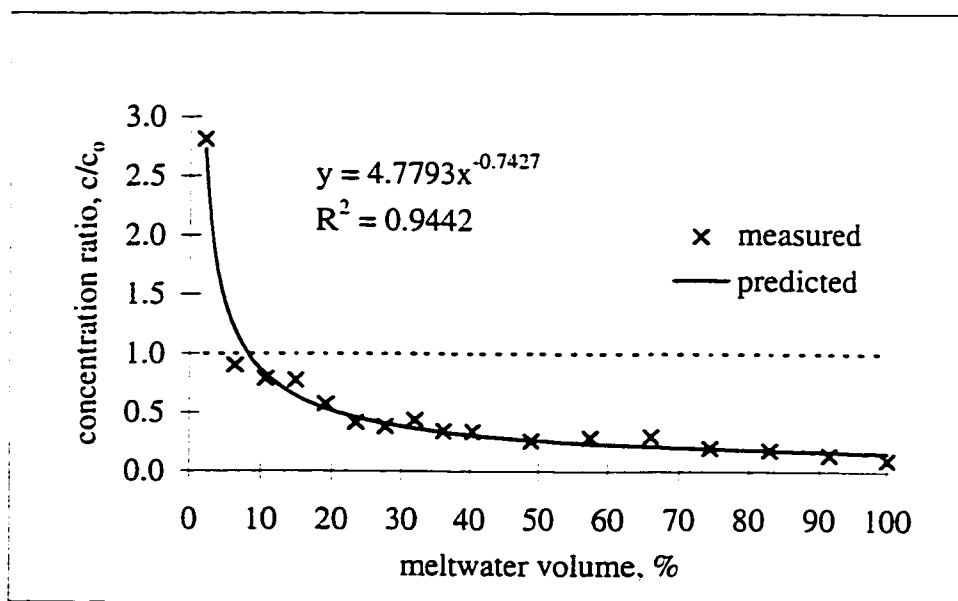


Figure 6-48 Predicted and measured meltwater conductivity ratio for the spray ice made from oil sands tailings pond water (spray ice was obtained at $-10\text{ }^{\circ}\text{C}$ and stored for 20 days).

Table 6-16 Coefficients of the meltwater impurity concentration prediction models for pulp mill effluent

Spray ice condition	Prediction model	Type of impurity	Coefficients		R ²
			k _m	L _o	
Air Temperature: - 10 °C storage time: 20 days	$y = L_o x^{-k_m}$	COD	0.673	6.138	0.879
		TOC	0.753	6.504	0.844
		color	0.661	4.548	0.810
		conductivity	0.667	3.694	0.833
40 days	$y = L_o x^{-k_m}$	COD	0.881	7.510	0.765
		TOC	0.753	4.167	0.748
		color	0.759	4.098	0.794
		conductivity	0.713	3.151	0.782
Air Temperature: - 24 °C storage time: 20 days	$y = L_o e^{-k_m x}$	COD	0.0393	3.633	0.985
		TOC	0.0396	4.055	0.988
		color	0.0404	3.743	0.990
		conductivity	0.0388	3.600	0.988
40 days	$y = L_o e^{-k_m x}$	COD	0.0336	2.856	0.995
		TOC	0.0337	3.300	0.995
		color	0.0349	3.009	0.996
		conductivity	0.0345	3.198	0.991

Table 6-17 Coefficients of the meltwater impurity concentration prediction models for oil sands tailings pond water

Spray ice condition	Prediction model	Type of impurity	Coefficients		R ²
			k _m	L _o	
Air Temperature: - 10 °C storage time: 20 days 40 days	$y = L_o x^{-k_m}$	COD	0.815	5.276	0.941
		TOC	0.768	5.318	0.948
		Cl ⁻	0.805	6.210	0.805
		SO ₄ ²⁻	0.786	6.461	0.913
		conductivity	0.743	4.779	0.944
		COD	0.963	6.513	0.636
		TOC	0.790	4.689	0.755
		Cl ⁻	0.793	4.884	0.709
		SO ₄ ²⁻	0.824	5.664	0.708
		conductivity	0.784	4.283	0.696
Air Temperature: - 24 °C storage time: 20 days 40 days	$y = L_o e^{-k_m x}$	COD	0.0279	2.340	0.920
		TOC	0.0285	2.309	0.862
		Cl ⁻	0.0359	3.330	0.941
		SO ₄ ²⁻	0.0371	3.640	0.938
		conductivity	0.0362	3.101	0.919
		COD	0.0294	3.009	0.875
		TOC	0.0337	3.009	0.872
		Cl ⁻	0.0372	3.330	0.938
		SO ₄ ²⁻	0.0363	3.198	0.926
		conductivity	0.0372	2.964	0.937

The spray freezing process is a batch treatment process which can be started when as needed and stopped when it is not needed. The spray freezing process is ideal for both small or large volume wastewater treatment and it can be used at any site given low winter temperatures. The ideal application of the spray freezing process would be for the industries or small communities located in the remote areas in the cold regions.

As the spray freezing process can effectively be used to remove both organic and inorganic contaminants, it is insensitive to the type of wastewater being treated. The process is an alternative for the treatment of the wastewater which can not be treated by biological treatment and is too expensive or complex to be treated by chemical or other processes. The process can also be used in conjunction with biological treatments (such as pond treatment process) which have low efficiency during the winter. Therefore, the spray freezing process should be selected as winter treatment method while biological treatment is used in the summer. The sizes of the ponds or lagoons can be reduced to store the volume of wastewater produced in the summer. Livestock farms, mining, pulp mill, and food processing industries are the examples of the possible users of the spray freezing process. After the spray freezing process, these industrial wastewaters could be discharged or recycled. Meanwhile, utilization of the spray freezing process will reduce the volume requirement for the tailings ponds or lagoons. The spray freezing process could also provide treatment and disposal alternatives for the sewage effluent (disinfection may be required for raw sewage effluent) for the small communities which face effluent disposal restriction during the winter.

Selection of the site for the spray ice containment depends on the characteristics and the volume of the wastewater to be treated. The site may be an abandoned lagoon, a piece of farm land or a special area designed to hold the spray ice. The containment area should be designed that the base of the containment area has a slope ($> 1\%$) to ensure positive drainage of the runoff during the spraying and that all the subsequent meltwater will drain from the containment area. The drainage pipes should be placed and have

access for water sampling both during and after the spraying operation. The discharge of the containment area should be down slope and beyond the spray pump location, to ensure that it does not become blocked during the spraying operation. If a liner is required for the containment area, it should be determined by the nature of the wastewater and the permeability of the foundation soil.

The maximum design depth (height) of a spray ice mound is determined by the duration and intensity of the freezing and thawing seasons. Similar to Martel's (1991) sludge freezing bed, the maximum height of the spray ice mound that can be built is controlled by freezing in United States and southern Canada. However, total depth of the ice that can be melted will determine the depth of the spray ice mound in the northern areas of Alaska and Canada.

The results obtained from the spray freezing test presented in this thesis should not be used to scale-up for the field applications due to the obvious differences in the drainage conditions in the runoff during the spraying operation and meltwater between the small ice columns used in this study and large ice piles in the field. Blocking of the runoff or meltwater that occurred when spray ice was placed in the plastic glass columns will unlikely happen in field conditions if the containment areas are properly designed. The greater ice mound depth in field applications will certainly improve impurity removal efficiency. Therefore, the impurity removal efficiency for the field applications will be higher than that of the small scale laboratory tests. The results obtained from the field test (Gao et al., 1996) conducted in Syncrude mine site showed much higher impurity removal efficiency than the small scale test conducted in this study.

6.5 Summary

Without any pretreatment, spray freezing process can effectively remove organic, inorganic contaminants contained in the pulp mill effluent and oil sands tailings pond water. The spray freezing process is also effective for toxicity reduction.

Observations and the experimental results justified the impurity removal hypothesis proposed in Chapter 5. The spray ice was first purified by releasing certain amount of impurities to the runoff generated (if there was any) during spraying operation. Then the water was further purified by discharging large amount of impurities with the early meltwater. The high impurity content in the early meltwater was induced by the redistribution of the impurities in the spray ice column after the sprayed wastewater froze. The redistribution of the impurities in the spray ice column is caused by water contained in the ice mound (the water freezes afterwards), metamorphism and sublimation of the ice grains, and freeze-melt cycling (did not occur in this study).

Ambient air temperature affected impurity removal efficiency by affecting the freezing rate of the sprayed wastewater. When the freezing rate was relatively low, runoff was generated and a considerable amount of impurities were carried away from the spray ice. The spray ice had lower impurity concentrations. At a high freezing rate, the sprayed wastewater completely froze during the spraying and no impurities were removed from the spray ice. The spray ice contained the same total mass of impurities as the source water.

The impurity removal efficiency was influenced by the age (storage time) of the spray ice when the spray ice was produced and stored in a warmer air temperature (-10°C). Higher percentage of impurity removal was achieved from the spray ice with longer storage time. Organic contaminants were eluted more effectively than the inorganics from the melting spray ice which was formed and stored at a warmer temperature. The

warmer ambient air temperature and the longer storage time might cause more effective and selective exclusion of impurities to the surface of the ice grains.

Fractionation of impurities from melting ice column is a complex process. Experimental results indicated that nature of the wastewater, the ice column density, distribution of impurities within the ice column and the spray ice impurity concentrations all influenced the meltwater impurity concentration. The spray ice obtained at colder temperature (-24 °C) had lower density and higher impurity concentrations.

More high quality meltwater was produced when the spray ice was formed with runoff generation. Therefore, certain amount of runoff generation is necessary for the spray freezing process to achieve higher impurity removal efficiency.

CHAPTER 7 SUMMARIES AND CONCLUSIONS

The fundamental research for using spray freezing technique to treat industrial wastewater is the principle that when water freezes, impurities present in the wastewater are rejected by growing ice crystals and are concentrated in the liquid phase when the sprayed water partially freezes (wet growth condition) during the spraying operation. The liquid carries away the highly concentrated impurities from the spray ice mound as runoff and leaves a relatively purer ice. The impurities remained in the ice mound become concentrated in the early meltwater during the spring thaw by metamorphism, sublimation and melt-freeze process. The spray ice is further purified by discharging large amount of impurities with the initial meltwater. The purer meltwater may be directly discharged or reused when it meets the corresponding standards.

In this research project, three sets of experiments were carried out to investigate the ice nucleation characteristics, the freezing behavior of freely suspended piggery wastewater, pulp mill effluent and oil sands tailings pond water as well as the treatability of pulp mill effluent and oil sands tailings pond water by the spray freezing process. A mathematical model was developed to predict impurity concentration in the spray ice. Two models were obtained by curve fitting to estimate meltwater impurity concentrations. The summaries and conclusions drawn from this study are presented in the following sections.

Conclusions on the freezing characteristics of industrial wastewater droplets

This experiment was set up to investigate the freezing characteristics of the three types of industrial wastewaters (piggery wastewater, pulp mill effluent and oil sands

tailings pond water) in comparison to distilled water. The experimental results were evaluated using Vali's (1971) nucleus spectra model. The concentration vs. temperature functions (nucleus spectra) were used to determine the nucleus content and the effectiveness of these nuclei in a wastewater droplet. The 'freezeability' of the wastewater was compared based on the derived nucleus concentration. The effect of pH, impurity concentration and size (volume) on the freezing temperature of the wastewater drops were examined. The conclusions drawn from this experiment are:

1. The wastewater generated from different industries freezes at different temperatures. The pulp mill effluent has highest nucleus concentration or highest 'freezeability' among the three types of wastewaters tested, and piggery wastewater has the lowest nucleus concentration. The nucleus concentration of oil sands tailings pond water (T.P.W.) is between the other two. The T_{90} 's (a temperature at which 90% of the droplets tested froze) of 4.2 μL (equivalent spherical diameter: 2.0 mm) wastewater drops were $-9.7\text{ }^{\circ}\text{C}$ for piggery wastewater, $-7.5\text{ }^{\circ}\text{C}$ for T.P.W. and $-6.4\text{ }^{\circ}\text{C}$ for pulp mill effluent. Under the same experimental condition, the T_{90} for distilled water droplets which had served as a reference was $-20.8\text{ }^{\circ}\text{C}$.
2. pH of the wastewater affected the freezing temperature of the wastewater droplets. The effect was specific to each wastewater. The initial freezing temperature was lower when the wastewaters were adjusted to an acidic pH. Comparing with the droplets at original liquid pH, nucleus concentrations of pulp mill effluent and piggery wastewater drops decreased when the wastewater pH was adjusted to 4.0. The T_{90} dropped $1.6\text{ }^{\circ}\text{C}$ for piggery wastewater and $0.6\text{ }^{\circ}\text{C}$ for pulp mill effluent but it increased $0.1\text{ }^{\circ}\text{C}$ for T.P.W. Basic pH (pH = 11.0) caused wastewater drops to freeze at a slightly warmer temperature. Under basic pH (pH = 11.0), the increase in T_{90} was 0.7, 0.4 and 0.4 degree for piggery wastewater, pulp mill effluent and T.P.W..

respectively. The pH adjustment had the least effect on the freezing temperature of T.P.W. droplets.

3. The droplet freezing temperature was influenced by the amount of the impurities present in the wastewater. When impurity concentration of the wastewaters was reduced to 2% and 50% of the original amount by 1:50 and 1:2 dilutions, the nucleus concentration in the piggery wastewater reduced by 97% and 40%, respectively. The reduction in nucleus concentration for pulp mill effluent was 83% when the wastewater contains 2% of its original impurity content. The concentration of active nuclei was only decreased by 20% under 50% of the original impurity content. For T.P.W., the decline in the nucleus concentration under 2% and 50% impurity concentration was 96% and 20%, respectively.
4. The freezing temperature of the wastewater drops were volume dependent. The larger drops froze at warmer temperature than the small ones. Lower freezing nucleus concentration was required for larger drops to freeze.

Conclusions on the freezing behavior of freely suspended wastewater droplets

A small vertical wind tunnel was built to study the behavior of freely suspended wastewater drops during the freezing process. The observations on the freezing of wastewater drops have revealed some interesting and important phenomena. Basic information about freezing characteristics of the wastewaters and the time required for the wastewaters to freeze under different experimental conditions was obtained under these relatively simple laboratory conditions. The information obtained can be used in the design and the optimization of a spray freezing process because of the simulation of the experimental conditions to the conditions under which drops freeze in the atmosphere during a spray freezing process. The conclusions drawn from the observations and results obtained from this experiment are:

1. Freezing of a water drop starts at the bottom and propagates over the surface to enclose the drop in an ice shell. The speed of the droplet surface freezing is a function of the ambient air temperature and the nature of the water. Most droplets decrease in terminal velocity after freezing due to the change in the droplet shape (larger cross section and lower density). Fracture of the ice shell is unlikely to occur to the droplets in a spray freezing operation due to the short air residence time of the sprayed water drops. For a droplet frozen at $-18\text{ }^{\circ}\text{C}$ (humidity: $\sim 71\%$) ambient air temperature, the time required to fracture the ice shell was in the range of 14.7 to 246.5 seconds for oil sands tailings pond water and 18.0 to 223.8 seconds for pulp mill effluent drops. No fracture of ice shell ever happened to the piggery wastewater drops. Longer time was required to break the ice shell when droplets were frozen at warmer air temperatures.
2. The time required for freezing of a collection of visibly identical drops spreads over a certain range. Under a given air temperature and initial droplet temperature, smaller drops needed less time to freeze. Generally, the ice nucleation in the larger droplets occurred at a slightly warmer temperature when compared to smaller drops. The difference in the freezing time required by large and small droplets reduced as air temperature decreased. The cooling rate increased with increasing temperature difference between the droplet and the ambient air, i.e. less time was required for the wastewater drops to freeze under colder air temperatures. The average time required for freezing of a piggery wastewater drop was in the range of 16.0 (for 3.4 mm diameter drops) to 19.4 seconds (for 4.2 mm diameter drops) at $-10\text{ }^{\circ}\text{C}$ (humidity: 75%) and the time decreased to 7.0 (3.4 mm diameter drops) to 7.4 (4.2 mm diameter drops) seconds when air temperature was at $-18\text{ }^{\circ}\text{C}$ (humidity: 71%). For pulp mill effluent droplets, the average time was 7.6 seconds for 2.8 mm diameter drops and 12.0 seconds for 4.2 mm diameter drops at $-10\text{ }^{\circ}\text{C}$. The

time was reduced to 2.5 (2.8 mm diameter drops) to 4.3 (4.2 mm diameter drops) seconds when air temperature dropped to - 18 °C. The average time for oil sands tailings pond water drops to freeze was in the range of 8.4 to 13.3 seconds at - 10 °C and 3.1 to 5.6 seconds at - 18 °C. Less time was required by the smaller drops (2.8 mm diameter) to freeze.

3. The ice nucleation temperature of a suspended water droplet varied with the ambient air temperature. The ice nucleation in the wastewater drops took place at warmer temperatures as air temperature fell, i.e. drops were less supercooled before freezing began. However, wastewater drops were deeply supercooled under warmer air temperatures which are colder than the warmest ice nucleation temperature of the wastewater. Freezing did not occur until droplet temperature approached the ambient air temperature.
4. The estimated freezing temperature for freely suspended pulp mill effluent drops (including both 4.2 mm diameter and 2.8 mm diameter) was in the range - 5.5 °C (at air temperature = - 10 °C) to - 1.8 °C (at air temperature = - 18 °C). Under the same conditions, the freezing temperature of the freely suspended oil sands tailings pond water drops was predicted between - 6 °C to - 3.4 °C. At - 10 °C air temperature, the ice nucleation temperature for piggery wastewater drops would be - 7.5 °C for a 4.2 mm diameter drop and - 7.9 °C for a 3.4 mm diameter drop. The freezing temperature would increase to - 5.3 °C for a 4.2 mm diameter drop and - 7.1 °C for a 3.4 mm diameter drop when air temperature decreased to - 18 °C.
5. The calculated results indicated that pulp mill effluent has the warmest ice nucleation temperature among the wastewaters tested and piggery wastewater drops have the lowest freezing temperature. The freezing temperature of oil sands tailings pond water drops is between the pulp mill effluent and the piggery wastewater drops. Piggery wastewater drops usually freeze at a

temperature about 2 to 3 °C lower than the pulp mill effluent and oil sands tailings pond water. Therefore, under the same conditions, a pulp mill effluent drop will have the highest ice fraction in the spray freezing process, while the ice fraction in the oil sands tailings pond water is slightly lower than that of the pulp mill effluent drop. The portion of frozen water in the piggery wastewater drops will be lowest because of the lower ice nucleation temperature of the piggery wastewater drops compared with the other wastewaters.

Conclusions on wastewater treatment by spray freezing process

Experimental results obtained from this study have demonstrated that spray freezing is a simple and effective method to treat pulp mill effluent and oil sands tailings pond water. In cold regions the spray freezing process provides a practical treatment alternative for the industrial wastewater which may be otherwise too expensive to be treated. The process can also be used to treat water or other types of wastewater with various volumes. Organic and inorganic contaminants including toxic substances can be effectively removed from the wastewater by the spray freezing process. Conclusions drawn from the spray freezing test include:

1. Ambient air temperature affected the freezing rate of the sprayed wastewater in the spray freezing process. The volume of runoff generated was directly related to the freezing rate of the sprayed wastewater. When runoff was produced, the sprayed wastewater had a relatively lower freezing rate and the spray ice formed contained a lower amount of impurities. A considerable amount of the impurities present in the wastewater was removed from the spray ice by the runoff. The impurity concentrations of the ice core samples (including both pulp mill effluent and oil sands tailings pond water) were only about 30% to 60% of the source water when runoff was generated. While the spray ice obtained at a higher freezing rate (no runoff generation) contained

the same amount of impurities as the source water. More impurities were transported to the bottom of the ice column when runoff was produced while the distribution of impurities was relatively uniform in the ice column when the sprayed water completely froze during spraying.

2. The age of the spray ice influenced the efficiency of impurity removal during melting when the wastewater was spray frozen and stored in a warmer ambient air temperature (- 10 °C). The percentage of the total amount of impurities removed from the ice column (about 300 mm in height) with the first 30% of the meltwater was 55% for COD, 53% for color, 57% for TOC and 54% for conductivity when spray ice of pulp mill effluent was aged for 20 days by storage. For the 40-day old pulp mill effluent spray ice, the percentage of impurity removal increased by 7% for COD and 5% for color. Under the same spraying and storage conditions, for the 20-day old oil sands tailings pond water spray ice, the percentage of impurity reduction by the first 30% of the meltwater was 60% for COD, 56% for TOC, 54% for conductivity, 57% for Cl^- and 54% for SO_4^{2-} . An extra 10% to 13% of the contaminants was removed with the initial meltwater for the older (40-days) spray ice. The organic contaminants were removed more effectively than the inorganics by the meltwater when spray ice was obtained and stored at a warmer air temperature.
3. Higher percentage of impurity removal by the initial 30% of the meltwater was achieved when the spray ice was formed and stored at a colder air temperature (-24 °C) due to the lower ice density and high impurity concentrations. The percentage of the total amount of impurities discharged with first 30% of the meltwater was in the range of 72% to 73% for 20-day old pulp mill effluent spray ice and 66% to 69% for the 40-day old pulp mill effluent spray ice. The impurities in the spray ice of oil sands tailings pond water was reduced by 66% to 76% after the first 30% of the meltwater was

discharged. The age of the spray ice had no significant effects on the meltwater impurity concentrations for the oil sands tailings pond water under this temperature condition. No obvious preferential elution of any type of impurity occurred during melting of the spray ice (including both pulp mill effluent and oil sands tailings pond water) obtained at - 24 °C. organic and inorganic contaminants were removed with equal efficiency.

4. The meltwater had higher quality when the runoff was generated during the spraying operation. More meltwater samples of the spray ice had above 80% impurity reduction (i.e. the meltwater contained less than 20% of the source water impurity content) even when the volume of the runoff was accounted (about 30% of the total volume of wastewater sprayed turned into runoff). Only 17% to 28% of the meltwater of the spray ice obtained at - 24 °C (including both 20-day and 40-day old ice) reach above 80% impurity reduction. For meltwater from - 10 °C spraying 24% to 48% of the meltwater (based on total volume of the sprayed water) reached the same degree of impurity removal when runoff was generated (the percentage of the meltwater that reached above 80% impurity reduction was 34% to 67% when runoff volume was not accounted). Slightly higher percentage of the meltwater reached above 50% impurity reduction for the spray ice obtained at - 24 °C (no runoff).
5. The spray freezing process can effectively remove the toxic substances present in the oil sands tailings pond water. To reduce toxicity from oil sands tailings pond water to the level that the negative effect on the test bacteria population is less than 50% (i.e. to achieve $EC_{50} (15, 15) > 100\%$), the meltwater of the spray ice could only contain less than 20% of the source water impurity content (or > 80% impurity reduction in the meltwater). About 50% of the total meltwater volume for the spray ice produced at - 10 °C (with runoff) and with 40-day storage had EC_{50} value greater than 100%. Less than 20% of the

meltwater volume for the spray ice obtained at the colder temperature (no runoff) obtained $EC_{50} > 100\%$. The toxicity in the source pulp mill effluent did not cause mortality to 50% of the test population ($EC_{50} > 100\%$). Reduction of toxicity indicated by EC_{20} (15, 15) (20% mortality of the test bacterial population) was discovered in the meltwater of the spray ice made from pulp mill effluent. The EC_{20} (15, 15) value of the pulp mill effluent increased from 77% in the source water to $> 100\%$ in the meltwater samples which achieved greater than 80% impurity reduction.

6. To achieve higher impurity removal efficiency by the spray freezing process. the spraying operation should be always controlled to produce certain amount of runoff (i.e. the sprayed wastewater only partially froze). The volume of the runoff generated should be small; less than 30% of the total volume of the sprayed wastewater is suggested.

Prediction of the spray ice and meltwater impurity concentrations

A mathematical model was developed to predict impurity concentrations in the spray ice based on the mass balance of the impurity in the continuous spray freezing process:

$$k = \frac{C_i}{C_o} = \frac{k^*}{k^* - \frac{Q_r}{Q_o} (k^* - 1)}$$

where:

Q_o = flowrate of the source sprayed (influent), m^3/s

Q_r = flowrate of the runoff, m^3/s

C_o = impurity concentration in the source water, g/m^3

C_i = impurity concentration in the spray ice, g/m^3

C_r = impurity concentration in runoff, g/ m³

$k^* = C_i/C_r$ = the interfacial distribution coefficient, and

$k = C_i/C_o$ = the effective distribution coefficient

If either the interfacial distribution coefficient k^* or the effective distribution coefficient, k of the wastewater to be treated is known, the spray ice impurity concentration can be estimated using above equation.

Two simple empirical formulations were developed for prediction of the meltwater impurity concentrations. For practical purposes, the relationship between the meltwater impurity concentration (ratio) and the cumulative meltwater percentage can be described by a power function when the spray ice is produced with runoff generation and a first order exponential decay function if no impurity is removed from the spray ice during spraying. The meltwater impurity concentration (ratio) is given by:

$$y = L_o x^{-k_m} \quad (\text{for the spray ice produced with 30\% runoff generation})$$

and

$$y = L_o e^{-k_m x} \quad (\text{for spray ice produced without runoff generation})$$

where:

y = meltwater impurity concentration ratio, c/c_o (where c_o is the source water impurity concentration)

L_o = the initial impurity concentration ratio

k_m = wash-out coefficient

x = cumulative meltwater fraction (%)

The nature of the wastewater, the freezing rate, the spray ice storage time, the amount of impurities within the spray ice mound, and the water flow through the melting ice column all affect the decay rate, k_m .

Conductivity of a water sample can be used as an indicator to measure the spray freezing process. The conductivity ratios of the runoff or meltwater samples to a source water give a direct indication on the impurity removal efficiency.

CHAPTER 8 RECOMMENDATIONS FOR FUTURE STUDIES

There are many phenomena and mechanisms which deserve more investigation and experimentation. The recommended future research on spray freezing process for wastewater treatment include:

1. Prediction of impurity participation in the liquid phase and solid phase in a freezing process will always involve the impurity partition coefficients. Therefore, the interfacial coefficient k^* (equation 5.6) of pulp mill effluent and oil sands tailings pond water should be determined and the factors that control k^* should be studied in detail. When information on k^* is available, equation 5.6 can be verified by an experimental study.
2. Larger scale laboratory melting test is recommended to investigate the influences of ice column density, depth and meltwater flow on the meltwater quality.
3. Large scale field tests should be conducted to check the results of this research under natural conditions and to get the process design information such as land use, spraying system selection, process capacity (the total volume of spray ice can be produced in the winter season) as well as capital and operating cost.

REFERENCES

Allyn, N. and Masterson, D. 1989. Spray ice construction and simulation. Proceedings of the Eight International Offshore Mechanics and Arctic Engineering Symposium (OMAE), The Hague, The Netherlands, IV: 253-262.

American Public Health Association, American Water Works Association and American Environment Federation, 1995. Standard Methods for the Examination of Water and Wastewater. Edited by: Eaton, A.D., Clesceri, L.S. and Greenberg, A.E. American Public Health Association, Washington, DC.

Applied Science Laboratory, Inc. 1971. Purification of mine water by freezing. US EPA, Water Quality Office, Water Pollution Control Research Series: 14010 DR7.

Baeth, C.L. and Polkowski, L.B. 1972. Correlation OII and odorous components in stored dairy manure. Paper No. 72-950. ASAE, St. Joseph, MI.

Bailey, I.H. and Macklin, W.C. 1968. The surface configuration and the internal structure of artificial hailstones. *Quart. J. R. Met. Soc.*, 94, No. 399: 1-11.

Baker, R.A. 1967a. Trace organic contaminant concentration by freezing - I : Low inorganic aqueous solutions. *Water Research*, 1: 61-77.

Baker, R.A. 1967b. Trace organic contaminant concentration by freezing - II : Inorganic aqueous solutions. *Water Research*, 1: 97-113.

Baker, R.A. 1969. Trace organic contaminant concentration by freezing -III: Ice washing. *Water Research*, 3: 717-730.

Baker, R.A. 1970. Trace organic contaminant concentration by freezing - IV: Ionic effects. *Water Research*, 4: 559-573.

Bales, R.C., Davis, R.E. and Stanley, D.A. 1989. Ion elution through shallow homogeneous snow. *Water Resources Research*, 25: 1869-1877.

- Bales, R.C. 1991. Modeling in-pack chemical transformation. In: *Seasonal Snowpacks: Process of Compositional Changes*. T.D. Davies, T. Tranter and H.G. Jones. Ed. Berlin. Germany: Springer-Verlag: 139-163.
- Bardulin, A.J., Rose, A. and Sweeny, R. 1963. Wastewater renovation. Part 1: A design study of freezing and gas hydrate formation. US Department of Health Education and Welfare, P.H.S., Environmental Health Series AWTR-4.
- Barth, C.L., Elliot, L.F. and Melvin, S.W. 1982. Using odor control technology to support animal agriculture. Paper No. 82-4035. ASAE, St. Joseph, MI.
- Barthakur, N. and Maybank, J. 1963. Anomalous behavior of some amino acids as ice nucleators. *Nature, Lond.* 200: 866-869.
- Bashkirova, G.M. and Krasikov, P.N. 1957. Investigation of certain substances as crystallization reagents of supercooled fog. *Trudy glav. geofiz. Obs. A. I. Voeikova*. 72: 118-126.
- Bigg, E.K. 1953. The supercooling of water. *Proc. Phys. Soc. (London)* B. 66:688-694.
- Blanchard, D.C. 1950. The behavior of water drops at terminal velocity in air. *Trans. Amer. Geophys. Union*, 31, No. 6: 836-842.
- Blanchard, D.C. 1955. The supercooling, freezing and melting of giant waterdrops at terminal velocity in air. *Artificial Stimulation of Rain*. Pergamen Press. 233-245.
- Brimblecobe, P.; Tranter, M., Abrahams, P.W., Blackwood, I., Davies, T.D. and Vincent, C.E. 1985. Relocation and preferential elution of acidic solute through the snowpack of a small, remote, high-altitude Scottish catchment. *Annals of Glaciology*, 7: 141-147.
- Brimblecobe, P., Clegg, S.L., Davies, T.D., Shooter, D. and Tranter, M. 1987. Observation of the preferential loss of major ions from melting snow and laboratory ice. *Water Res.*, 21, No. 10: 1279-1286.
- Bryant, G.W., Hallett, J. and Mason, B.J. 1959. Epitaxial growth of ice on single crystalline substrates. *J. Phys. Chem. Solids*, 12: 189-195.
- Burton, J.A., Prim, P.C. and Slichter, W.P. 1953. Distribution of solute in crystals grown from the melt II. *Experimental. J. Chem. Phys.* 21: 1987-1991.
- Campbell, R.J. and Emmerman, D.K. 1972. Freezing and recycling of plating rinsewater. *Industrial Water Engineering*, June/July: 38-39.
- Chalmers, B. 1959. How water freezes. *Scientific American*, 200: 114-122.

- Chen, K.H. and Trezek, G.J. 1977. The effect of heat transfer coefficient, local wet bulb temperature and drop size distribution function on the thermal performance of sprays. *J. Heat Transfer*, 99: 381-385.
- Cissé, J. and Bolling, G.F. 1971. A study of the trapping and rejection of insoluble particles during the freezing of water. *J. Crystal Growth*, 10: 67-76.
- Cobb, A.W. and Gross, G.W. 1969. Interfacial electrical effects observed during the freezing of dilute electrolytes in water. *J. Electrochem. Soc.* 116: 796-804.
- Colbeck, S.C. 1981. A simulation of the enrichment of atmospheric pollutants in snow cover runoff. *Water Resource Res.*, 17: 1283-1388.
- Colbeck, S.C. and Anderson, E.A. 1982. The permeability of a melting snow cover. *Water Resour. Res.* 18: 904-908.
- Colbeck, S.C., 1987. Snow metamorphism and classification. In: *Seasonal Snowpack: Physics, Chemistry and Hydrology*, H.G. Jones and W.J. Orville-Thomas, Ed. Dordrecht: D. Reidel: 1-35.
- Corte, A.E. 1962. Vertical migration of particles in front of a moving freezing plane. *J. Geophysical Res.*, 67: 1085-1090.
- Cox, G.F.N. and Weeks, W.F. 1975. Brine drainage and initial slat entrapment in sodium chloride ice. USA Cold Regions Research and Engineering Laboratory. CRREL Reprot 354: 85.
- Cragin, J.H., Hewitt, A.D. and Colbeck, S.C. 1993. Elution of Ions from Melting Snow: Chromatographic Versus Metamorphic Mechanisms. US Army Corps of Engineers. Cold Region Research & Engineering Laboratory (CRREL) Report 93-8.
- Crooks, R. and Sikes, J. 1991. Environmental effects of bleached kraft mill effluents. *Appita J.*, 43: 67-76.
- Davies, T.D., Vincent, C.E. and Brimblecombe, P. 1982. Preferential elution of strong acids from a Norwegian ice cap. *Nature*, 300: 161-163.
- Davies, T.D., Brimblecombe, P., Tranter, M., Tsiouris, S., Vincent, C.E., Abrahams P.W. and Blackwood, I.L. 1986. The removal of soluble ions from melting snowpacks. In *Seasonal Snowcovers: Physics, Chemistry, Hydrology*. H.G. Jones and W.J. Orville-Thomas, Ed. Dordrecht: D.Reidel: 337-392.
- De Micheli, S.M. de and Iribarne, J.V. 1963. *J. Chim. Phys.* (France), 60: 767.

- De Pena, R.G., Iribarne, J.V. and De Achával, E.M. 1962. The freezing of supercooled droplets of electrolytic solutions. *J. Atmos. Sci.*, 19: 302-308.
- Dearborn Chemical Company Ltd. 1991. Plant wide Wastewater Treatment Development Study. Syncrude Canada Ltd., Final Report. Contract No.: C7224-26. DECG File No.: S10-641.
- Dickinson, D.R. and Marshall, W.R. 1968. The rates of evaporation of sprays. *AIChE J.* 14: 541-552.
- Dorsch, R.G. and Hacker, P.T. 1950. Photomicrographic investigation of spontaneous freezing temperatures of supercooled water drops. NACA Tech. Note 2142, Washington, D.C.
- Douglas, J. 1989. Freeze Concentration: An energy-efficient separation process. *EPRI Journal*, 14, No.1, Jan-Feb.: 16-21.
- Drost-Hansen, W. 1967. The water-ice interface as seen from the liquid side. *J. Colloid and Interface Science*, 25: 131-160.
- Dryden, H.L. and Schubauer, G.B. 1947. The use of damping screens for the reduction of wind-tunnel turbulence. *J. Aeronautical Sciences*, April, 1947: 221-228.
- Dye, J.E. and Hobbs, P.V. 1966. Effect of carbon dioxide on the shattering of freezing water drops. *Nature, Lond.*, 209: 464-466.
- Dye, J.E. and Hobbs, P.V. 1968. The influence of environmental parameters on the freezing and fragmentation of suspended water drops. *J. Atmos. Sci.*, 25: 82-96.
- Elmore, W.M. 1968. Water Purification by Natural Freezing. Master Thesis, University of Wyoming, Laramie, Wyoming.
- Evans, L.F. 1966. Ice nucleation by amino acids. *J. Atmos. Sci.*, 23: 751-752.
- Fletcher, A.H. 1958. Size effect in heterogeneous nucleation. *J. Chem. Phys.* 29: 572-576.
- Fletcher, A.H. 1970. The Chemical Physics of Ice. Cambridge University Press. p. 271.
- Fletcher, A.N. 1972. High-temperature contact nucleation of supercooled water by organic chemicals. *J. Appl. Met.*, 11: 988-993.
- Foster, P.M. 1978. The modeling of pollutant concentrations during snowmelt. CEGB Report RD/L/N 46/78 Job no. VC455.

- Frankel, J. 1946. *Kinetic Theory of Liquids*. Oxford University Press. p. 488.
- Freudenberg, K. 1955. Lignins. *Lignin Modern Methods of Plant Analysis* (Edited by K. Paech and M.V. Tracey, Springer, Berlin) III: 499-516.
- Fukuta, N. 1958. Experimental investigations on the ice-forming ability of various chemical substances. *J. Met.*, 15: 17-26.
- Fukuta, N. and Mason, B.J. 1963. Epitaxial growth of ice on organic crystals. *J. Phys. Chem. Solids*, 24: 715-718.
- Fukuta, N. 1965. Activated ice nucleation by sprayed organic solutions. *J. Atmos. Sci.* 22: 207-211.
- Fukuta, N. 1966. Experimental studies of organic ice nuclei. *J. Atmos. Sci.* 23: 191-196.
- Fukuta, N., 1975. A study of the mechanism of contact ice nucleation. *J. Atmos. Sci.* 32: 1597-1603.
- Gao, W.; Sego, D and Smith, D.W., 1996. Spray freezing to treat oil sands tailings pond water. In: *Proceedings of 8th International Cold Regions Engineering Conference*. Fairbanks, Alaska, August 12-17, 1996: 60-70.
- Gates, E.M. and Lozowski, E.P. 1985. An overview of marine icing research. *Proceedings Fourth International Symposium on Offshore Mechanics and Arctic Engineering*, Dallas, 10 pp.
- Gilpin, R.R. 1979. A model of the "liquid-like" layer between ice and a substrate with applications to wire regelation and particle migration. *J. Colloid and Interface Science*. 68: 235-253.
- Gilpin, R.R. 1979. Theoretical studies of particle engulfment. *J. Colloid and Interface Science*, 74: 44-63
- Glen, J.W. 1974. The physics of ice. USA Cold Regions Research and Engineering Laboratory, Cold Regions Science and Engineering Monograph IIC2A. ADA 778 009.
- Glen, J.W., Homer, D.R. and Paren, J.G. 1977. Water at grain boundaries: Its role in the purification of temperature glacier ice. *IAHS-AISH, Publ.* 118, 263-271.
- Gokhale, N.R. 1965. Dependence of freezing temperature of supercooled water drops on rate of cooling. *J. Atmos. Sci.*, 22: 212-216.
- Götz, G., Mészáros, E. and Vali, G. 1991. *Atmospheric Particles and Nuclei*. Akadémiai Kiadó, Budapest, Hungary, p. 131-192.

- Gross, G.W. 1965. The Workman-Reynolds effects and ionic transfer processes at the ice-solution interface. *J. Geophysical Res.*, 70, No. 10: 2291.
- Gross, G.W. 1967. Ion distribution and phase boundary potentials during the freezing of very dilute ionic solutions at uniform rates. *J. Colloid Interf. Sci.*, 25: 270-279.
- Gross, G.W. 1968. Some effects of trace inorganics on the ice/water system. In: Trace Inorganics in Water, American Chemical Society, Washington, D.C., 27-93.
- Gross, G.W. 1971. Freezing potentials in the system $H_2O-NH_3-CO_2$ at controlled concentrations. *J. Atmospheric Sci.* 28: 1005-1014.
- Gross, G.W., Wu, C., Bryant, L. and McKee, C. 1975. Concentration dependent solute redistribution at the ice/water phase boundary. II. Experimental investigation. *J. Chem. Phys.*, 62, No. 8: 3085-3092.
- Grulich, G., 1969. Improved Methods of Spent Sulfite Liquor Disposal. Ph.D. Thesis. Dartmouth College.
- Hagen, A. and Langeland, A. 1973. Polluted snow in southern Norway and the effect of the meltwater on freshwater and aquatic organisms. *Environmental Pollution*. 5: 45-57.
- Halde, R. 1980. Concentration of impurities by progressive freezing. *Water Research* 14: 576-580.
- Hammond, E.G., Kuczala, P., Junk, G.A. and Kozel, J. 1974. Constituents of swine house odours. In: Livestock Environment, ASAE Proceedings, St. Joseph, MI. p. 364-372.
- Hartung, L.D., Hammong, E.G. and Miner, J.R. 1970. Identification of carbonyl compounds in a swine-building atmosphere. Proceedings of the International Symposium on Livestock Wastes, ASAE, St. Joseph, MI. p. 105-106.
- Head, R.B. 1961. Steroids as ice nucleators. *Nature, Lond.* 191: 1058-1059.
- Heverly, J.R., 1949. Supercooling and crystallization. *Trans. Am. Geophys. Un.*, 30: 205.
- Hewitt, A.D., Cragin, J.H. and Colbeck, S.C. 1989. Does snow have ion chromatographic properties? In Proceedings of the Forty-Sixth Annual Eastern Snow Conference, Quebec City, Quebec, pp. 165-171.
- Hobbs, P.V. 1974. Ice Physics. Clarendon Press, Oxford.

- Hoffer, T.E. 1961. A laboratory investigation of droplet freezing. *J. Met.*, 18: 766-778.
- Hughes, P.R. and Gilliland, E.R. 1952. The mechanics of drops. *Chemical Eng. Progress*, 48, No. 10: 497-504.
- Instanes, Arne, 1993. An Experimental Study of the Mechanical Behavior of Spray Ice. Doctoral Dissertation, University of Alberta, Edmonton, Alberta, Canada.
- Iribarne, J.V. and Pyshnov, T. 1990. The effect of freezing on the composition of supercooled droplets — I. Retention of HCl, HNO₃, NH₃ and H₂O₂. *Atmospheric Environment*, 24A, No. 2: 383-387.
- Jaccard, C. and Levi, L. 1961. Ségrégation d'impuretés dans la glace. *Z. Angew. Math. Phys.*, 12: 70-76.
- Johannes, A.H., Galloway, J.N. and Troutman, D.E. 1981. Snowpack storage and ion release. In: Integrated Lake-Watershed Study, EPRI Report, EA-125, 6-1.
- Johannessen, M., Dale, T., Gjessing, E.T., Henriksen, A. and Wright, R.F. 1975. Acid precipitation in Norway: The regional distribution of contaminants in snow and chemical processes during snowmelt. In proceedings of Isotopes and Impurities in Snow and Ice. Grenoble. International Association of Sci. Hydrology Publication, 118:116-120.
- Johannessen, M. and Henriksen, A. 1978. Chemistry of snow meltwater: Changes in concentration during melting. *Water Resources Research*, 14: 615-619.
- Johnson, D. and Hallett, J. 1968. Freezing and shattering of supercooled water drops. *Quart. J. R. Met. Soc.*, 94: 468-482.
- Jones, H.G. and Deblois, C. 1987. Chemical dynamics of N-containing ionic species in a boreal forest snowcover during the spring melt period. *Hydrological Processes*, 1: 271-282.
- Jones, H.G. 1991. Snow chemistry and biological activity: A particular perspective on nutrient cycling. In: *Seasonal Snowpacks: Processes of Compositional Change*. T.D. Davies, M. Tranter and H.G. Jones, Ed. Berlin, Germany: Springer-Verlag, p. 173-228.
- Kamra, A.K. and Ahire, D.V. 1985. A simple technique for simultaneous suspension of multiple drops in a small vertical wind tunnel. *J. Atmospheric and Oceanic Technology*, 2, Sept. 1985: 408-411.
- Kenny, R., Gorgal, R.G., Marlineau, D. and Prahacs, S. 1991. Freeze crystallization of TEMCELL's BOTMP effluent. In: 1991 Environment Conference Publication by Canadian Pulp & Paper Association, Montreal, Quebec, 141-145.

Knollenberg, R.G. 1966. Urea as an ice nucleant for supercooled clouds. *J. Atmos. Sci.*, 23: 197-201.

Knollenberg, R.G. 1969a. A laboratory study of the local cooling resulting from the dissolution of soluble ice nuclei having endothermic heats of solution. *J. Atmos. Sci.* 26: 115-124.

Knollenberg, R.G. 1969b. The local cooling ice nucleation model. *J. Atmos. Sci.* 26: 125-129.

Komabayashi, M. and Ikebe, Y. 1961. Organic ice nuclei: ice-forming properties of some aromatic compounds. *J. Met. Soc. Japan*, 39: 82-94.

Komabayasi, M., Gonda, T. and Isono, K. 1964. Lifetime of water drops before breaking and the size distribution of fragment droplets. *J. Meteor. Soc. Japan*, 42: 330-340.

Krepchin, I.P. 1985. Fresh water from the sea. *High Techno.*, Sept.1985: 64-65.

Kringstad, K.P. and Lindström, K. 1982. Spent liquors from pulp bleaching. In: Proceedings of 1982 TAPPI Research and Development Conference, Atlanta. TAPPI Press, pp. 191-200.

Kringstad, K.P. and Lindström, K. 1984. Spent liquors from pulp bleaching. *Environ. Sci. Technol.*, 18: 236a-248A.

Kuhns, L.E. and Mason, B.J. 1968. The supercooling and freezing of small water droplets falling in air and other gases. *Proc. Roy. Soc. A*, 302: 437-452.

Kuo, V.H.S. and Wilcox, W.R. 1973. Removal of particles by solidification. *Industrial Eng. Chem. Process Des. Development*, 12, No. 3: 376-379.

Langer, G., Rosinski, J. and Bernsen, S. 1963. Organic crystals as icing nuclei. *J. Atmos. Sci.* 20: 557-562.

Lafarque, C. 1958. Sur rôle joué par les ions dans le phénomène de la surfusion de l'eau. *Compt. Rend.*, 246: 1894-1896.

Lane, W.R. 1951. Shatter of drops. *Industrial and Engineering Chemistry*, 43, No. 6: 1312-1316.

Langer, G., Rosinski, J. and Edwards, C.P. 1963. Organic crystals as icing nuclei. *J. Atmos. Sci.*, 20: 557-562.

Langham, E.J. and Mason, B.J. 1958. The heterogeneous and homogeneous nucleation of supercooled water. *Proc. R. Soc. A*, 247: 493-504.

- Laws, J.Q. and Parson, D.A. 1943. The relation of raindrop size to intensity. *Trans. Of American Geopgysical Union*, 24: 452-460.
- Leach, J.M. and Thakore, A.N. 1975. Isolation and identification of constituents toxic to juvenile rainbow trout (*Salmo gairdneri*) in caustic extraction effluents from kraft pulp mill bleach plants. *J. Fish Res. Board Can.*, 32: 1249-1257.
- Leivestad, H. and Muniz, I.P. 1976. Fish kill at low pH in a Norwegian river. *Nature*. 259 (5542): 391-392.
- Lenard, P., 1904. Uber regen. *Met. Z.*, 21: 248-262.
- Levine, J. 1950. Statistical explanation of spontaneous freezing of water droplets. Natl. Advisory Committee for Aeronautics, NACA Technical Note 2234, pp. 27.
- Levin, Z. and Yankofsky, S.A. 1988. Ice nuclei of biological origin. Atmospheric Aerosols and Nucleation, P.E. Wagner and G.Vali (Editors), Proceedings of the Twelfth International Conference on Atmospheric Aerosols and Nucleation, Held at the University of Vienna, Austria, August 22-27, 1988, pp.620-633.
- Lindenmeyer, C.S. 1959. The solidification of supercooled aqueous solutions. Ph.D. Thesis, Harvard University, pp.117.
- List, R., 1959. Wachstum von Eis - Wassergemischen im Hagelversuchskanal. *Helv. Phys. Acta*, 32: 293.
- Loeb, L.B., 1958. Static Electrification. Springer, Berlin, pp. 240.
- Makkonen, L. 1986. Salt Entrapment in spray ice. Proceedings of IAHR Ice Symposium 1986, Iowa City, Iowa, II: 165-178.
- Malo, B.A. and Baker, R.A. 1968. Cationic concentration by freezing. In: Trace Inorganics in Water, American Chemical Society, Washington, D.C., pp.149-163.
- Marsh, A.R.W. and Webb, A.H. 1979. Physico-chemical aspects of snowmelt. D.M. Gray and D.H. Male, eds. Pergamon Press.
- Martel, C.J. and Diener, C.J. 1991. A pilot-scale study of alum sludge dewatering in a freezing bed. *Journal of the American Water Works Association*, 28, No. 12: 51-55.
- Mason, B.J. 1953. Progress in cloud physics research. A progress report on recent investigation at Imperial College, London. *Archiv für Met. Geopgys. u. Bioklima*, A. 6, 1-52.

Mason, B.J. 1956. The nucleation of supercooled water clouds. *Sci. Prog. Lond.* No.175, pp.479.

Mason, B.J. 1974. *The Physics of Clouds*, 2nd Edition, Clarendon Press, Oxford.

Mason, B.J. and Van Den Heuvel, A.P. 1959. The properties and behavior of some artificial ice nuclei. *Proc. Phys. Soc.*, 74: 744.

Mason, B.J. and Maybank, J. 1958. Ice nucleating properties of some natural mineral dusts. *Quart. J. R. Met. Soc.*, 84: 235-241.

Mason, B.J. and Maybank, J. 1960. The fragmentation and electrification of freezing water drops. *J. Atmos. Sci.*, 86: 176-186.

Matsubara, K. 1973. Ice-forming properties of oxides of some rare earth elements. *J. Met. Soc. Japan*, 51, No.1: 54-60.

McDonald, J.E. 1954. The shape and aerodynamics of large rain drops. *J. Metro.*, 11: 478-494.

McKague, A.B. 1988. Characterization and identification of organic chlorine compounds in bleach plant effluents. In: Proc. Colloquim on Measurement of Organic chlorines, Pulp Pap. Res. Center, University of Toronto, Toronto. ON.

Merkel, J.A., Hazen, T.E. and Miner, J.R. 1969. Identification of gases in a confinement swine building atmosphere. *Trans. Of ASAE*, 12, No. 3: 310-315.

Miner, J.R. 1982. Controlling odors from livestock production facilities. Research Results in Manure Digestion, Runoff, Refeeding, Odor. North Central Regional Research Publication No. 284. Midwest Plan Service, Iowa State University, Ames. IA. pp. 30-35.

Montgomery, D.N. and Dawson, G.A. 1969. Collisional charging of water drops. *J. Geophys. Res.* 74: 962-972.

Müller, M. and Sekoulov, I. 1992. Wastewater reuse by freeze concentration with a falling film reactor. *Water. Sci. Tech.* Vol. 26, No7-8: 1475-1482.

National Research Council of Canada, 1981. Acidification in the Canadian aquatic environment: scientific criteria for assessing the effects of acidic deposition on aquatic ecosystems, Ottawa, National Research Council of Canada (Publication 18475 196).

Nebbia, G. and Menozzi, G.N. 1968. Early experiments on water desalination by freezing. *Desalination*, 5: 49.

Parungo, F.P. and Lodge, Jr., J.P. 1965. Molecular structure and ice nucleation of some organics. *J. Atmos. Sci.*, 22: 309-313.

Parungo, F.P. and Lodge, Jr., J.P. 1967a. Freezing of aqueous solutions of non-polar gases. *J. Atmos. Sci.*, 24: 439-441.

Parungo, F.P. and Lodge, Jr., J.P. 1967b. Amino acids as ice nucleators. *J. Atmos. Sci.* 24: 274-277.

Pena, J. and De Pena, R.G. 1970. Freezing temperatures of water droplets in equilibrium with different gases. *J. Geophys. Res.*, 75, No. 15: 2831-2835.

Pfann, W.G. 1966. Zone Melting. John Wiley, New York, pp. 310.

Pitter, R.L. and Pruppacher, H.R. 1973. A wing tunnel investigation of freezing of small water drops falling at terminal velocity in air. *Quart. J. R. Met. Soc.*, 99: 540-550.

Power, B.A. and Power, R.F. 1962. Some amino acids as ice nucleators. *Nature, Lond.* 194: 1170-1171.

Prandtl, L. 1933. Attaining a Steady Air Stream in Wind Tunnels. N.A.C.A. T.M. No. 726, October, 1933.

Priem, R. and Maton, A. 1980. The influence of the content of trace elements in the feed on the composition of liquid manure of pigs. In: Effluents from Livestock. Edited by Grasser, J.K.R. and assisted by J.C. Hawkin, J.R. O'Callaghan and B.F. Pain, Applied Science Publisher Ltd. London. pp. 712.

Pruppacher, H.R. and Neiburger, M. 1963. The effect of water soluble substances on the supercooling of water drops. *J. Atmos. Sci.*, 20: 376-385.

Prupacher, H.R. 1967a. Some relations between the structure of the ice-solution-solution interface and the free growth rate of ice crystals in supercooled aqueous solutions. *J. colloid Interf. Sci.*, 25: 285-294.

Prupacher, H.R. 1967b. On the growth of ice crystals in supercooled water and aqueous solution drops. *Pure and Appl. Geophys.*, 68: 186-195.

Pruppacher, H.R. and Schlamp, R.J. 1975. A wing tunnel investigation on ice multiplication by freezing of waterdrops falling at terminal velocity in air. *J. Geophys. Res.*, 80, No. 3: 380-386.

Rabinowitz, B., Vassos, T.D. and Hyslop, W.F. 1988. The use of snowmaking for wastewater treatment and disposal. In: Proceedings of Environment Canada et.al. Wastewater Treatment 11th International Symposium, Montreal, 1988: 1-13.

- Ramchandra Murty, A.S. and Ramana Murty, Bh.V. 1972. Freezing characteristics of rain water drops with different solutes and their implication on anomalous ice. *Tellus*. 24. No. 2: 150-160.
- Ramchandra Murty, A.S. and Ramana Murty, Bh.V. 1972a. A new effect of evaporation accelerating the ice phase in supercooled water. *J. Atmos. Sci.*, 29: 781-784
- Ramchandra Murty, A.S. and Ramana Murty, Bh.V. 1972b. Conditions governing drop freezing at warm temperatures. *J. Atmos. Sci.*, 29: 1322-1328.
- Ranz, W.E. and Marshall, W.R. 1952. Evaporation from Drops. *Chem. Eng. Prog.*, 48: 141-180.
- Reischel, M.T. and Vali, G. 1974. Freezing nucleation in aqueous electrolytes. *Tellus*. 27, No. 4: 414-427.
- Reischel, M.T. 1984. Freezing -nucleation in aqueous solutions of clathrate forming gases. *Tellus*, 36B: 73-84.
- Richards, C.N. and Dawson, G.A. 1971. The hydrodynamic in stability of water drops falling at terminal velocity in vertical electric fields. *J. Geophys. Res.*, 76: 3445-3455.
- Roberts, P. and Hallett, J. 1968. A laboratory study of the ice nucleating properties of some mineral particulates. *Quart. J. R. Met. Soc.*, 94: 25-34.
- Römkens, M.J.M. and Miller, R.D. 1973. Migration of mineral particles in ice with a temperature gradient. *J. Colloid and Interface Science*, 42, No. 1: 103-111.
- Rosinski, J. and Nagamoto, C.T. 1972. Ice nucleation as a function of hydrogen ion concentration. *J. Rech. Atmos*, 6, No. 1/3: 469-478.
- Rosinski, J., Langer, G., Nagamoto, C.T., Bayaard, M.C. and Parungo, F.P. 1976. Chemical composition of surfaces of natural ice-forming nuclei. *J. Rech. Atmos*. 10. No. 4: 201-210.
- Schmid, L.A. and Lipper, R.I. 1969. Swine waste, characterization and anaerobic digestion. In: Animal Waste Management. Cornell University Conference on Agricultural Waste Management. Jan. 13-15, 1969, Syracuse, NY.
- Schnell, R.C. and Vali, G. 1976. Biogenic ice nuclei. Part 1: Terrestrial and marine sources. *J. Atmos. Sci.*, 33: 1554-1564.

- Seip, H.M., Abrahamsen, G., Christophersen, N., Gjessing, E.T. and Stuanes, A.O. 1980. Snow and Meltwater Chemistry in Minicatchments. SNSF-project IR 53/80. Norwegian Forest Research Institute, Aas, Norway, 51pp.
- Serpolay, R. 1958. L'activité glaciogène des aérosols d'oxydes métalliques. *Bull.Obs. Puy de Dôme*, pp. 81.
- Serpolay, R. 1959. L'activité glaciogène des aérosols d'oxydes métalliques. II les oxydes catalyseurs. *Bull.Obs. Puy de Dôme*, pp. 81
- Soulage, G. 1958. Contribution des fumées industrielles à l'enrichissement de l'atmosphère en noyaux glaciogènes. *Bull. Obs. Puy de Dôme*, No.4:121.
- Spengler, J.D. and Gokhale, N.R. 1972. Freezing of freely suspended, supercooled water drops in a large vertical wind tunnel. *J. Appl. Met.*, 11: 1101-1107.
- Spengler, J.D. 1971. Experimental Studies of Hydrometer Interation Using a Large Vertical Wind Tunnel. Ph.D. Thesis, State University of New York at Albany.
- Springer, A.M. 1986. Industrial Environmental Control: Pulp and Paper Industry. John Wiley & Sons. 430 pp.
- Spyker, J.W. 1982. Desalination of Brackish Water by Spray Freezing. Saskatchewan Research Council (SRC), Technical Report No. 140, SPC Publication No. E-835-3-B-82.
- Steinemann, S. 1958. Experimentelle Untersuchungen zur Plastizität von Eis. *Beit Geologie der Schweiz. Geotechnische Serie. Hydrologie*, Nr. 10, 72 pp.
- Stoyanova, V., Kashchiev, D. and Kупenova, T. 1994. Freezing of water droplets seeded with atmospheric aerosols and ice nucleation activity of the aerosols. *J. Aerosol. Sci.* 25. No. 5: 867-877.
- Suntio, L.R., Shiu, W.Y. and Mackay, D. 1988. A review of the nature and properties of chemicals present in pulp mill effluents. *Chemosphere*, 17, No.7: 1249-1290.
- Suzuki, K. 1991. Diurnal variation of the chemical characteristics of meltwater. *Seppyo*, 53: 21-31.
- Szilder, K., Forest, T.W. and Lozowski, E.P. 1991. A comparison between different construction methods of ice islands. 1991 OMAE, IV, Arctic/Polar Technology: 9-15.
- Tammann, G. and Büchner, A. 1935. Die lineare kristallisationsgeschwindigkeit des Eises aus gewöhnlichem und schwerem Wasser. *Z. anorg. allg. Chem.*, 222: 12-16.

Taylor, G.I. 1935. Turbulence in a contracting stream. *Zeit. Fur angew. Math. U. Mech.*, 15: 91-96.

Telford, J. 1960. Freezing nuclei from industrial processes. *J. Met.*, 17: 676.

Terwilliger, J.P. and Dizio, S.F. 1970. Salt rejection phenomena in the freezing of saline solutions. *Chem. Eng. Science*, 25: 1331-1349.

Tranter, M., Brimblecombe, P., Davies, T.D., Vincent, C.E., Abrahams, P.W. and Blackwood, I. 1986. The composition of snowfall, snowpacks and meltwater in the Scottish highlands: Evidence for preferential elution. *Atmospheric Environment*. 20: 517-525.

Tranter, M., Tsiouris, S., Davies, D.T. and Jones, H.G. 1992. A laboratory investigation of the leaching of solute from snowpack by rainfall. *Hydrological Processes*, 6: 169-178.

Tsiouris, S., Vincent, C.E., Davies, T.D. and Brimblecombe, P. 1985. The elution of ions through field and laboratory snowpacks. *Annals of Glaciology*, 7: 196-201.

Uhmman, D.R., Chalmers, B. and Jackson, K.A. 1964. Interaction between particles and a solid-liquid interface. *J. Applied Physics*, 35, No. 10: 2986-2993.

U.S. EPA 1982. Development Document for Effluent Limitations Guidelines and New Source Performance Standards for the Pulp, Paper, and Paperboard – Point Source Category, EPA 440/1-82/025, October, 1982.

Vali, G. and Stansbury, E.J. 1966. Time-dependent characteristics of the heterogeneous nucleation of ice. *Can. J. Phys.*, 44: 477-502.

Vali, G. 1971. Quantitative evaluation of experimental results on the heterogeneous freezing nucleation of supercooled liquids. *J. Atmo. Sci.*, 28: 402-409.

Vonnegut, B. 1947. The nucleation of ice formation by silver iodide. *J. Appl. Phys.*, 18: 593-595.

Waller, R. 1966. A Study of Aggregate Ice Formation as a Method of Concentrating Impurities in Aqueous Solution. Doctoral Dissertation, The Johns Hopkins University. University Microfilms No.66-12532.

Weeks, W.F. and Ackley, S.F. 1982. The growth, structure and properties of sea ice. USA Cold Regions Research and Engineering Laboratory, CRREL Monograph 82-1. pp. 136.

Weeks, W.F. and Lofgren, G. 1967. The effective solute distribution coefficient during the freezing of NaCl solution. In: *Physics of Snow and Ice*. Institute of Low Temperature Science, 1: 579-597.

Wood, G.R. and Walton, A.G. 1969. Kinetics of ice nucleation from water and electrolyte solutions. Office of Saline Water Research and Development Progress Report No. 500, 171 pp.

Workman, E.J. and Reynolds, S.E. 1950. Electrical phenomena occurring during the freezing of dilute aqueous and their possible relationship to thunderstorm electricity. *Phys. Rev.*, 78: 254-259.

Yao, S.C. and Schrock, V.E. 1975. Heat and mass transfer from freely falling drops. *J. Heat Transfer, ASME*, 98, No. 1: 120-125.

Yasuhara, A. and Fuwa, K. 1979. Odour and volatile compounds in liquid swine manure: Volatile and odourous components in anaerobically or aerobically digested liquid swine manure. *Bulletin of the Chemical Society of Japan*, 52, No.1: 114-117.

Zapf-Gilje, R. 1985. Treatment and Disposal of Secondary Sewage Effluent through Snowmaking. Doctoral Dissertation. University of British Columbia, Vancouver, BC.

Zarling, J.P. 1980. Heat and Mass Transfer from Freely Falling Drops at Low Temperatures. CRREL Report 80-18, ADA090522.

APPENDIX - A CHAMICAL ANALYSIS DATA

TAP WATER

I. Source Water

A. Measurements of source water which was used to produce spray ice at - 10 °C

Sample	TOC (mg/L)	COD (mg/L)	Color (TCU)	Cl ⁻¹ (mg/L)	SO ₄ ²⁻ (mg/L)	Conductivity (μs/cm)	pH
1	2	2	0	3	54	232	7.21
2	2	2	2	4	53	232	7.21
3	1	15	0	3	54	248	7.26

B. Measurements of source tap water which was used to produce spray ice at - 24 °C

Sample	TOC (mg/L)	COD (mg/L)	Color (TCU)	Cl ⁻¹ (mg/L)	SO ₄ ²⁻ (mg/L)	Conductivity (μs/cm)	pH
1	1	7	7	3	59	301	7.93
2	2	7	9	3	60	319	7.91
3	2	9	11	3	59	271	7.94

II. Runoff Which Was Obtained During Spraying Operation at - 10 °C

Sample	TOC (mg/L)	COD (mg/L)	Color (TCU)	Cl ⁻¹ (mg/L)	SO ₄ ²⁻ (mg/L)	Conductivity (μs/cm)	pH
1	4	10	2	5	72	251	7.33
2	4	18	4	4	72	258	7.35
3	3	16	4	6	74	278	7.33

III. Meltwater of Spray Ice Formed at - 10 °C and Stored for 20 Days (two ice columns)

meltwater of ice column 1:

Sample	TOC (mg/L)	COD (mg/L)	Color (TCU)	Cl ⁻¹ (mg/L)	SO ₄ ²⁻ (mg/L)	Conductivity (μs/cm)	pH
1	25	68	17	32	471	1210	8.41
2	3	10	4	0	48	170	9.05
3	3	22	2	1	27	118	8.90
4	3	10	2	2	36	145	8.97
5	4	22	4	3	50	182	8.94
6	6	22	4	6	73	242	9.01
7	6	24	2	7	92	280	8.98
8	4	1	4	0	35	146	8.60
9	1	8	1	0	12	84	8.46
10	1	0	0	0	7	64	8.48
11	2	7	0	2	11	74	8.32
12	1	8	0	0	8	52	8.03
13	1	9	0	0	3	28	8.60
14	1	4	0	0	1	20	8.57

meltwater of column 2:

Sample	TOC (mg/L)	COD (mg/L)	Color (TCU)	Conductivity (μ S/cm)	pH
1	16	40	2	825	8.68
2	8	24	1	373	8.85
3	3	16	8	140	8.96
4	4	16	0	199	8.83
5	3	7	0	139	9.02
6	3	16	1	170	9.00
7	5	14	2	216	9.12
8	7	11	0	285	9.10
9	5	8	0	248	8.97
10	3	7	0	144	8.55
11	1	11	0	79	8.52
12	1	7	0	55	8.26
13	2	6	0	35	8.44
14	1	13	0	31	8.88

IV. Meltwater of Spray Ice Formed at - 10 °C and Stored for 40 Days (two ice columns)

meltwater of ice column 1:

Sample	TOC (mg/L)	COD (mg/L)	Color (TCU)	Cl ⁻¹ (mg/L)	Conductivity (μs/cm)	pH
1	14	54	14	10	617	8.50
2	4	20	3	18	222	8.90
3	4	14	1	0	214	8.88
4	4	11	3	0	215	8.87
5	4	8	0	0	222	8.83
6	4	26	1	0	226	8.89
7	4	38	0	0	241	8.89
8	3	19	0	0	195	8.60
9	1	24	0	0	117	8.18
10	1	9	0	0	89	8.00
11	1	5	1	0	67	7.75
12	1	5	0	0	68	7.79
13	2	7	5	0	76	8.48
14	0	11	1	0	26	8.70
15	1	18	3	5	29	9.09

meltwater of ice column 2:

Sample	TOC (mg/L)	COD (mg/L)	Color (TCU)	Cl ⁻¹ (mg/L)	SO ₄ ²⁻ (mg/L)	Conductivity (μs/cm)	pH
1	21	113	10	27	359	1100	8.58
2	5	33	3	5	72	233	9.01
3	4	53	1	5	70	226	9.02
4	4	34	0	5	63	206	8.94
5	4	32	1	4	60	201	8.90
6	5	7	0	5	59	201	8.88
7	3	3	0	4	57	203	8.85
8	4	7	1	5	53	199	8.86
9	3	6	1	4	54	200	8.87
10	2	18	3	4	51	200	8.76
11	2	10	3	3	34	157	8.51
12	2	10	1	2	12	93	7.93
13	1	5	1	0	7	64	7.88
14	0	6	1	0	7	59	8.08
15	1	4	0	0	6	48	8.50

V. Meltwater of Spray Ice Formed at - 24 °C and Stored for 20 Days (two ice columns)

meltwater of ice column 1

Sample	TOC (mg/L)	COD (mg/L)	Color (TCU)	Cl ⁻¹ (mg/L)	SO ₄ ²⁻ (mg/L)	Conductivity (μs/cm)	pH
1	8	28	8	18	145	948	8.59
2	2	4	6	3	123	215	8.73
3	2	9	6	3	93	205	8.71
4	3	6	8	2	80	217	8.74
5	1	1	5	3	73	167	8.73
6	2	2	8	2	71	180	8.96
7	1	9	6	3	70	155	8.57
8	1	6	6	0	56	77	7.49
9	0	18	6	0	53	49	7.43
10	0	0	5	0	36	34	7.65
11	0	1	5	0	34	29	7.33
12	1	6	6	0	23	51	7.19
13	2	2	6	0	17	79	8.54
14	1	9	6	0	8	33	9.03

meltwater of ice column 2

Sample	TOC (mg/L)	COD (mg/L)	Color (TCU)	Cl ⁻ (mg/L)	Conductivity (μs/cm)	pH
1	7	18	10	3	500	9.14
2	8	16	8	6	339	9.16
3	4	14	8	5	289	9.03
4	3	10	5	3	261	8.92
5	3	9	8	3	248	8.73
6	2	2	5	4	244	8.57
7	3	6	6	6	247	8.43
8	1	6	6	3	209	8.34
9	2	8	6	3	201	8.19
10	1	11	6	0	160	8.11
11	1	4	8	0	150	8.20
12	1	6	6	0	115	8.20
13	0	0	6	0	93	8.32
14	2	10	6	0	74	9.16

VI. Meltwater of Spray Ice Formed at - 24 °C and Stored for 40 Days (two ice columns)

meltwater of ice column 1:

Sample	TOC (mg/L)	COD (mg/L)	Color (TCU)	Cl ⁻ (mg/L)	Conductivity (μs/cm)	pH
1	6	19	0	9	668	8.50
2	4	10	0	6	509	8.96
3	4	10	0	5	305	8.69
4	3	7	0	4	274	8.42
5	2	1	0	4	250	8.21
6	2	4	1	3	230	8.12
7	2	1	0	0	206	7.96
8	2	3	0	2	198	7.88
9	3	1	3	2	197	7.83
10	2	10	1.1	0	181	7.83
11	3	10	0	0	149	7.77
12	2	6	0	0	113	7.72
13	2	7	3	0	83	7.68
14	1	10	1.1	0	51	7.65

meltwater of ice column 2:

Sample	TOC (mg/L)	COD (mg/L)	Color (TCU)	Cl ⁻¹ (mg/L)	SO ₄ ²⁻ (mg/L)	Conductivity (μs/cm)	pH
1	5	19	0	6	131	333	9.08
2	4	17	0	6	128	332	8.93
3	3	12	0	5	112	323	8.79
4	4	12	0	5	101	310	8.75
5	3	4	0	4	87	283	8.62
6	2	4	0	4	75	259	8.47
7	2	11	0	3	59	228	8.34
8	2	7	0	3	51	206	8.27
9	2	2	0	3	44	185	8.14
10	2	0	0	0	37	170	7.92
11	1	0	0	0	29	140	7.84
12	1	2	0	0	27	133	7.90
13	3	5	0	0	16	104	8.62
14	2	8	0	0	4	62	8.54

PULP MILL EFFLUENT

I. Source Water

A. Measurements of source water used to produce spray ice at - 10 °C

Sample	TOC (mg/L)	COD (mg/L)	Color (TCU)	Conductivity (μ s/cm)	pH
1	261	520	1333	2800	7.20
2	254	597	1305	2760	7.25
3	258	520	1305	2770	7.25

B. Measurements of source water used to produce spray ice at - 24 °C

Sample	TOC (mg/L)	COD (mg/L)	Color (TCU)	Conductivity (μ s/cm)	pH
1	231	641	1348	2500	7.57
2	224	677	1401	2560	7.53
3	274	682	1401	2450	7.63

II. Runoff Which Was Obtained During Spraying Operation at - 10 °C

Sample	TOC (mg/L)	COD (mg/L)	Color (TCU)	Conductivity (μ s/cm)	pH
1	413	791	2012	4150	7.73
2	442	857	2058	4150	7.73
3	385	736	1856	3780	7.77
4	355	802	1856	3740	7.33

III. Ice Core Samples of the Spray Ice

A. Ice core sample formed at - 10 °C and stored for 20 days

Sample	TOC (mg/L)	COD (mg/L)	Color (TCU)	Conductivity (μ s/cm)	pH
1	74	184	271	570	9.46
2	94	294	429	616	9.71
3	228	510	1033	2265	9.37

B. Ice core sample formed at - 10 °C and stored for 40 days

Sample	TOC (mg/L)	COD (mg/L)	Color (TCU)	Conductivity (μ s/cm)	pH
1	28	235	345	639	9.90
2	79	212	338	611	9.87
3	185	483	494	1675	9.45

C. Ice core sample formed at - 24 °C and stored for 20 days

Sample	TOC (mg/L)	COD (mg/L)	Color (TCU)	Conductivity (μ s/cm)	pH
1	292	686	1355	2073	10.00
2	268	682	1361	2063	10.04
3	257	685	1375	2090	10.03

D. Ice core sample formed at - 24 °C and stored for 40 days

Sample	TOC (mg/L)	COD (mg/L)	Color (TCU)	Conductivity (μ s/cm)	pH
1	253	633	1298	2153	10.09
2	227	584	1195	2005	10.15
3	268	740	1517	2425	10.17

IV. Meltwater of Spray Ice Formed at - 10 °C and Stored for 20 Days (two ice columns)

meltwater of ice column 1:

Sample	TOC (mg/L)	COD (mg/L)	Color (TCU)	Conductivity (μ S/cm)	pH
1	1837	3522	7658	13520	8.85
2	409	859	1747	3120	9.30
3	602	1228	2659	4600	8.60
4	148	655	584	1044	9.34
5	174	827	848	1452	9.43
6	145	752	705	1204	9.44
7	94	613	450	806	9.27
8	125	289	585	1032	9.24
9	159	356	764	1292	9.37
10	188	428	886	1640	9.42
11	205	484	1017	1820	9.47
12	141	359	761	1364	9.43
13	63	148	304	550	9.20
14	69	177	359	668	9.21
15	122	305	652	1088	9.21
16	77	224	476	854	9.28
17	58	167	330	574	9.42
18	53	195	319	578	9.53
19	50	198	333	596	9.63

meltwater of ice column 2:

Sample	TOC (mg/L)	COD (mg/L)	Color (TCU)	Conductivity (μ s/cm)	pH
1	728	1699	3948	7000	9.01
2	177	385	852	1392	9.32
3	134	256	545	900	9.42
4	143	294	584	940	9.35
5	182	320	742	1204	9.34
6	189	357	790	1274	9.24
7	177	320	695	1188	9.23
8	194	363	771	1270	9.34
9	304	533	1243	1034	9.33
10	101	276	567	984	9.04
11	22	62	101	196	9.29
12	53	139	276	450	9.25
13	53	123	271	440	9.10
14	73	173	373	538	9.22
15	71	177	392	586	9.17
16	120	305	666	1090	8.91
17	49	128	275	432	9.29
18	30	105	163	256	9.60

V. Meltwater of Spray Ice Formed at - 10 °C and Stored for 40 Days (two ice columns)

meltwater of ice column 1:

Sample	TOC (mg/L)	COD (mg/L)	Color (TCU)	Conductivity (µs/cm)	pH
1	867	2537	4089	7980	9.21
2	308	1025	1481	2370	9.01
3	132	426	637	1140	9.32
4	122	428	607	1090	9.27
5	179	504	856	1490	9.44
6	131	382	624	1130	9.45
7	107	368	530	992	8.92
8	36	154	184	330	8.42
9	44	198	250	481	9.00
10	46	87	221	453	8.84
11	43	80	214	445	8.58
12	71	143	344	682	8.59
13	90	196	463	875	8.76
14	69	139	342	666	8.62
15	62	108	272	544	9.07
16	21	44	127	235	9.15
17	10	14	63	143	9.28

meltwater of ice column 2:

Sample	TOC (mg/L)	COD (mg/L)	Color (TCU)	Conductivity (μ S/cm)	pH
1	596	1513	3279	5400	9.45
2	231	613	1157	1980	9.38
3	91	227	435	811	9.21
4	93	254	481	907	9.27
5	92	235	488	916	9.29
6	97	255	522	936	9.30
7	119	283	590	1050	9.22
8	90	213	443	833	9.02
9	74	111	367	687	8.84
10	44	89	214	464	8.68
11	47	109	206	433	8.68
12	107	247	491	973	8.61
13	90	192	389	773	8.61
14	64	142	286	583	8.81
15	47	104	199	441	9.03
16	49	142	188	342	9.39

VI. Meltwater of Spray Ice Formed at - 24 °C and Stored for 20 Days (two ice columns)

meltwater of ice column 1:

Sample	TOC (mg/L)	COD (mg/L)	Color (TCU)	Conductivity (µs/cm)	pH
1	1348	3176	6876	12420	9.63
2	767	1798	3996	8040	9.63
3	595	1577	3252	5970	9.62
4	518	1312	2729	5070	9.60
5	417	990	2164	4170	9.56
6	377	855	1985	2890	9.54
7	311	720	1524	2400	9.39
8	228	564	1245	2080	9.26
9	197	452	1007	1790	9.19
10	152	370	790	1420	9.11
11	102	242	522	980	9.09
12	65	141	295	611	9.12
13	36	91	178	332	9.14
14	30	78	150	294	9.17
15	21	61	103	228	9.33
16	15	40	70	168	9.69

meltwater of ice column 2:

Sample	TOC (mg/L)	COD (mg/L)	Color (TCU)	Conductivity (μ S/cm)	pH
1	501	1234	2657	5340	9.56
2	499	1228	2620	4980	9.61
3	543	1342	2806	5190	9.54
4	607	1472	3026	5700	9.54
5	504	1764	2640	5040	9.48
6	387	933	2014	3990	9.40
7	318	774	1632	2550	9.31
8	296	742	1528	2450	9.30
9	262	664	1364	2310	9.20
10	228	530	1158	1940	9.15
11	139	299	619	1140	9.00
12	72	181	376	738	9.00
13	54	135	278	574	8.92
14	35	91	181	336	9.08
15	39	100	183	424	9.53
16	30	76	152	303	9.23

VII. Meltwater of Spray Ice Formed at - 24 °C and Stored for 40 Days (two ice columns)

meltwater of ice column 1:

Sample	TOC (mg/L)	COD (mg/L)	Color (TCU)	Conductivity (μ S/cm)	pH
1	751	1818	3877	7800	9.48
2	718	1785	3615	7740	9.49
3	587	1435	2904	6420	9.45
4	508	1161	2417	4860	9.39
5	456	1110	2404	4800	9.41
6	344	865	1805	3900	9.36
7	257	652	1354	2960	9.27
8	248	579	1208	2180	9.24
9	212	517	1084	1980	9.22
10	174	426	896	1600	9.21
11	167	367	801	1450	9.13
12	126	284	621	1150	9.04
13	118	249	518	1000	9.07
14	94	187	400	806	9.08
15	60	144	302	672	9.30
16	41	106	194	344	9.70

meltwater of ice column 2:

Sample	TOC (mg/L)	COD (mg/L)	Color (TCU)	Conductivity (μ S/cm)	pH
1	708	1749	3690	7020	9.65
2	617	1581	3091	6150	9.61
3	502	1217	2492	5130	9.62
4	483	1175	2434	4920	9.57
5	468	1178	2479	4920	9.57
6	419	1007	2135	4290	9.52
7	295	727	1534	2500	9.43
8	256	601	1242	2160	9.37
9	235	573	1208	2150	9.3
10	227	528	1121	1920	9.28
11	150	346	728	1340	9.17
12	111	224	470	927	9.07
13	81	163	346	724	9.02
14	46	119	237	540	9.03
15	38	100	188	352	9.18
16	34	94	166	326	9.49
17	24	68	117	257	9.52

OIL SANDS TAILINGS POND WATER

I. Source Water

A. Measurements of source water used to produce spray ice at - 10 °C

Sample	TOC (mg/L)	COD (mg/L)	Cl ⁻¹ (mg/L)	SO ₄ ²⁻ (mg/L)	Conductivity (µs/cm)	pH
1	143	415	474	145	3320	8.20
2	158	393	473	137	3340	8.19
3	140	476	472	140	3339	8.22
4	151	354	472	142	3340	8.25

B. Measurements of source water used to produce spray ice at - 24 °C

Sample	TOC (mg/L)	COD (mg/L)	Cl ⁻¹ (mg/L)	SO ₄ ²⁻ (mg/L)	Conductivity (µs/cm)	pH
1	134	400	476	165	3640	8.68
2	137	416	476	136	3200	8.62
3	139	439	475	108	3220	8.49

II. Runoff Which Was Obtained During Spraying Operation at - 10 °C

Sample	TOC (mg/L)	COD (mg/L)	Cl ⁻¹ (mg/L)	SO ₄ ²⁻ (mg/L)	Conductivity (μs/cm)	pH
1	234	619	727	214	4500	8.30
2	225	708	726	216	4700	8.30
3	226	730	758	226	5080	8.35
4	234	592	757	236	5060	8.34

III. Ice Core Samples of the Spray Ice

A. Ice core sample formed at - 10 °C and stored for 20 days

Sample	TOC (mg/L)	COD (mg/L)	Cl ⁻¹ (mg/L)	SO ₄ ²⁻ (mg/L)	Conductivity (μs/cm)	pH
1	50	196	154	52	1085	9.86
2	47	99	66	21	489	9.65
3	130	332	414	139	2335	9.35

B. Ice core sample formed at - 10 °C and stored for 40 days

Sample	TOC (mg/L)	COD (mg/L)	Cl ⁻¹ (mg/L)	SO ₄ ²⁻ (mg/L)	Conductivity (μs/cm)	pH
1	46	146	118	383	806	10.16
2	38	124	85	26	576	10.17
3	115	328	370	117	2025	9.49

C. Ice core sample formed at - 24 °C and stored for 20 days

Sample	TOC (mg/L)	COD (mg/L)	Cl ⁻¹ (mg/L)	SO ₄ ²⁻ (mg/L)	Conductivity (μs/cm)	pH
1	98	445	358	109	1918	9.87
2	95	432	372	108	2010	10.03
3	228	449	802	250	4930	9.68

D. Ice core sample formed at - 24 °C and stored for 40 days

Sample	TOC (mg/L)	COD (mg/L)	Cl ⁻¹ (mg/L)	SO ₄ ²⁻ (mg/L)	Conductivity (μs/cm)	pH
1	143	471	484	141	3788	9.87
2	146	473	487	143	3735	10.04
3	143	455	486	139	3788	9.88

IV. Meltwater of Spray Ice Formed at - 10 °C and Stored for 20 Days (two ice columns)

meltwater of ice column 1:

Sample	TOC (mg/L)	COD (mg/L)	Cl ⁻¹ (mg/L)	SO ₄ ²⁻ (mg/L)	Conductivity (μs/cm)	pH
1	539	1176	1932	609	10650	8.97
2	222	574	763	242	4680	9.59
3	138	359	468	155	2690	9.98
4	164	444	574	189	3780	9.75
5	121	313	392	121	2550	10.01
6	73	158	209	71	1590	9.93
7	52	144	147	51	1190	9.85
8	72	185	232	80	1580	9.85
9	70	160	222	76	1520	9.83
10	78	141	273	99	1620	9.84
11	70	68	150	50	1040	9.87
12	38	43	110	33	747	9.82
13	30	35	90	42	668	9.77

meltwater of ice column 2:

Sample	TOC (mg/L)	COD (mg/L)	Cl ⁻¹ (mg/L)	SO ₄ ²⁻ (mg/L)	Conductivity (μs/cm)	pH
1	371	854	1369	426	8100	9.03
2	62	178	199	58	1340	9.76
3	114	335	424	129	2570	9.60
4	65	208	209	64	1380	9.75
5	62	160	191	59	1260	9.75
6	56	152	178	55	1190	9.78
7	50	177	204	61	1350	9.78
8	57	147	212	65	1330	9.39
9	31	77	115	59	762	9.35
10	32	45	89	40	631	9.42
11	31	53	104	52	693	9.50
12	47	111	180	53	1160	9.59
13	49	139	197	62	1310	9.57
14	22	82	104	31	667	9.65
15	19	66	85	24	600	9.72
16	24	41	52	23	467	9.72
17	19	41	47	14	334	9.60

V. Meltwater of Spray Ice Formed at - 10 °C and Stored for 40 Days (two ice columns)

meltwater of ice column 1:

Sample	TOC (mg/L)	COD (mg/L)	Cl ⁻¹ (mg/L)	SO ₄ ²⁻ (mg/L)	Conductivity (μs/cm)	pH
1	515	1218	1783	554	11760	8.97
2	93	262	316	103	1910	9.69
3	114	321	420	129	2350	9.30
4	60	173	184	79	1140	9.90
5	63	176	192	64	1220	9.75
6	55	166	182	60	1170	9.99
7	19	66	54	19	407	9.44
8	15	40	38	17	257	9.45
9	25	44	46	15	292	9.46
10	11	6	40	9	231	9.63
11	11	6	43	11	235	9.59
12	20	34	78	24	510	9.76
13	49	104	182	55	1130	9.75
14	41	101	161	48	1070	9.78
15	31	75	107	31	732	9.63

meltwater of ice column 2:

Sample	TOC (mg/L)	COD (mg/L)	Cl ⁻ (mg/L)	SO ₄ ²⁻ (mg/L)	Conductivity (μs/cm)	pH
1	369	957	1371	430	9780	9.25
2	105	292	350	110	2070	10.03
3	94	264	322	99	1930	10.04
4	83	242	284	93	1810	10.08
5	85	254	290	92	1840	10.08
6	111	315	392	123	2310	9.62
7	75	171	205	65	1350	9.53
8	31	88	89	31	635	9.59
9	28	64	79	24	562	9.47
10	17	22	59	17	326	9.00
11	18	20	57	16	385	9.33
12	19	19	64	18	410	9.40
13	30	55	101	30	660	9.75
14	24	24	82	25	531	9.49
15	29	78	104	33	725	9.64

VI. Meltwater of Spray Ice Formed at - 24 °C and Stored for 20 Days (two ice columns)

meltwater of ice column 1:

Sample	TOC (mg/L)	COD (mg/L)	Cl ⁻¹ (mg/L)	SO ₄ ²⁻ (mg/L)	Conductivity (μs/cm)	pH
1	240	703	1024	309	7680	9.84
2	247	715	1045	321	7020	9.81
3	248	731	1072	327	7140	9.73
4	244	739	1088	330	7140	9.84
5	232	678	1013	310	6720	9.84
6	158	456	797	242	5340	9.80
7	102	370	576	174	4080	9.75
8	93	309	503	150	2720	9.77
9	74	243	425	98	2260	9.79
10	99	290	396	115	2150	9.80
11	60	183	230	65	1370	9.69
12	42	135	160	48	1010	9.60
13	34	134	115	34	720	9.46
14	33	128	73	20	472	9.38
15	21	97	44	12	256	9.31
16	17	89	17	7	148	8.82

meltwater of ice column 2:

Sample	TOC (mg/L)	COD (mg/L)	Cl ⁻ (mg/L)	SO ₄ ²⁻ (mg/L)	Conductivity (μs/cm)	pH
1	856	2377	3800	1111	27150	8.97
2	457	1091	1632	775	10920	9.21
3	265	811	1015	298	6840	9.83
4	132	456	624	185	4530	9.96
5	128	459	622	186	4530	9.98
6	157	493	666	193	4800	10.02
7	332	869	1169	352	7830	9.86
8	82	324	318	98	1940	9.92
9	71	266	277	86	1700	9.95
10	55	215	220	63	1360	9.91
11	42	182	167	49	1050	9.93
12	30	130	78	22	519	9.75
13	39	137	107	32	716	9.89
14	56	167	166	50	1040	9.98
15	45	135	142	41	900	9.96
16	44	106	116	33	763	9.95
17	30	68	68	19	473	9.81

VII. Meltwater of Spray Ice Formed at - 24 °C and Stored for 40 Days (two ice columns)

meltwater of ice column 1:

Sample	TOC (mg/L)	COD (mg/L)	Cl ⁻¹ (mg/L)	SO ₄ ²⁻ (mg/L)	Conductivity (μs/cm)	pH
1	418	1009	1436	445	8370	9.76
2	360	902	1318	379	8040	9.77
3	264	683	997	282	6330	9.75
4	235	608	896	250	5880	9.75
5	233	612	877	256	5880	9.74
6	187	469	676	188	4680	9.72
7	132	334	483	130	3420	9.69
8	92	246	350	96	2110	9.68
9	74	194	271	76	1650	9.60
10	90	163	253	70	1480	9.55
11	96	187	259	69	1450	9.56
12	64	131	165	47	970	9.41
13	60	131	140	39	864	9.39
14	7	195	109	33	714	9.36
15	3	130	83	21	570	9.39

meltwater of ice column 2:

Sample	TOC (mg/L)	COD (mg/L)	Cl ⁻¹ (mg/L)	SO ₄ ²⁻ (mg/L)	Conductivity (μs/cm)	pH
1	1327	1749	4614	1302	28500	9.39
2	591	1581	2113	598	13680	9.87
3	270	1217	1006	281	6420	9.87
4	162	1175	627	167	4230	9.82
5	139	1178	549	152	2900	9.81
6	103	1007	408	113	2300	9.78
7	76	727	285	79	1750	9.75
8	92	601	254	71	1560	9.68
9	83	573	237	67	1440	9.68
10	52	151	191	57	1200	9.57
11	54	124	150	43	939	9.52
12	50	126	127	36	798	9.45
13	30	105	91	25	593	9.46
14	28	101	75	23	510	9.44
15	27	92	62	24	338	9.32
16	32	112	43.3	14	273	9.32

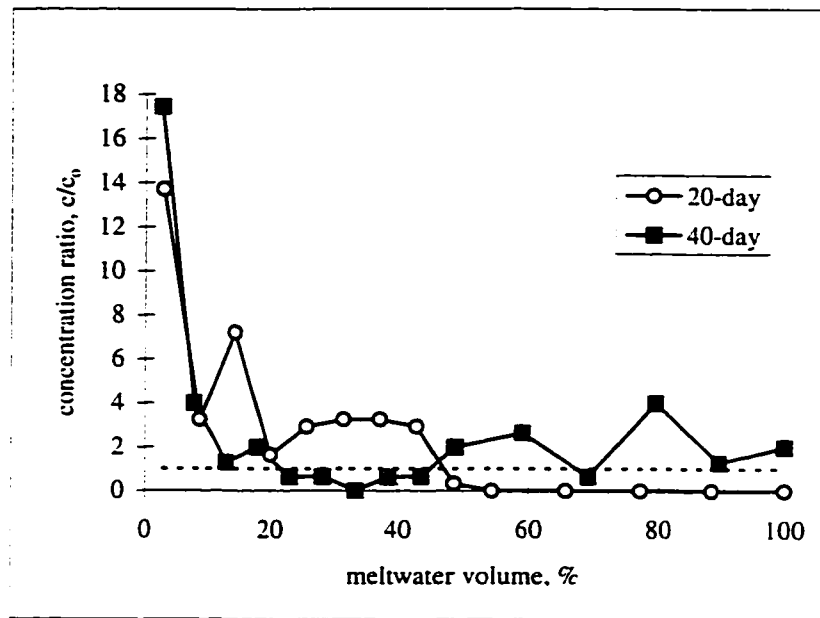


Figure AA-1 Variation of the normalized color concentration in the sequential meltwater samples of the spray ice made from tap water (the spray ice was obtained in a - 10 °C environment). The source water color concentration, $c_0 = 1$ (TCU).

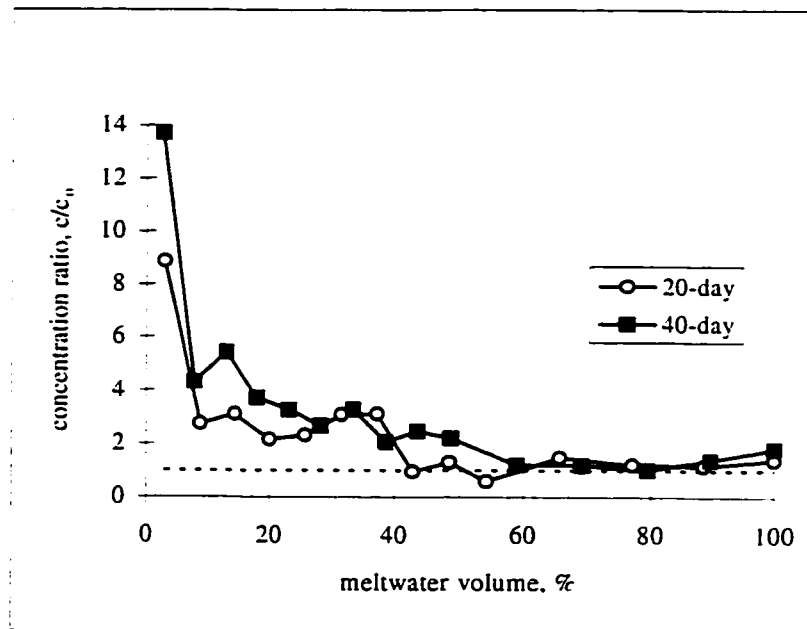


Figure AA-2 Variation of the normalized COD concentration in the sequential meltwater samples of the spray ice made from tap water (the spray ice was obtained in a - 10 °C environment). The source water COD concentration, $c_0 = 6$ mg/L.

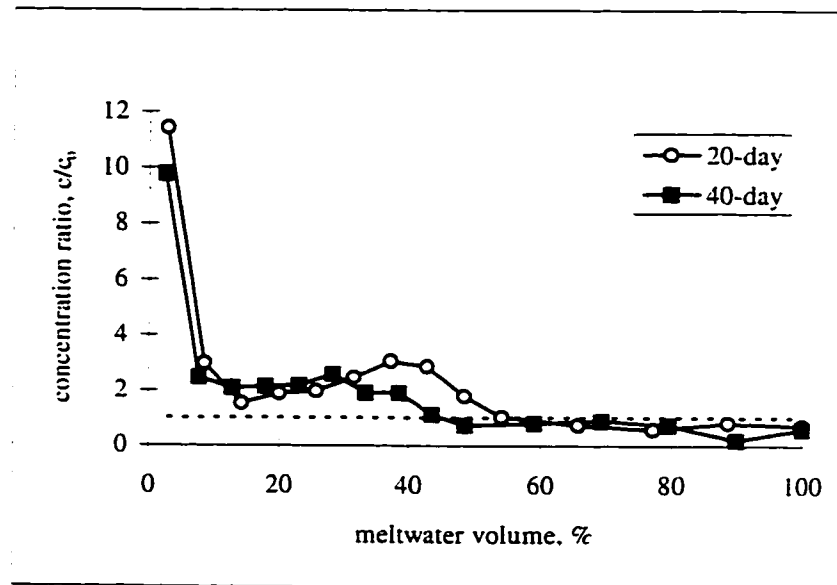


Figure AA-3 Variation of the normalized TOC concentration in the sequential meltwater samples of the spray ice made from tap water (the spray ice was obtained in a - 10 °C environment). The source water TOC concentration, $c_0 = 2 \text{ mg/L}$.

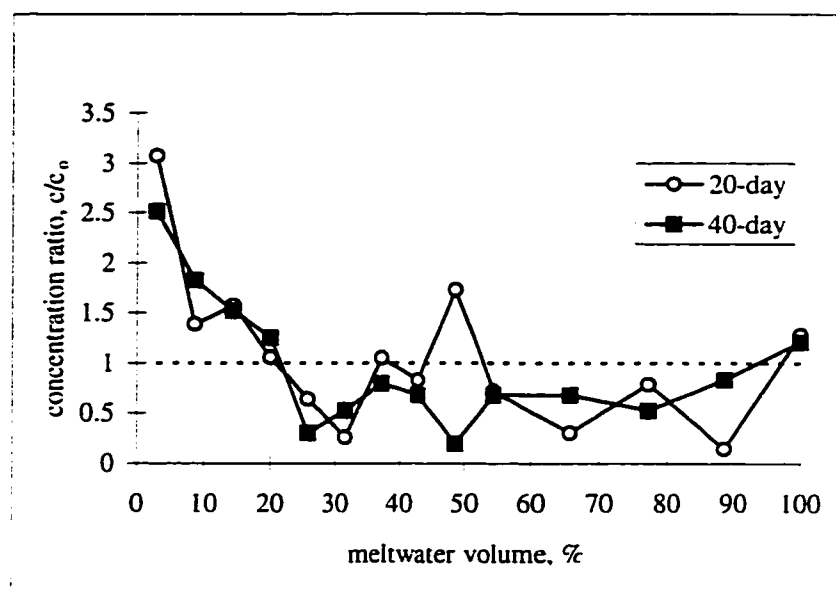


Figure AA-4 Variation of the normalized COD concentration in the sequential meltwater samples of the spray ice made from tap water (The spray ice was obtained in a - 24 °C environment). The source water COD concentration, $c_0 = 7$ mg/L.

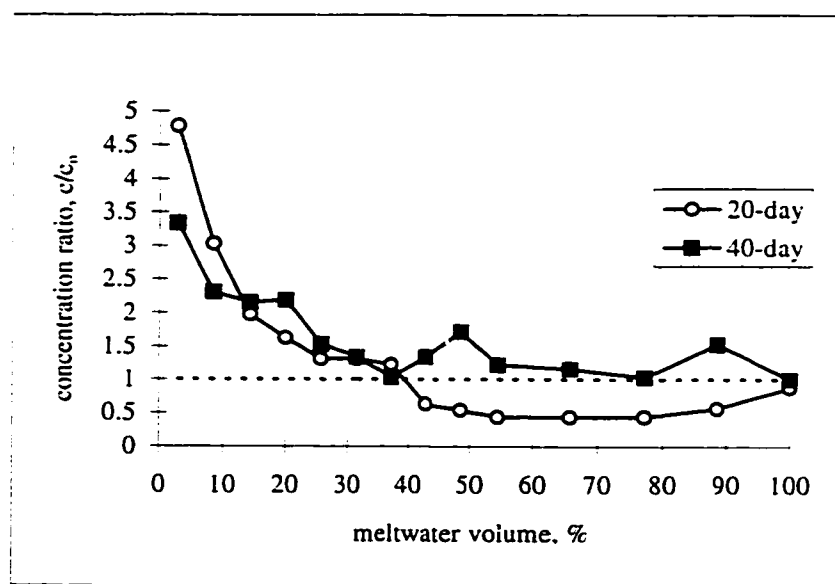


Figure AA-5 Variation of the normalized TOC concentration in the sequential meltwater samples of the spray ice made from tap water (The spray ice was obtained in a - 24 °C environment). The source water TOC concentration, $c_0 = 2$ mg/L.

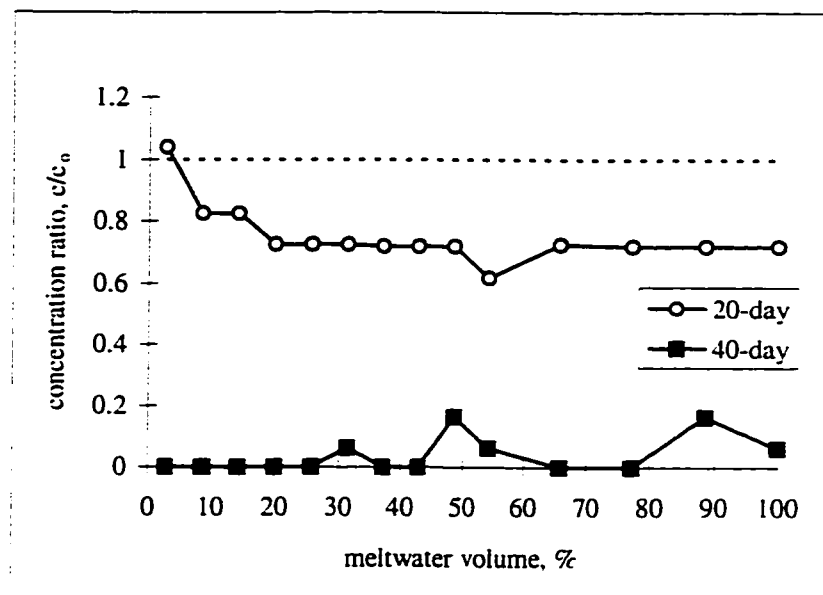


Figure AA-6 Variation of the normalized color concentration in the sequential meltwater samples of the spray ice made from tap water (The spray ice was obtained in a -24°C environment). The source water color concentration, $c_0 = 9$ TCU.

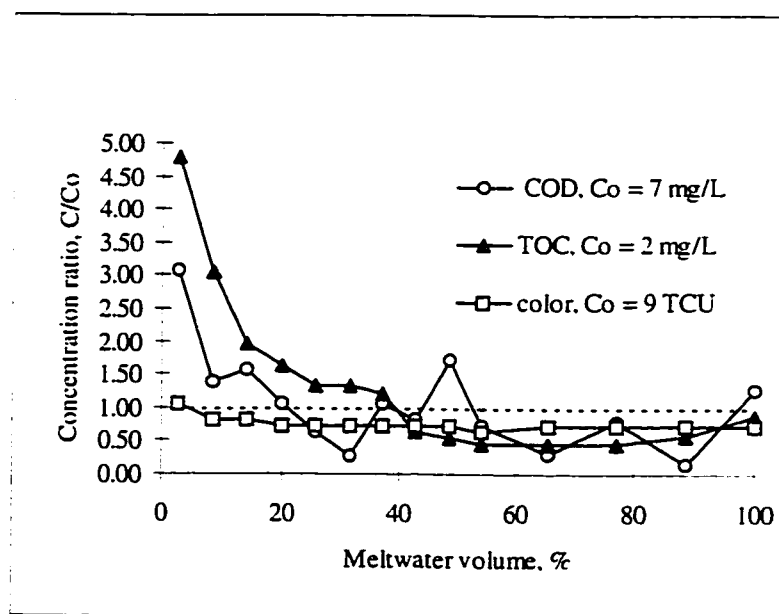


Figure AA-7 Variation of the concentration ratios of the selected organic contaminants versus meltwater volume for the 20-day old spray ice made from tap water in a -24°C environment.

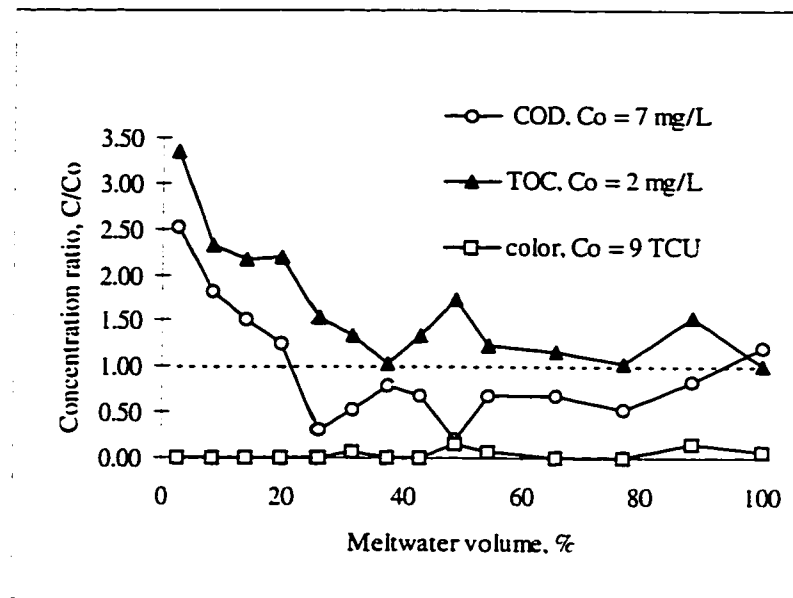
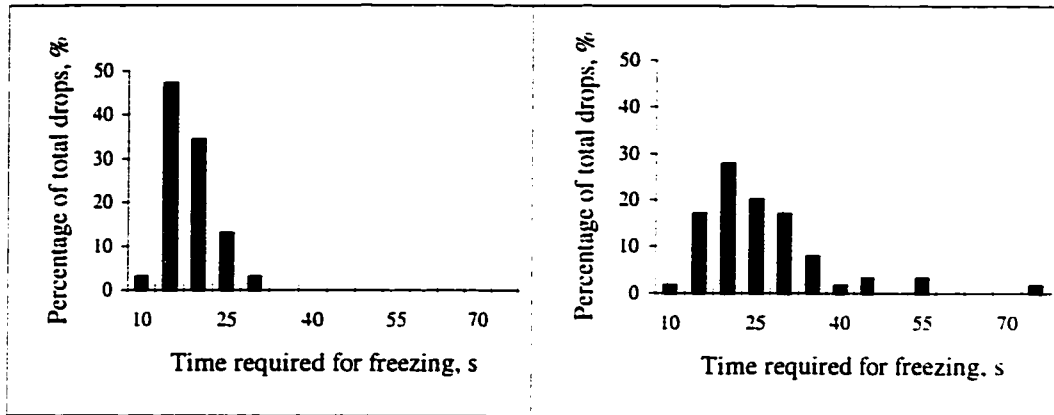


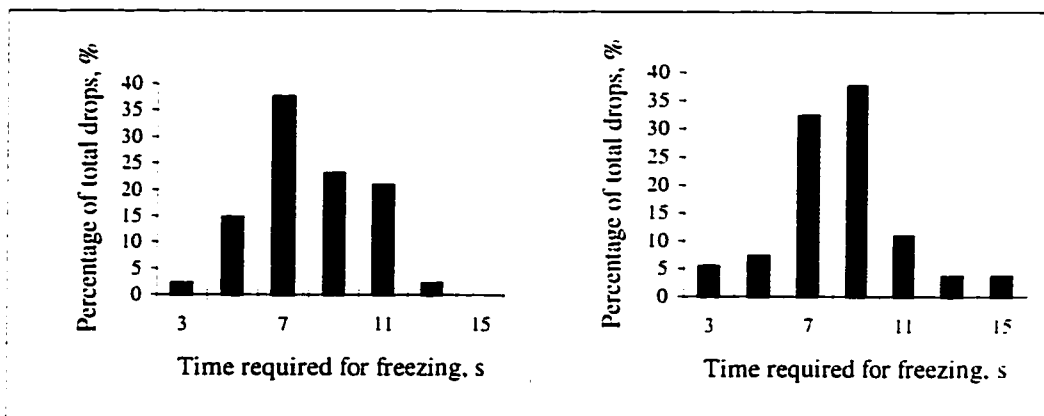
Figure AA-8 Variation of the concentration ratios of the selected organic contaminants versus meltwater volume for the 40-day old spray ice made from tap water in a - 24 °C environment.

**APPENDIX - B FREEZING TIME REQUIRED BY FREELY
SUSPENDED WASTEWATER DROPLETS**



(a)

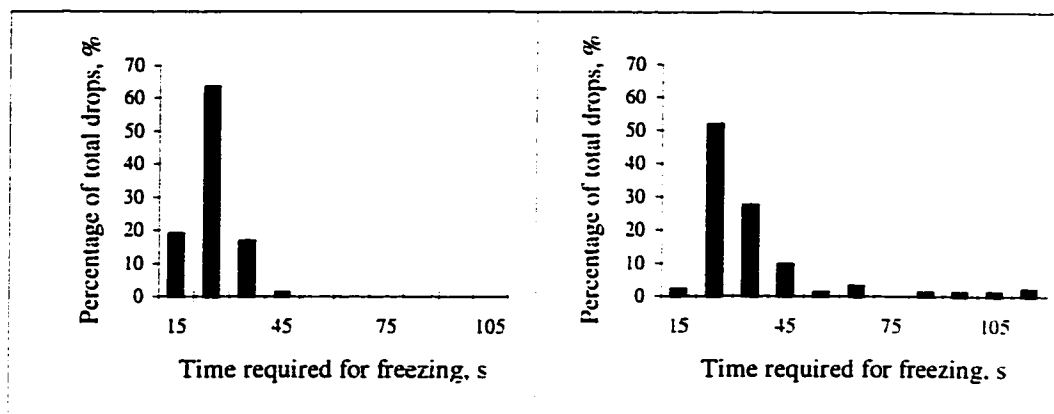
(b)



(c)

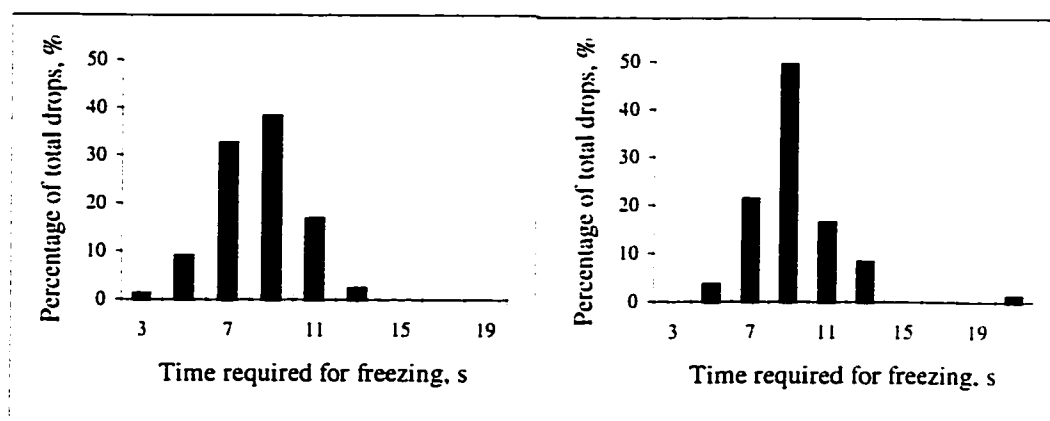
(d)

Figure AB-1 Distribution of required freezing times for 3.4 mm diameter (21.2 μ L) piggery wastewater drops: (a) air temp. = - 10 °C, liquid pH = 7.1; (b) air temp. = - 10 °C, liquid pH = 11.0; (c) air temp. = - 18 °C, liquid pH = 7.1 and (d) air temp. = - 18 °C, liquid pH = 11.0.



(a)

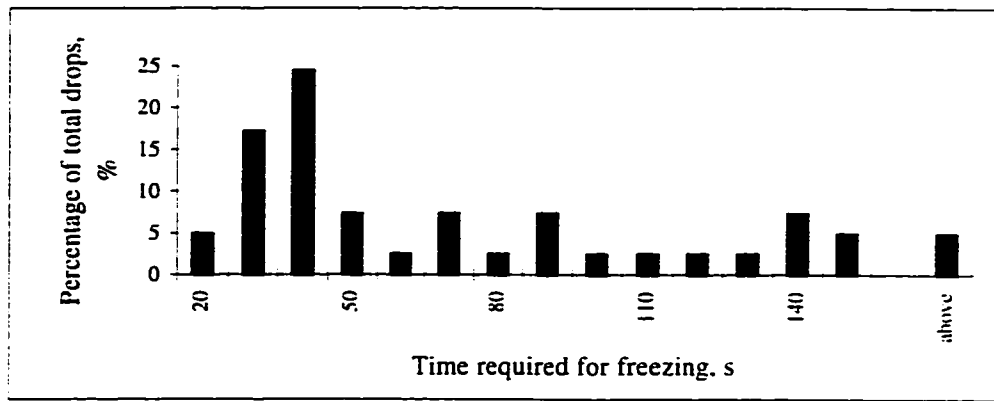
(b)



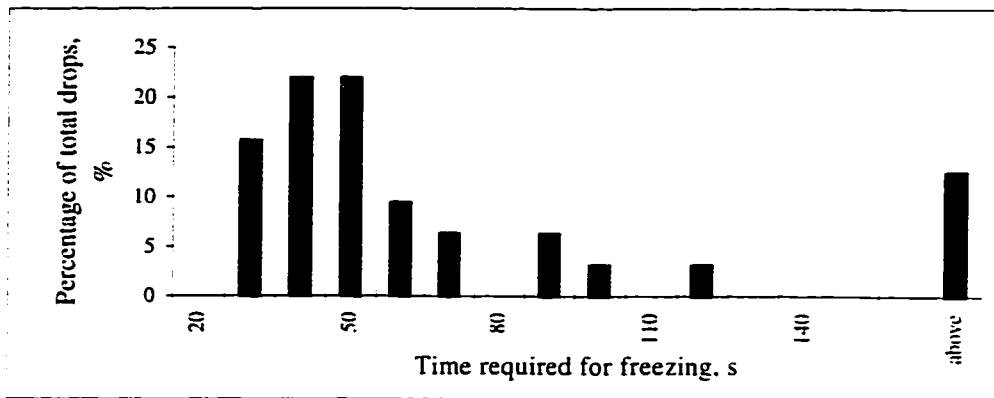
(c)

(d)

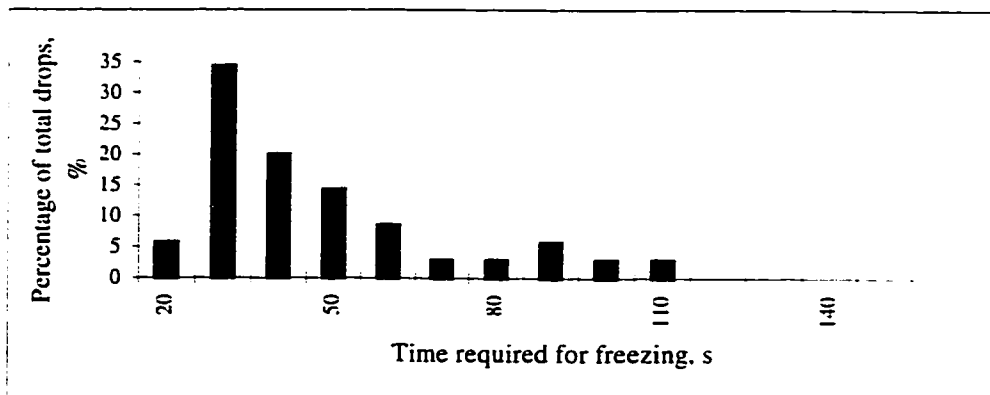
Figure AB-2 Freezing time distribution for 4.2 mm diameter (37.7 μ L) piggy wastewater drops: (a) air temp. = - 10 °C, liquid pH = 7.1; (b) air temp. = - 10 °C, liquid pH = 11.0; (c) air temp. = - 18 °C, liquid pH = 7.1 and (b) air temp. = - 18 °C, liquid pH = 11.0



(a)



(b)



(c)

Figure AB-3 Piggery wastewater droplet freezing time distribution under various ambient air temperatures: (a) 3.4 mm diameter drops, air temperature = - 6.7 °C; (b) 3.4 mm diameter drops and air temperature = - 7.4 °C; (c) 4.2 mm diameter drops, air temperature = - 6.7 °C.

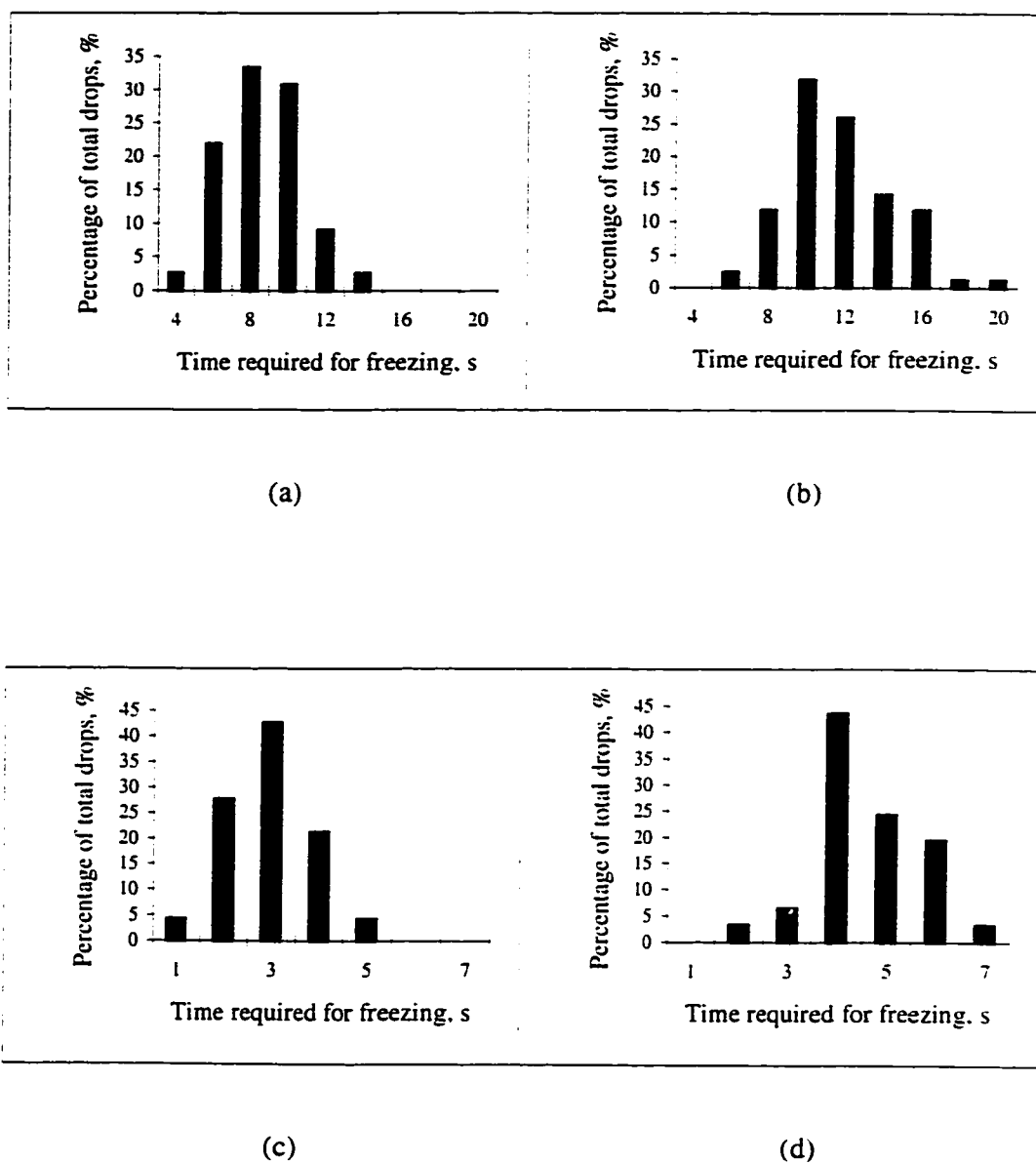
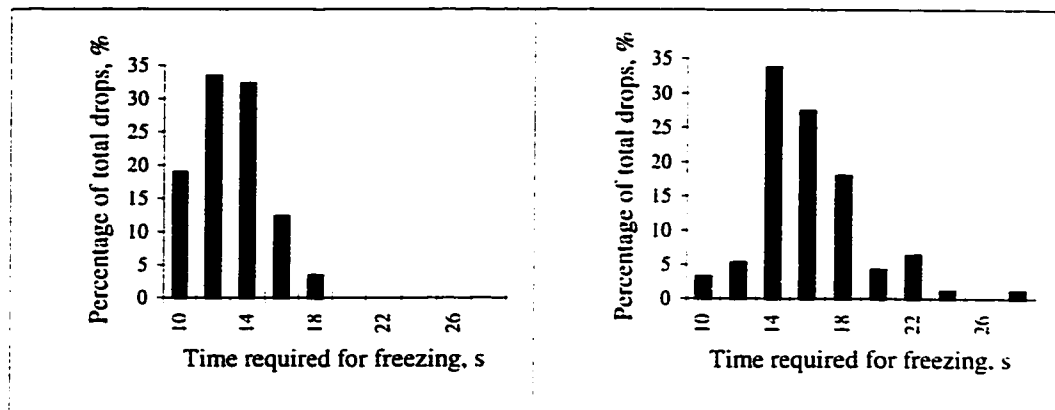
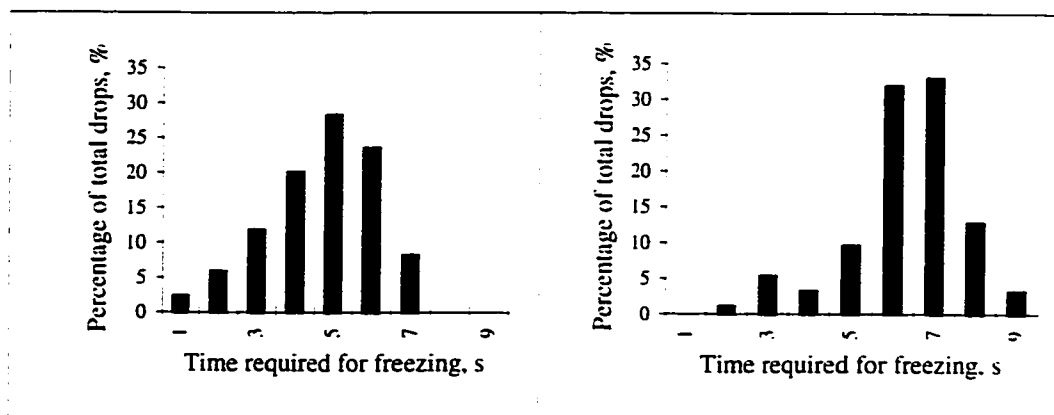


Figure AB-4 Freezing time distribution for 2.8 mm diameter pulp mill effluent drops: (a) air temp. = -10 °C, liquid pH = 7.6; (b) air temp. = -10 °C, liquid pH = 11.0; (c) air temp. = -18 °C, liquid pH = 7.6 and (d) air temp. = -18 °C, liquid pH = 11.0.



(a)

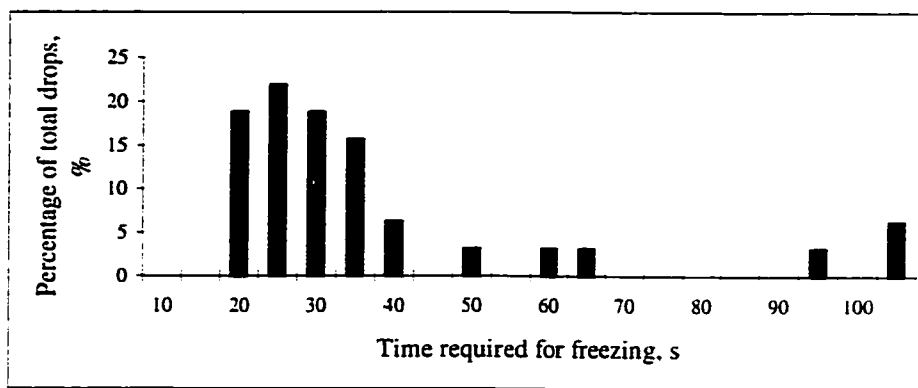
(b)



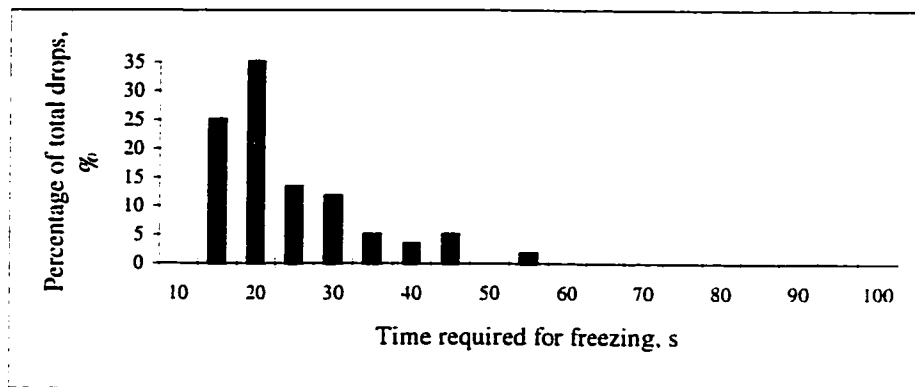
(c)

(d)

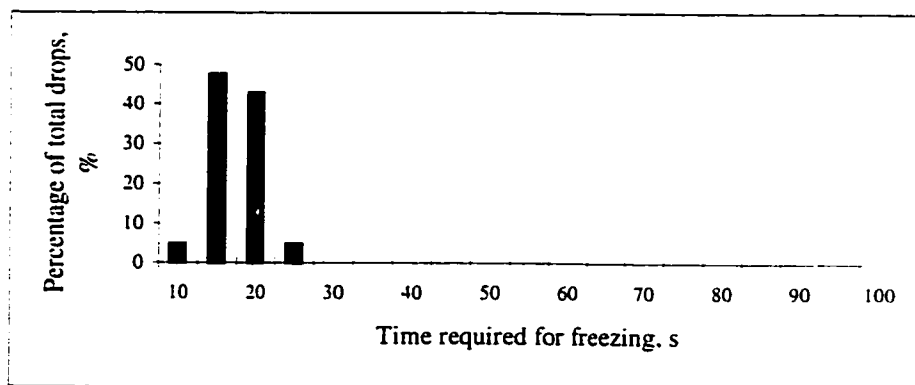
Figure AB-5 Droplet freezing time distribution for 4.2 mm diameter pulp mill effluent drops: (a) air temp. = -10 °C, liquid pH = 7.6; (b) air temp. = -10 °C, liquid pH = 11.0; (c) air temp. = -18 °C, liquid pH = 7.6 and (d) air temp. = -18 °C, liquid pH = 11.0.



(a)

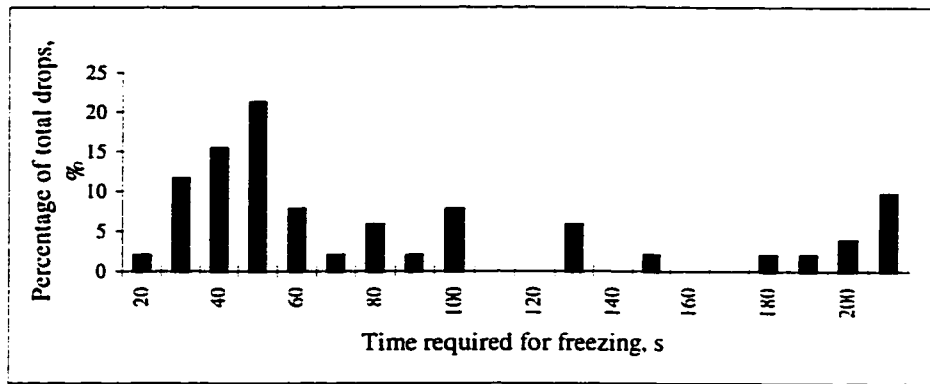


(b)

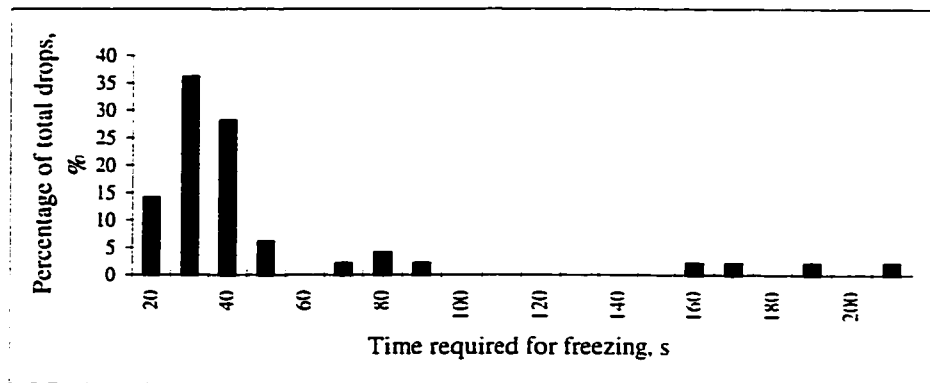


(c)

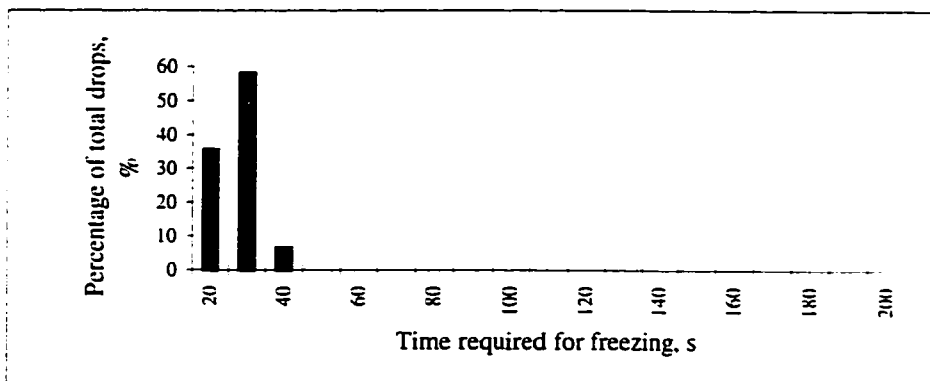
Figure AB-6 Freezing time distribution for 2.8 mm diameter pulp mill effluent drops under different ambient temperatures: (a) ambient temperature = -5.5°C , (b) ambient temperature = -6.7°C and (c) ambient temperature = -7.4°C .



(a)

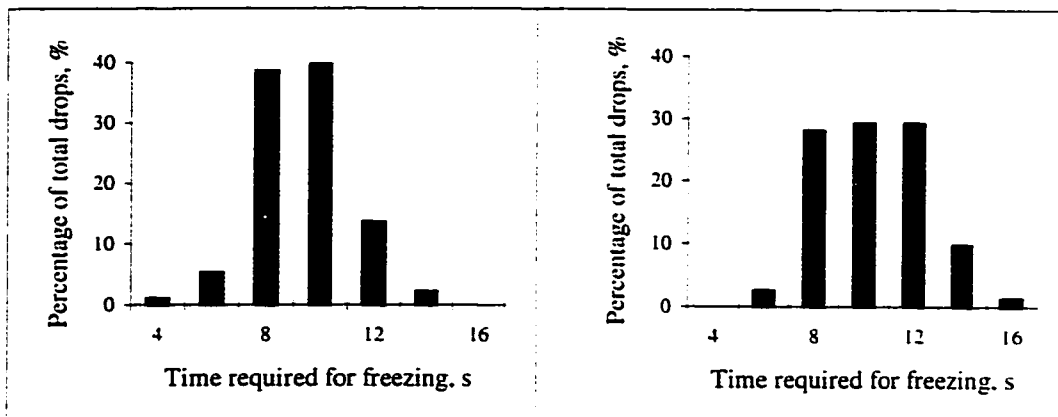


(b)



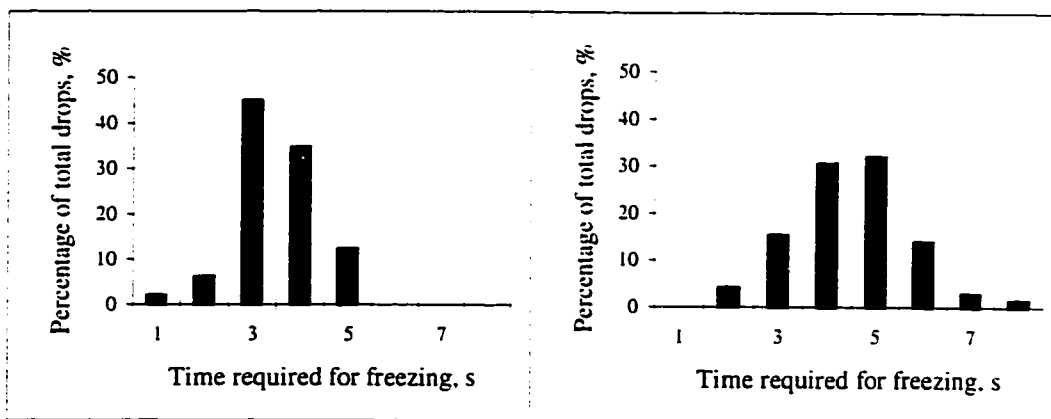
(c)

Figure AB-7 Freezing time distribution for 4.2 mm diameter pulp mill effluent drops under different ambient temperatures: (a) ambient temperature = -5.5 °C, (b) ambient temperature = -6.7 °C and (c) ambient temperature = -7.4 °C.



(a)

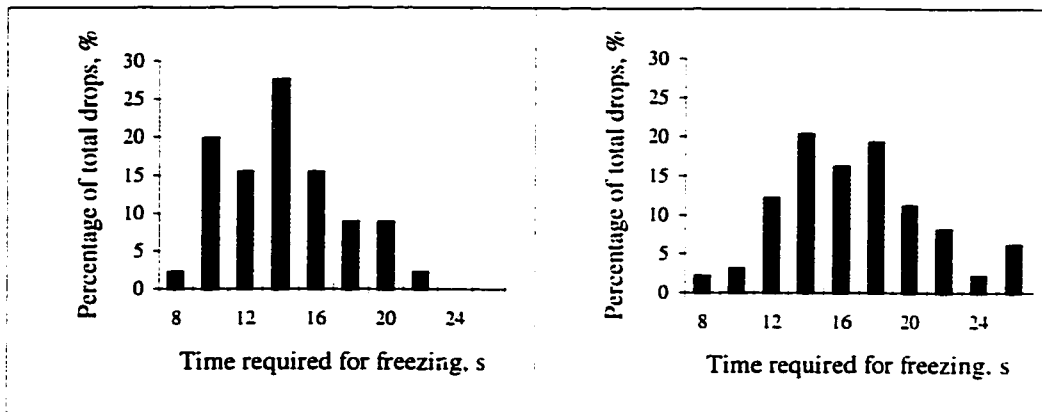
(b)



(c)

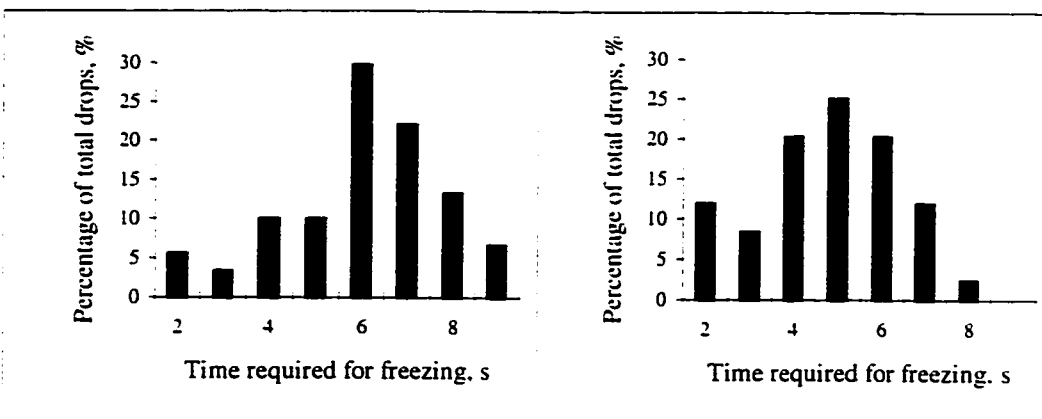
(d)

Figure AB-8 Freezing time distribution for 2.8 mm diameter oil sands tailings pond water drops: (a) air temp. = -10 °C, liquid pH = 8.1; (b) air temp. = -10 °C, liquid pH = 11.0; (c) air temp. = -18 °C, liquid pH = 8.1 and (b) air temp. = -18 °C, liquid pH = 11.0.



(a)

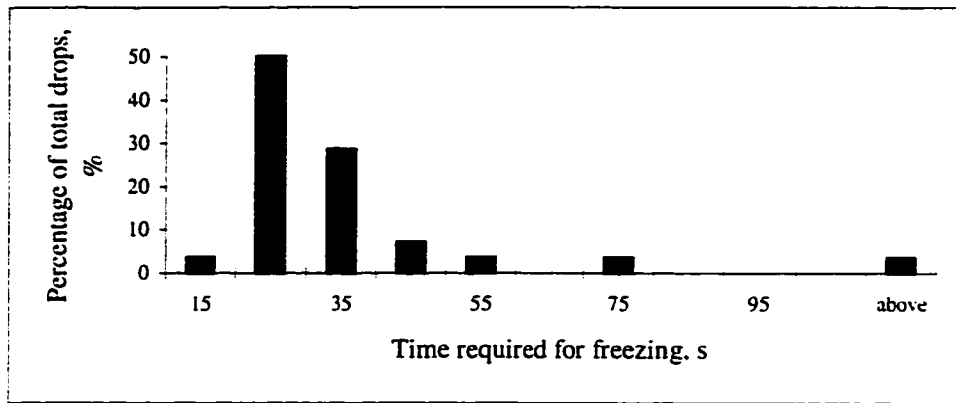
(b)



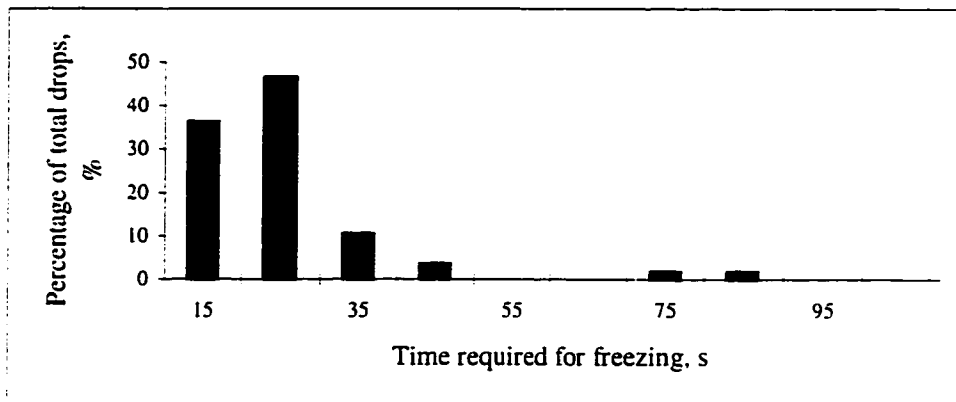
(c)

(d)

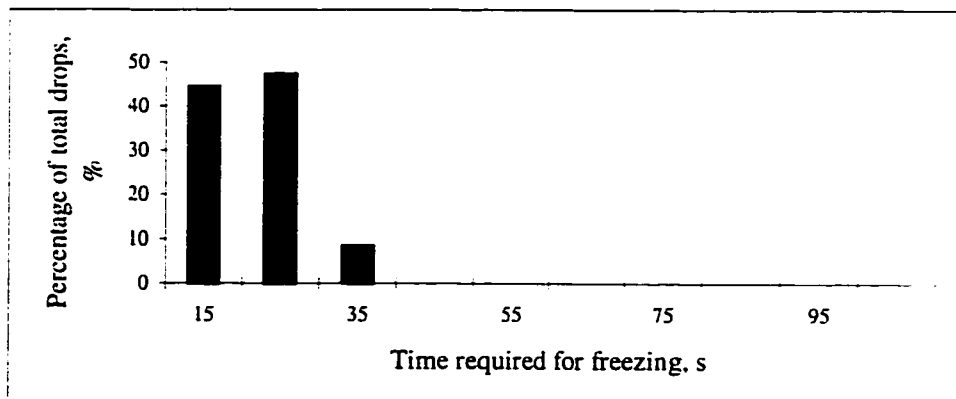
Figure AB-9 Freezing time distribution for 4.2 mm diameter oil sands tailings pond water drops: (a) air temp. = - 10 °C, liquid pH = 8.1; (b) air temp. = - 10 °C, liquid pH = 11.0; (c) air temp. = - 18 °C, liquid pH = 8.1 and (b) air temp. = - 18 °C, liquid pH = 11.0.



(a)

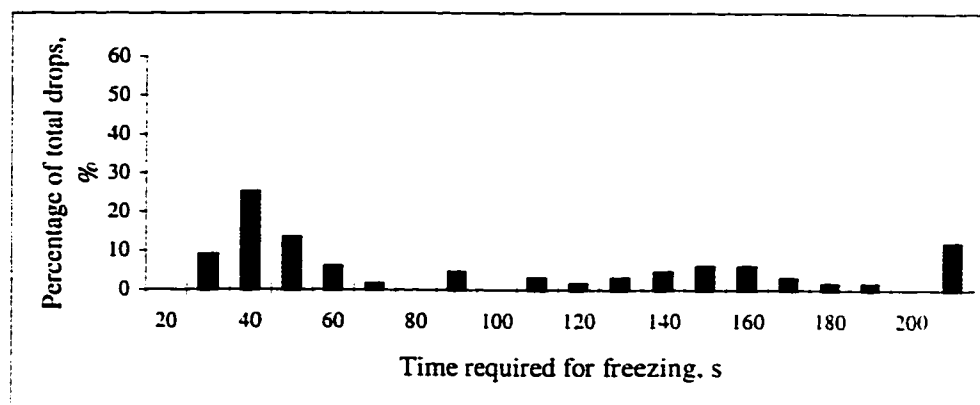


(b)

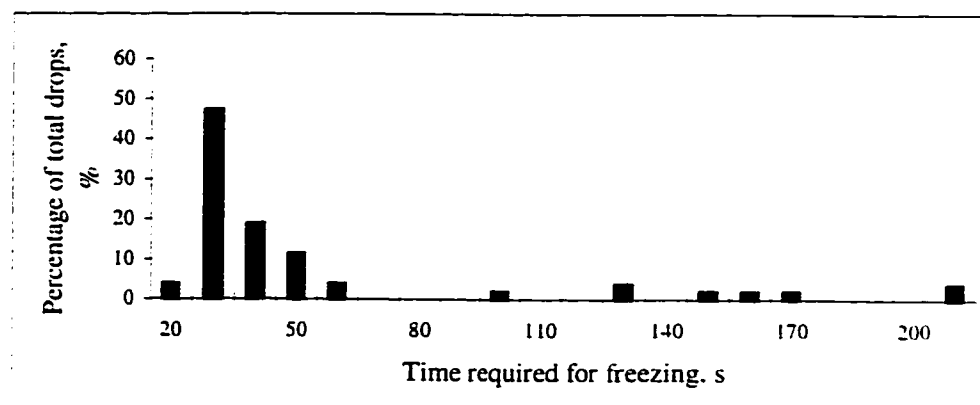


(c)

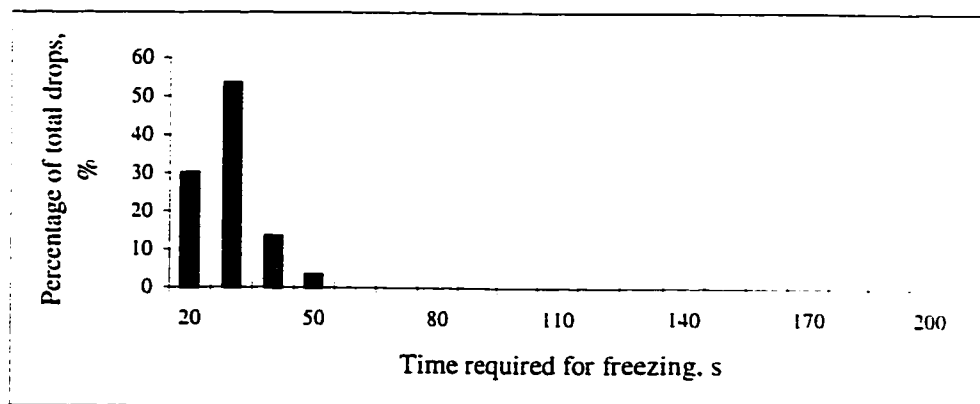
Figure AB-10 Freezing time distribution for 2.8 mm diameter oil sands tailings pond water drops under different ambient temperatures: (a) ambient temperature = -5.5 °C, (b) ambient temperature = -6.7 °C and (c) ambient temperature = - 7.4 °C.



(a)



(b)



(c)

Figure AB-11 Freezing time distribution for 4.2 mm diameter oil sands tailings pond water drops under different ambient temperatures: (a) ambient temperature = -5.5°C , (b) ambient temperature = -6.7°C and (c) ambient temperature = -7.4°C .

APPENDIX - C PHOTOGRAPHS OF THE EXPERIMENTS

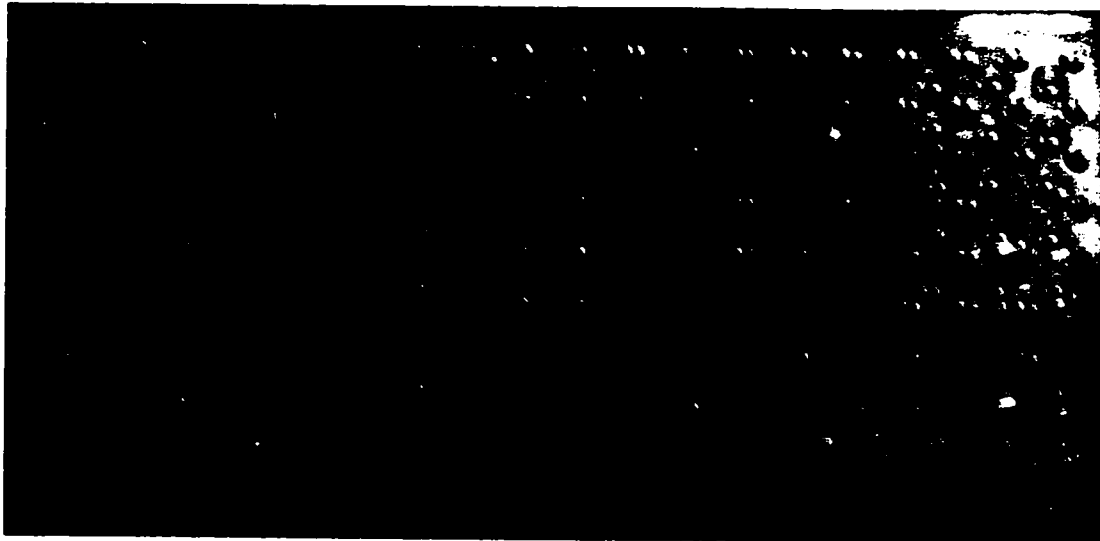


Photo - 1: Water drops were placed on the surface of the cooling device

Photo - 1 to Photo - 3 show the sequence of the ice nucleation in the water drops tested. Photo - 1 shows the drops were placed on the surface of the cooling device at room temperature. The drops in the area of letter D were made from distilled water, in the area of letter A, piggery wastewater, in the area of letter P, pulp mill effluent and in the area of letter T were oil sands tailings pond water drops. Photo - 2 shows that most of the pulp mill effluent and oil sands tailings pond water drops had frozen while no freezing occurred in the piggery wastewater and distilled water drops. Photo - 3 shows that all wastewater drops froze but still no freezing occurred in the distilled water.

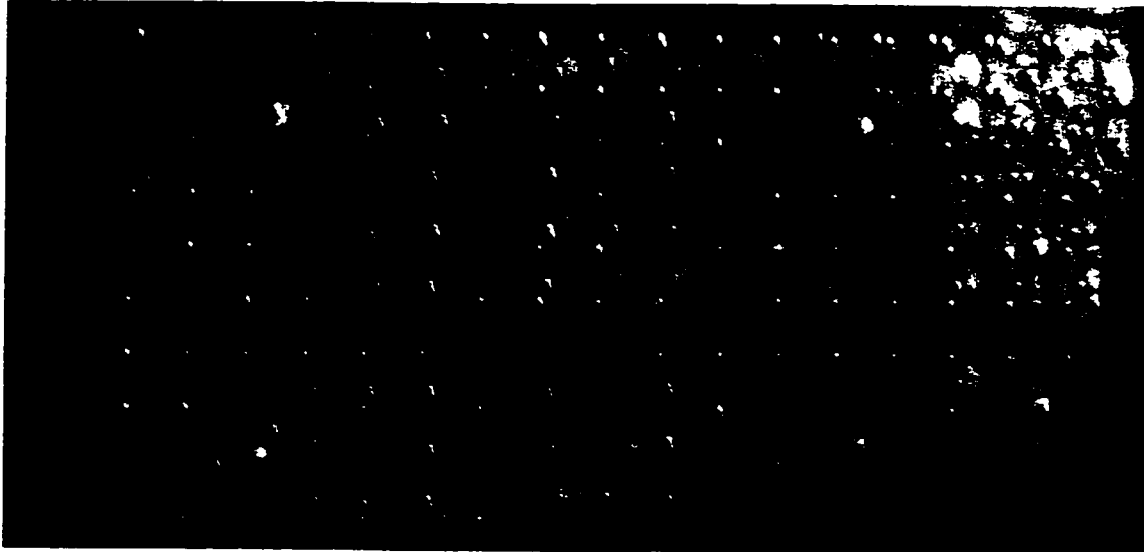


Photo - 2: Most of the pulp mill effluent (P area) and oil sands tailings pond water drops (T area) froze while no freezing occurred in the piggery wastewater (A area) and distilled water drops (D area).



Photo - 3: All wastewater drops had frozen while freezing did not start in the distilled water drops.

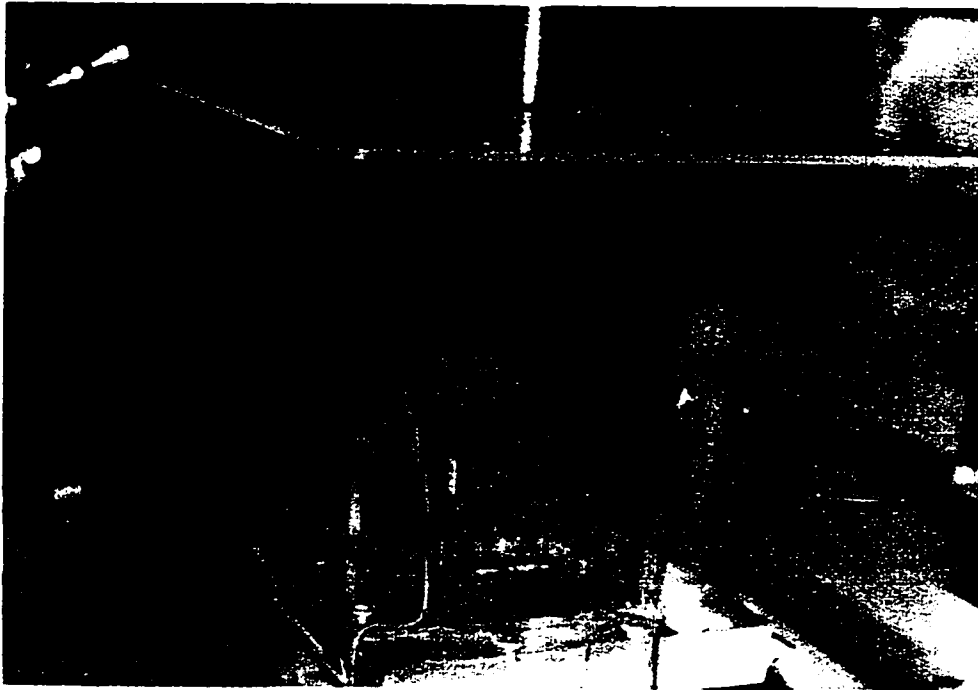


Photo - 4: Working section of the vertical wind tunnel, back pressure plate and a freely suspended water drop.

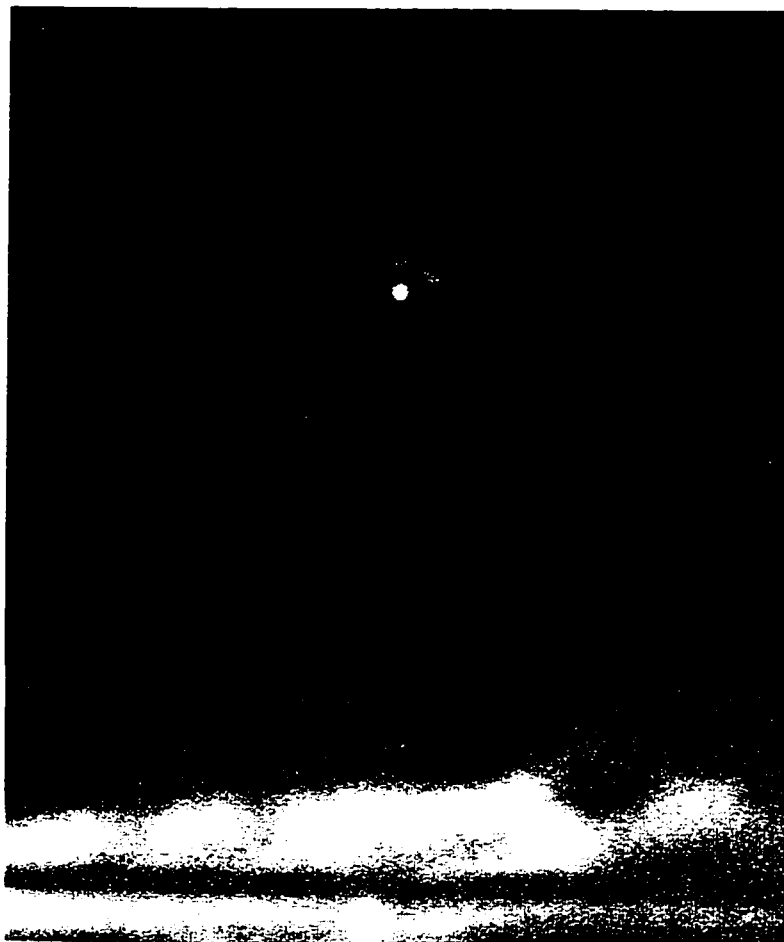


Photo - 5: A frozen oil sands tailings pond water drop suspending in the air.



Photo - 6: Pulp mill effluent spray ice core sample. The spray ice was formed at - 10 °C and runoff was generated during spraying.



Photo - 7: Spray ice core sample of oil sands tailings pond water. The spray ice was formed at - 10 °C and runoff was generated during spraying.

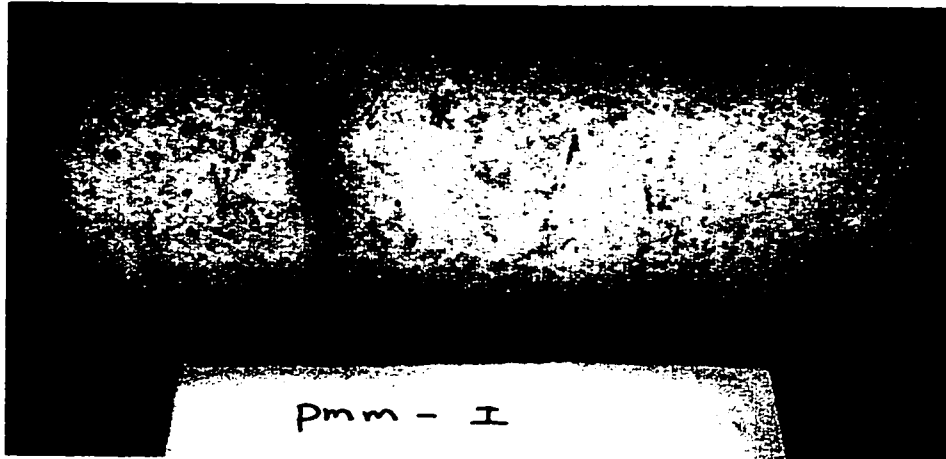


Photo - 8: Pulp mill effluent spray ice core sample. The spray ice was formed at - 24 °C and no runoff was generated during spraying.

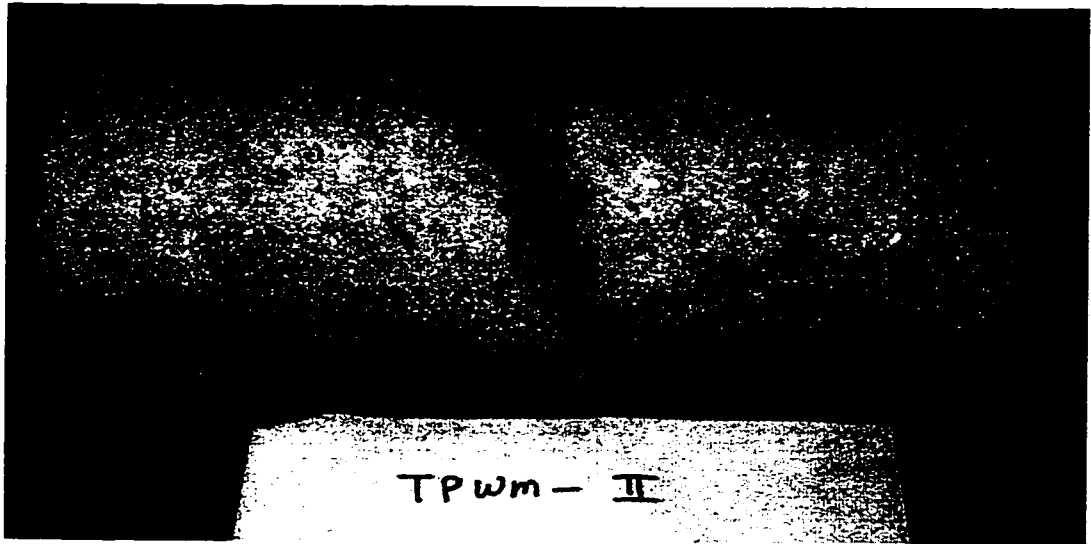


Photo - 9: Spray ice core sample of oil sands tailings pond water. The spray ice was formed at - 24 °C and no runoff was generated during spraying.

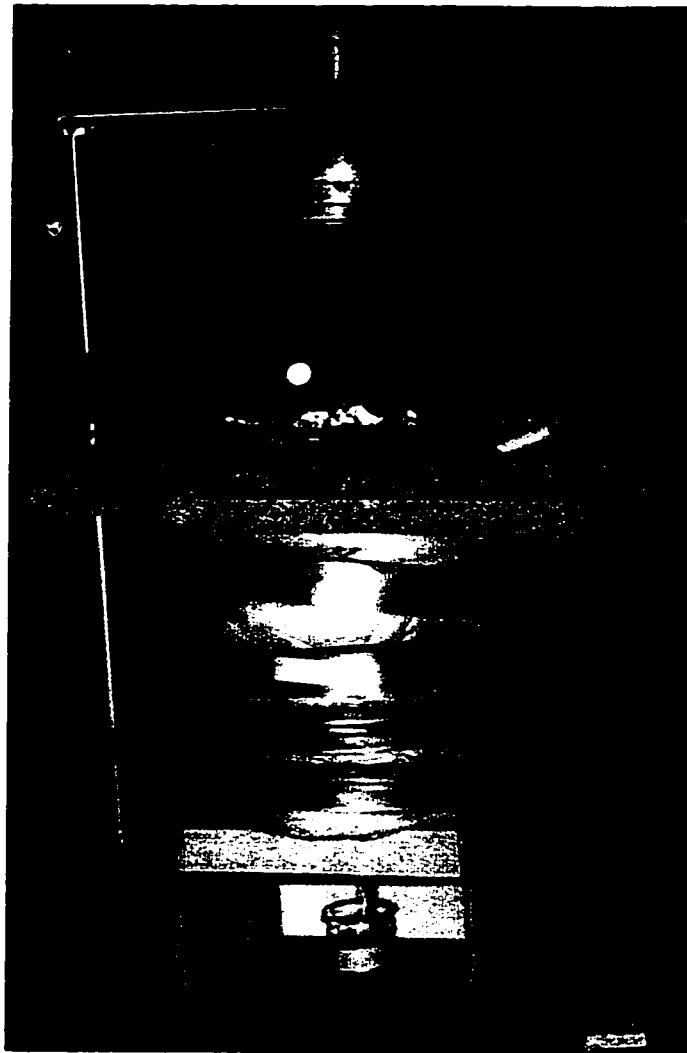


Photo - 10: Set-up of the spray ice melting test.

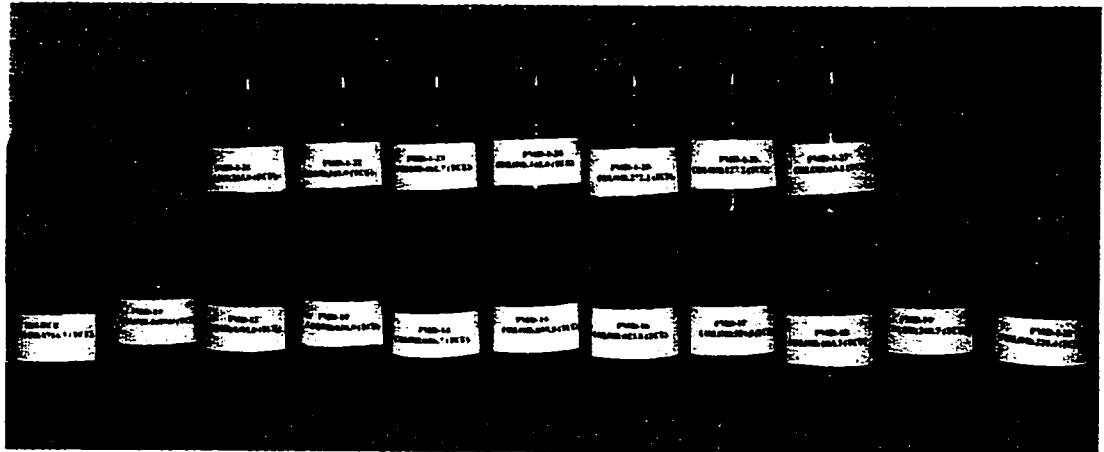


Photo - 11: Color comparison of the source pulp mill effluent sample and the meltwater samples. The leftmost bottle of the lower row is the source water sample. The sequence of the meltwater samples starts at the second bottle from left of the lower row (the first meltwater sample, with highest color concentration) and ends at the rightmost bottle of the upper row (the last meltwater sample, with lowest color concentration). The spray ice was formed at - 10 °C (with runoff generation during spraying) and stored for 40 days.

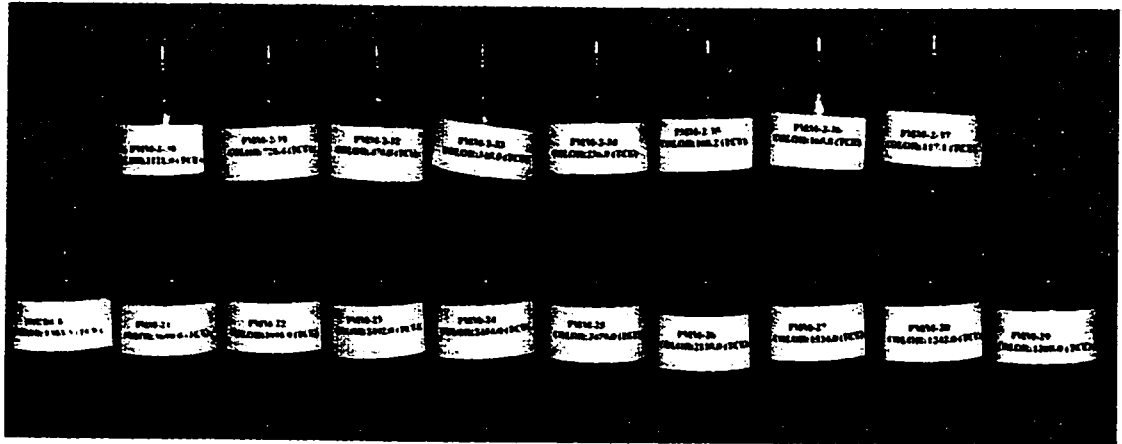
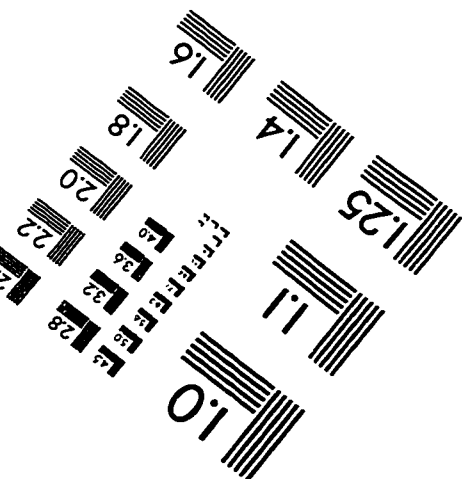
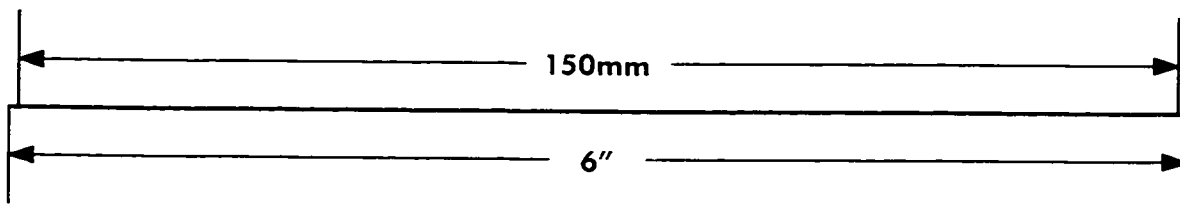
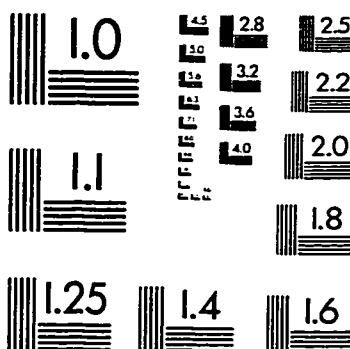
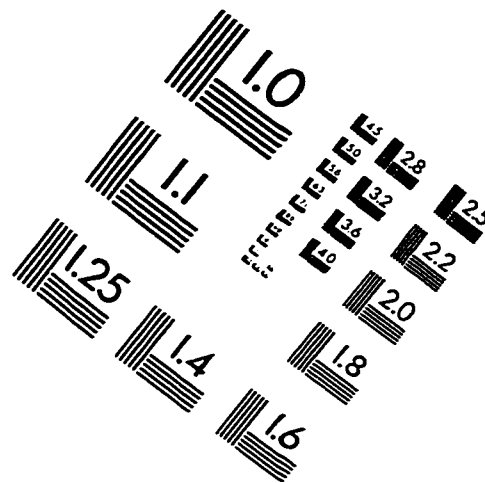
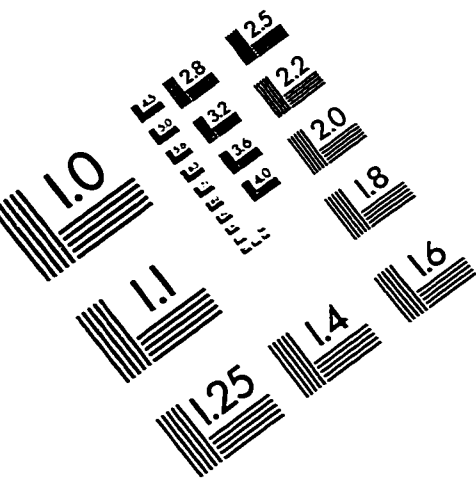


Photo - 12: Color comparison of the source pulp mill effluent sample and the meltwater samples. The leftmost bottle of the lower row is the source water sample. The sequence of the meltwater samples starts at the second bottle from left of the lower row (the first meltwater sample, with highest color concentration) and ends at the rightmost bottle of the upper row (the last meltwater sample, with lowest color concentration). The spray ice was formed at - 24 °C (no runoff generation during the spraying) and stored for 40 days.

IMAGE EVALUATION TEST TARGET (QA-3)



APPLIED IMAGE, Inc
1653 East Main Street
Rochester, NY 14609 USA
Phone: 716/482-0300
Fax: 716/288-5989

© 1993, Applied Image, Inc.. All Rights Reserved

